ESA / EUMETSAT Contract No. 16007/02/NL/SF

"Absorption Spectra Measurements with the GOME-2 FMs using the IUP/IFE-UB's Calibration Apparatus for Trace Gas Absorption Spectroscopy CATGAS"

Final Report

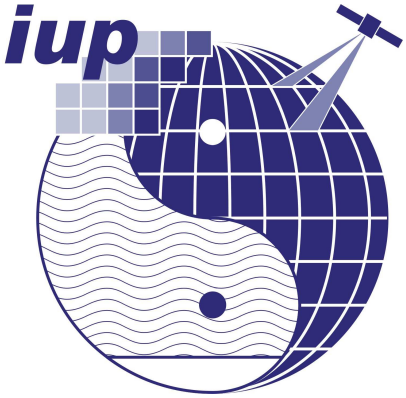

Institute of Environmental Physics
Molecular Spectroscopy and Chemical Kinetics Group
University of Bremen, October 2005

Bilgehan Gür, Peter Spietz, Johannes Orphal and John P. Burrows

Abstract

The present report documents measurements of absorption spectra of O_3, NO_2 and O_2 with the GOME-2 flight models (FM's) by using the CATGAS setup.

CATGAS (Calibration Apparatus for Trace Gas Absorption Spectroscopy) is a mobile absorption spectroscopy setup, developed by the Molecular Spectroscopy Group of the Institute of Environmental Physics in Bremen, Germany.

GOME-2 (Global Ozone Monitoring Experiment) is an enhanced follow-up project of GOME-1, which was launched on ESA's second European Remote Sensing Satellite (ERS-2) in 1995. GOME-2 is a nadir-viewing spectrometer that observes solar radiation transmitted or scattered from the Earth atmosphere or from its surface. The recorded spectra are used to derive a detailed picture of the atmospheric content and profile of O_3, NO_2 and other trace gases.

In this project temperature dependent absorption cross sections of O_3 and NO_2 have been measured in the 240 - 790 nm region by using the GOME-2 flight models FM2, FM2-1 (a refurished version of FM2) and FM3. The absorption spectra of O_3 have been measured at five temperatures in the 203-293 K range, NO_2 at four temperatures between 223 and 293 K. Furthermore O_2 were measured at ambient temperature.

This new set of laboratory measurements of O_3 absorption spectra is in very good agreement (about 1-3 % at 293 K) with the recommended O_3 absorption cross-sections at 10 different wavelengths. They also clearly confirm the previously observed temperature-dependence of the O_3 absorption coefficients in the Chappuis band, i.e. a slight increase of the peak absorption at 604 nm (about 1 % between 293 K and 203 K) and an increase and shift of the differential cross-sections in the 400-500 nm region.

The measurements of NO_2 absorption spectra is in very good agreement with previous published and recommended NO_2 absorption coefficients (about 1-2 % in the main DOAS window between 400 and 500 nm).

In both cases the newly achieved spectra are important as reference data for remote sensing. It will furthermore help to validate and improve the spectroscopic database.

• **Acknowledgements**

We would like to express our gratitude to ESA and EUMETSAT for funding this project under contract No. 16007/02/NL/SF. We especially thank Jörg Callies and Alain Lefebvre from ESA and Abelardo Perez-Albinana and Rose Munro from EUMETSAT for fruitful discussions during several CATGAS-GOME-2 progress meetings.

We furthermore express high appreciation to Gerard Otter, Luud van Riel, Martin Eschen, Pepijn Kenter and further members of the TPD/TNO team for outstanding support and cooperation before, during and after the CATGAS campaigns in Delft, Holland.

Contents

Chapter 1

Introduction

The GOME-2 instrument is part of the core payload of the MetOp satellite series, which forms the space segment of the EUMETSAT Polar System (EPS). It is an enhanced version of the GOME-1 (Global Ozone Monitoring Experiment) instrument, which has been operating in-orbit since its launch on April the 20th 1995 aboard the second European Research satellite, ERS-2, of the European Space Agency.

Similar to its predecessor, GOME-2 is a scanning double spectrometer system, which makes simultaneous observations in the 230-790 nm wavelength range of the extra terrestrial solar irradiance and the up-welling earthshine earth radiance in nadir viewing geometry. In addition GOME-2 makes regular measurements of the moon for long term calibration purposes.

Inversion of the observed earthshine radiance and extraterrestrial irradiance made by GOME 2, a large number of geophysical parameters can be derived. The primary target parameters are total column densities and vertical profiles of O_3. It has been demonstrated that total column densities of several other trace gases (e.g., H_2O, NO_2, SO_2, BrO, OClO, HCHO) and information on aerosols, clouds, and polarisation can be also be retrieved from GOME-1 data. Furthermore it has been shown that tropospheric column amounts can be retrieved from GOME-1 measurements.

• Previous Measurements

During the development of GOME-1, a recommendation was made by the GOME Science Advisory Group (GSAG)/Characterisation and Calibration Sub-group, that the temperature dependent trace gas absorption spectra should be measured under representative in-flight conditions with the GOME Flight Model. These measurements were made by the IFE/IUP-UB spectroscopy team using an absorption spectroscopy set-up dedicatedly developed for this purpose. The development of the set up was funded in large part by the University of Bremen.
Absolute absorption cross sections were derived by the IUP/IFE-UB team from these GOME-FM measurements for NO_2, O_3 and SO_2. This required laboratory measurements at the University of Bremen too.

Subsequently a study at the IUP/IFE-UB, supported by the DLR and the ESA, yielded high resolution absorption spectra of NO_2 and O_3 at a selected set of temperatures. One of the intentions of this study was to provide the data to investigate the accuracy of combining an accurate knowledge of the instrument response function coupled with high resolution gas absorption spectra to reduce the requirement for the measurement of trace gas spectra with the FM during calibration. In the case of unstable absorbers (e.g., free radicals BrO and OClO) it is difficult to measure reference spectra using the Flight Models at all, as either time resolved measurement modes for the FM would be needed or impractically high absorber concentrations were needed.

In practice at least for the dominant absorbers in the spectral range to be measured by GOME, the error on the reference spectra has not been reduced by using the two step procedure. The reason is that it is not feasible to measure the instrument response function of the spectrometers with sufficient accuracy. So in spite of their limitations the GOME-1-FM spectra, when adjusted to account for the different dispersion between one atmosphere and vacuum, still provide the best reference spectra for the GOME-1 analysis. The GOME-1-FM spectra have therefore been used as the reference spectra in the generation of GOME Level 2 data products.

The above result has been confirmed by a study commissioned by ESA and entitled "A Comparison between Predicted and Measured GOME Spectra". This investigation has shown explicitly that significant errors can be introduced if the high resolution reference spectrum is convoluted with the instrument response function, rather than absorption spectra measured with the Flight Models themselves are used as reference spectra for DOAS retrieval algorithms. These errors are dependent on the knowledge of the characterization of the instrument response function.

For the above reasons, the SCIAMACHY calibration programme measured both high resolution trace gas reference spectra of the relevant gases, accurate instrument response functions and a limited set of trace gas measurements of the majority of the target gases at a variety of temperatures and pressures with the SCIAMACHY FM.

In conclusion in order to maximize the information content and to guarantee the quality of Level 2 data products from GOME-2, it is necessary to make on-ground pre-flight measurements of the trace gas absorption spectra with the GOME-2 Flight Models under operational temperature and pressure conditions (i.e. under vacuum, the instrument being at approximately 5°C).

• Overall Objectives of the GOME-2 FM/CATGAS study

The main objectives of the GOME-2 FM/CATGAS study were:

– The measurement and subsequent analysis of high quality absorption spectra of at least O_3, NO_2, and possibly O_2 with all three GOME-2 FMs. This provides important information about the performance of the GOME-2 FMs and yields the desired absorption spectra as a function of temperature under instrumental conditions of the in-flight operation aboard MetOp.

– The detailed analysis of the measured absorption spectra and the generation of reference spectra as candidate spectra for use in the retrieval algorithms for operational and scientific processing of GOME-2 data.

This general approach agrees with the recommendations in the report of the GOME Science Advisory Group (GSAG), Characterisation and Calibration Sub-group (October 1992), reiterated by the majority of scientists in recent GSAG meetings.

The present report documents the measurements of absorption spectra with GOME-2 using the IFE/IUP CATGAS set- up, which were performed at the TPD/TNO facilities in Delft, Netherlands. During this period measurements were taken with O_3 and NO_2 at five different temperatures (293K, 273K, 243K, 223K, 203K), and O_2 at ambient temperature. Based on the experience from previous campaigns with GOME-1 and SCIAMACHY the CATGAS set-up was modified and improved, which is documented in chapter 3.

With respect to the overall scientific management and administration the IUP/IFE-UB study team was led by Prof. Dr. J. P. Burrows, head of the Institute of Environmental Physics and Remote Sensing at the University of Bremen (IUP/IFE-UB). Professor Burrows initiated and participated in the CATGAS measurements for GOME-1 and initiated those for SCIAMACHY.

The operating of the CATGAS setup was performed by Dipl.-Phys. Bilgehan Gür and Dipl.-Phys. Peter Spietz. Further support regarding documentation, preparation and analysis were given by the team members Dipl.-Phys. Heike Kromminga, Dipl.-Phys. Juan-Carlos Gomez-Martin, Christian Albers (student) and Petra Schumacher (technician). The IUP/IFE team is furthermore supported by former IUP/IFE scientist Dr. Johannes Orphal as a consultant.

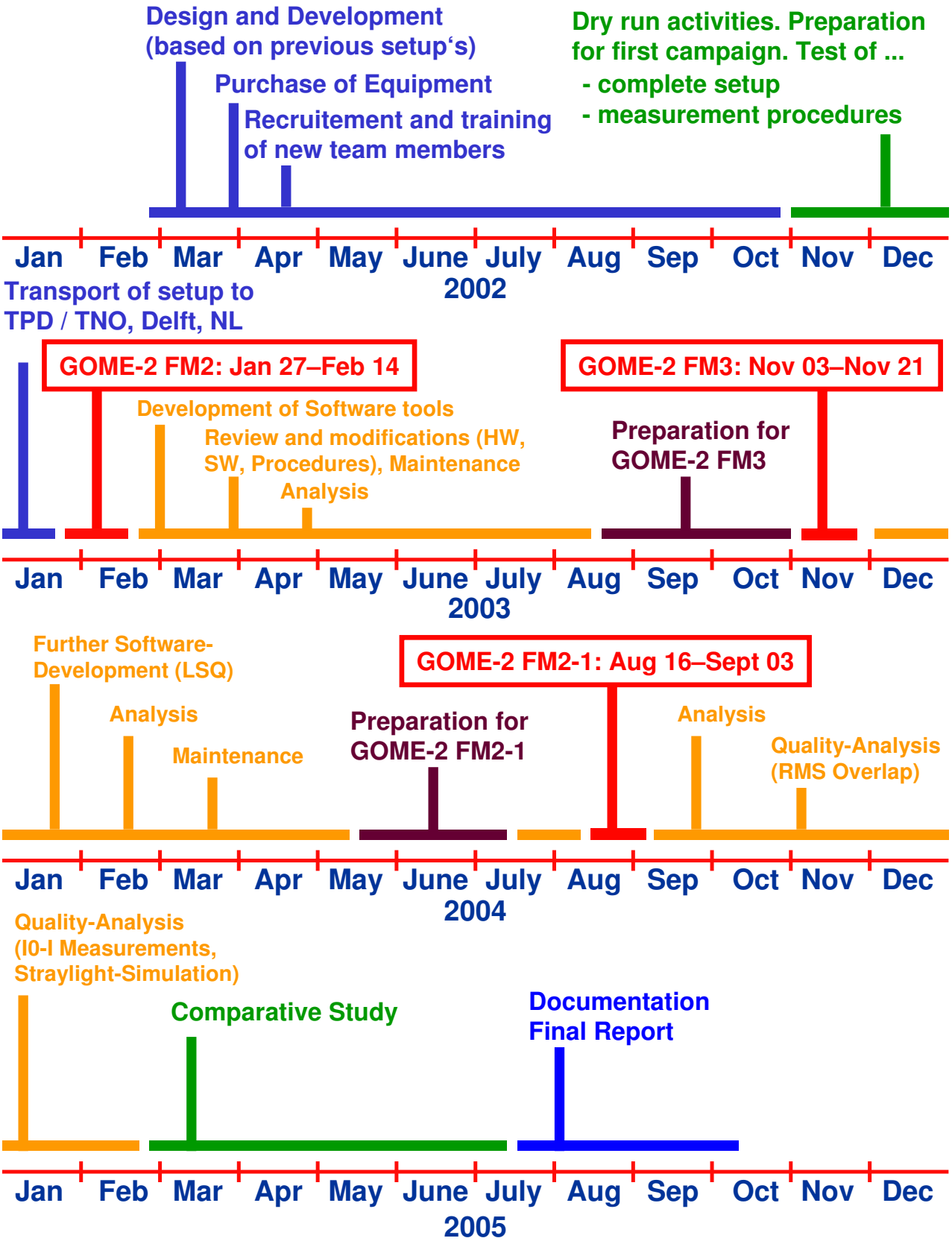

Figure 1.1: Timeline during the CATGAS GOME-2 project

Chapter 2

Absorption Spectroscopy

The basic principle used for the absorption measurements is the Lambert-Beer-Law. When passing a homogeneous gas-probe of concentration ρ electromagnetic radiation can be absorbed or scattered in dependence of wavelength λ. In every layer of the gas probe the same amount of the incident light with intensity I is absorbed:

$$\frac{dI(\lambda)}{dl} = -k(\lambda) \cdot I(\lambda) \tag{2.1}$$

- l Optical pathlength
- k Absorption coefficient

The absorption coefficient depends on the amount of absorbers along the path l:

$$k(\lambda) = \sigma(\lambda) \cdot \rho \tag{2.2}$$

$\sigma(\lambda)$ is the absorption cross section in cm^2 /molecule.
Integration of 2.1 and constitution of 2.2 leads to the absorption law of Lambert-Beer:

$$I_{Abs}(\lambda) = I_0(\lambda) \cdot e^{-\sigma(\lambda)\cdot\rho\cdot l} \tag{2.3}$$

- I_0 ... Initial light intensity
- I_{Abs} ... Intensity after passage of gas-probe

The ratio I/I_0 is designated as transmission. The optical density is defined as:

$$OD(\lambda) = \ln\left(\frac{I_0(\lambda)}{I_{Abs}(\lambda)}\right) = \sigma(\lambda) \cdot \rho \cdot l \tag{2.4}$$

By reconverting eqn. 2.4 the absorption cross section can be expressed as follows:

$$\sigma(\lambda) = \frac{1}{\rho \cdot l} \cdot \ln\left(\frac{I_0(\lambda)}{I_{Abs}(\lambda)}\right) \tag{2.5}$$

The absorption cross section σ is a function of wavelength λ and temperature T as well. Its determination by measurements of the absorption spectrum $I_{Abs}(\lambda)$, the reference-spectrum (or spectrum of analysis light-source) $I_0(\lambda)$, the concentration ρ and the optical pathlength l is influenced by the experimental setup.
It was however not the intention to measure absolute cross sections but the intensities I_{Abs} and I_0 and scale the resulting optical density to values given in the literature.

2.1 Absorption-Spectrum of O_3

The observing window of GOME-2 will cover the wavelength range between 220 and 790 nm. In the following figure a typical absorption spectrum of O_3 at ambient temperature in this range is shown:

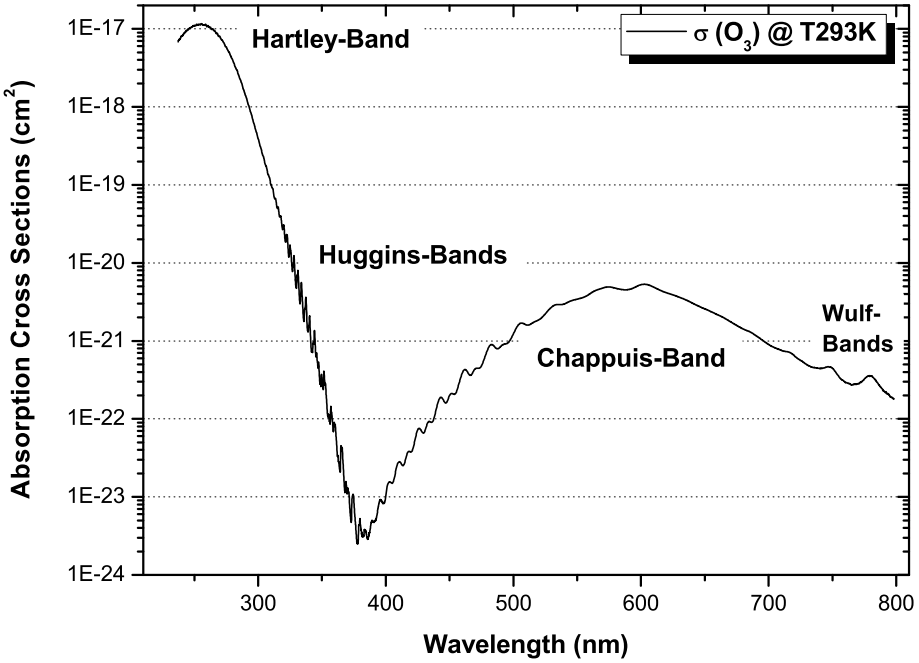

Figure 2.1: Absorption spectrum of O_3 at ambient temperature in the 220 - 790 nm range

As seen in figure 2.1 the absorption cross sections of O_3 vary in the region of interest over seven orders of magnitude. This requires several measurements with different experimental conditions in order to cover only a certain part of the spectrum and finally to compound the certain measurements to an overall spectrum. The approach regarding this issue will be addressed in detail in chapter 3.3.1.
The absorption spectrum of O_3 in this region consists of several electronic transition

systems, which are named Hartley-, Huggins-, Chappuis- and Wulf-bands.

The Hartley band is the strongest absorption band of O_3 in UV region and covers approximately the 200-310 nm region. It consists of a broad continuum with a peak around 255 nm which is superimposed by small diffuse structures. The strong absorption of O_3 in this wavelength range prevents harmful solar radiation from reaching the earth's surface.

The region between 310 and 370 nm is known as the Huggins bands and is mainly characterized by a series of peaks superimposed on the continuum of the UV range. I contrast to the Hartley band the Huggins structures show a strong temperature dependence, which increases progressively when approaching the longer wavelengths. The range between 325 and 345 nm represents an important window for remote sensing, one part of the analysis in chapter 5.1 will therefore focus on this issue.

The Chappuis absorption bands cover the 400-690 nm range with a maximum absorption cross section around 600 nm. It shows mainly a continuum absorption feature, which is superposed by an irregular series of vibrational bands in the blue wing between 400 and 550 nm, which is an important window for ground based measurements.

Starting at the red wing of the Chappuis band the Wulf bands reach the NIR at about 1050 nm and will only be covered partly by the GOME-2 instrument.

2.2 Absorption-Spectrum of NO_2

The second main target gas of GOME-2 is NO_2. The following graphics show a typical absorption spectrum of NO_2 in the range to be observed:

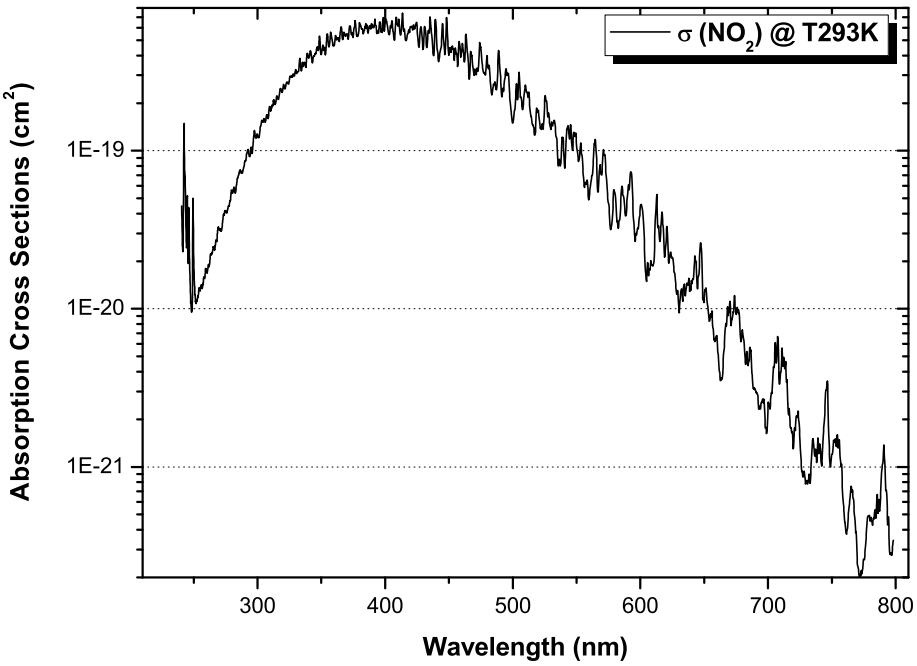

Figure 2.2: Absorption spectrum of NO_2 at ambient temperature in the 220 - 790 nm range

As seen in figure 2.2 the absorption cross sections of NO_2 vary also over several orders of magnitude. Therefore the same principle is applied to the measurements with NO_2, where several measurements with different experimental conditions have to be performed in order to cover one part of the spectrum. A detailed description about the settings and how these experimental conditions were achieved will be given in chapter 3.4.2.

Chapter 3

Experimental Setup

The concept is a modular compounded mobile absorption spectroscopy setup consisting of gas-vessel, optics and gas-system. This chapter describes the setup with the several sub-components. The following graphics gives a principle overall overview of the setup:

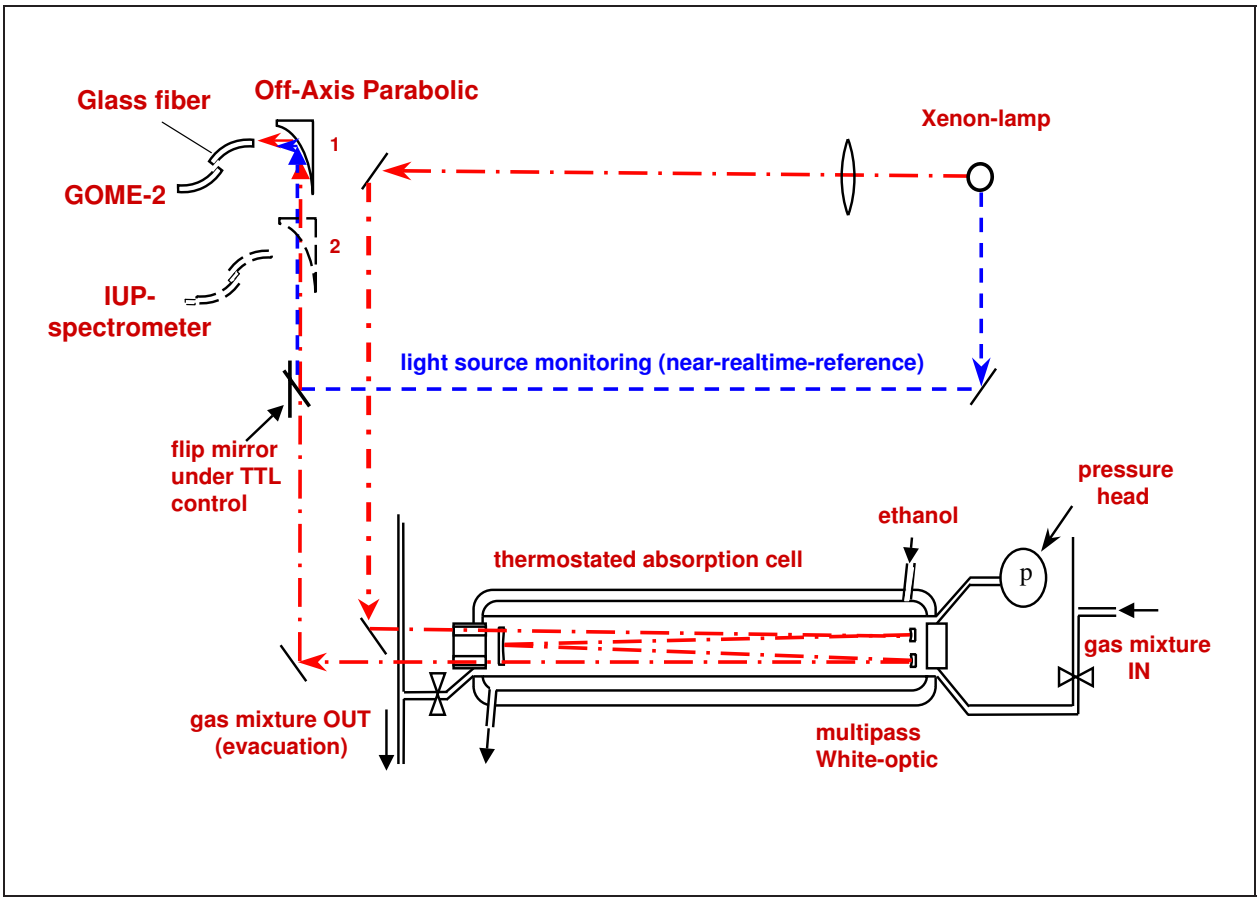

Figure 3.1: Principle absorption spectroscopy setup

The analysis light passes a vessel containing the gas of interest (red path in figure 3.1) and can then be analyzed by either the GOME-2 instrument or, for verifications of the

experimental conditions, by the commercial IUP-spectrometer. Two major differences have been made compared to previous CATGAS setup's:

- An integration of a TTL-controlled flip mirror for monitoring the light source during the absorption measurements (blue path in figure 3.1)
- Development of new gas mixing units for measurements with O_3 and NO_2, respectively and integration of a pressure regulator in order to maintain a constant pressure in the vessel during gas exchange.

Both efforts lead to a significant improvement in baseline stability.

In the following picture the complete set up on the optical bench is shown:

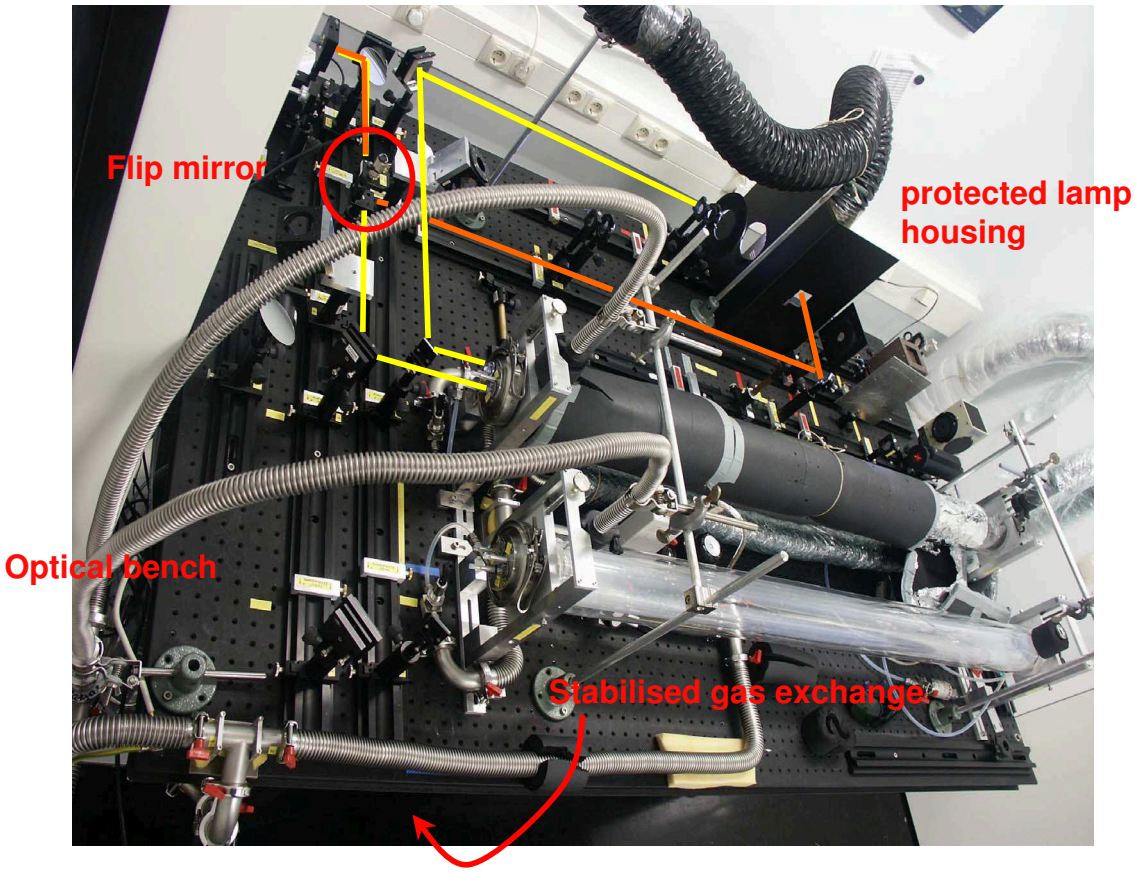

Figure 3.2: CATGAS setup on the optical bench

A detailed description of the several sub components is given in the following sections.

3.1 Light-Source and optics

As a light source a new xenon-lamp of the typ Hamamatsu was used. In contrast to previous setup's a higher stability could be gained by a protected lamp housing. A lens focuses the light into the entrance window of the gas cell, which is equipped with a so-called White-optics. This optical arrangement, following the method of White [3], allows multiple reflections within the vessel and therefore optical pathlengths up to 33m. The analysis light coming from the CATGAS setup is directed either to

1. the actual optical CATGAS-GOME-2 connection consisting of a multi fibre bundle and an optical interface developed by TPD (see section 3.1.1) or
2. a small glass fibre leading to the commercial IUP-spectrometer (used for verification of the experimental conditions or checking the stability of the system e.g. after temperature change)

Once the correct experiment conditions are set, the off-axis parabolic mirror No. 2 in figure 3.1, can be removed and the light can than be guided to the GOME-2 fibre by the off-axis parabolic mirror No. 1.

3.1.1 Optical Interface

As mentioned before the light coming from the CATGAS setup is to be guided to the GOME-2 instrument. This is done by a multi fibre bundle and and optical interface. The fibre bundle has a circular (front) entrance and a rectangular exit (spatial), as seen in figure 3.3.

(a) Fibre-Entrance (b) Fibre-Exit

Figure 3.3: Fibre bundle connecting the CATGAS set-up and TPD optical interface

The detailed characteristics are listed in the following table:

Length	5 m
Diameter single fibre	70 μm
Front aperture	Ø 6.2 mm
Exit aperture	19 x 1.6 mm
NA fibre	0.25

These characteristics, especially the exit aperture and NA of the fibre need to be adapted to the GOME-2 instrument spatial entrance acceptance area and field:

FOV	2.75° x 0.286°
Aperture	25 x 5 mm

In order to correctly transfer the light coming from the fibre into the spectrometer TPD developed an optical interface consisting of a 3 mirror system. Figure 3.4 illustrates the optical and mechanical layout of the interface.

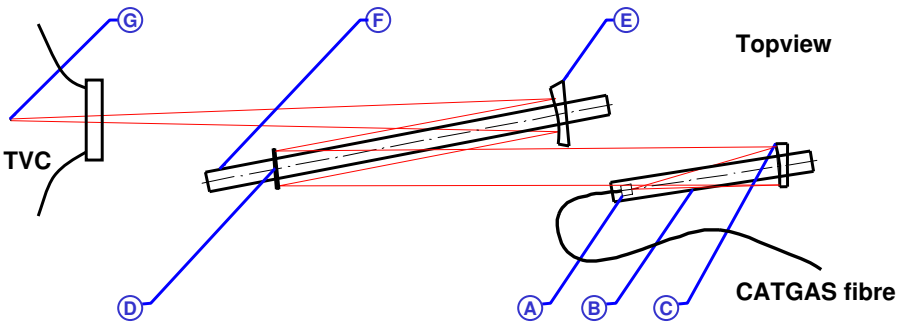

A: Fibre input (from the CATGAS setup)

B: Optical rail

C: Mirror 1 **f = 700mm; D (min) = 210mm (parabolic and off-axis)**

D: Mirror 3 **f = ∞ ; D (min) = 200mm (spherical)**

E: Mirror 2 **f = 3175mm; D (min) = 317mm (fold mirror)**

F: Optical rail

G: Focal plane (on the GOME scanning mirror)

Figure 3.4: Optical and mechanical layout of optical interface[1]

Mirror 2 and 3 are coated with an aluminium layer, furthermore mirror 2 is optimized for the UV-range by having an additional UV enhanced layer. Due to the high optical surface quality of mirror 1 (manufactured in the TPD optical workshop on an optical precision diamond turning machine) an aluminium layer on this mirror is not needed.
Further characteristics are given in the following table:

Input NA	0.13 (total light cone $\sim 15°$)
Aperture Stop	D = 183 mm
Magnification	4.5
Image Dimensions (on	85.5 mm (length)
GOME Scanning mirror)	7.2 mm (width)

[1]Kindly provided by TPD

Further details regarding optical homogeneity and detailed calculations regarding the interface are given in MO-TN-TPD-GO-0060i1 in the GOME calibration report by TPD.

3.2 Gas-Vessel

The gas vessel is a double jacketed fused silica gas cell. The inner cell is the gas reservoir and also contains the White-optics. Through the middle cell a flow of ethanol can be used from a thermostated reservoir in order to cool down the temperature down to -70°C. The outer cell can be evacuated for insulation. This is illustrated in figure 3.5.

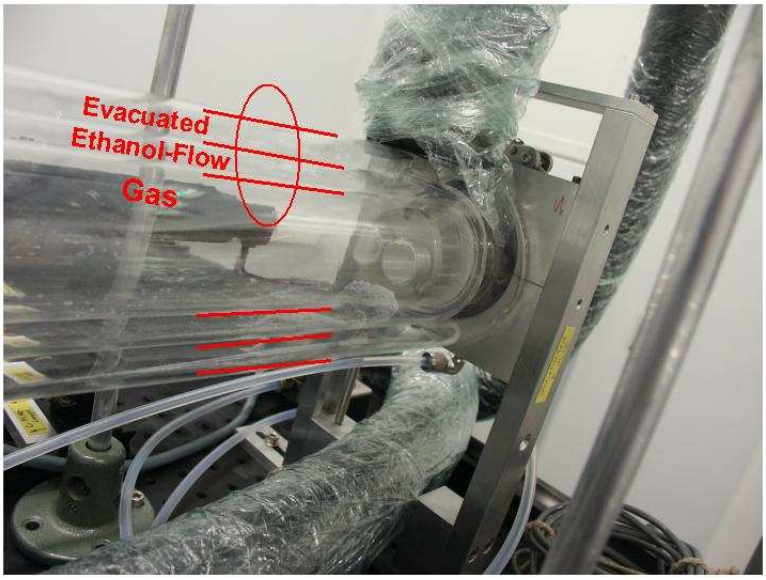

Figure 3.5: Double-jacketed gas-vessel

The setup consists of two such vessels, one for O_3 one for NO_2-measurements (figure 3.2).

3.3 Gas-System O_3

In principle the O_3 gas-system consists of a 50l oxygen-bottle (5.0 purity), a newly developed gas-exchange unit ($O_2/_3$-Flow switching unit), two 2000 sccm (standard cubic centimeter) flowcontrollers, ozonisers and an ozone-destroyer unit. For measurements with O_3 a setup was chosen for using a flow modus. It was intended to keep the pressure in the cell constant, even at gas exchange.

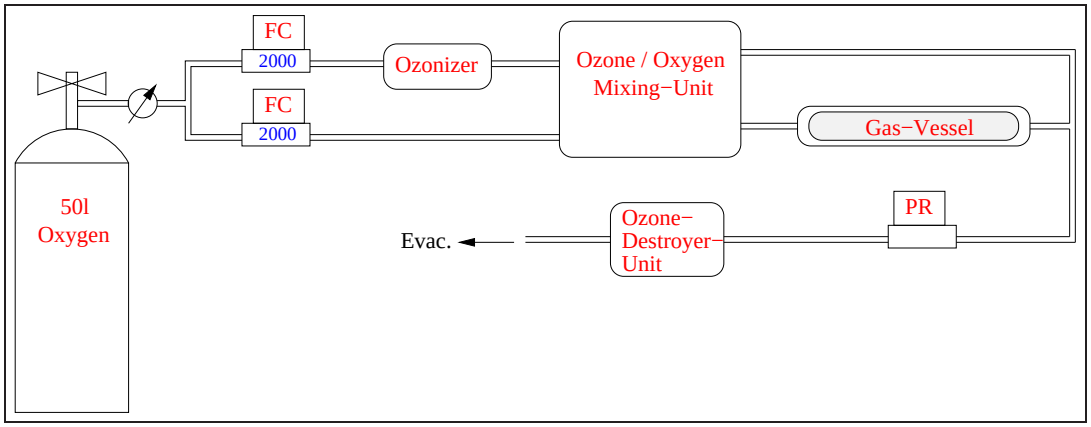

Figure 3.6: O_3 gas system

The initial gas-flow coming from the gas bottle is separated into two lines: One line is connected directly with the gas-exchanging unit, the other flow passes the ozonizer in which O_3 is produced by electrical discharge. Two types of ozonizer (one commercial one [typ OG5] and one built at IUP/IFE) were used depending on the amount of O_3 needed. The OG5 produces higher O_3-concentrations and is therefore used for ranges with low absorption cross section. The efficiency can be regulated by a power control. For measurements in regions with high absorption cross sections as in the Hartley-band (mixtures 6 to 8) the IUP/IFE ozonizer with a much lower production of O_3 concentrations was used.

This branch with a O_2 / O_3-mixed flow is also connected with the gas exchanging unit. Each line is connected with a 3-way-valve, depending on its position the flow is either directed in the reaction vessel or evacuated. The two valves from each line are connected with each other through a hand gear in a way that they react anticorrelated. That means that, if one flow is connected with the reaction vessel the other one is automatically evacuated and vice versa. In this way the flow towards the vessel is hardly disturbed and the pressure remains within +/- 0,1mbar.

Figure 3.7 illustrates more detailed the O_3 mixing unit.

The above described method about changing the flows to the vessel by using the gear is however only valid for measurements referred to mixtures 1 to 5. For measurements regarding mixtures 6 to 8, covering the Hartley-band in channel 1, a slight modification is required:

Due to the high absorption cross sections of O_3 in the 220 to 310 nm region, even with the lowest amount of produced O_3 one reaches far to high optical densities. As seen in figure 3.7 we have an interconnection between the two lines, which has no effect as long as the valve in this connection is closed.

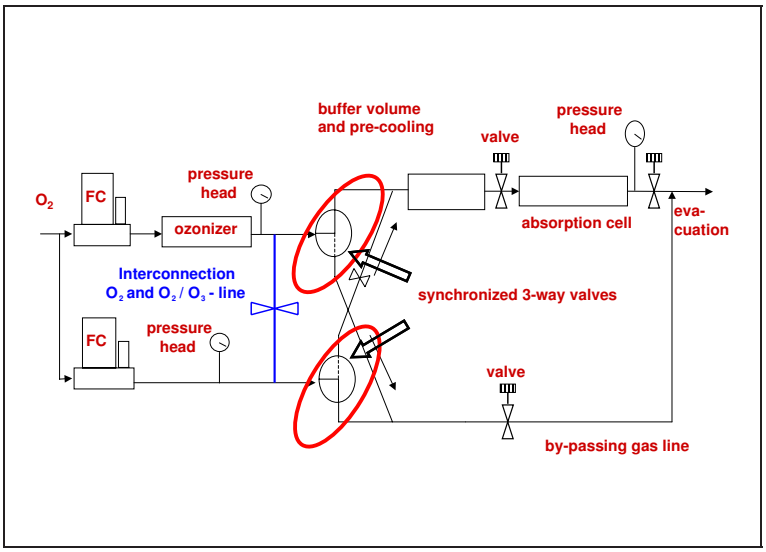

Figure 3.7: O_3 mixing unit I

Opening the valve however allows additional diluting of the O_3-flow with O_2. The rate of dilution can be controlled by the settings for the flow-controller of the O_2 branch. The change from a reference to an absorption measurement and back is simply achieved by switching the ozonizer on and off.

Figure 3.8 shows the mixing unit with the hand gear (red circle), with which the flow can be changed and the interconnection of the two branches (blue circle).

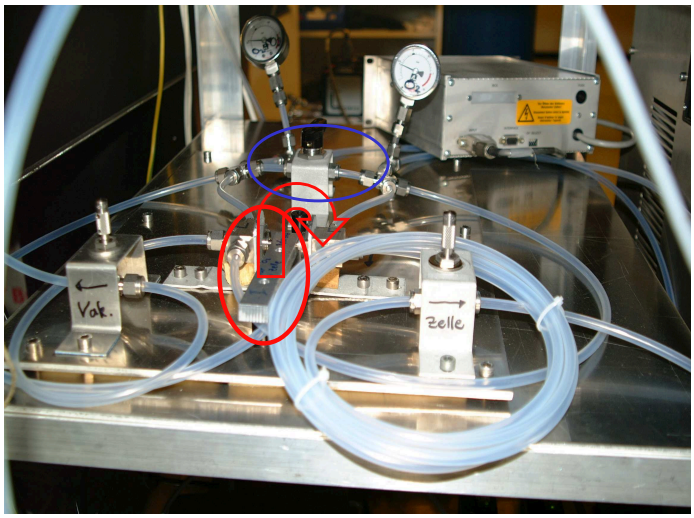

Figure 3.8: O_3 mixing unit II

As mentioned before it was an important requirement for the baseline stability to keep the pressure in the vessel constant during all measurements regarding one mixture, even and especially at gas-exchange. Beside the above described gas mixing unit for this purpose a pressure regulator was integrated at the output of the vessel.

Once the desired pressure in the vessel is reached the regulator is activated and the flows and pressure in the vessel remain constant(figure 3.9).

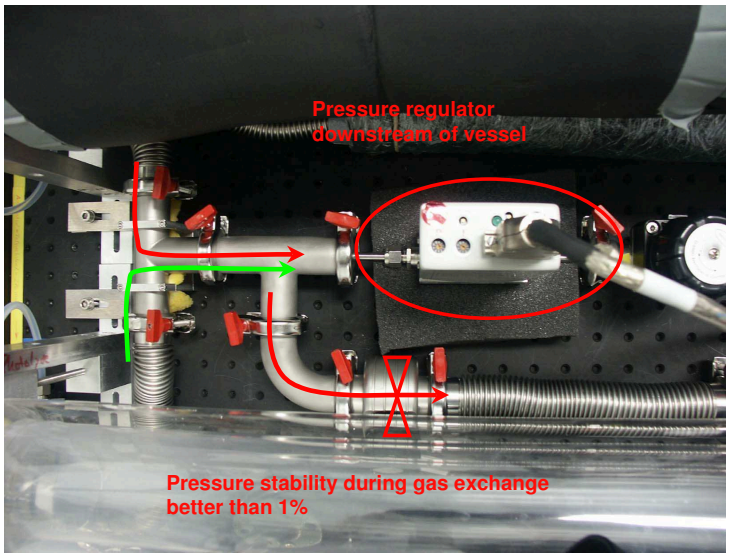

Figure 3.9: Pressure regulator at the output of the gas vessel

3.3.1 Experimental Settings for O_3-Measurements

As mentioned in chapter 2.1 several absorption measurements with different experimental conditions are required due to the variation of the O_3 absorption cross sections over seven orders of magnitude in the 240-790 nm range.

Different conditions can be achieved by different combinations of optical pathlength and O_3 concentration, which we will call 'mixtures' in the following. As for instance expressed in equation 2.4 high concentrations are required in regions with small absorption cross sections and vice versa.

In figure 3.10 again an absorption spectrum of O_3 at ambient temperature is shown. The spectrum is divided into eight areas, shown by the horizontal lines, which represent different experimental settings (named mix1, mix2, ..., mix8) of optical pathlength and O_3-concentration. In the respective combination of these parameters the optical density will ideally be between 0.1 and 1 in a certain range and cover a certain part of the spectrum. For instance, the settings for "mix1" will mainly cover the minimum range of the O_3-spectrum between 350 and 450 nm.

In Table 3.1 the certain combinations of experimental conditions (optical pathlength, power of the O_3 generator, total pressure and gas flow rate) are listed. Please note that after the first campaign with GOME-2 FM2 the procedure was slightly changed. Due to the importance of the DOAS window between 325 and 345 nm for remote sensing, it was decided to cover the Huggins bands with more than three measurements (originally declared as "mix3, mix4, mix5"). Combination 3 in table 3.1 therefore represents seven different measurements each with different settings for the O_3 generator. Combinations 1-3 and 6-8 have been measured with different O_3 generators.

As explained in the preceding section the gas mixing and exchanging method differs for measurements regarding mixture 6 to 8. Beside the use of a different O_3 generator the valve between both branches in the mixing module is open (see figure 3.7).

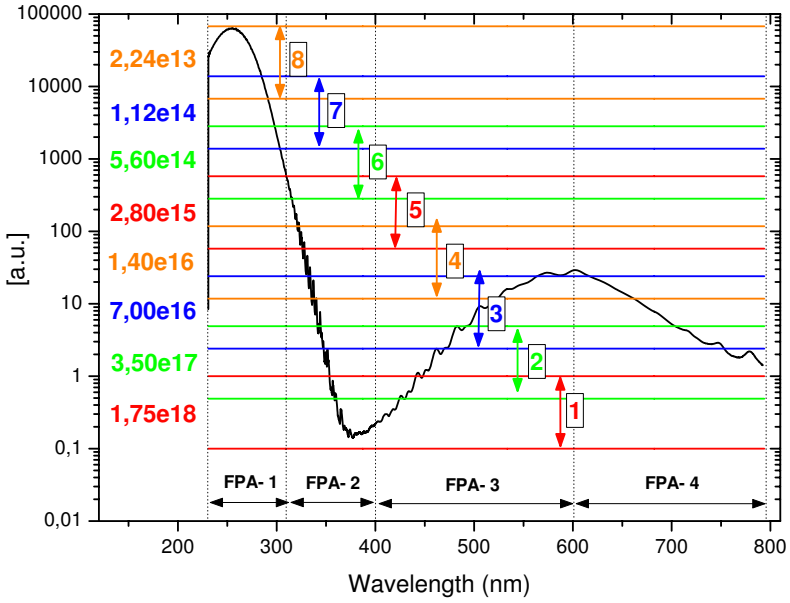

Figure 3.10: Absorption spectrum of O_3 with different regions of interest. The numbers on the left give roughly the achieved O_3 concentrations in the certain experimental settings. Note that the channel borders have always been covered by one combination.

Combination and Channel	Wavelength range [nm]	Optical Pathlength [m]	Power OG (1-3, [a.u.]) (6-8, [V])	Pressure in reaction vessel [mbar]	Flow in O_2-branch [sccm]	Flow in O_3-branch [sccm]
1 (FPA-2+3)	355-455	28.40	260	800	100	100
2 (FPA-2)	340-365	28.40	60	800	400	400
(FPA-3)	430-500					
3[2] (FPA-2)	315-350	28.40	40-120	100	400	400
(FPA-3+4)	475-790					
6 (FPA-1)	300-325	2.40	12	320	0	1000
7 (FPA-1)	280-310	2.40	8.5	65	0	1000
8 (FPA-1)	240-290	2.40	12	36	200	200

Table 3.1: Experimental conditions for O_3 measurements. The units for the flow controllers sccm stand for standard cubic centimeter per minute. Since relative measurements have been performed an accuracy statement for the flow controllers is not necessary.

[2]Combination 3 represents seven different measurements, each with different settings for the O_3 generator and covers the range, which was originally declared as "mix3, mix4, mix5" (fig. 3.10). More details are given in the text.

3.4 Gas-System NO_2

The NO_2 system differs from the O_3 system, although the principle of a constant cell pressure remains. The principal item for the NO_2 gas-system is, similar as in the O_3 set up, the mixing unit, with which two flows of synthetic air and synthetic air with 2,5% NO_2 can be combined to the right mixing ratio with the required NO_2 concentration in the vessel. The principle NO_2 gas-system is illustrated in figure 3.11.

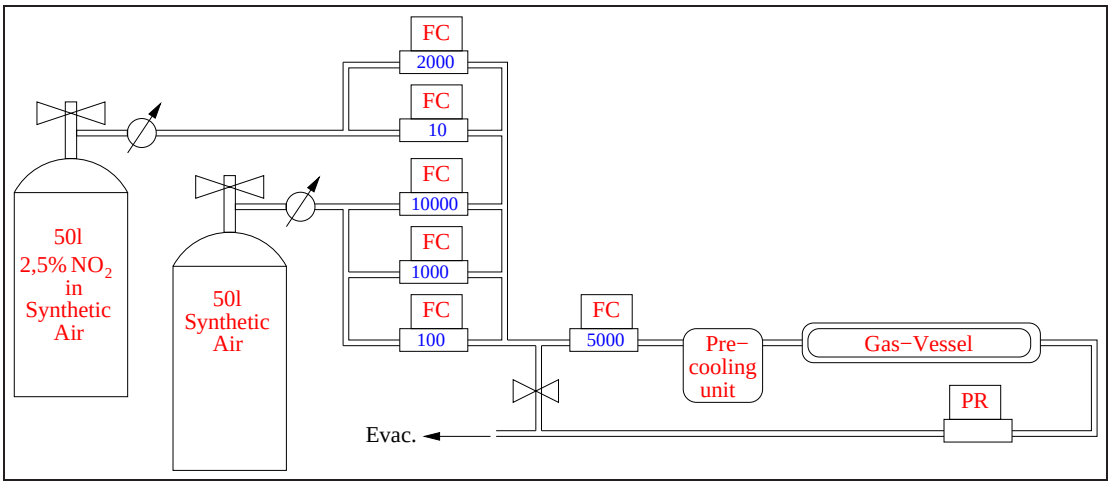

Figure 3.11: NO_2 gas system

Two 50l gas bottles, containing synthetic air and NO_2 (2,5% NO_2 in synthetic air) respectively, are connected with the mixing unit; synthetic air with 3 flowcontrollers, allowing a maximum flow of 10000, 1000 or 100 sccm, NO_2 with 2 flowcontrollers allowing a maximum flow of 2000 or 10 sccm respectively. After passing the fc's both branches are united and then directed to the vessel.

Between the mixing unit and the vessel an additional flowcontroller (5000sccm) is integrated, the flow of which is in general lower than the sum of the flows of the mixing unit. The resulting overpressure is deflated through another valve into the vacuum. A pressure regulator at the output of the vessel ensures, similar to the O_3 system, a stable pressure in the cell. The switch from reference measurement to absorption measurement is simply done by activating the NO_2 -flow. The required concentration of NO_2 in the vessel is achieved by diluting the NO_2-flow with the synthetic air flowcontrollers. This will be described more detailed in section 3.4.1

3.4.1 Calculation of NO_2-Concentrations and Dimerisation

Figure 2.2 in chapter 2.2 shows an absorption spectrum of NO_2, which varies, similar to an O_3 spectrum, over several orders of magnitude. Here as well it is necessary to take several measurements for complete coverage in the 240-79 nm range, whereas an additional factor has to be respected: The dimerisation of NO_2 to N_2O_4.
This issue needs to be introduced before listing the experimental settings and conditions for NO_2 measurements.

As already seen in figure 3.10 with the O_3 absorption spectrum the NO_2 spectrum as well can be divided into six sections representing different experimental conditions (see figure 3.16). The numbers given on the left are again indications for NO_2-concentrations. The maximum possible concentration of NO_2 in the vessel (based on a 2,5% NO_2 in synthetic air mixture) can be determined as follows:

Avogadro's number gives the amount of molecules in 1 mole of a gas under norm conditions, meaning at 273K and atmospheric pressure. Under these conditions the gas has a volume of $22{,}4 \cdot 10^3 \mathrm{cm}^2$. This corresponds to a concentration of

$$[\mathrm{c}] = \frac{6,022 \cdot 10^{23} \mathrm{molecules}}{22,4 \cdot 10^3 \mathrm{cm}^3} \approx 2,7 \cdot 10^{19} \ \mathrm{molecules/cm}^3 \tag{3.1}$$

With 2,5% NO_2 in synthetic air this would mean a concentration of NO_2 in a vessel with 1000mbar:

$$[\mathrm{NO_2}] = \frac{25\mathrm{mbar} \cdot 2,7 \cdot 10^{19} \mathrm{molec/cm}^3}{1000\mathrm{mbar}} = 6,75 \cdot 10^{17} \mathrm{molec/cm}^3 \tag{3.2}$$

This value can then be used as a reference value. In figure 2.2 the highest concentration is however given one order of magnitude lower. This is due to the requirement of a second flow needed for dilution. Only with a second flow of pure synthetic air the flow of the NO_2-branch can be stopped (as needed for reference measurements) without interrupting the flow through the vessel(as needed for baseline stability).

Initiating from this point the other required concentrations can be estimated by the following procedure: The concentration of NO_2 at any temperature can be expressed by

$$[\mathrm{NO_2}]_{\mathrm{a,b}} = P_{NO_2 a,b} \cdot 2.7 \cdot 10^{19} \mathrm{molec/cm}^3 \cdot \frac{273.15\mathrm{K}}{T} \tag{3.3}$$

where P is the partial pressure and $2.7 \cdot 10^{19}$ molec / cm^3, as calculated before, the concentration under norm conditions. At this point another critical issue to be thought of is the following: NO_2 is constantly in an equilibrium with its dimer N_2O_4.

$$2NO_2 \rightleftharpoons N_2O4$$

This equilibrium is shifted towards N_2O_4 at lower temperature or higher NO_2 partial pressure. This has to be respected in the calculations of further concentrations of NO_2 at different temperatures and partial pressures. The index a or b in the foregoing equation is referred to a concentration without and with dimerisation respectively. $P_{NO_2 b}$ can be determined by the following equation

$$P_{NO_2 b} = \frac{K_p}{4} \left[\sqrt{1 + \frac{8 P_{\mathrm{vessel}} \cdot \chi}{K_p}} - 1 \right] \tag{3.4}$$

where K_p is the equilibrium constant of NO_2 with N_2O_4 as given in [5] and χ the percentage of NO_2 in the flow, in this case 2,5%. An additional flow of synthetic air

reduces the partial pressure of NO_2 in the vessel:

$$P_{NO_2a} = 0,025 \cdot P_{\text{vessel}} \cdot \frac{\text{FlowFC1}}{\text{FlowFC1} + \text{FlowFC2}} \tag{3.5}$$

Based on these deliberations the interaction of both flowcontrollers at different temperatures could be determined, which was done with the scientific software origin. The following table shows such an origin-project for calculations at 293 K, which can also be used for future references.

The pressure in the vessel is 500 mbar, the flow of the flowcontroller FC1 (2.5% NO_2 in synthetic air) is 10 sccm.

Worksheet: "Dilution at 293 K and 500 mbar pressure in the vessel":

T	Kp	Pvessel	FlowFC2	PNO2a	concNO2a	...
Kelvin	mbar	mbar	sccm	mbar without Dimerisation	molec / ccm without Dimerisation	...
292,99585	97,04215	500	0	12,5	3,13101E17	...
292,99585	97,04215	500	20	4,16667	1,04367E17	...
292,99585	97,04215	500	40	2,5	6,26203E16	...
:	:	:	:	:	:	...

...	PNO2b	concNO2b	PN2O4	concN2O4
... ...	mbar with Dimerisation	molec / ccm with Dimerisation	mbar with Dimerisation	molec / ccm with Dimerisation
...	10,30949	2,58233E17	2,19051	5,4868E16
...	3,85965	9,66769E16	0,30702	7,69024E15
...	2,38297	5,96889E16	0,11703	2,93144E15
...	:	:	:	:

The meaning of the abbreviations in the worksheet are as follows:

T	...	Temperature in Kelvin
Kp	...	Equilibrium constant
Pcell	...	Overall pressure in cell
FlowFC2	...	Flow of second flowcontroller, with which the NO_2-flow is diluted
PNO2a	...	Partial pressure of NO_2 **without** Dimerisation
concNO2a	...	Concentration of NO_2 **without** Dimerisation
PNO2b	...	Partial pressure of NO_2 **with** Dimerisation
concNO2b	...	Concentration of NO_2 **with** Dimerisation
PN2O4	...	Partial pressure of N_2O_4
concN2O4	...	Concentration of N_2O_4

With the created worksheets the desired NO_2-concentration in the vessel can easily be read off in dependence of temperature and partial pressure. Figures 3.12 to 3.15 illustrate exemplarily the NO_2-concentration (10 sccm 2.5 % NO_2 in s.a.) in dependence of the dilution, i.e. additional flow of synthetic air coming from FC2.

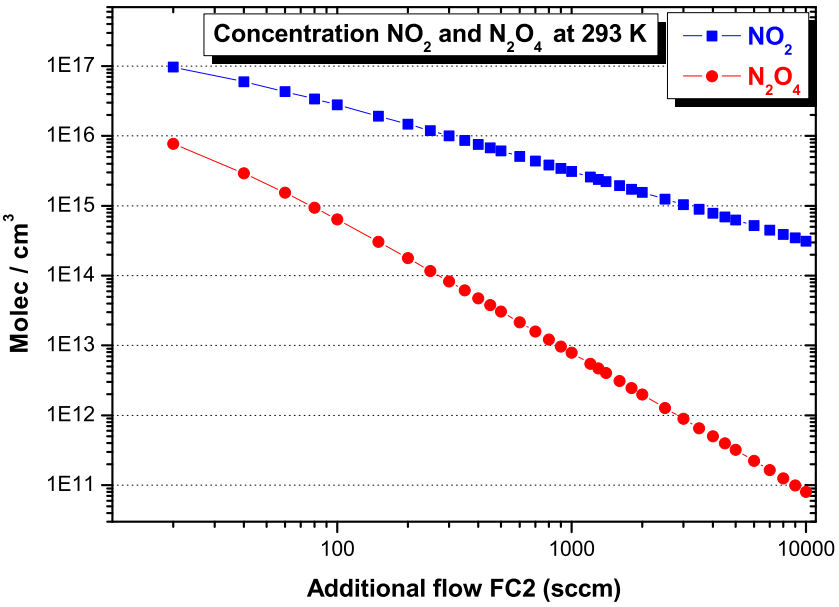

Figure 3.12: NO_2-concentration (10 sccm of 2.5 % NO_2 in s.a.) as a function of diluting synthetic air flow coming from FC2 for T 293 K

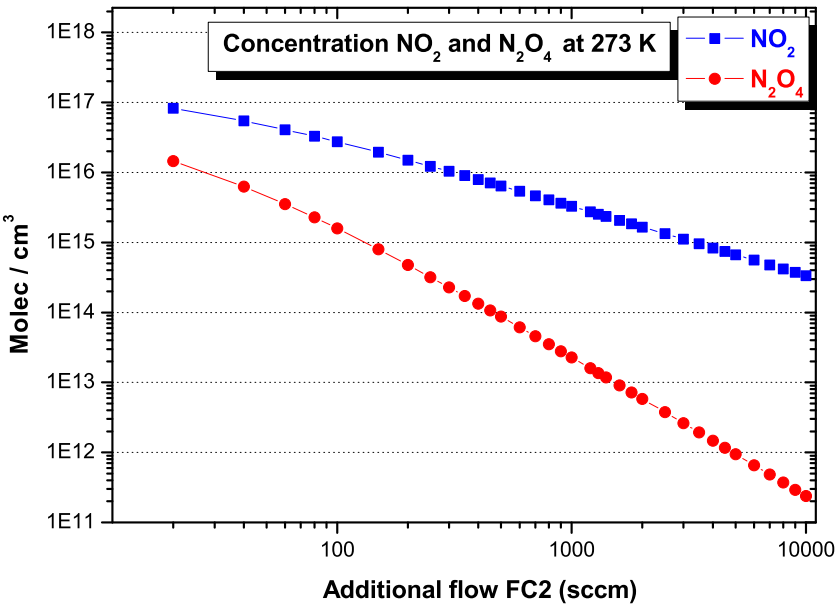

Figure 3.13: NO_2-concentration (10 sccm of 2.5 % NO_2 in s.a.) as a function of diluting synthetic air flow coming from FC2 for T 273 K

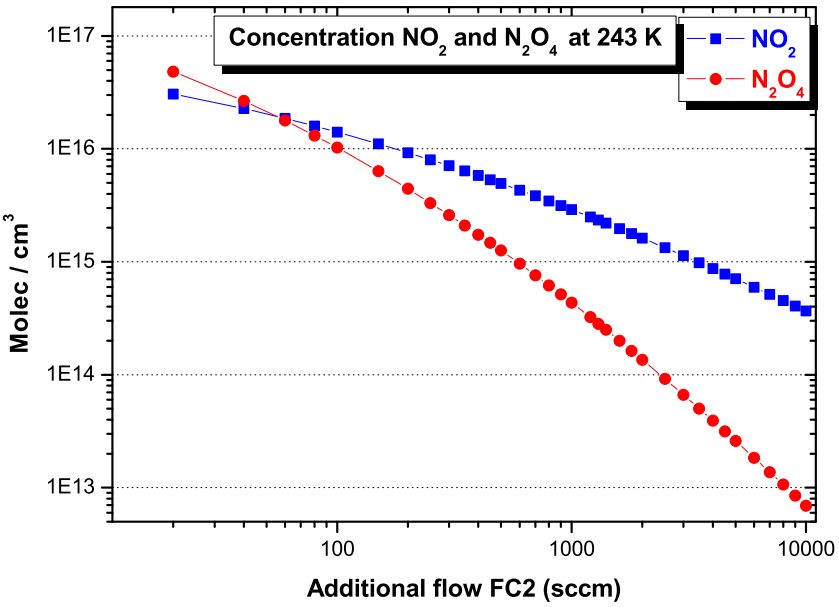

Figure 3.14: NO_2-concentration (10 sccm of 2.5 % NO_2 in s.a.) as a function of diluting synthetic air flow coming from FC2 for T 243 K

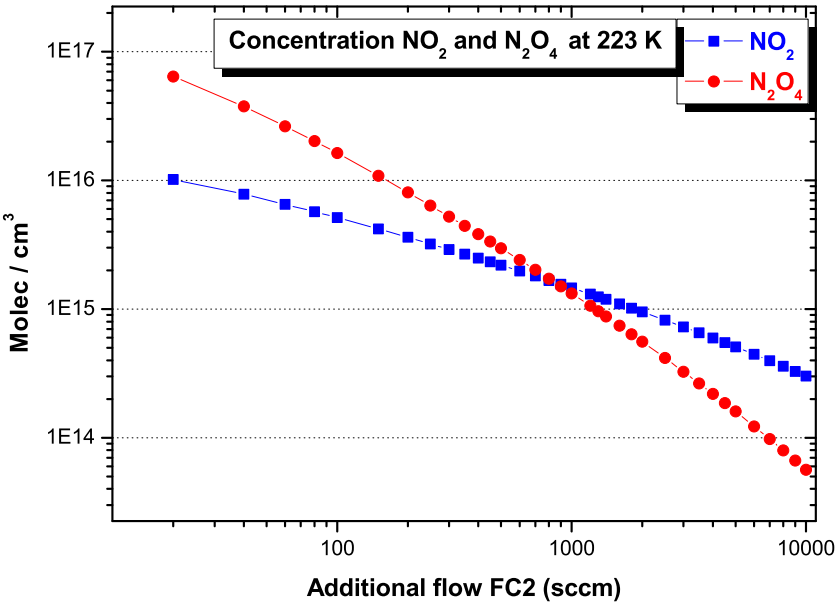

Figure 3.15: NO_2-concentration (10 sccm of 2.5 % NO_2 in s.a.) as a function of diluting synthetic air flow coming from FC2 for T 223 K

3.4.2 Experimental Settings for NO_2-Measurements

In this section we list the experimental settings and conditions for NO_2 measurements (table 3.2). As illustrated in figure 3.16 the complete NO_2 absorption spectrum in the 240-790 nm range can be covered with six measurements under different experimental conditions, whereas it has to be noted that during the measurements N_2O_4 is produced as well and has to be extracted.

Following this section we will describe the required procedure to achieve N_2O_4 corrected NO_2 absorption spectra.

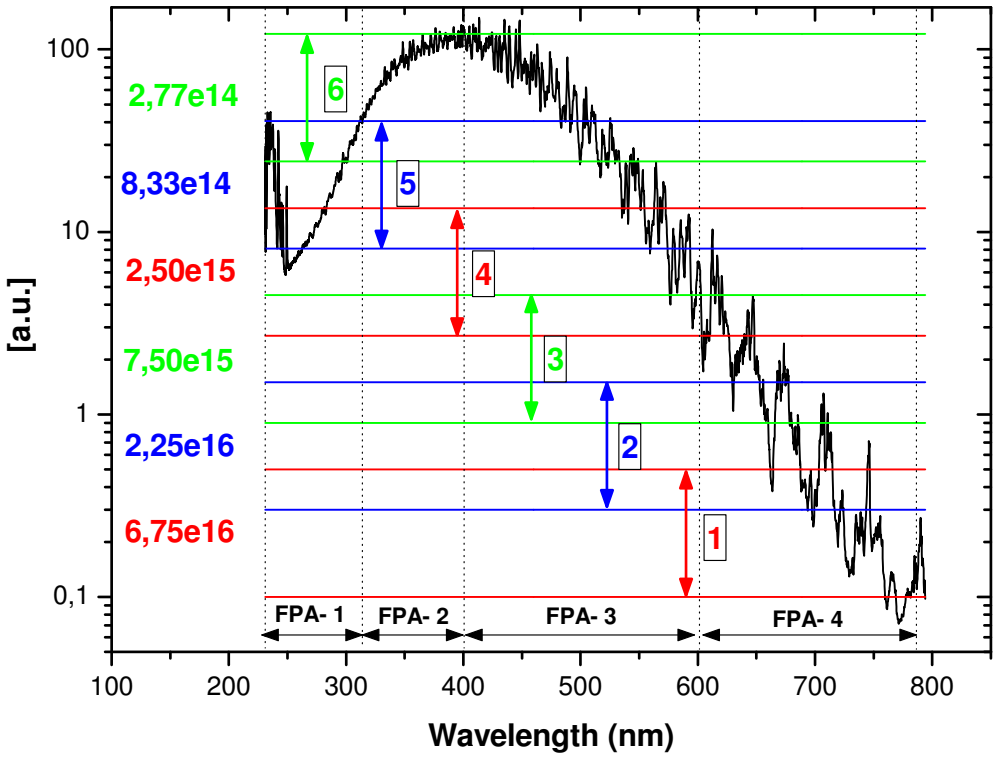

Figure 3.16: Absorption spectrum of NO_2 with different regions of interest. The numbers on the left give roughly the achieved NO_2 concentrations in the certain experimental settings.

Temperature [Kelvin]	**Mixture**	**FC[10] NO_2-Flow [sccm]**	**FC[2000] NO_2-Flow [sccm]**	**FC[10000] Dilution [sccm]**	**FC[5000] Flow to Vessel [sccm]**
293	1	5,5	-	3300	1000
	2	10	-	2800	1000
	3	10	-	1050	1000
	4	-	50	2200	1000
	5	-	90	1800	1000
	6	-	350	1800	1000
273	1	4	-	3600	1000
	2	4	-	1400	1000
	3	10	-	1300	1000
	4	4	-	1200	1000
	5	-	93	1250	1000
	6	-	140	1250	1000
243	1	2,8	-	2000	1000
	2	5	-	1300	1000
	3	10	-	1200	1000
	4	10	-	800	1000
	5	-	50	1600	1000
	6	-	250	1500	1000
223	1	2,8	-	1500	1000
	2	5	-	1500	1000
	3	8,5	-	2000	1000
	4	-	37	1600	1000
	5	-	170	1200	1000
	6	-	220	1200	1000

Table 3.2: Experimental conditions for NO_2 measurements

3.4.3 Correction of the N_2O_4-Absorption

NO_2 is constantly in an equilibrium with its dimer N_2O_4.

$$2NO_2 \rightleftharpoons N_2O4$$

This equilibrium is shifted towards N_2O_4 at lower temperature or higher NO_2 partial pressure. N_2O_4 is absorbing below 400nm, therefore the measured NO_2 absorption spectra in this spectral range are a superposition of a NO_2- and N_2O_4-spectrum. In order to achieve a pure NO_2-spectrum the superposed N_2O_4-spectrum needs to be separated. For this purpose a method is applied, which was described by Eisinger in 1994 [4]. For application the following requirements need to be fulfilled:

- constant temperature in absorption cell
- Measurement of three absorption spectra at different NO_2 partial pressures
  1. A spectrum with low NO_2 partial pressure and therefore low N_2O_4-absorption. This will , according to the notation given in [4], in the following be notated as spectrum B and can be seen as the NO_2-reference.
  2. A spectrum with intermediate NO_2 partial pressure (the actual measurement-spectrum). This will be notated as NO_2-spectrum or spectrum A.
  3. A spectrum with high NO_2 partial pressure and therefore strong N_2O_4-absorption. This will be notated as N_2O_4-spectrum or spectrum F.
- NO_2 and N_2O_4 in an equilibrium in the cell

$$[NO_2] \text{ and } [N_2O_4] \approx \text{const}$$

The spectral separation is based on the assumption that N_2O_4 does not absorb at wavelength above 400nm. The spectra to be corrected must therefore content this spectral range. This is due to the broad spectral range of the GOME-2 spectrometer fulfilled. The knowledge of the temperature dependent equilibrium constant K_p is not required for the application of this method. In the following the several steps of the Eisinger-procedure are described:

1. Isolation of the N_2O_4-absorption in the NO_2-spectrum and N_2O_4-reference with respect to the NO_2-reference.
   (a) Calculation of the relative NO_2-absorption in the NO_2-spectrum and N_2O_4-reference with respect to the NO_2-reference.
   $$r_A = \frac{[NO_2]_A}{[NO_2]_B} \quad \text{and} \quad r_F = \frac{[NO_2]_F}{[NO_2]_B} \tag{3.6}$$
   (b) Subtraction of the scaled NO_2-reference from the NO_2-spectrum and N_2O_4-reference respectively.
   $$C = A - r_A \cdot B \tag{3.7}$$
   $$D = F - r_F \cdot B \tag{3.8}$$
   C and D content only the N_2O_4-absorption

2. Calculation of the relative N_2O_4-absorption in spectrum C, in the NO_2-reference and in the NO_2-spectrum with respect to spectrum D. For spectrum C it is:

$$s_C = \frac{[N_2O_4]_C}{[N_2O_4]_D} \tag{3.9}$$

s_C is ascertained by division of the spectra C and D and averaging of the ratios in a pixel range close to the maximum of the N_2O_4-absorption in channel 2. According to the definition of C the following expression is valid:

$$s_C = s_A + r_A \cdot s_B \tag{3.10}$$

s_A and s_B are the sought scaling factors. Due to the equilibrium condition, s_A and s_B can be found in the following relation:

$$r_A = \frac{s_A}{s_B} \tag{3.11}$$

¿From this it follows that:

$$s_A = \frac{r_A}{r_A - 1} \cdot s_C \tag{3.12}$$

and

$$s_B = \frac{r_A}{r_A(r_A - 1)} \cdot s_C \tag{3.13}$$

r_A is to be significantly larger than 1, meaning that the NO_2-concentration in the NO_2-reference and the NO_2-spectrum must be different.

3. Removal of the N_2O_4-absorption from the NO_2-spectrum and the NO_2-reference.

$$E = A - s_A \cdot D \tag{3.14}$$
$$G = B - r_B \cdot D \tag{3.15}$$

E and G content only the NO_2-absorption.

Chapter 4

Data-Aquisition / Data-Handling

4.1 Measurement-Procedure with GOME-2

Operating CATGAS starts with turning on the system and letting it stabilize for about two to seven hours depending on the desired temperature. Whether the system is stable or not, after the desired settings (gas flow, pressure in the vessel, temperature) are set, can be checked with the commercial spectrometer. Once stable conditions are reached the off-axis parabolic mirror No.2 (see figure 3.1) is removed and measurements with GOME-2 can be done. For a measurement with GOME-2 the following sequence was performed:

1. Measurement of first reference ⇒ vessel contains no gas of interest (O_3, NO_2)
2. Measurement of absorption measurements with gas of interest in the vessel
3. Measurement of second reference ⇒ vessel contains no gas of interest

Each measurement consisted of the following sub-steps: First the TTL-controlled flip-mirror was in a position, where the light going trough the vessel (signed as "VESSEL") was detected. In this position two measurements were taken by GOME-2. The flip-mirror switched then in a position, where the light coming directly from the Xe-lamp (signed as "DIRECT") could be monitored. Also two measurements were taken. Then the ratio VESSEL / DIRECT was build. This sequence was repeated three times. These "ratio-files" contain the mean value of these three pairs. The label gives reference to each measurement, containing information about mixture, temperature, date, time and type of measurement(O_3 or NO_2, reference or absorption):

ratio_2003-02-03_14_08_47_O3b1m1t203r_01.FPA-1.dat

These steps are provided by TPD. The data is in ascii-format and contains pixel number, wavelength, ratio average, ratio standard deviation, ratio max and min.

4.1.1 I_0-I Documentation

A further required procedure in preparation for measurements were the settings of the pixel exposure times (PET). For a linear response of the photodiodes the signal should not exceed 50.000 bu and should not fall below 3 % of this maximum value. The documentation of the light intensities in binary units therefore provides an additional technical quality check.

Table 4.1 shows exemplarily the light intensities in binary units for measurements with GOME-2 FM2-1 at 293 K. Column 1 gives the respective mixture, column 2 and 3 the regarding relevant channel and wavelength range. Column 4 and 5 contain the intensities in binary units for I_0 (reference) and I (absorption), respectively.

Regarding mixtures 6 to 8 there is additional information given. These particular wavelengths correspond to certain Hg-lines (253nm, 289nm, 296nm, 302nm) and are indicators for the quality of the spectra in comparison to the literature, especially at 253 nm. Therefore these information are included in the table.

The table is followed by graphical illustration of the intensities. The upper part of the respective figure shows the complete channel, the lower part a zoom of the actual corresponding, relevant wavelength range. Only the measurements at 293 K are given here as an example. Appendix B contains the complete documentation (tables and graphics) regarding the intensities at all temperatures and all FM's.

Mixture	**FPA**	λ **[nm]**	$\mathbf{I_0}$ **[bu]**	**I [bu]**
1	2	353 - 400	15000 - 18000	5000 - 17000
1	3	400 - 455	5000 - 15000	4000 - 8000
2	2	340 - 360	20000	5000 - 15000
2	3	430 - 490	10000 - 20000	8000 - 15000
3	2	310 - 345	5000 - 18000	2500(low c) - 15000(high c)
3	3	475 - 600	20000 - 33000	15000 - 5000
3	4	590 - 790	5000 - 27000	2000 - 15000
6	1	298 - 310	17000 - 5000	7000 - 2500
		Hg(302)	16000	7000
6	2	310 - 315	7000 - 22000	5000 - 13000
7	1	285 - 303	15000 - 28000	6000 - 25000
		Hg(289)	20000	10000
		Hg(296)	26000	20000
8	1	240 - 290	2000 - 20000	1800 - 19000
		Hg(253)	3000	2000

Table 4.1: Intensities in binary units for measurements with GOME-2 FM2-1 @ 293 K

Please note that this documentation is only given for O_3 measurements. One reason is the documentation in the UV region (especially at 253 nm, which is an indicator for the quality of the spectra), where the light intensity drops rapidly due to the properties of the Xe-lamp and the optics. In general, the handling, measurement and analysis of O_3 is more difficult and critical than NO_2 measurements.

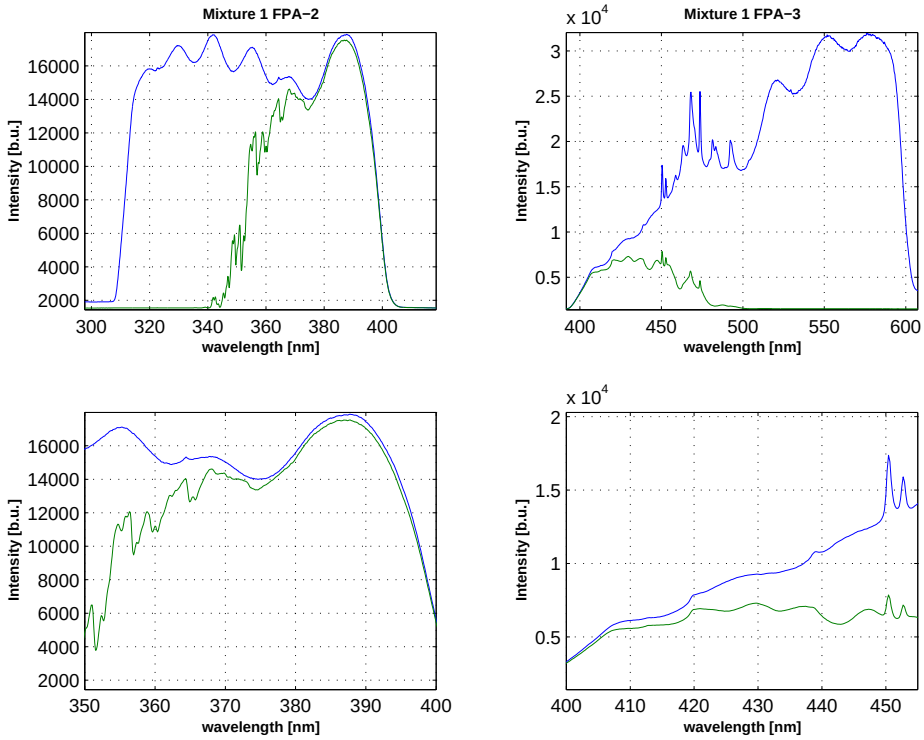

Figure 4.1: Intensities regarding mixture 1 measured with GOME-2 FM2-1 @ 293K. The lower graphics show the corresponding relevant wavelength range

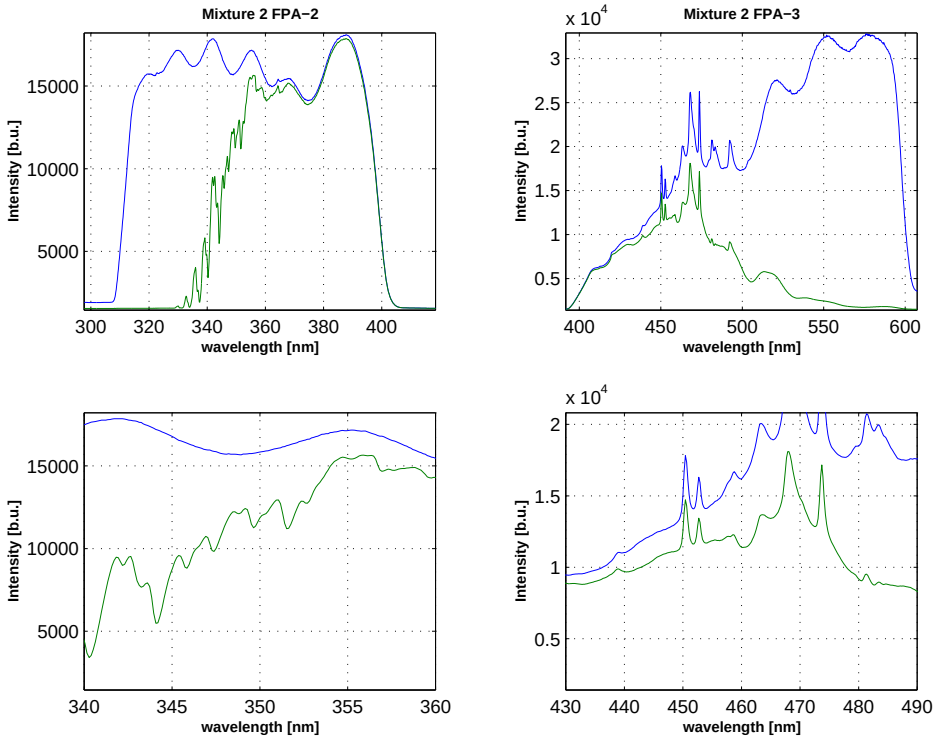

Figure 4.2: Intensities regarding mixture 2 measured with GOME-2 FM2-1 @ 293K. The lower graphics show the corresponding relevant wavelength range

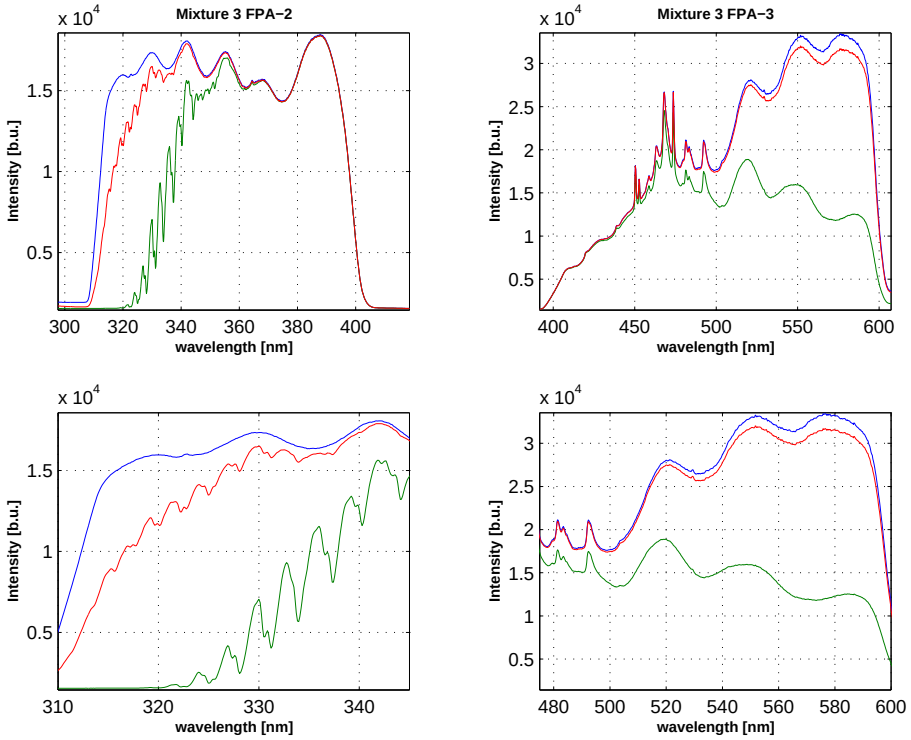

Figure 4.3: Intensities regarding mixture 3 measured with GOME-2 FM2-1 @ 293K. As described in the report mixture 3 corresponds to several measurements with slightly different concentrations. The red line shows the intensity with the lowest and the green line the highest concentration regarding mixture 3

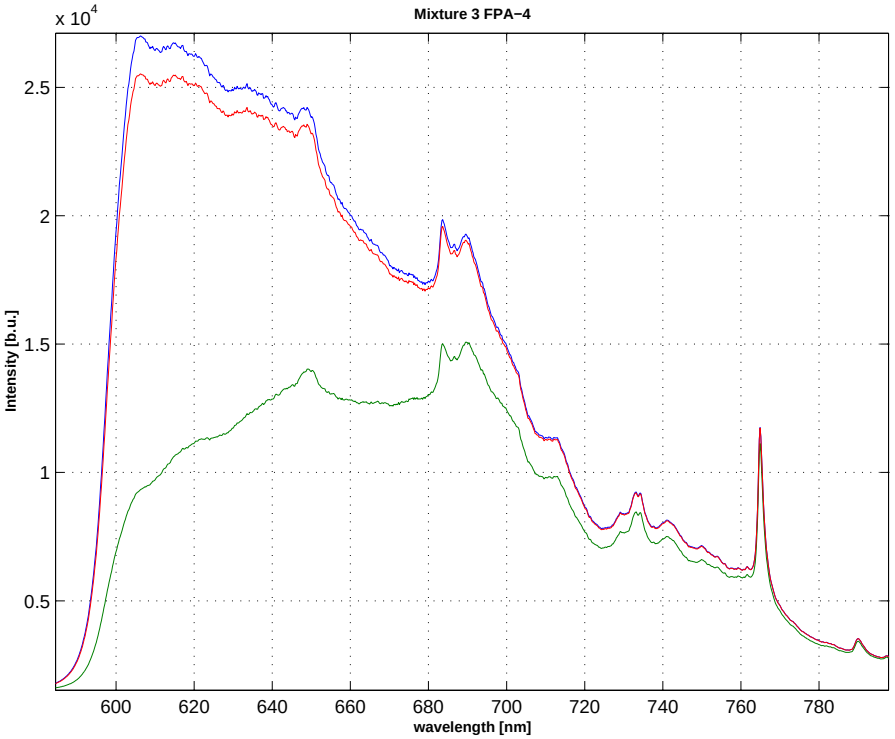

Figure 4.4: Intensities regarding mixture 3 in channel 4 measured with GOME-2 FM2-1 @ 293K.

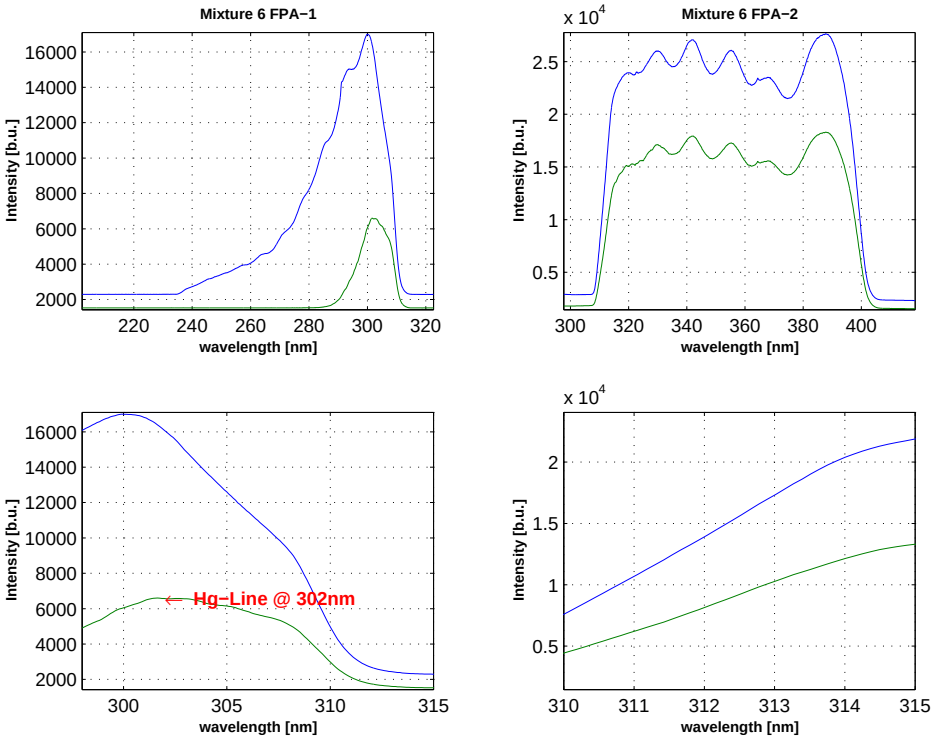

Figure 4.5: Intensities regarding mixture 6 measured with GOME-2 FM2-1 @ 293K. The lower graphics show the corresponding relevant wavelength range

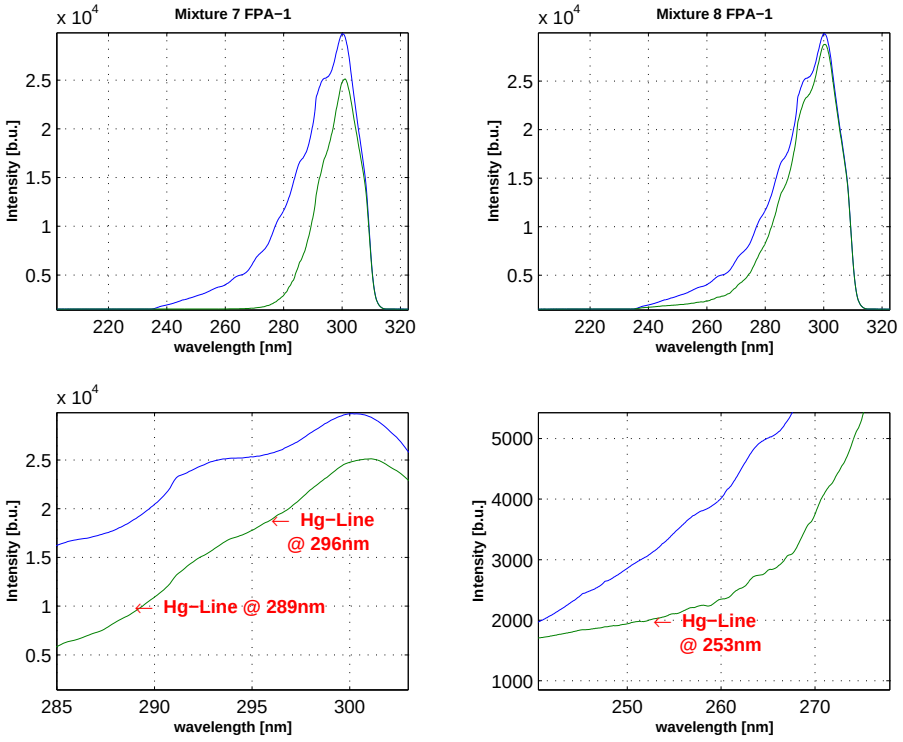

Figure 4.6: Intensities regarding mixture 7 and 8 measured with GOME-2 FM2-1 @ 293K. The lower graphics show the corresponding relevant wavelength range together with arrows indicating the location of Hg-Lines, where comparisons with literature data have been done.

4.2 Reference-Interpolation and Calculation of Optical Densities

With the ratio-files in ascii-format the following procedure is required. As described above a sequence starts with a reference measurement. In case of O_3-measurements this means that the cell is filled with pure O_2. That is followed by an absorption measurement, the vessel is now filled with an O_3 / O_2 mixture. After the absorption measurements the vessel is filled again with pure O_2 and another reference measurement is taken. The second reference measurement is required to characterize a baseline shift, meaning whether and how the optical property of the setup has changed. This can be expressed in terms of optical density by applying the natural logarithm to the ratio of both reference measurements:

$$\mathrm{OD_{Baseline}} = \ln\left(\frac{\mathrm{I_{0,1}}}{\mathrm{I_{0,2}}}\right) \tag{4.1}$$

Since a change is very likely the absorption measurements, or more precisely the reference measurements before and after the absorption measurements, need to be time-interpolated, before the optical density can be calculated by applying Lambert-Beer's law.

The assumption is made that the optical property changes linearly, therefore a linear time-interpolation is applied. May

$$\mathrm{OD_{Ref1}} = \ln\left(\frac{\mathrm{I_{0,1}}}{\mathrm{I_{LM,0,1}}}\right) \qquad \text{and} \qquad \mathrm{OD_{Ref2}} = \ln\left(\frac{\mathrm{I_{0,2}}}{\mathrm{I_{LM,0,2}}}\right) \tag{4.2}$$

be the reference-measurements at times t_1 and t_2 before and after an absorption measurement at time t_i. The first step is to find the time-interpolated reference at time t_i, on which together with the absorption measurement at time t_i the Lambert-Beer law can be applied. The interpolated reference can be obtained by the following equation:

$$\mathrm{OD_{Ref_i}} = \mathrm{OD_{Ref_1}} \cdot \left(\frac{\mathrm{t_2 - t_i}}{\mathrm{t_2 - t_1}}\right) + \mathrm{OD_{Ref_2}} \cdot \left(\frac{\mathrm{t_i - t_1}}{\mathrm{t_2 - t_1}}\right) \tag{4.3}$$

This leads to Lambert-Beer:

$$\mathrm{OD} = \ln\left(\frac{\mathrm{I_{0,i}}}{\mathrm{I_{LM,0,i}}} \cdot \frac{\mathrm{I_{A,i}}}{\mathrm{I_{LM,A,i}}}\right) = \mathrm{OD_{Ref_i}} + \mathrm{OD_{Abs_i}} \tag{4.4}$$

This sequence is also illustrated in figure 4.7 and consists of 12 single operations. We have developed a software package for automation of this procedure. The software tool is started in a prepared directory and goes then through the subdirectories and calculates automatically the baselines and optical densities (figure 4.8), with which the actual compounding of the spectra can be started, at least for O_3. The NO_2-measurements are still superimposed with an absorption spectrum of the dimer N_2O_4. This has to be separated first, which was described in chapter 3.4.3.

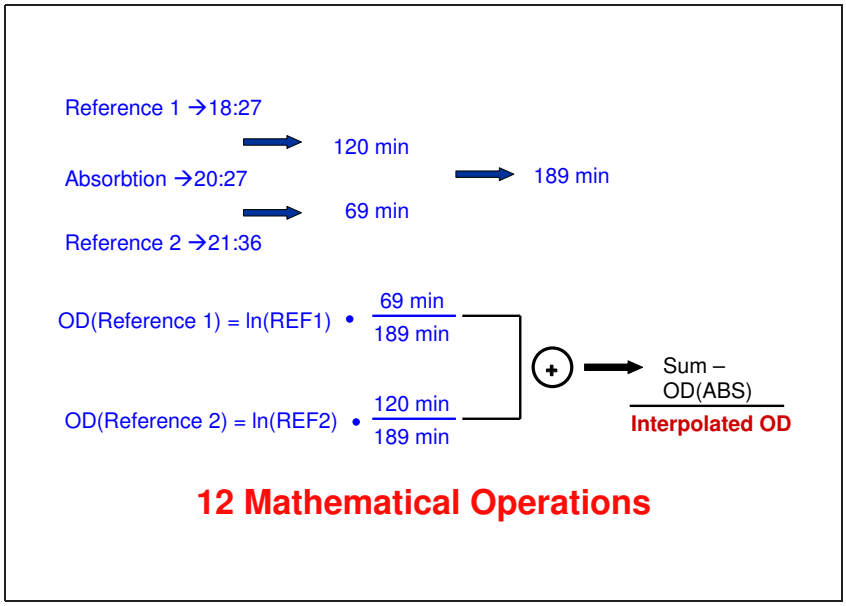

Figure 4.7: Calculation of time-interpolated optical density

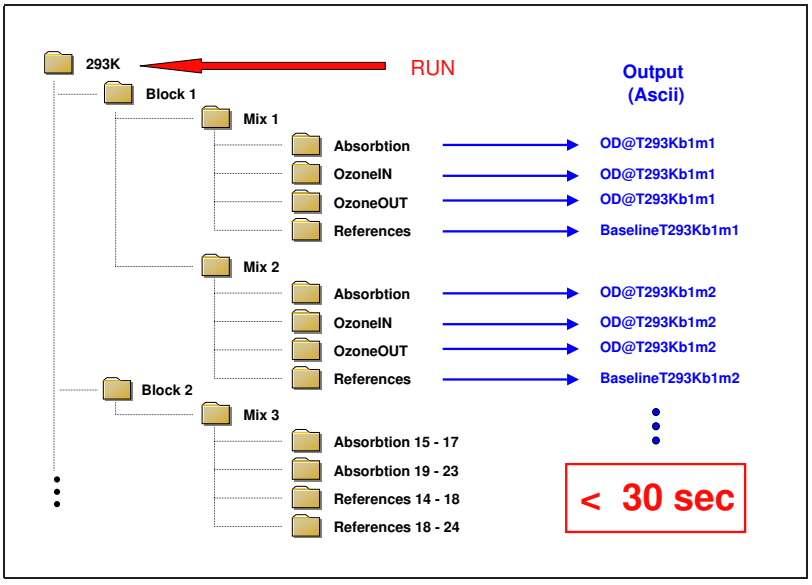

Figure 4.8: Directory-structure and application of software tool

4.3 Compounding a Spectrum

In this section we want to describe the method and procedure we have applied for compounding the certain parts of the spectra to one spectrum. As an example we use the O_3-measurements at 293 K, the basic principle is valid for the NO_2 spectra as well.
The gluing has been done manually using the scientific software origin, the description of the specific projects is given in section 4.4.

An optical density between ~ 0.1 and 1 is assumed to be optimal in the O_3 measurements, in this range the pixel response is expected to be linear. Therefore the gluing of two measurements is to be done in an overlapping region, where both measurements fulfill this requirement. It can be stated though that optical densities of up to 2.5 showed also good results due to the high linearity of the GOME-2 instruments.

The starting point is a measurement, where the optical density at 576.96nm (Hg-Line) in channel 3 is around 1, which is usually the case with experimental settings referring to mixture 3 (table 3.1). This measurement is then as a first approximation scaled to 0.0477, representing the average absorption cross section (in units of 10^{-19}cm^2)[1] at 298 +/- 5K, as given in the "Critical Review of the Absorption Cross-Sections of O_3 in the 240 - 790 nm Region" by Johannes Orphal [1]. This step is illustrated in Figure 4.9.

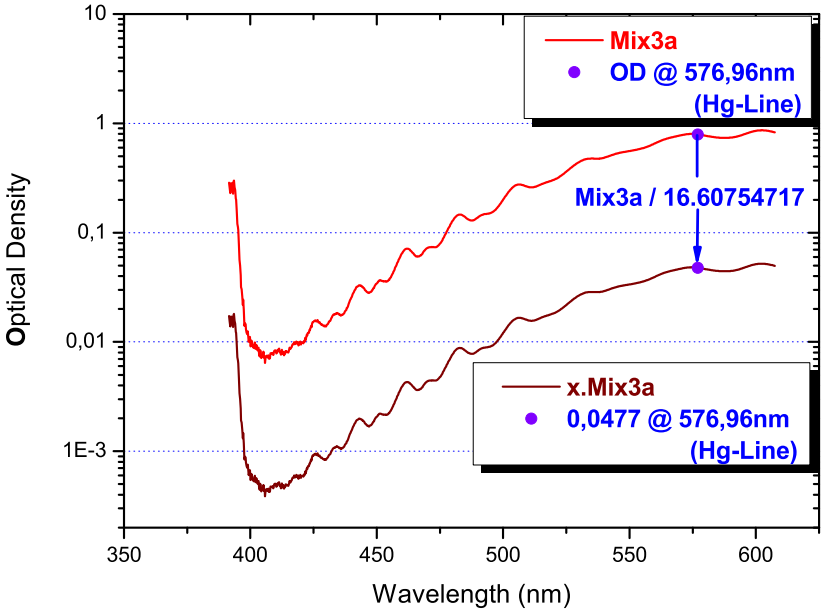

Figure 4.9: Initial scaling @ 576.96nm (Hg-line)

One advantage of measurements with the GOME-2 spectrometer is the simultaneous coverage of the Chappuis band and parts of the Huggins band.

[1] In [1], page 43, Table 6-11 the unit for this point is erroneously given in 10^{-20}cm^2

The same scaling factor is therefore then transferred to channel 2 of the same measurement, covering a part of the Huggins bands (figure 4.10).

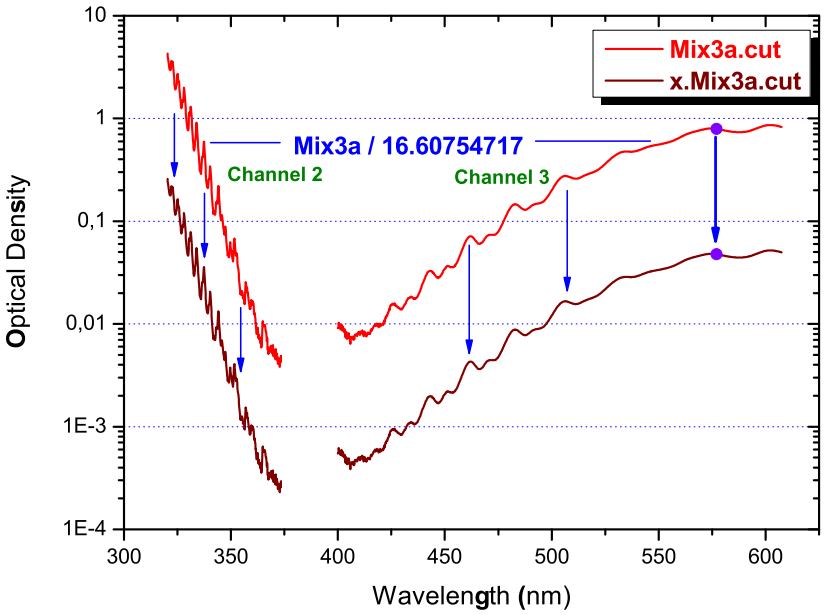

Figure 4.10: Equal scaling factor of the same measurement in channel 2

According to the current scientific state the temperature dependence in the peaks of the Chappuis band is not expected to be larger than 1 %. The initial scaling itself does not influence the compounding itself but will allow a first estimation about the quality of the spectra by, for instance, checking the temperature dependence in the Hartley band. It is therefore important to note that this doesn't necessarily have to be the final scaling to absolute absorption cross sections.

In order to compound now another measurement to mixture 3, in an initial step a wavelength window is defined, in which both mixtures meet the requirement to have optical densities between 0.1 and 1. For this purpose the original optical densities are plotted in one plot. An example is given in 4.11. In the same plot also the scaled measurement 3a, as seen in figure 4.10, is given (labelled as **x**.Mix3x).
One can see that an optimal overlapping region between mixture 2 and 3a is given mainly in the wavelength range 475 to 500 nm. Therefore the next step would then be to scale mixture 2 to the scaled mixture 3a in a way that in this range the congruence between both measurements is as good as possible. The congruence between both measurements in the overlap region can then be verified with the ratio between both measurements. Based on the ratio it can then be decided where to finally cut the measurement and concatenate to the other (figures 4.12 to 4.14).

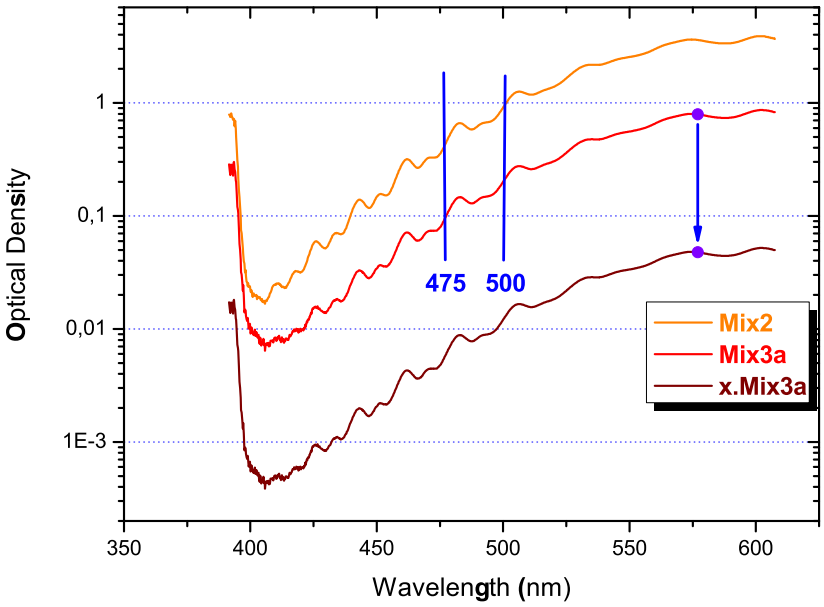

Figure 4.11: Compounding of two mixtures

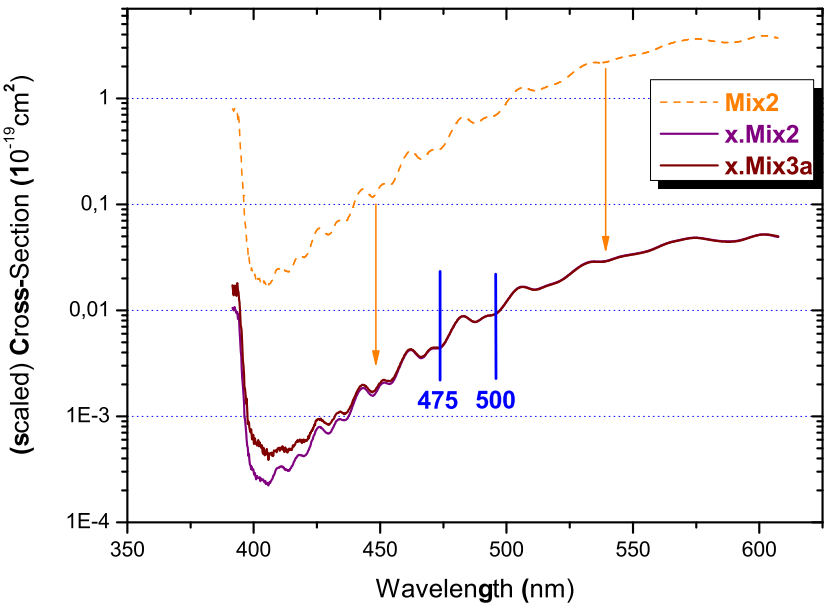

Figure 4.12: Scaling of two measurements in optimal overlap region

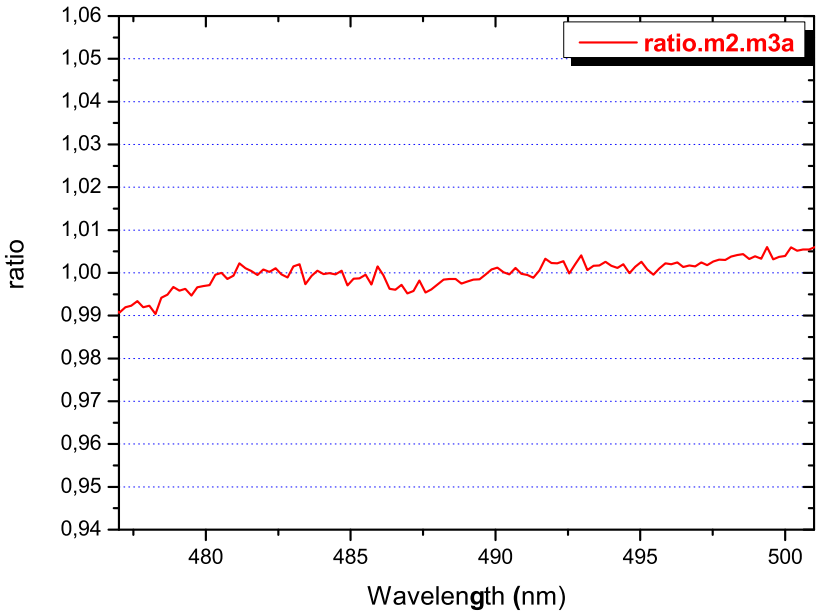

Figure 4.13: Ratio between two measurements in the overlap

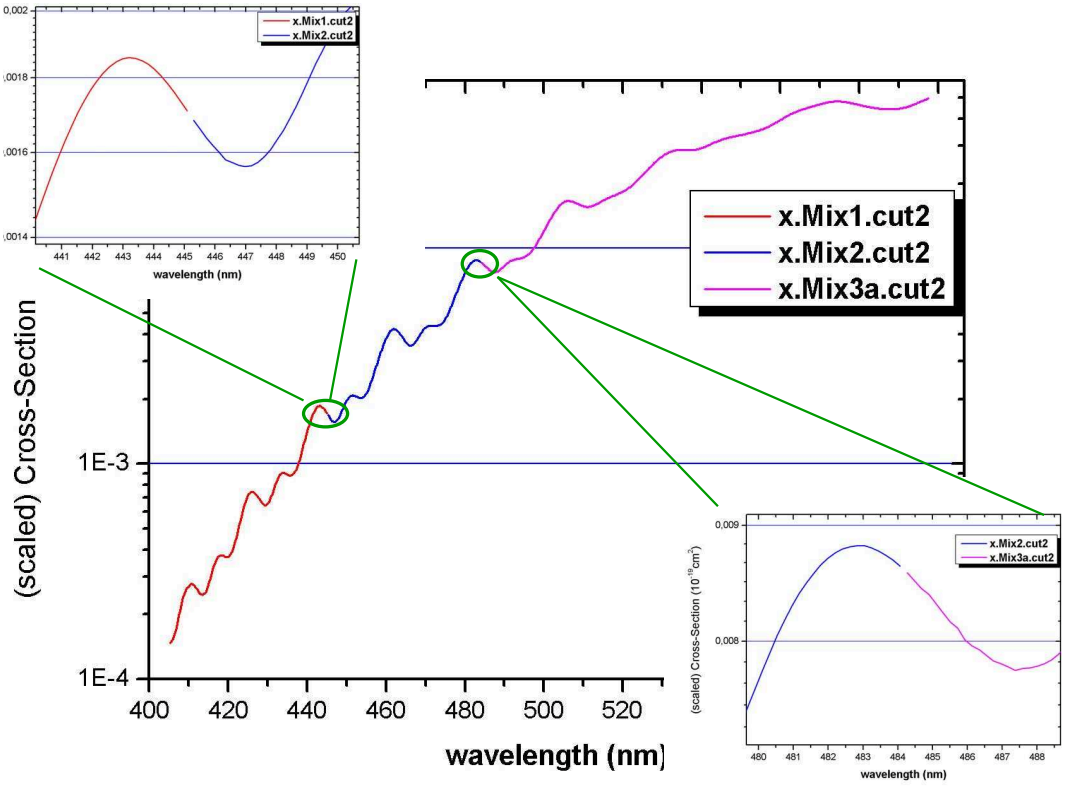

Figure 4.14: Concatenation of different measurements in channel 3

4.3.1 Quality analysis of overlap region

An overlap region between two measurements is, as mentioned above, in principle defined by the wavelength range, where both measurements have an optical density between 0.1 and ≈ 1.5. Some ratios show however that even regions with higher OD can be used. A final decision regarding the gluing was therefore not only based on an optimal density but also on the ratio.

In an optimal case the ratio is horizontal around 1 in the corresponding wavelength range. Figure 4.15 illustrates such a ratio between mixture 6 and 7 in channel 1 at 243K. The left part around 295nm corresponds to an optical density of mixture 6 of about 2.5. Also included in the graphics is the mean value with the standard deviation in the certain wavelength window. Both the mean value and the standard deviation in the overlap region can therefore be used as a quality criteria.

In appendix A a table listing of gluing points, overlap region and quality criteria by the above mentioned parameters is given for every gluing point. In general the standard deviation is smaller than 1%, only for the measurements at 223K it amounts about 1.2%.

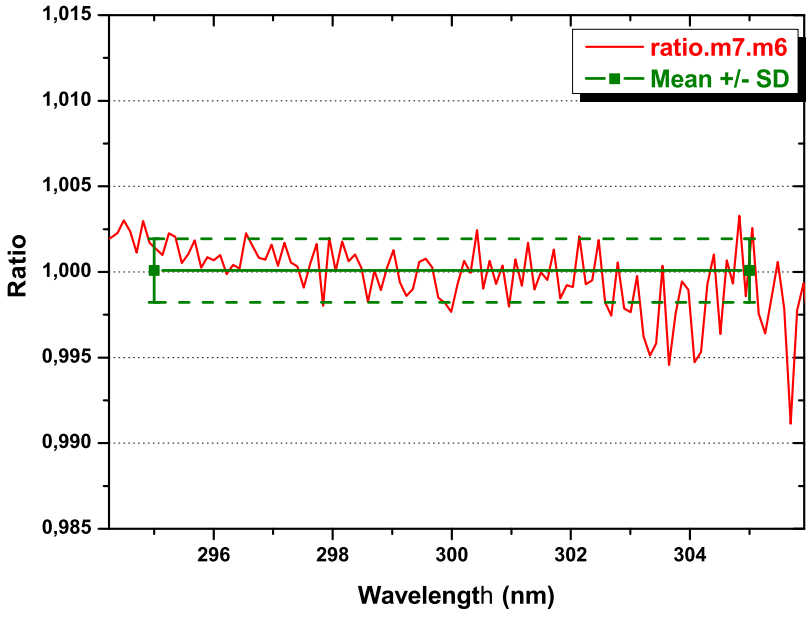

Figure 4.15: Ratio between two "scaled" measurements corresponding to mixture 6 and 7 in Channel 1 (GOME-2 FM3 @ 243 K).

4.4 Origin-Projects

4.4.1 Data

The data handling after the optical densities were calculated was done with the scientific software origin. The description of the certain projects, the labels of the worksheets, graphics, etc. is topic of this chapter. As an example still the O_3-measurements (measured with FM3) are used. In a first step a new project is started and named in the following way: **"GOME-2_FM3_O3_[Temperature]_Data"**. For the data at 293K measured with GOME-2 FM3 this leads to:
"GOME-2_FM3_O3_T293K_Data".

In this project the relevant data, meaning the reference interpolated and calculated optical densities are imported in respective subfolders and origin-worksheets. Not every mixture is useful for every channel. For the O_3 analysis usually the following mixtures are imported:

Channel 1: Mixture 6 - 8
Channel 2: Mixture 1 - 6
Channel 3: Mixture 1 - 3
Channel 4: Mixture 3

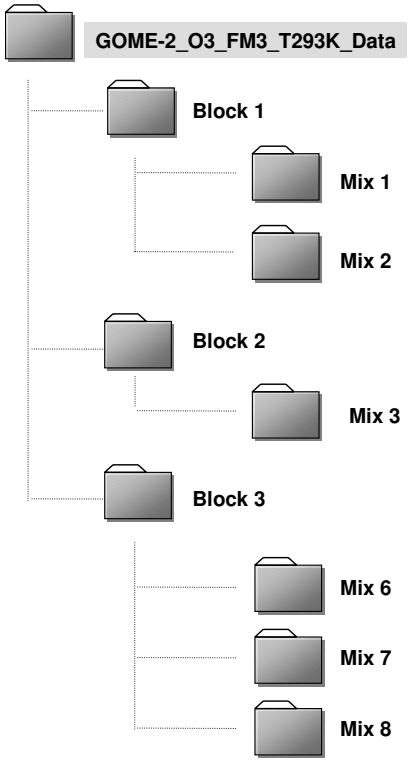

Figure 4.16: Origin-Project "Data"

The project itself contains several subfolders named Block1, Block2, Block3, which in itself consists of several folders as well, named by the mixtures. The directory structure in such a project is therefore as in figure 4.16. The NO_2-projects differ only slightly: The subdirectories are not divided into blocks but only into mixtures and the project has also (besides "Data") a further subdirectory labelled as "[Temperature]_Eisinger_corrected_data", which contains the worksheets from the N_2O_4-correction.

The certain subfolders contain worksheets which are labelled as follows:
"T293Km8c1" for instance contains the information:

- T293K ... Temperature 293K
- m8 ... Mixture 8
- c1 ... Channel 1

Additional information is given for worksheets of mixture 1 and 2 in the O_3 projects:

- O3IN ... Optical densities during the time period, when O_3 was filled in the vessel
- O3OUT ... Optical densities during the time period, when O_3 was evacuated
- ABS ... Actual absorption measurement, corresponds usually to the last measurement of O3IN

The columns are named as follows:

- LambdaCh1 ... Wavelength channel 1
- Mix8 ... Column contains the optical densities corresponding to mixture 8
- Mix8.cut ... A first cut version of column mix8, where parts with saturation or bad signal to noise have been cleared in the worksheet

4.4.2 Spectra

With the imported data the project is saved as **"GOME-2_FM3_O3_T293K_Spectrum"**. That means we have two separate projects containing the data. Not only is this a safety back up, but also simplifies the trouble shooting in case of need. It was part of our philosophy during the analysis that with every new operation a new project, file, worksheet or column would be created. In this way a permanent check up would be given (for instance after "copy" and "paste" actions) and, in case of errors, it could be easily gone back one step in the procedure.

In the new project a subfolder is created named "Spectra", in which the actual compounding was done in separate files, which are named by the channel. Every "Channel"-file itself contains also folders regarding the compounding of two measurements. These are named "Overlap_[Mixture]_[Mixture]". Figure 4.17 illustrates the directory structure in the "Spectrum"-project.

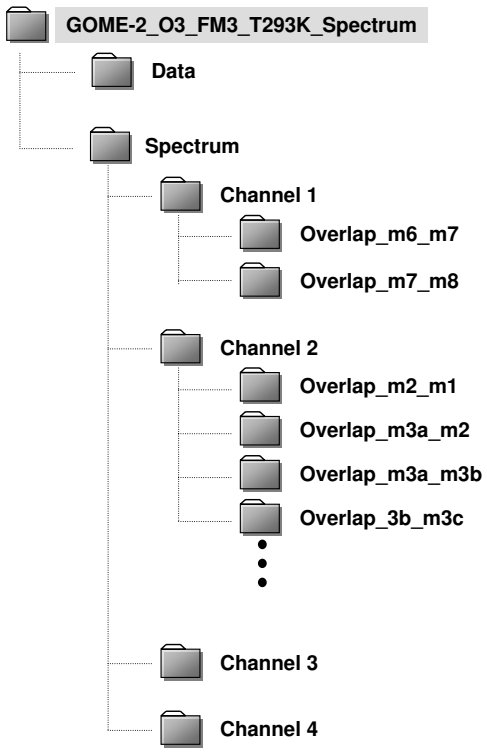

Figure 4.17: Origin-Project "Spectrum"

The content in the certain files are as follows:

- **"Spectrum"**
  - **Channel 1:**
    - **Worksheet "T293c1" (Temperature 293 K Channel 1)**
      This worksheet contains initially the columns "LambdaCh1", "Mix8.cut", "Mix7.cut", "Mix6.cut", which are imported from the "Data"-file. During the analysis procedure this is then added by further columns, for example like

x.Mix8.cut	...	scaled version of Mix8.cut
x.Mix8.cut2	...	final cut version
x.Mix7.cut	...	scaled version of Mix7.cut
...		

The following table illustrates this form:

LambdaCh1	**Mix8.cut**	**x.Mix8.cut**	**x.Mix8.cut2**	...
:	:	:	:	...
288,2141	0,20928	16,90148	16,90148	...
288,3226	0,20701	16,69759	16,69759	...
288,4312	0,20485	16,52362	-	...
:	:	:	:	...

* **Subfolder "Overlap_m7_m8"** This subfolder contains the information regarding the compounding of mixture 7 and mixture 8. It includes the following worksheet and graphics:
  - `Worksheet "Ratm8m7c1 - Ratio x.Mix8.cut / x.Mix7.cut - Channel 1"`

LambdaCh1	**x.Mix8.cut**	**x.Mix7.cut**	**ratio.m8.m7**
:	:	:	:
288,2141	16,89944	16,90148	0,99988
288,3226	16,71632	16,69759	1,00112
288,4312	16,54128	16,52362	1,00107
:	:	:	:

  - `Graphics "T293Km7m8c1"`
    Shows the initial optical densities *without* scaling, important for validating the overlap in the proper wavelength range

  - `Graphics "Overlapm7m8c1 - Scaled data x.Mix7.cut and x.Mix8.cut - Channel 1"`
    Shows the *scaled* optical densities of both mixtures, in this case mixture 7 and 8.

  - `Graphics "GrRatm7m8c1 - Ratio x.Mix7.cut / x.Mix8.cut - Channel1"`
    Shows the ratio between mixture 7 and 8, mainly in the overlapping region.

It is likewise as described above for the certain "Channel"-files and its subfolders. Once the individual gluing has been done, the certain parts have to be concatenated to the overall spectrum. The file "Spectrum" consists therefore, beside the certain subdirectories, of the following worksheets:

– **Worksheet "cut2c1" ... "cut2c4":** When the data have been scaled and cut to the final state (labelled by "cut2"), they have been copied in an extra worksheet. This also gives at the same time a chance for a validation-check:

The following table illustrates this form:

LambdaCh1	x.Mix8.cut2	x.Mix7.cut2	x.Mix6.cut2
:	:	:	:
288,2141	16,89944	–	–
288,3226	16,71632	–	–
288,4312	–	16,52362	–
288,5397	–	16,37435	–
:	:	:	:
300,5292	–	3,60879	–
300,6368	–	3,56429	–
300,7444	–	–	3,51657
300,8521	–	–	3,456

– **Worksheet "FM3T293K"** Contains finally the overall spectra in just one column. The column named `"sigma.T293K.FM3"` is the spectrum divided by 10^{-19}, representing the absorption cross section in units of cm^2.

wavelength	T293K	sigma.T293K.FM3
:	:	:
306,8737	1,57052	1,57052E-19
306,9811	1,53816	1,53816E-19
:	:	:

4.4.3 Baselines

The origin-project **"Baselines(T)_FM2-1.OPJ"** contains the baselines at all temperatures and mixtures. The directory structure is similar to the one in the data-projects. The worksheets are named as "[Temperature][Block][Mixture]" (only "[Temperature][Mixture]" for NO_2 respectively) and contains all 4 channels with the baselines:

LambdaCh1	BaselineCh1	LambdaCh2	BaselineCh2	...
:	:	:	:	...
288,2141	0,00193	375,4274	0,0021	...
288,3226	0,00268	375,544	0,0021	...
288,4312	0,00238	375,6605	0,00221	...
:	:	:	:	...

The graphics are labelled as "Gr[Temperature][Block][Mixture]" and show the baseline shift in all 4 channels. Figure 4.18 shows exemplary the baseline shift for "GrT293Kb3m7" (measured with FM3):

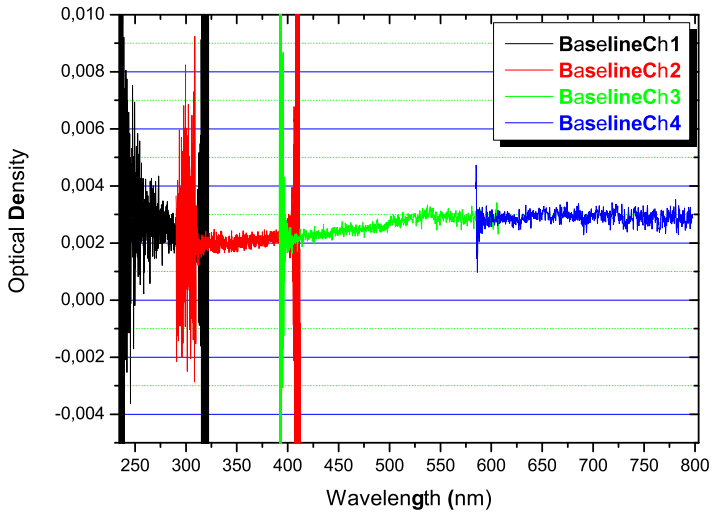

Figure 4.18: Exemplary baseline for mixture 7 at 293K

The baseline stability is in general (60-70 % of all measurements) better than 0.5 %, especially for the mixtures 6 to 8. In measurements regarding mixture 1, where the references before and after the absorption measurements have been taken in a time distance of up to 4 hours, the baseline stability is still better than 2 %, usually around 1 %. Very rarely ($\approx$ 10 % of all measurements the) we could see a baseline shift larger than 2 %, however in general not more than 3.5 %.

4.5 Error Analysis and Propagation

As a general measure of the error present in the individual recorded spectra of optical density the baselines have to be analysed. They contain a systematic error as a more or less long term drift across all four channels and statistical noise superimposed to that.

The systematic error is of the order of 0.001 to 0.005 (”50 % of measurements), around 0.01 to 0.02 (30-40% of measurements) and 0.02 to 0.04 (remaining 10-20% of measurements). All errors in units of optical density. By interpolation of references between the first and last reference measurement, the systematic error can be partly eliminated from the determined spectra of optical density. This elimination is the better, the closer the true temporal behaviour of observed drift - i.e. the observed systematic error is to being linear in time. Based on this it is well justified to estimate this error for the majority of measurements (80-90%) to be of the order of 10^{-3} or even better. The remaining 10-20% of measurements could have larger systematic errors of some 10^{-2}.

The statistical error, i.e. the noise on the calculated optical densities, is much smaller. It is determined by firstly removing the systematic error by subtracting a polynomial and secondly determination of the standard deviation of the resulting noise within each channel. The statistical error varies from $2 \cdot 10^{-3}$ in the left (”blue”) half of channel 1 to $4.9 \cdot 10^{-4}$ in the right (red) half of channel 1. In the remaining channels 2,3 and 4 it takes on values of $1.6 \cdot 10^{-4}$, $1.4 \cdot 10^{-4}$, and $1.8 \cdot 10^{-4}$ respectively (all in units of optical density).

Both errors have to be put into perspective to the selected optimal range of optical density of 0.1 to 1.0 (O_3) and 0.1 to 0.5 (NO2). The dominant contribution results from the systematic error limiting the error of the final product, the spectrum. With 80-90% of measurements having a systematic error of the order of a few 10^{-3} or even better and a minimum signal of 0.1 optical density the final error of these measurements is of the order of some 10^{-2} meeting the required accuracy of 3%. As pointed out in the proposal to this study, the error will be larger wherever the maximum optical density reached in the experiment is smaller than 0.1. In such regions the resulting error will be above 3%.

Apart from this more general statement, the error propagation was also determined for each spectrum yielding a relative error, see next chapter. The initial error measure of peak to peak variation within three subsequently measured ratios is crude and therefore results in a number of cases into relative errors, which are larger than the demanded 3%. Due to the crude initial error measure the relative error determined in 5.1 rather defines an upper limit of error.

• Error Propagation

As described in chapter 4.2 the initial point of calculating optical densities and absolute absorption cross sections are the ratio-files provided by TPD (see chapter 4.1). These files contain the following information: Pixel number, wavelength, ratio average, ratio standard deviation, ratio max and min. Figure 4.7 illustrates the mathematical operations required for the calculation of a time-interpolated optical density. The error can be estimated in the following way:

Originally there are three ratio files from three measurements:

- Reference R_1, ΔR_1
- Absorption A, ΔA
- Reference R_2, ΔR_2

with Δ = ratio_max - ratio_min. May t_1 be the time between R_1 and A, t_2 the time between A and R_2 and t_{Total} the time between R_1 and R_2. As illustrated in Figure 4.7 the first term of the sum is given by:

$$\text{OD}(R_1) = \ln R_1 \cdot \frac{t_2}{t_{\text{Total}}} \tag{4.5}$$

The uncertainty can be estimated via the standard propagation of errors:

$$\Delta\text{OD}(R_1) = \sqrt{\left(\frac{t_2}{t_{\text{Total}}} \cdot \frac{\Delta R_1}{R_1}\right)^2 + \left(\frac{\ln R_1}{t_{\text{Total}}}\Delta t\right)^2 + \left(\frac{t_2 \cdot \ln R_1}{(t_{\text{Total}})^2}\Delta t\right)^2} \tag{4.6}$$

The calculation for the second term is likewise, only t_2 is replaced by t_1 and R_1 by R_2. The final time-interpolated optical density OD is given by:

$$\text{OD} = \text{OD}(R_1) + \text{OD}(R_2) - \text{OD}(A) \tag{4.7}$$

Accordingly the error can be estimated by:

$$\Delta\text{OD} = \sqrt{\Delta\text{OD}(R_1)^2 + \Delta\text{OD}(R_2)^2 + \Delta\text{OD}(A)^2} \tag{4.8}$$

The same way is applied when the optical densities are scaled to absolute absorption cross sections:

$$\sigma = OD \cdot c \tag{4.9}$$

$$\Delta\sigma = \sqrt{(\text{c}\Delta\text{OD})^2 + (\text{OD}\Delta\text{c})^2} \tag{4.10}$$

The results of the achieved absorption spectra with GOME-2 will be discussed in detail in chapter 5. However a brief outlook may be given at this place. Figure 4.19 shows ratios of the O_3 absorption spectra at ambient temperature between different FM's in comparison with the statistical error. One can see a good agreement between the FM's, especially in the Hartley and Chappuis band, and furthermore a consistency with the estimated statistical errors. Note that the ratio of two data sets with 1-2 % accuracy each can produce uncertainties of 3-4 %. The larger deviations in the Huggins bands between 310 and 360 nm is mainly caused by differences in the wavelength axis. This will be discussed in detail in chapter 5.4

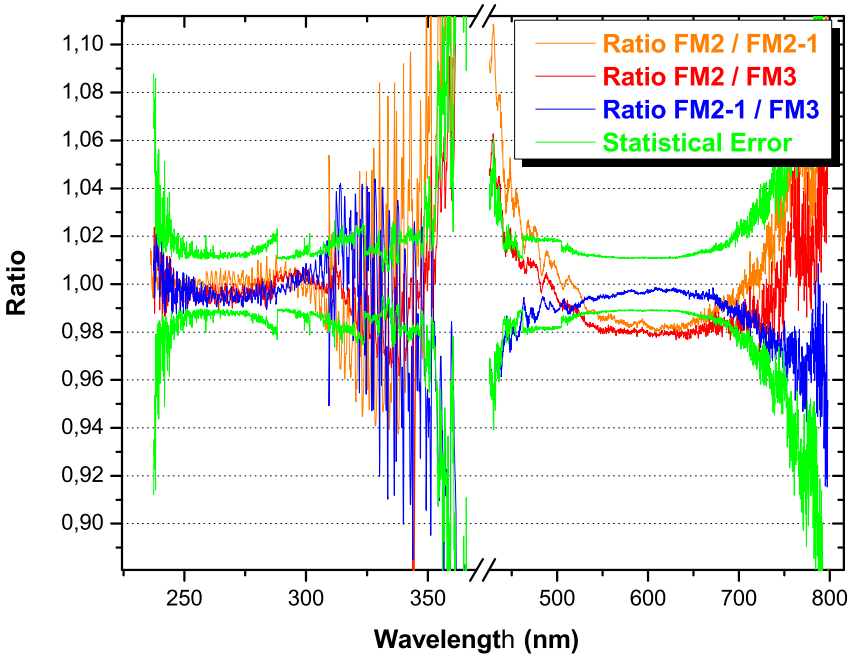

Figure 4.19: Ratios of the O_3 absorption spectra at ambient temperature between different FM's in comparison with the statistical error

Chapter 5

Results for FM's & Comparison of Results

In this chapter we will present the obtained results from the GOME-2 study for the individual flight models (FM's) and also the comparison between the FM's. As mentioned before, measurements have been performed with three FM's: FM2, FM2-1 (a refurbished version of FM2) and FM3.

The individual sections regarding the O_3 and NO_2 measurements will contain discussions about temperature dependence and comparison with literature. Furthermore it will be described, how the relative measurements have been scaled to absolute absorption spectra.

- We will first discuss the achieved absorption spectra of the O_3 measurements (section 5.1), which have been measured at five different temperatures, i.e. 293 K, 273 K, 243 K, 223 K and 203 K.
- The results and discussion regarding the obtained NO_2 absorption spectra will be topic in section 5.2. NO_2 measurements have been taken at four different temperatures, i.e. 293 K, 273 K, 243 K and 223 K.
- Section 5.3 contains the results of the O_2 measurements at ambient temperature.
- Also part of this chapter is the wavelength calibration, which will be presented in section 5.4.
- One goal of the comparative study was the investigation of a potentially new approach regarding compounding a spectrum and data analysis for future studies by using a Least-Square-Method. The results of this investigation are topic of section 5.5.
- The chapter will then finally be closed by giving a short format description of the delivered absorption spectra in ascii format.

5.1 O_3 Absorption Cross Sections

In this section we will discuss the O_3 absorption spectra obtained in this study. First, we will investigate the relative temperature dependence of relative spectra and compare the results with previous measurements of absolute absorption cross sections given in the literature.

Following that we will describe the method of scaling the relative spectra to absolute absorption cross sections, which will base on the results of the foregoing part. Finally we will again compare the scaled absorption spectra of this study with data given in the literature. Included in this section is furthermore the comparison of the results between the FM's.

5.1.1 Determination of relative temperature dependence

A critical issue in determining the temperature dependence of O_3 absorption cross sections from relative spectra is how to avoid dependence of the desired result from previous data. This can be achieved through integrated absorption cross sections. Molecular absorption cross sections that are integrated over entire electronic transitions present two main advantages in comparison to measurements at single wavelengths: Firstly they are nearly independent of temperature (which has been observed for O_3, NO_2, BrO, OClO, H_2CO) because of the Born-Oppenheimer principle. This separates electronic and nuclear motion (e.g. ref. [8]) and thereby allows to assume constant electronic transition moment between the ro-vibrational states involved, which in turn justifies the assumption on integrated cross section being independent of temperature. Secondly integrated cross sections are much less sensitive to instrumental effects such as spectral resolution or accuracy of wavelength calibration.

Therefore relative spectra, which were recorded at different temperatures and which are normalized to unity integrated optical density (integration across all bands of an electronic transition), will directly be placed on a common scale, which provides correct relative temperature dependence among them. Dividing the series of spectra at different temperatures by one spectrum at an arbitrarily chosen reference temperature, yields the temperature dependence relative to the chosen one. The GOME-2 spectra were normalized in the described way based on the sum of two integration regions from 245 to 340 nm and from 410 to 690 nm. This covers the Hartley, Huggins and Chappuis bands and is the best available approximation to the requirement that full electronic bands have to be covered.

¿From the in this way scaled relative spectra the relative temperature dependence of the O_3 absorption spectrum was determined at selected wavelengths, where a large number of reference data for determination of absolute absorption cross section as a function of wavelength is available from literature, see [1] and references therein, and [9]. This included wavelengths 253.65 nm, 289.36 nm, 296.73 nm, 302.15 nm, 334.15 nm and 604.61 nm with special focus on the latter one. In the 400 to 450 nm region the differential structure of the relative absorption cross section spectra was determined by subtracting a suitable polynomial of 2nd or 3rd order following the procedure well known from the analysis of atmospheric remote sensing data as zenith sky measurements or Differential Optical Absorption Spectroscopy DOAS [10, 11] and references therein. Thereby variations of any background absorption, which could possibly be present in the

data, are suppressed and the relative temperature dependence of differential absorption cross section can be determined. Finally the relative temperature dependence for all wavelengths was determined by fitting a suitable polynomial to the found variation of cross section at each wavelength.

5.1.2 Relative temperature dependence at selected single wavelengths

In the past several measurements of absorption cross sections have been performed at single wavelength as well as over large spectral regions (e.g. [12, 13, 14, 15, 16, 17]). From this data relative temperature dependence was determined and compared to that obtained from our relative spectra, which - by the described normalization to integrated optical density - nevertheless display the correct relative temperature dependence among them.

Figure 5.1 shows the relative temperature dependence of the O_3 cross section at 253.65 nm as observed in previous measurements [12, 13, 14, 15, 16] compared to those obtained from the three GOME-2 campaigns.

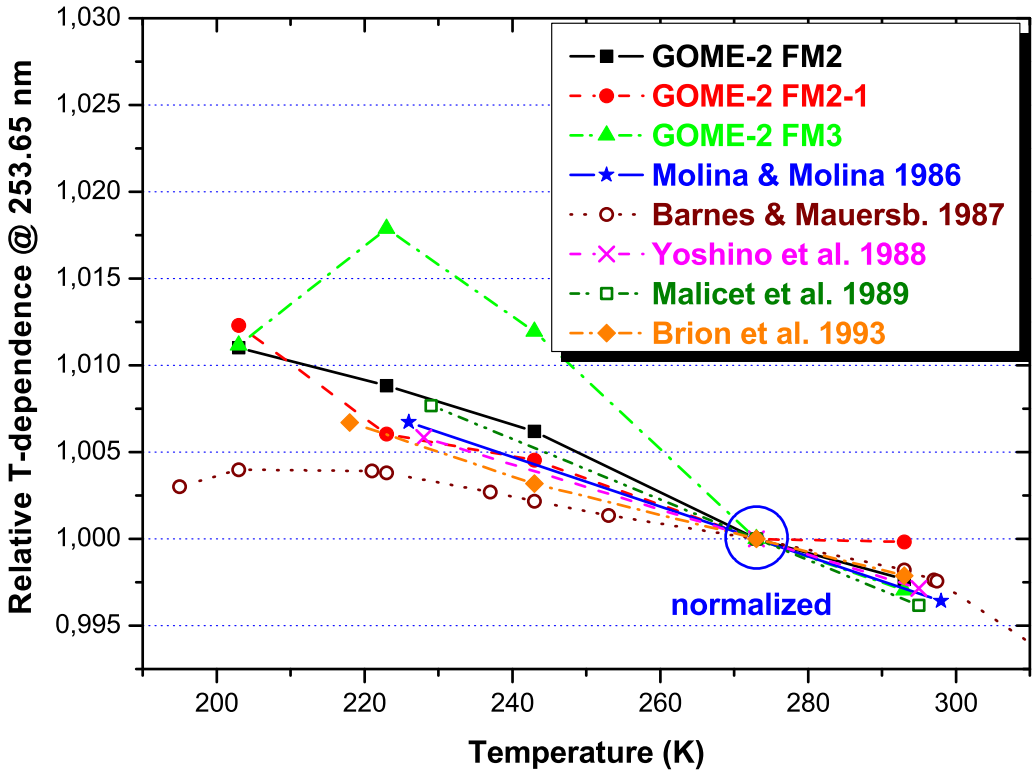

Figure 5.1: Relative temperature dependence of the O_3 cross section at 253.65 nm

Even though by some authors the data by Molina & Molina [12] is considered as overes-

timating the true absolute cross section, it is nevertheless considered for relative temperature dependence based on the notion that the relative scaling of the spectra is correct. This is supported by the following figures 5.2 to 5.5. The reference data at 253.65 show an increase of about 1 % with temperature decreasing from 293 K to 203 K. The temperature dependences obtained in this study agree well with the observed behavior while yielding a slightly larger increase with temperature. The data from the GOME-2 FM3 campaign shows a large deviation at 223 and 243 K, which is most likely due to the signal to noise ratio, which was significantly poorer in these particular measurements (combination 8 in Table 3.1).

A previous comparison of literature data in ref. [1] showed the appearance of a crossing point around 260 nm, where the temperature dependence changes its direction. In agreement with that, our data at 289.36 nm, 296.73 nm, 302.15 nm, and 334.15 nm show a clear decrease of the O_3 absorption cross sections with decreasing temperature, while the magnitude of the temperature dependence increases up to 10 %. This is illustrated in figures 5.2 to 5.5.

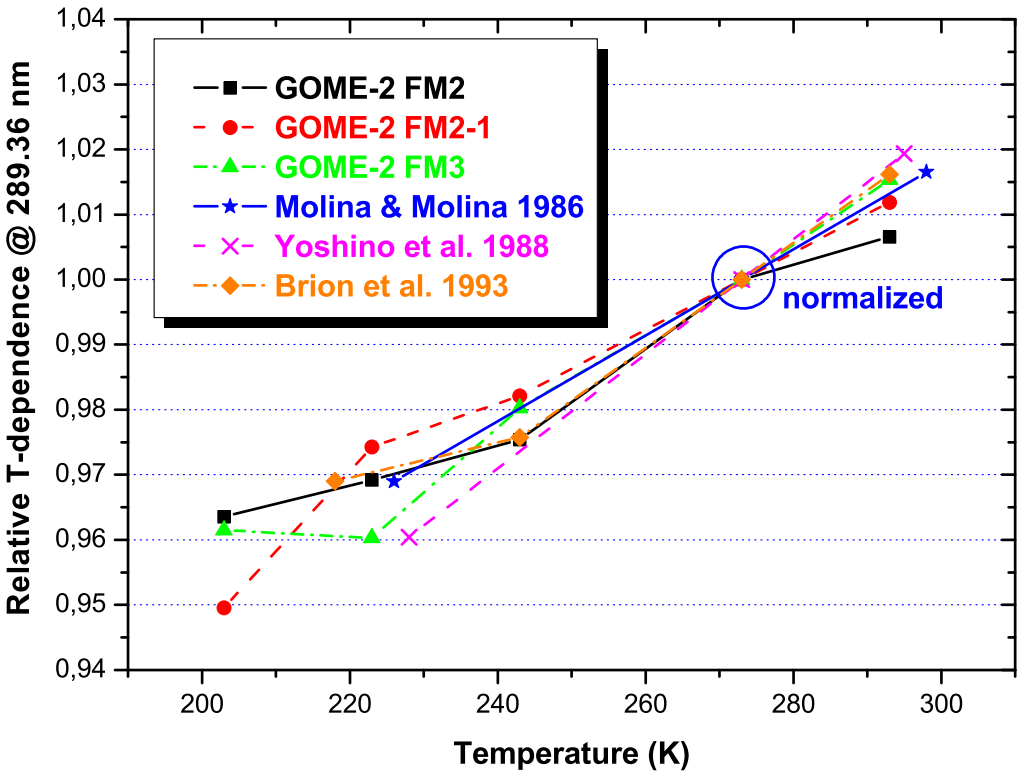

Figure 5.2: Relative temperature dependence at 289.36 nm

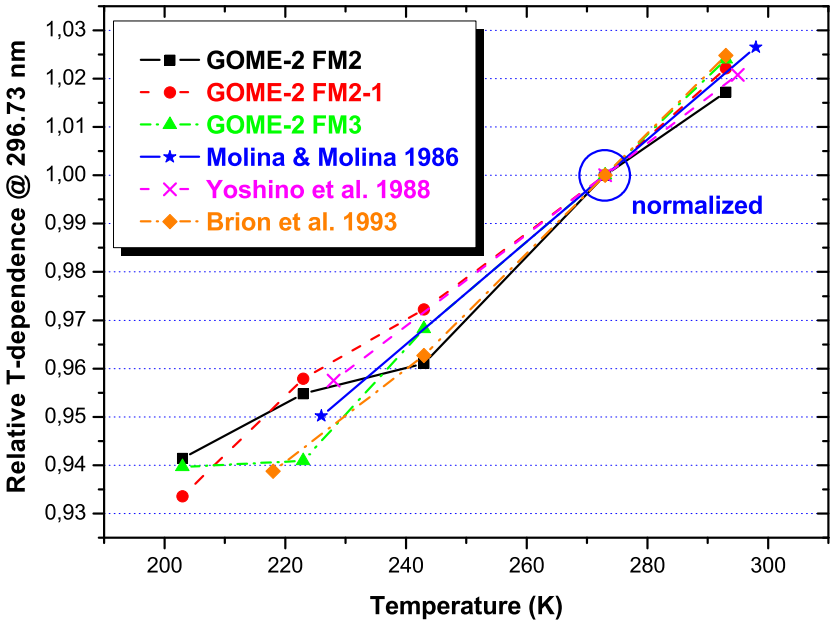

Figure 5.3: Relative temperature dependence at 296.73 nm

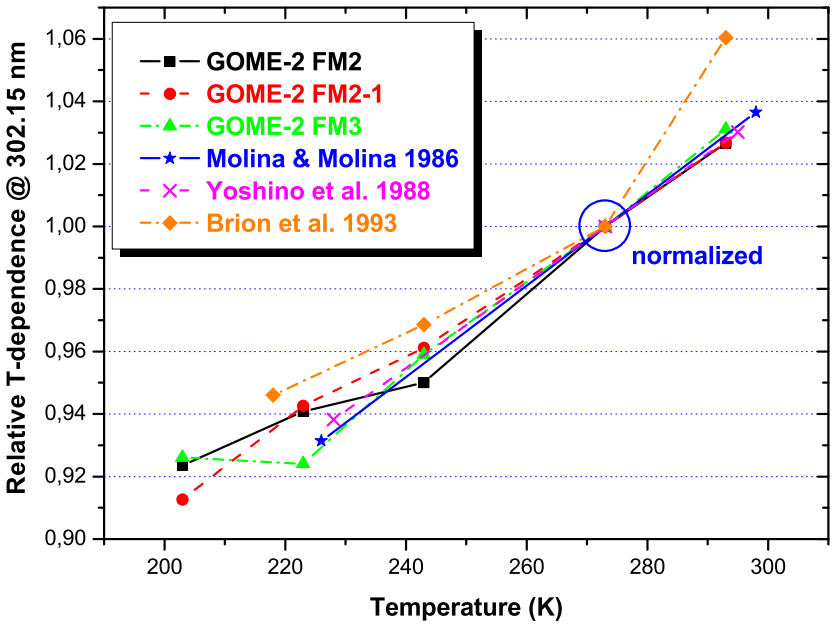

Figure 5.4: Relative temperature dependence at 302.15 nm

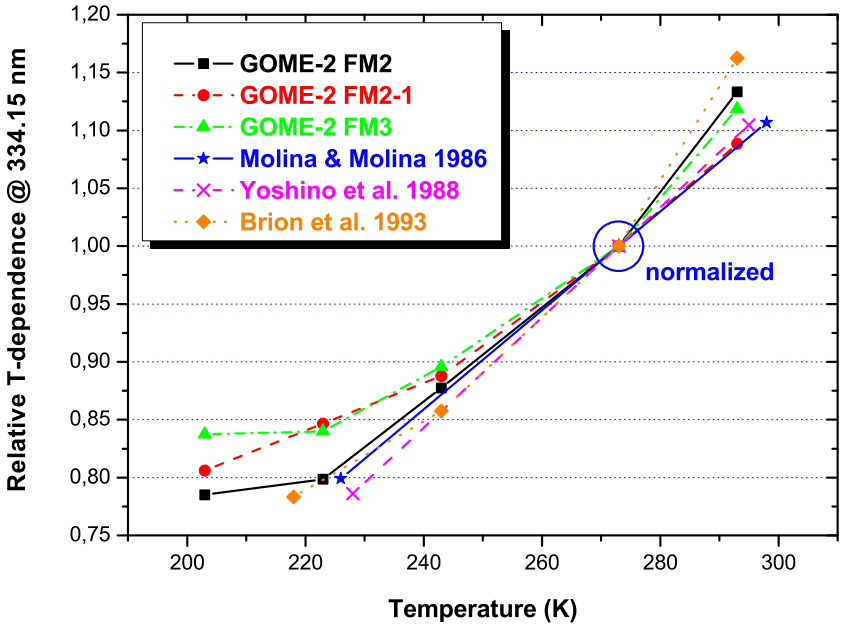

Figure 5.5: Relative temperature dependence at 334.15 nm

The relative temperature dependence obtained from all three GOME-2 campaigns shows an excellent consistency with previous measurements [12, 14, 16]. Note that at this point only comparisons have been made with literature data, which was based on measurements of absolute absorption cross sections. All of them were converted from absolute to relative temperature dependence. This high degree of consistency found between the available reference data and our data supports the assumption that the selected interval of integration and the quality of our observational data are sufficient to indeed preserve relative temperature dependence of spectra.

Furthermore, as the Huggins and Chappuis bands had been covered simultaneously by a large number of measurements, it is reasonable to assume that the systematic behavior of relative temperature dependence is also preserved in the range of 400 to 450 nm and at the maximum of the Chappuis band at 604.61 nm. There are only a few measurements available in literature.

At 420 nm a temperature dependent decrease of ≈40 % when reducing temperature from 298 K to 220 K was reported [18]. Our data do not support this observation. Relative temperature dependence at 426.1 nm and 429.5 nm as obtained from the three GOME-2 campaigns shows a decrease with falling temperature of at maximum 10 % for the scattered data of FM2 and FM3 and for the more systematic data of FM2-1 of no more than a few percent. This is illustrated in figure 5.6. These two wavelengths have been chosen on peak (426.1 nm) and off peak (429.5 nm). As these data points were obtained at comparatively small optical densities - as was the case in the measurements of ref. [18] - the possible effects of instability of throughput and background absorption could have played a critical role in their determination. This can be seen from the be-

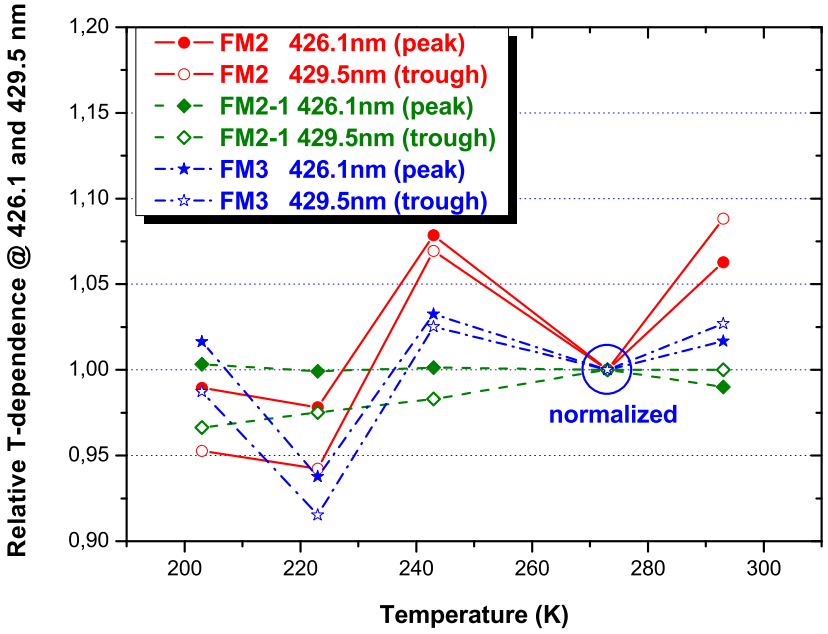

Figure 5.6: Relative temperature dependence at 426.1 and 429.5 nm

havior of data points, which varied significantly differently between the three series. But checks on stability of optical throughput of those measurements unequivocally proved that the observed behavior was not caused by instabilities of the optical system. Instead, comparison of the temporal behavior of differential structures belonging to the O_3 absorption spectrum during the filling of the vessel to temporal behavior of the spectrally broad background clearly showed that both behaved significantly differently. This clearly proved that in those measurements, which focussed on that spectral region a further absorption must be present. O_3 concentrations had to be high at $\approx 10^{17}$ molec/cm^3 due to the O_3 cross sections being very small in that region and with O_2 as bath gas - both as in ref. [18]. With the available data it is not possible to decide, whether the observed additional absorption is caused by a gas phase absorber - which could possibly be an O_3/O_2 or O_3/O_3 dimer - or an interaction of O_3 with the molecular layers of H_2O on mirrors and windows. Such molecular layers of water are always present at the typical pressures and temperatures of such measurements. Changes in these molecular layers by interaction of O_3 and H_2O would slightly and spectrally broadly change the reflectance and transmittance of mirrors and windows respectively. The effect would be similar to that observed. Considering this effect as a possible source for the scatter of FM2 and FM3 data in figure 5.6 one can consider the systematic behavior of data of FM2-1 as a criterion which indicates the absence of background effects. This is supported by the fact that the data points of FM2-1 show a systematic decrease of cross section of ≈ 3 % with falling temperature at 429.5 nm, which is located in a minimum of the band structure. Opposed to that at 426.1 nm - the maximum of the neighboring band - the cross section slightly increases by ≈ 1 % with falling temperature. Both observations indicate an increase of differential structure and a decrease of the underlying continuum. But the decrease of

the continuum absorption is significantly smaller than that observed in ref. [18]. As their measurements were performed at similarly high O_3, with O_2 as bath gas and with similarly low optical densities as in our work, it appears possible that their observed strong decrease of continuum absorption could have been caused by changes of the same continuous background absorption as it was found in our measurements. To eliminate effects of continuous background absorption we determined the differential structure of the O_3 absorption spectrum by subtracting a slowly varying polynomial. The amplitude of these differential structures at 426 nm clearly shows a systematic increase of 10 %, 15 % and 15 % (campaigns FM3, FM2, FM2-1 resp.), on average 13 % with falling temperature (293 K to 203 K), see figure 5.7. This is in agreement with the observation stated quali-

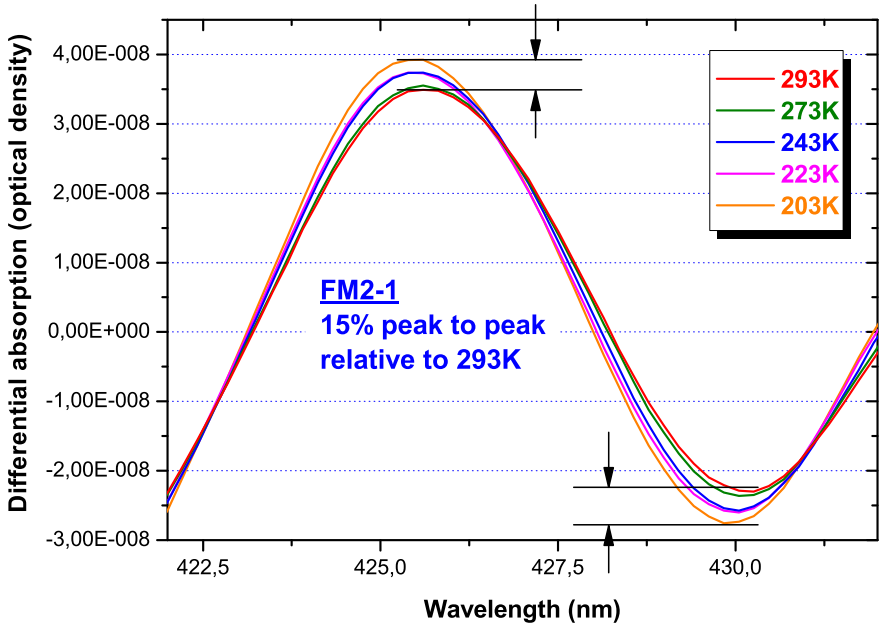

Figure 5.7: Relative temperature dependence of differential absorption cross section

tatively in the text of ref. [18]. Apart from these changes of differential cross section also slight shifts in wavelength are observed in the 400-500 nm region which is frequently used for O_3 retrieval from ground based measurements. This is in agreement with previous publications (e.g. [18, 19]).

At 604.61 nm at the maximum of the Chappuis band, where larger optical densities are reached with clearly lower O_3 concentrations and where no problems with continuous background absorptions were observed, the data by [17, 16, 18] show a slight increase of absorption cross section of less than 0.5 %, $\approx$ 1 % and $\approx$ 0.5 % respectively, when temperature decreased from room temperature to about 220 K. Please note: In some publications, e.g. [20], the data of Amoruso et al. [17] is considered as underestimating the absolute cross section. In our context of relative temperature dependence the data is nevertheless included based on the assumption that the relative magnitude of spectra at different temperatures is preserved.

Opposed to the increase reported in the aforementioned publications [18, 17, 20] a

recent study claims the observation of a clear decrease of 3 % over the same temperature range [9]. Figure 5.8 compares the available data to the relative temperature dependence obtained from the average of our measurements.

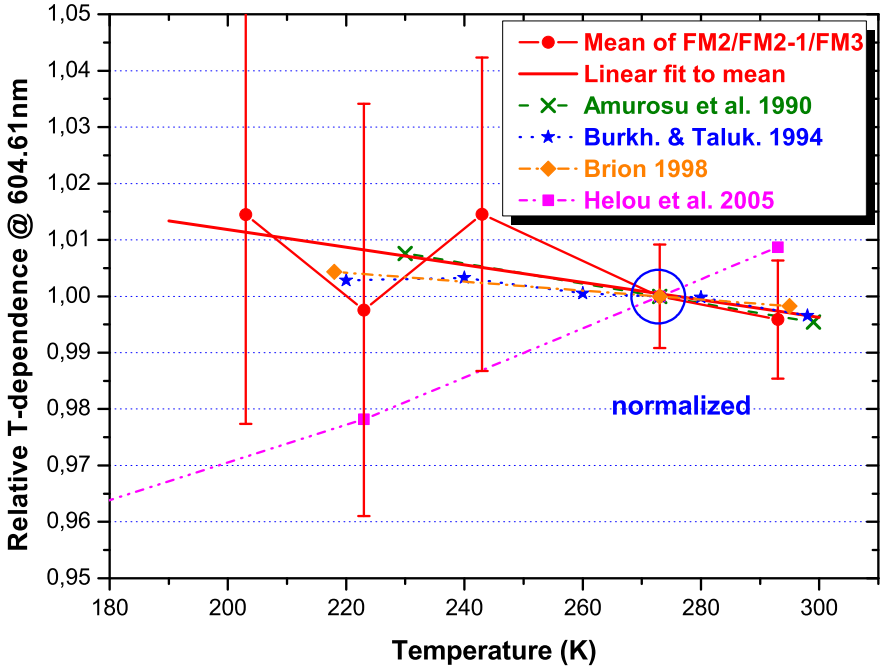

Figure 5.8: Relative temperature dependence at 604.61 nm

Even though our data points (average from relative temperature dependence from all three campaigns FM2, FM2-1, and FM3) show some scatter, they clearly show an increase of cross section with falling temperature, which agrees with an increase of 0.5 to 1 % as reported in ref. [18, 17, 20]. A linear fit to the data points obtained in our work, which eliminates irregular scatter clarifies this even more. Our result does not support a reduction of absorption cross section as reported in ref. [9].

The statistical error of our spectra in the region of the Chappuis maximum varies from 0.4 % (293 K) to 1 - 2.3 % (203 K) which transforms to 0.6 % (293 K) to 1.4 - 3.2 % (203 K) for the ratio of two spectra, as considered for the relative temperature dependence. A measure for the systematic error is the standard deviation obtained from the average of results obtained in the three different campaigns and which resulted to 0.5 % (293 K) to 1.8 % (203K). As a conservative worst case error estimate the sum of statistical and systematic error is considered and plotted in figure 5.8. Even though the result in ref. [9] at 223 K falls within this conservative (and very likely too pessimistic) error interval of our data, the continuation of their data to lower temperatures lies clearly outside the error interval. One might argue that data which displays an error of the magnitude of our worst case error estimate can not be used to deduce a statement about a temperature dependence below this threshold of error. But the isolated consideration of error bars neglects the systematic trend, which is clearly visible in our data and which can

be determined by a liner fit, which smoothes out irregular variations. The disagreement between on one hand [18, 17, 20] and our data and on the other hand that of [9] is not easily understood, especially as the latter used the original vessel of Brion et al. [20] and their own. The discussion of their result in comparison to previous measurements, especially that of reported in ref. [20] does not indicate possible reasons for the disagreement.

5.1.3 Modelling the temperature dependence of O_3 by a polynomial fit

In the past several empirical models have been proposed to reproduce the temperature dependence of O_3 absorption cross sections (e.g. second-order polynomials, exponential functions etc. See [1] and references therein). Such models help to improve the accuracy of the data since instrumental effects (like straylight or baseline differences), which have no systematic temperature variation can be reduced. In this study we therefore followed this line of thinking by applying a quadratic polynomial fit with three parameters to model relative temperature dependence:

$$\frac{\sigma(\lambda, T)}{\sigma(\lambda, T_0)} = c_0(\lambda) + c_1(\lambda) \cdot T + c_2(\lambda) \cdot T^2 \tag{5.1}$$

Temperature is expressed in degree Celsius, and T_0 is set to 273.15 K. The coefficients obtained from these fits are shown in figures 5.9 and 5.10 for the Huggins and the Chappuis bands respectively (exemplarily for FM3). In the Huggins bands the sensitivity of the cross sections strongly increases towards longer wavelengths, while in the Chappuis band the spectrum is much more stable with respect to temperature changes. Only in the short- and long-wavelength wings of the Chappuis band, the temperature variation of the cross sections becomes more important.

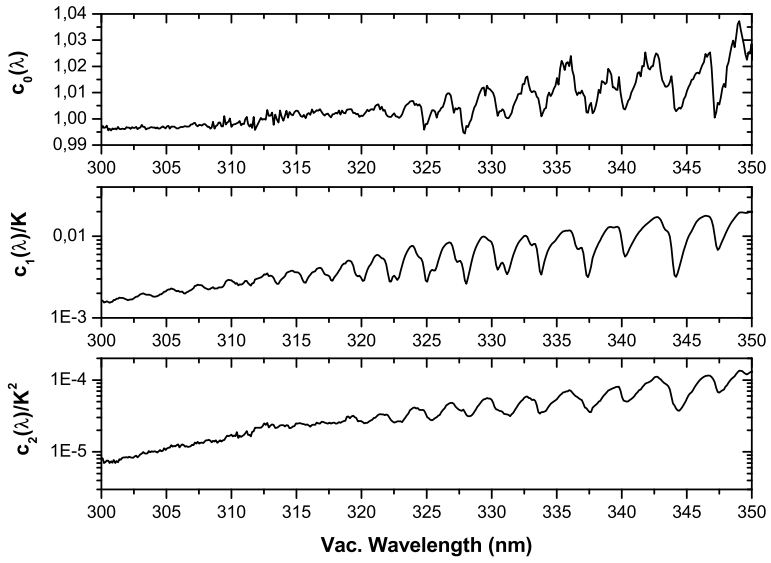

Figure 5.9: Huggins Coefficients

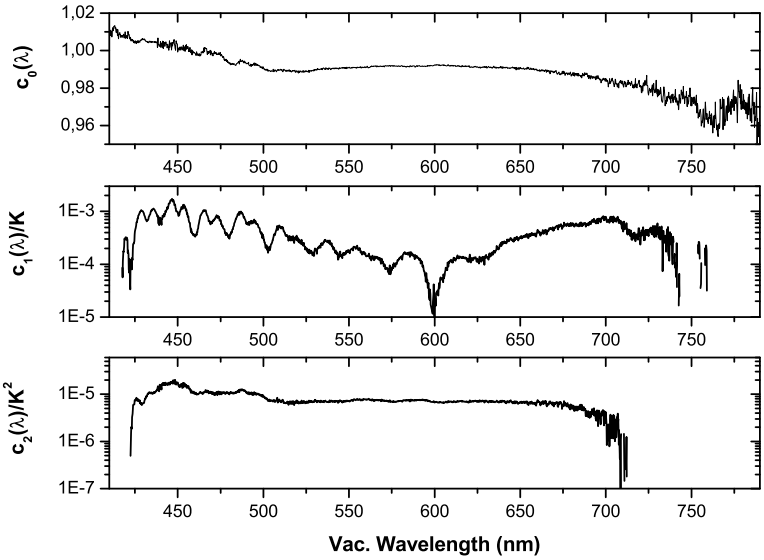

Figure 5.10: Chappuis Coefficients

5.1.4 Absolute scaling of the O_3 spectra obtained from the GOME-2 measurements

In section 5.1.1 it was described, how a series of relative spectra recorded at different temperatures was put on a common scale, which directly reflects the correct relative temperature dependence between them. This approach used integrated optical density. To scale this series of relative spectra to absolute cross sections, a single scaling factor has to be determined, which scales the whole temperature dependent series at once, rather than determining individual scaling factors for each spectrum at a given temperature. This procedure preserves the correct temperature dependence between them.

In the determination of the scaling factor only absolute determinations of O_3 absorption cross section were used. Any relative data, which itself had been scaled to absolute measurements, was rejected. This ensured that the scaling of our spectra is independent of any assumptions which had possibly been necessary in the scaling of the other relative data. With respect to absolute determinations both single wavelength absorption cross sections (from line source measurements) as well as continuous spectra of absorption cross section were used. From the latter single wavelength absorption cross sections were determined by interpolation, wherever resolution and shape of the spectrum allowed this.

Considered were all cross section data available at temperatures within or near the temperature range spanned by our data. Selected were the wavelengths 253.65 nm, 289.36 nm, 296.73 nm, 302.15 nm, 334.15 nm and 604.61 nm. At each wavelength a scaling factor was determined between the group of available absolute absorption cross section determinations at various temperatures and the group of our five optical densities from the GOME-2 spectra at that wavelength and at the five temperatures of our measurements. The scaling factor was determined by a least squares approach which minimized the deviation of the available reference data points from the scaled polygon of our five data

points, see figures 5.11 to 5.16. The uncertainties of the reference data points as stated in the corresponding references were used as weights in the least squares approach. As a large number of absolute determinations had been performed at temperatures slightly above our largest temperature of 293 K as well as some slightly below our lowest temperature of 203 K, it was allowed to extrapolate from the polygon of our data points within narrow limits, to also "catch" reference data points nearby. From each fit a standard error for the determined scaling factor was calculated. The final scaling factor was determined as a weighted average of the factors obtained at the considered individual wavelengths. Table 5.1 lists the individual results and the uncertainty estimations obtained from the fit.

	Scaling GOME-2 FM2 [10^{-16} cm^2/molec]	Scaling GOME-2 FM2-1 [10^{-16} cm^2/molec]	Scaling GOME-2 FM3 [10^{-16} cm^2/molec]
253.65 nm	3.542 ±1.61 %	3.528 ±1.61 %	3.545 ±1.61 %
289.36 nm	3.485 ±0.37 %	3.508 ±0.37 %	3.504 ±0.37 %
296.73 nm	3.454 ±0.41 %	3.454 ±0.41 %	3.484 ±0.40 %
302.15 nm	3.427 ±0.38 %	3.448 ±0.41 %	3.479 ±0.40 %
334.15 nm	3.225 ±0.34 %	3.105 ±0.35 %	3.156 ±0.35 %
604.61 nm	3.485 ±0.63 %	3.495 ±0.63 %	3.462 ±0.64 %
Ø	3.510 ±0.11 %	3.508 ±0.11 %	3.522 ±0.11 %

Table 5.1: Scaling Factors at selected wavelengths. These were determined as one factor per wavelength and per set of spectra, i.e. per flight model campaign FM2, FM2-1, and FM3.

Figures 5.11 to 5.16 illustrate the above described procedure.

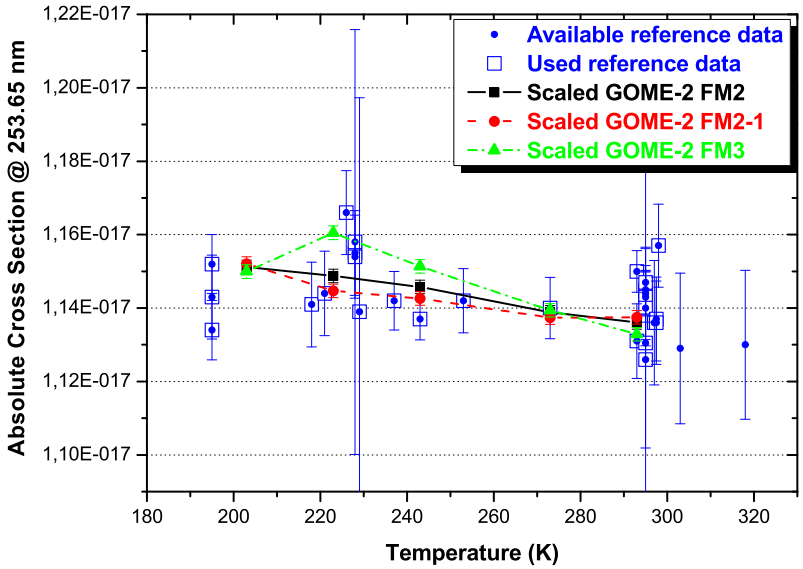

Figure 5.11: Scaling factor from data at 253.65 nm

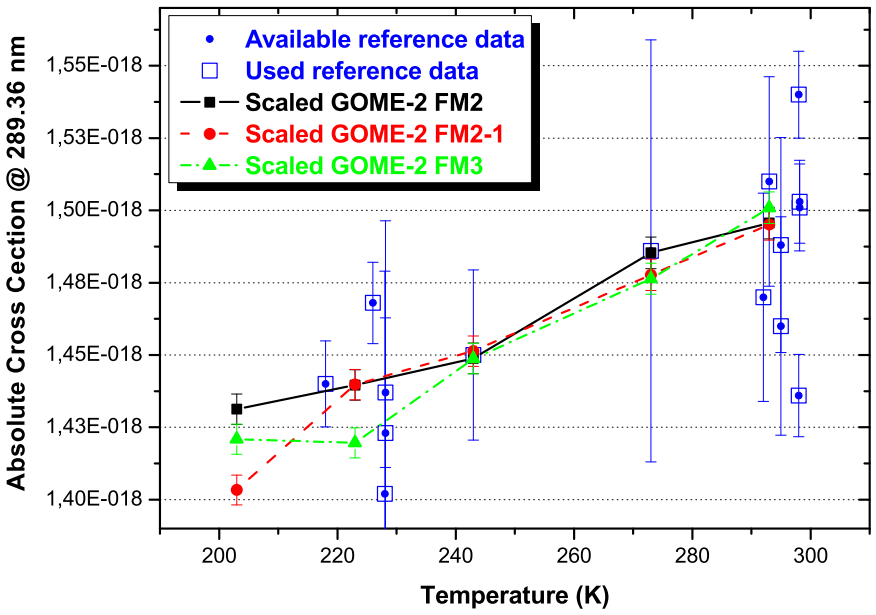

Figure 5.12: Scaling factor from data at 289.36 nm

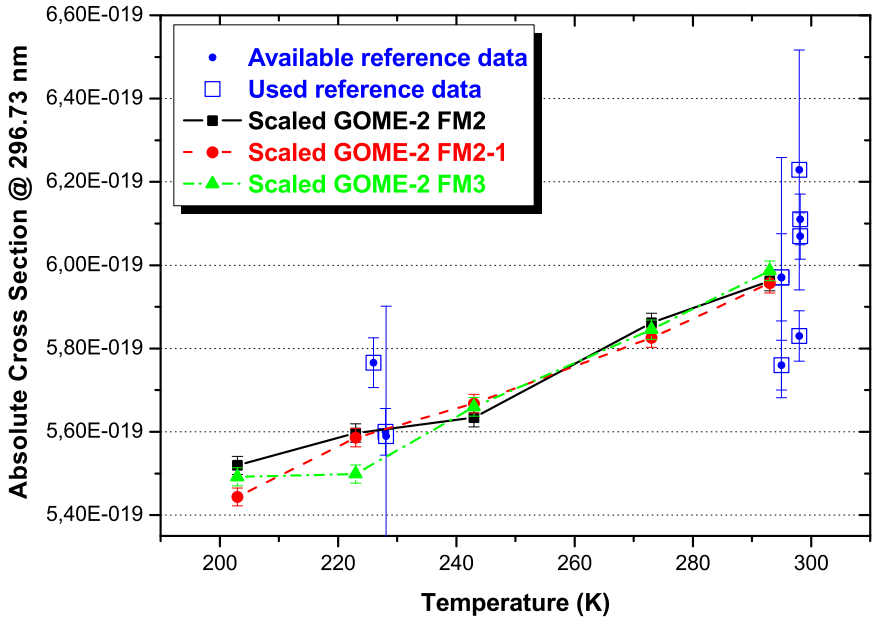

Figure 5.13: Scaling factor from data at 296.73 nm

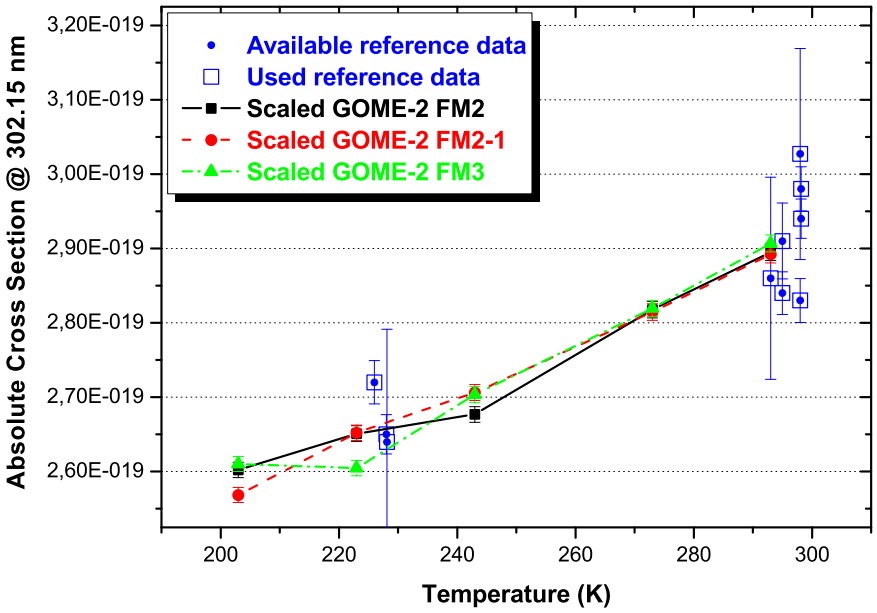

Figure 5.14: Scaling factor from data at 302.15 nm

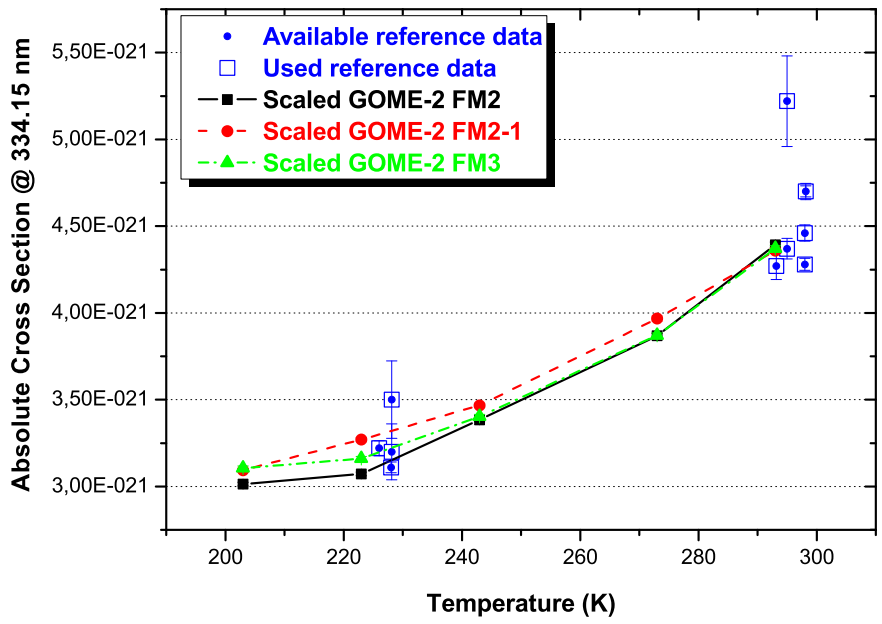

Figure 5.15: Scaling factor from data at 334.15 nm

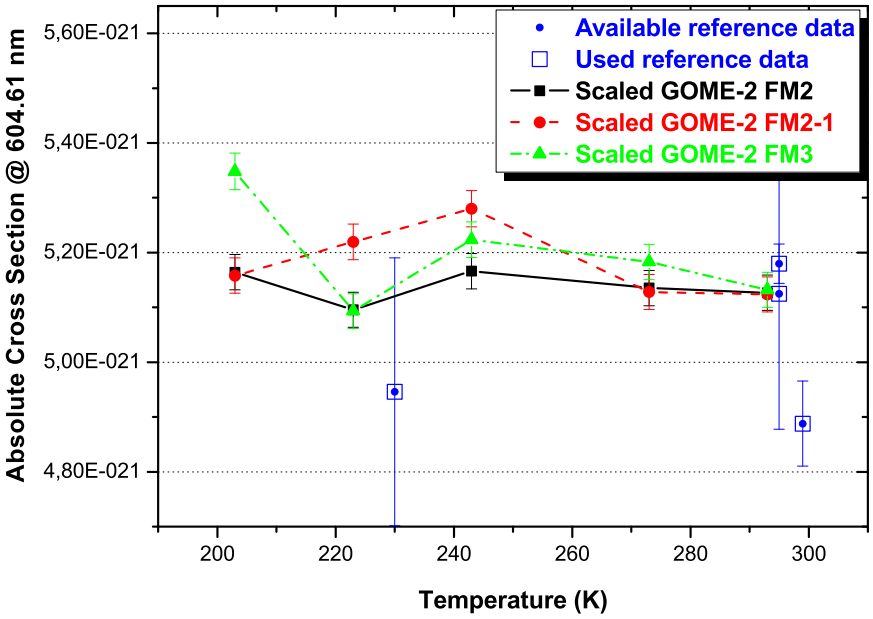

Figure 5.16: Scaling factor from data at 604.61 nm

Filled circles represent available reference data. Data used for the determination of the scaling factor is marked by an additional open square. The advantage of this approach is that it preserves the relative temperature dependence between spectra (see above) and takes all reference data into account, which is available at the selected wavelength and - this is important - at different temperatures. The scaling factors agree to within 1 % and better between the three campaigns emphasizing the consistency and reproducibility of the results. Especially the quality of concatenation of the numerous subsections of the spectrum obtained by the 12 different combinations (compare table 3.1) is clearly confirmed by this. The scaling factor obtained at 334.15 nm in the Huggins band falls low, which is most likely due to systematic effects of different resolution in the reference data and our comparatively low resolved spectra. For the determination of the final scaling factor for the spectra the results obtained at that wavelength is ignored. From the remaining data a weighted average was determined

5.1.5 Comparison of GOME-2 spectra at ambient temperature with literature values at 10 single wavelengths

In the literature exist many previous measurements at 10 selected wavelengths, corresponding to Hg lamp and He-Ne laser lines, which have been reviewed and summarized for room temperature in ref. [1]. Four of these wavelengths are located in the Hartley band, six in the Chappuis band (figure 5.17). Ref. [1] furthermore provides averages of absolute determinations of absolute cross sections at room temperature, which were obtained based on different selections of available data. For our comparison we selected those averages which were obtained without usage of scaled spectra to avoid

dependence of our approach on any assumptions possibly needed in the scaling of any previous relative spectra. Figure 5.18 shows exemplarily the O_3 absorption cross sections at 293 K obtained with GOME-2 FM3 in the present study and the comparison with the recommended values of Ref. [1]. The individual values are given in table 5.2.

The GOME-2 data show high consistency among the three FM's as well as in comparison with previous measurements. The deviations of our absolutely scaled spectra from the reference points are all well centered around zero not exceeding the range of ±2.2 %.

The deviations of our spectra from the room temperature reference value at 253.65 nm appear to be slightly larger than the remaining ones and are all negative. This could indicate either a slight systematic deformation of our spectra or a systematic deviation between the averaged reference data at different wavelengths. Or this deviation could have been caused by on one side using the average reference value from [1]. This was obtained from room temperature data only. Opposed to that on the other side our room temperature spectrum was scaled in such a way, that considered data points not only at room temperature, but - at each selected wavelength - of all data points within the considered temperature range were used. Considering the scatter of reference data in figure 5.11, it indicates that this interpretation could indeed be the reason for the observed small deviation between our spectra and the room temperature average from [1] at 253.65 nm.

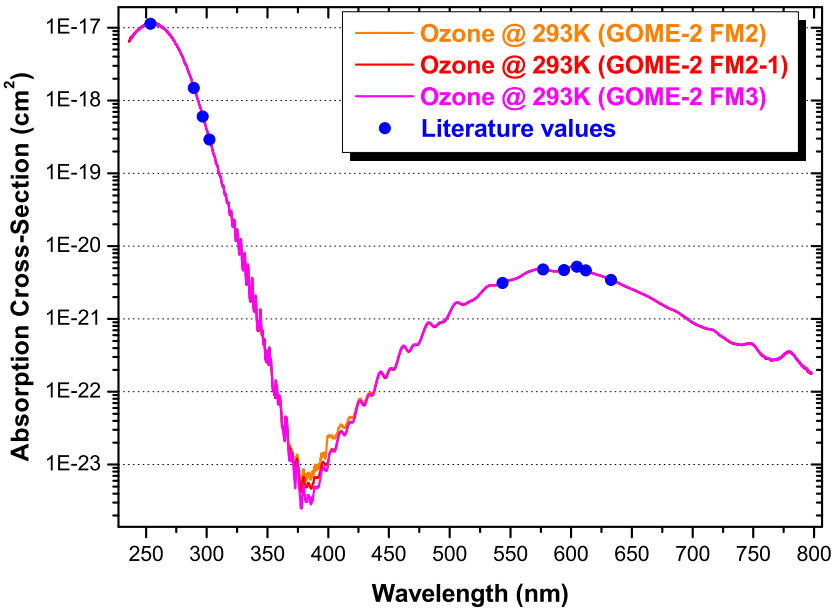

Figure 5.17: O_3 spectra @ 293 K obtained with GOME-2 and comparison at 10 single wavelengths with literature values

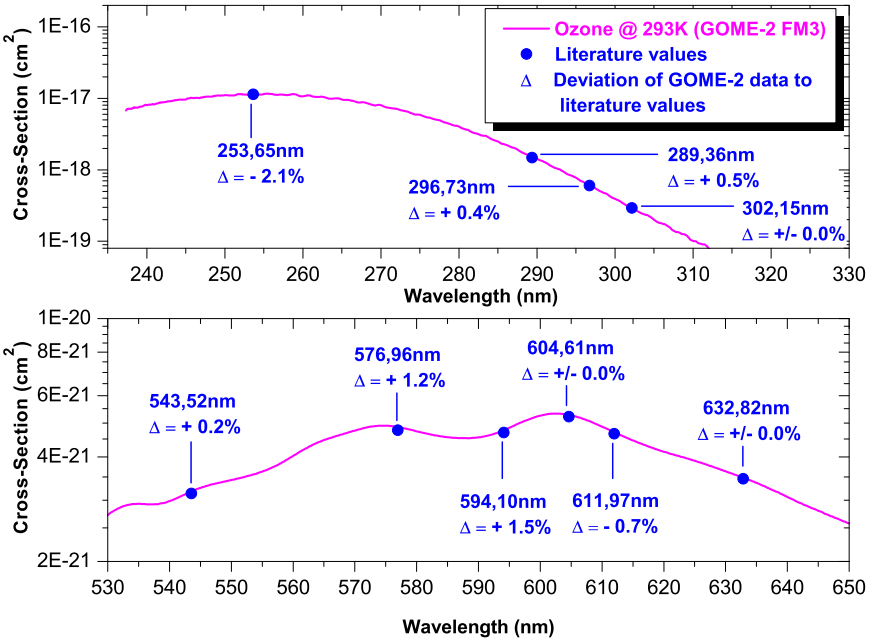

Figure 5.18: O_3 spectra @ 293 K obtained with GOME-2 FM3 and comparison at 10 single wavelengths with literature values

λ [nm]	Ref. [1]	RMS[%]	FM2	Δ[%]	FM2-1	Δ[%]	FM3	Δ[%]	Δ GOME-2 [%]	RMS[%]
253.65	1141	0.9	1116	-2.2	1124	-1.5	1117	-2.1	-1.9	0.4
289.36	149	2.0	149	0.2	149	-0.2	150	0.5	0.2	0.4
296.73	59.8	1.6	60.0	0.4	60.2	0.6	60.0	0.4	0.5	0.1
302.15	29.2	1.8	29.4	0.6	29.2	0.1	29.2	±0.0	0.2	0.3
543.52	0.311	1.3	0.307	-1.2	0.306	-1.5	0.312	0.2	-0.8	0.9
576.96	0.472	0.8	0.472	±0.0	0.471	-0.2	0.478	1.2	0.3	0.8
594.10	0.461	1.2	0.462	0.3	0.461	±0.0	0.468	1.5	0.6	0.8
604.61	0.518	1.0	0.512	-1.2	0.511	-1.3	0.518	±0.0	-0.8	0.7
611.97	0.465	0.7	0.456	-2.0	0.455	-2.1	0.462	-0.7	-1.6	0.8
632.82	0.342	1.2	0.337	-1.5	0.337	-1.4	0.342	±0.0	-1.0	0.8
mean values		1.3		-0.7		-0.8		0.1	-0.4	0.5

Table 5.2: Comparison of GOME-2 data with recommended cross sections at 293 K at 10 selected wavelengths. All cross section values are given in units of 10^{-20} cm^2. The second column gives the average values obtained in ref. [1] (NOTE: Average values of ABSOLUTE measurements) together with the RMS in the third column indicating the 1-σ root-mean-squared differences of the literature values given in ref. [1]. Δ indicates the relative differences between the values of this study and those from ref. [1]. The last two columns show the averaged differences of all three GOME-2 FM's at the selected wavelengths together with the RMS of these differences

5.1.6 Comparison of available spectra in the Huggins bands

The Huggins bands consist of a series of individual peaks in the 310 to 380 nm region, showing a strong temperature dependence both due to the varying slope of the Hartley band and to the sharpening of the individual bands at lower temperatures. Comparison of O_3 cross sections at single wavelengths in this region is critical because of the strong influence of small wavelength shifts and of spectral resolution. However, the range between 325 and 345 nm is an important spectral window for remote sensing of atmospheric O_3. In order to make a useful comparison in this region a different approach is required. Therefore, the following procedure was applied (as already used in ref. [1]):

- Convolution of high resolution spectra (Bass and Paur, Brion et al., and Voigt et al.) with a Gaussian of 0.3 nm FWHM (which is very close to the GOME-2 instrumental line shape as characterized by TPD/TNO)
- Comparison of the O_3 absorption cross sections with a non-linear least-squares fitting program using five parameters:
  - a second order baseline polynomial (3 parameters)
  - a scaling coefficient to adjust the amplitude of the cross sections (1 parameter)
  - a linear wavelength shift coefficient (1 parameter) to take into account differences in spectral calibration.

The convolution minimizes the influence of spectral resolution when comparing high resolution data with O_3 absorption cross sections recorded at lower resolution such as the GOME-2 data of the present study. The non-linear least-squares fitting program is applied to minimize the influence of wavelength uncertainties and of baseline drifts.

The comparisons were made with the data sets of Bass and Paur [21, 22], Brion et al. [16, 23, 24, 25] and Voigt et al. [26]. An example of such a fit is given in figure 5.19.

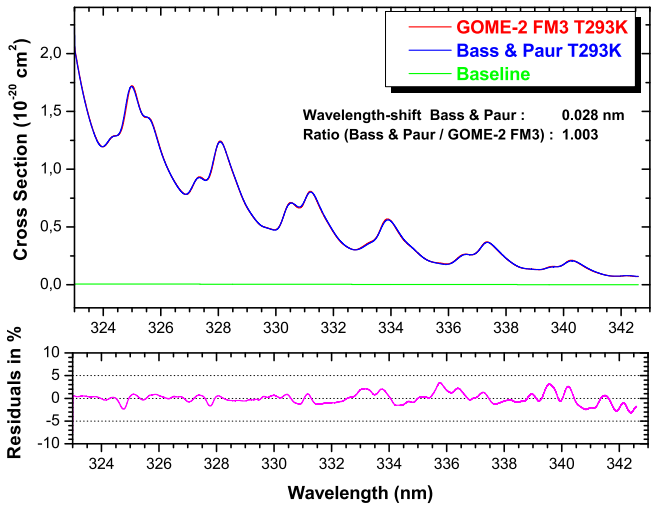

Figure 5.19: Comparison of GOME-2 data with high resolution data in the Huggins bands

The upper graph shows the two O_3 spectra (after the adjustments) together with the retrieved baseline difference. In the lower graph the residuals (differences between the two spectra after the adjustment) are shown. The comparison was made in the 323-343 nm region at five different temperatures between 203 and 293 K. A summary of all comparisons with the above mentioned high resolution spectra is given in table 5.3.

	GOME-2 FM2		**GOME-2 FM2-1**		**GOME-2 FM3**	
Reference	*λ-shift FM2*	*ratio Ref/FM2*	*λ-shift FM2-1*	*ratio Ref/FM2-1*	*λ-shift FM3*	*ratio Ref/FM3*
Voigt et al. [26]						
293 K	0.010	0.973	-0.034	0.993	-0.005	0.972
273 K	0.010	1.064	-0.035	1.100	0.000	1.054
243 K	0.013	1.061	-0.030	1.095	0.000	1.054
223 K	0.022	1.084	-0.030	1.095	-0.002	1.029
203 K	0.038	1.186	-0.013	1.157	0.023	1.178
Bass & Paur [21, 22]						
293 K	-0.018	1.002	-0.037	0.976	-0.028	1.003
273 K	-0.018	0.982	-0.029	0.933	-0.022	0.990
243 K	-0.017	0.999	-0.026	0.957	-0.021	1.004
223 K	-0.016	0.991	-0.033	0.964	-0.028	1.039
203 K	-0.014	0.974	-0.019	0.975	-0.017	0.977
Brion et al. [16, 23, 24]						
293 K	0.025	1.001	-0.019	0.980	0.010	1.002
273 K	0.008	0.979	-0.033	0.945	- 0.002	0.989
243 K	0.004	1.006	-0.038	0.974	- 0.009	1.013
223 K	0.010	1.002	-0.040	0.990	- 0.013	1.055

Table 5.3: Comparison with high resolution spectra

While the agreement of our data with the spectra of Bass and Paur as well as Brion et al. is good to very good (scaling of generally better than 3 % and of opposite sign with respect to the two data sets), the situation with respect to the FTS spectrum by Voigt et al. is considerably poorer. There in the low temperature measurement at 203 K the deviations reach up to +19 %, +16 %, and +18 % with respect to the three FMs and are of the order of +5 to +10 % for all other but the room temperature spectrum. Based on the agreement of our spectra with the two former data sets, this indicates problems with lamp drift or similar effects possibly being present in the spectra of [26]. Having been obtained with an FTS at high resolution, therefore long scanning times and without light source monitoring, the stability of the lamp could only have been monitored before and after the absorption measurements. Correction had to rely on linear interpolation to the time of the absorption measurement. This makes baseline drifts for these measurements a plausible possibility.

For the remaining reference data the ratios do not show a similarly clear systematic behavior. For FM2 and FM3 the deviations are with the exception of FM3, 223K of the order of 1-2 % and more or less centered around zero, i.e. scaling of 1.0. For FM2-1 the deviations are slightly larger of 3-4 % and all falling systematically low by approx. 1-2 %.

The wavelength shifts are given in nm and are defined with respect to the corresponding reference spectrum. As these are either FTS spectra or grating spectra obtained at higher resolution, it is reasonable to assume that their calibration is more precise than that of the GOME-2 instruments.

For the latter the width of pixels is approx. 0.1 - 0.2 nm, while the targeted wavelength accuracy was at 0.04 pixel [27]. Wavelength calibration of the GOME-2 spectra was provided by the GOME-2 instrument's calibration measurements by TPD/TNO. Similar as for the ratios also the wavelength shifts for the Voigt et al. spectrum at 203 K indicate a very clear systematic deviation. This is approx. +0.02 to +0.025 nm (i.e. to the red) relative to the others.

The surprising fact that this deviation occurs in the same way for all three FMs makes it unlikely that this deviation is caused by statistical errors in the three GOME-2 data sets, which were calibrated independently and obtained independently. Furthermore wavelength calibration for the GOME-2 spectra was identical within one campaign, i.e. for one individual FM at all temperatures. This indicates that the observed deviation is caused by wavelength calibration problems of the Voigt et al. spectrum.

A similar but much weaker effect is found for the 203 K data of Bass and Paur displaying an apparently red-shifted 203K spectrum relative to those at the remaining temperatures. On the other hand according to [1] the 203 K spectrum by Voigt et al. shows strongest shifts relative to Bass and Paur while the latter itself shows stronger shifts at low temperature relative to [19]. For the Brion et al. data no such effect occurs in the available data. But it has to be noted that for that data set no 203 K measurement exists. Therefore our data supports the conclusion, which is also indicated by the analysis in ref. [1] that the wavelength calibration of the 203 K spectra by Voigt et al. as well as by Bass and Paur might require a correction to the blue.

With the exception of the shifts between FM2-1 and Bass and Paur we see an excellent agreement of the shifts between reference spectra as found in table 6-14 in [1] and those, which one obtains when comparing the shifts for one FM relative to the corresponding reference spectra. For example the difference of the shifts of FM2 relative to Bass and Paur at 293 K (-0.018 nm) and to Voigt et al. (+0.01 nm) agrees very well with the shift between Bass and Paur and Voigt et al. (-0.029 nm) as given in table 6-14 in [1]. In the same way the shifts between the three FMs and the Brion et al. data as well as for the Voigt et al. data agree with the shifts determined between the different FM's data sets underlining the internal consistency of the analysis.

In ref. [1] it was shown that with respect to wavelength calibration the spectrum by Voigt et al. at room temperature is likely to be closest to the correct wavelength calibration, i.e. zero shift. This is in agreement with the consistency found for the higher temperature data as discussed above.

5.1.7 Integrated cross sections at different temperatures

As mentioned above the integrated absorption cross sections are rather insensitive to differences in spectral resolution and wavelength calibration. Therefore they provide a good means for comparing cross sections in different regions. Here especially a comparison between the region of the Huggins band and that of the Chappuis band is of interest. As these regions were in large parts covered simultaneously in a considerable number of our measurements, these measurements provide a well-suited set of data for an intercomparison of absorption cross sections between these two regions. We calculated integrated absorption cross sections from our spectra after they had been scaled to absolute cross sections. This is no limitation to the validity of the intercomparison as this scaling was the same factor for all spectra within a selected campaign (FM2/FM2-1/FM3). The obtained integrated cross sections will all be on the same common scale with respect to their temperature dependence. Cross sections were integrated over the following regions, according to those given in [1]:

- in the Hartley band between 245 and 340 nm: label "Hartley"
- in the Chappuis band between 410 and 690 nm: label "Chappuis"
- in the Huggins bands between 325 and 340 nm: label "Huggins"
- in the blue wing of the Chappuis band between 410 and 520 nm: label "Blue Wing"

The results are given in table 5.4. They show a high consistency between the three FMs, which is reflected in the small standard deviations of the averages, see bottom block of table 5.4. The results show a clear systematic in the integrated cross section of the Huggins band. In the other regions no clear systematic dependence on temperature is found. Considering the data for the Chappuis band it is found that the integral across this region is independent of temperature within less than ± 1 % corresponding to an average and standard deviation of $(6.44 \pm 0.05) \times 10^{-20}$ cm^2/molec.

	Hartley	Huggins	Blue Wing	Chappuis
	10^{-16}nm×cm^2/molec	10^{-20}nm×cm^2/molec	10^{-19}nm×cm^2/molec	0^{-20}nm×cm^2/molec
FM2				
203K	3.5036	5.45	6.27	6.40
223K	3.5037	5.66	6.20	6.36
243K	3.5036	6.21	6.31	6.53
273K	3.5036	7.10	6.25	6.30
293K	3.5036	8.10	6.28	6.44
FM2-1				
203K	3.5014	5.52	6.27	6.38
223K	3.5013	5.87	6.32	6.43
243K	3.5012	6.31	6.39	6.46
273K	3.5014	7.30	6.24	6.35
293K	3.5014	8.12	6.24	6.36
FM3				
203K	3.5160	5.70	6.55	6.64
223K	3.5163	5.77	6.26	6.33
243K	3.5161	6.29	6.42	6.54
273K	3.5161	7.19	6.41	6.55
293K	3.5162	8.20	6.36	6.56
average				
203K	3.5070±0.0079	5.56±0.13	6.36±0.16	6.47±0.14
223K	3.5071±0.0080	5.76±0.10	6.26±0.06	6.38±0.05
243K	3.5070±0.0080	6.27±0.05	6.37±0.06	6.51±0.04
273K	3.5070±0.0079	7.20±0.10	6.30±0.10	6.40±0.13
293K	3.5070±0.0080	8.14±0.06	6.30±0.06	6.45±0.10

Table 5.4: Comparison of integrated absorption cross sections at different temperatures and in selected wavelength regions

From these results the ratios between integrated cross sections from different regions were determined. It is important to note, that these ratios are independent of any scaling, which was performed to obtain the final spectra, as any scaling cancels from a ratio between two regions of the same spectrum. These ratios are the same, if calculated from the original unscaled and solely concatenated spectra. The ratios are listed in table 5.5.

They show no significant change with temperature between the integrated cross sections of the full Hartley region and that of the full Chappuis band. The same is true for the integrated values of the "Blue Wing" relative to the full Chappuis band. But the ratios between the integrated cross sections of the Huggins band relative to the "Blue Wing" as well as relative to the Chappuis band display a clear dependence on temperature, which has its origin in the temperature dependence of the Huggins band. The values obtained here are a direct measure for intercomparison of absorption cross sections between the different regions.

	Hartley/Chappuis	Huggins/BlueWing	Huggins/Chappuis	BlueWing/Chappuis
FM2				
203 K	558.71	0.852	0.0869	0.1020
223 K	565.09	0.890	0.0913	0.1026
243 K	555.58	0.951	0.0985	0.1036
273 K	560.56	1.127	0.1136	0.1008
293 K	557.68	1.257	0.1290	0.1026
FM2-1				
203 K	558.60	0.865	0.0881	0.1019
223 K	553.70	0.912	0.0928	0.1017
243 K	548.22	0.977	0.0989	0.1012
273 K	561.28	1.148	0.1170	0.1018
293 K	560.60	1.276	0.1300	0.1018
FM3				
203 K	536.46	0.859	0.0870	0.1012
223 K	561.42	0.910	0.0921	0.1011
243 K	547.82	0.962	0.0980	0.1018
273 K	548.14	1.098	0.1121	0.1022
293 K	552.46	1.251	0.1289	0.1030
average				
203 K	551.26 ± 12.8	0.858 ± 0.006	0.0873 ± 0.0007	0.1017 ± 0.0004
223 K	560.07 ± 5.8	0.904 ± 0.012	0.0920 ± 0.0007	0.1018 ± 0.0008
243 K	550.54 ± 4.4	0.963 ± 0.013	0.0984 ± 0.0005	0.1022 ± 0.0012
273 K	556.66 ± 7.4	1.124 ± 0.025	0.1142 ± 0.0025	0.1016 ± 0.0007
293 K	556.91 ± 4.1	1.262 ± 0.013	0.1293 ± 0.0006	0.1025 ± 0.0006

Table 5.5: Ratios of integrated cross sections from different spectral regions

5.2 NO_2 Absorption Cross Sections

In this section we will present the results of the NO_2 measurements. First we describe shortly the strategy of scaling to absolute absorption cross sections. Following that we will compare the obtained NO_2 spectra with previous measurements given in the literature. Finally we will discuss the temperature dependence of NO_2 in visible wavelength range.

5.2.1 Absolute scaling of NO_2 spectra

The absolute scaling of the NO_2-measurements has been done through integrated absorption cross sections in the 400 - 500 nm range, the main DOAS-window:

- Integration of the optical density in the 400 - 500 nm range
- Dividing the whole spectrum by the obtained integration value
- Multiply the spectrum with $4.50 \cdot 10^{-17}$ cm^2 nm as recommended in [6] and [2].

This is valid for all temperatures. The advantages of using integrated cross sections have been described in chapter 5.1.4.

5.2.2 Comparison of GOME-2 data with literature at ambient temperature

In ref. [2] it is recommended to define a standard of temperature dependent NO_2 absorption cross-sections for the entire region 240-790 nm, based on the available laboratory data. It is proposed to use the cross sections of Vandaele et al. (1998) at 294 K and at 220 K together with a linear model to interpolate for intermediate temperatures: This data set is consistent with other recent laboratory measurements of NO2 absorption cross-sections at both temperatures, and was recorded at a spectral resolution that is high enough for most remote-sensing applications.

In the following we compare the GOME-2 data with the (high resolution) data of Vandaele et al. at ambient temperature.

Figures 5.20 to 5.22 show a good agreement in the comparison of the absorption cross sections in different wavelength intervals. The differences in resolution are clearly visible. This can be more quantified by building the ratio between the GOME-2 and Vandaele et al. data. Figure 5.23 reveals a mean deviation of about 2%, only below 280 nm both data sets drift apart significantly. This is however not crucial for remote sensing applications, since the main DOAS window is between 400 and 500 nm. The high noise results from building the ratio of two data sets with different resolution. In figure 5.24 an application of a smoothing procedure is illustrated. This also confirms the mean deviation of about 2 %, together with a baseline, which has been already observed in the Vandaele data and reported in [2].

The deviation of about 2 % is highly consistent with the comparison of integrated cross sections in the 400-500 nm range between several data sets in ref. [2]. The integrated cross section of the Vandaele data set in this wavelength region is $4.58 \cdot 10^{-17}$ cm^2 nm, therefore approximately 2% higher than the recommended value in [6] and [2].

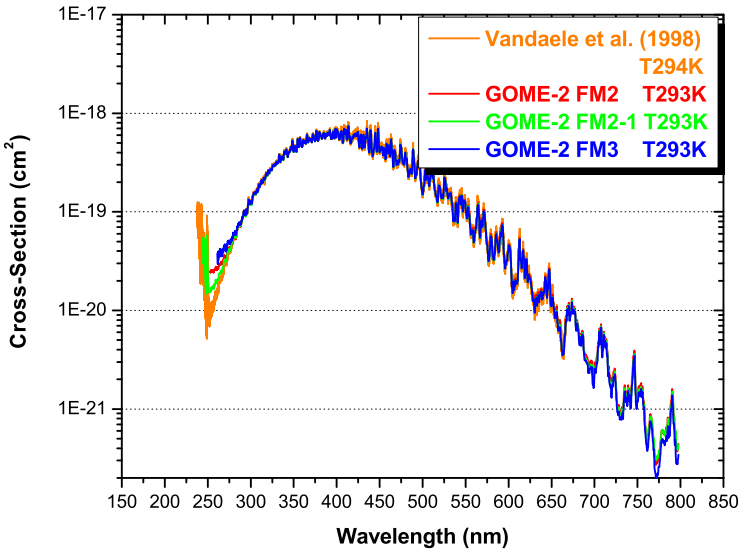

Figure 5.20: Comparison of GOME-2 data with Vandaele et al. at ambient temperature

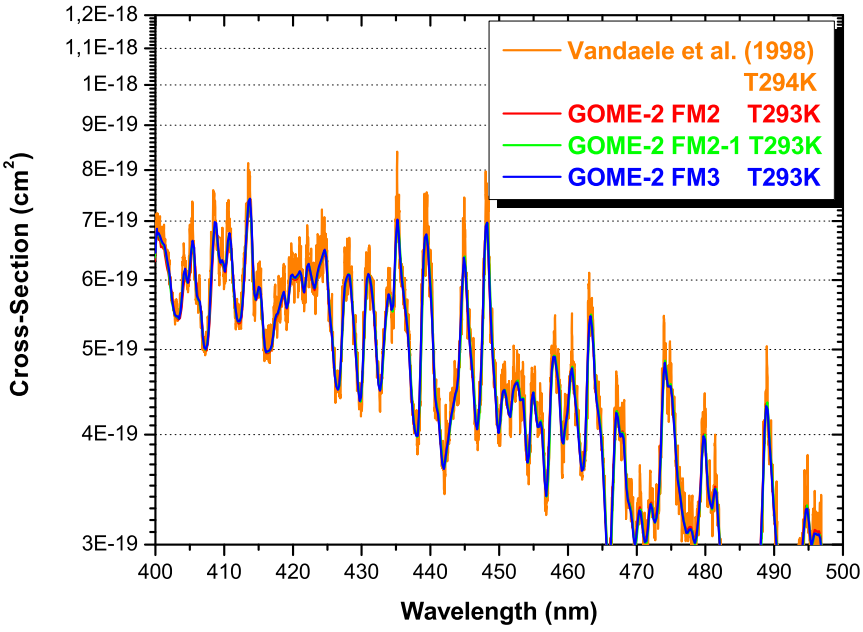

Figure 5.21: Comparison of GOME-2 data with Vandaele et al. at ambient temperature

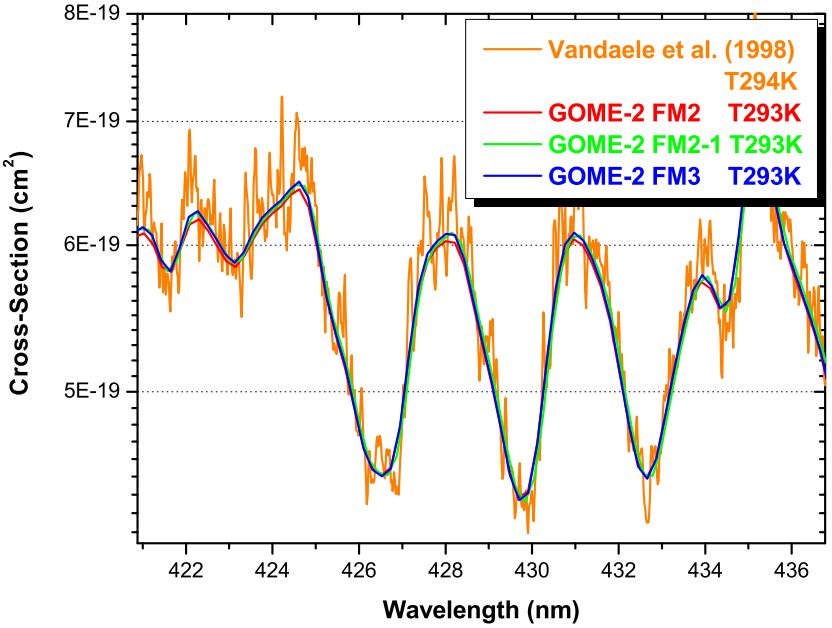

Figure 5.22: Comparison of GOME-2 data with Vandaele et al. at ambient temperature

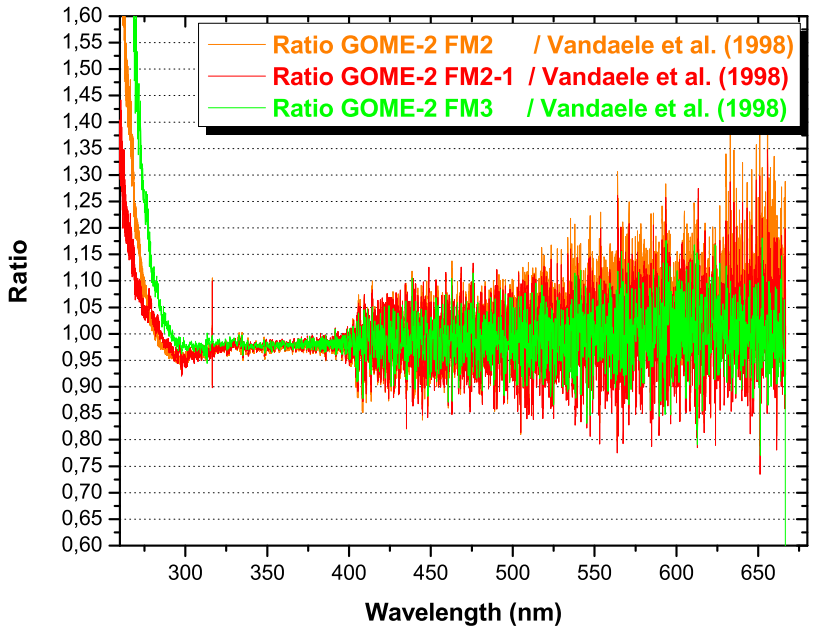

Figure 5.23: Ratio between GOME-2 FM2-1 data and Vandaele et al.

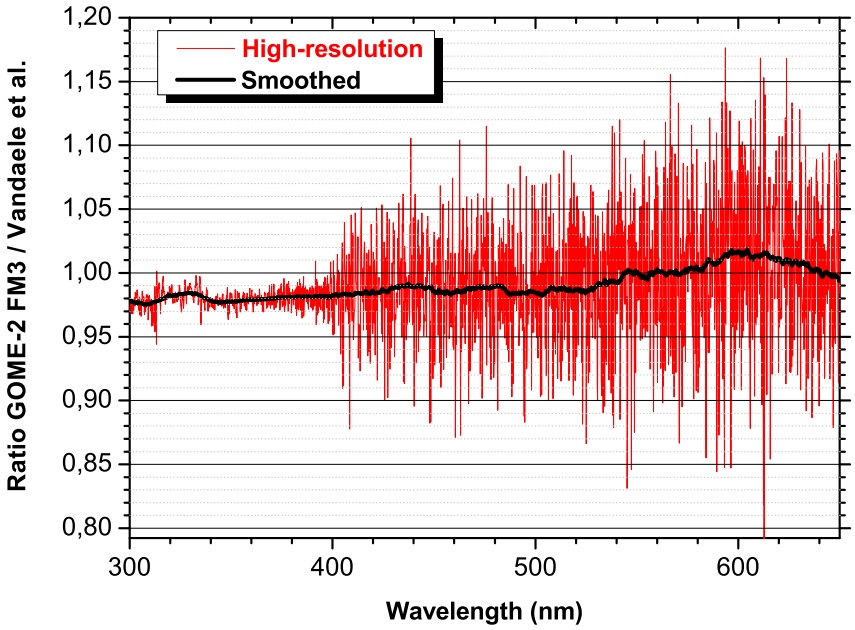

Figure 5.24: Ratio between GOME-2 FM2-1 data and Vandaele et al.

5.2.3 Temperature dependence of NO_2 spectra obtained from the GOME-2 study

In this section we will describe the results concerning the temperature dependence of the NO_2 spectra obtained from the GOME-2 study. As mentioned above a linear temperature behavior between 293 and 223 K is well established in the literature. Figure 5.25 shows the NO_2 absorption spectrum recorded with GOME-2 FM3 at four different temperatures. As described in 5.2.1 all spectra at all temperatures were scaled to absolute cross sections through integrated cross sections in the 400 to 500 nm region. Figures 5.26 and 5.27 show a more detailed picture in this range, which is the main DOAS window. In 5.27 we can see the curves at different temperatures at arbitrary progressions in the 400 to 500 nm range, which confirms a consistent temperature dependence, i.e. an increase of the differential structure with decreasing temperature.

The linearity of the temperature dependence is illustrated in figures 5.28 to 5.30. The absorption cross section at two arbitrary peaks ($\approx$ 428 and 431 nm) in the DOAS range between 400 and 500 nm have been plotted at different temperatures. In all cases the behavior could be reproduced with a linear interpolation. This is, as mentioned before in high consistency with previous measurements.

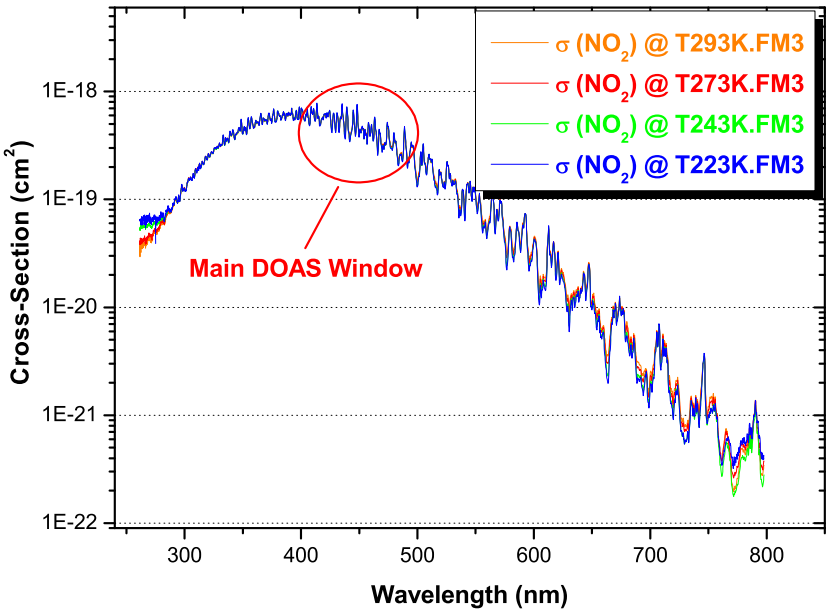

Figure 5.25: NO_2 spectra at different temperatures

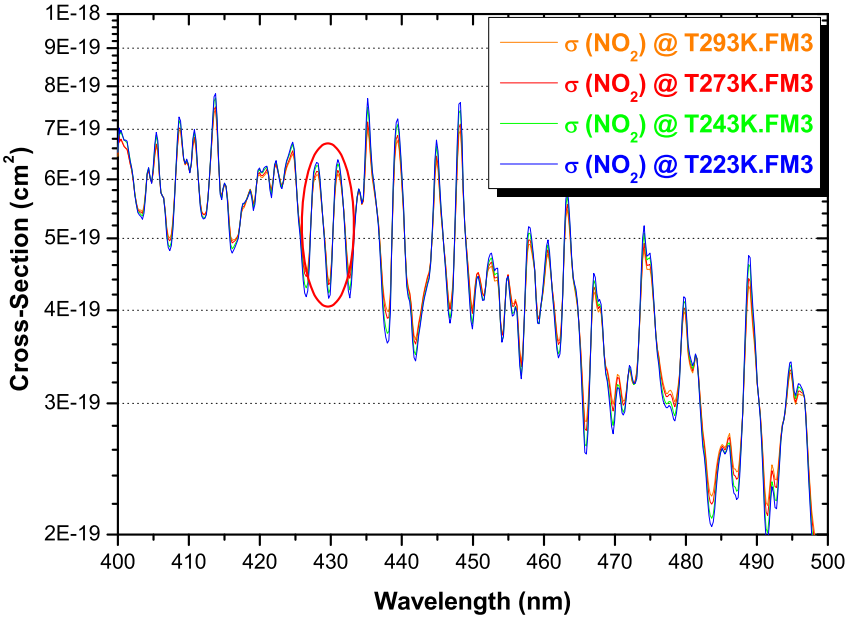

Figure 5.26: NO_2 spectra in the main DOAS window (Zoom I)

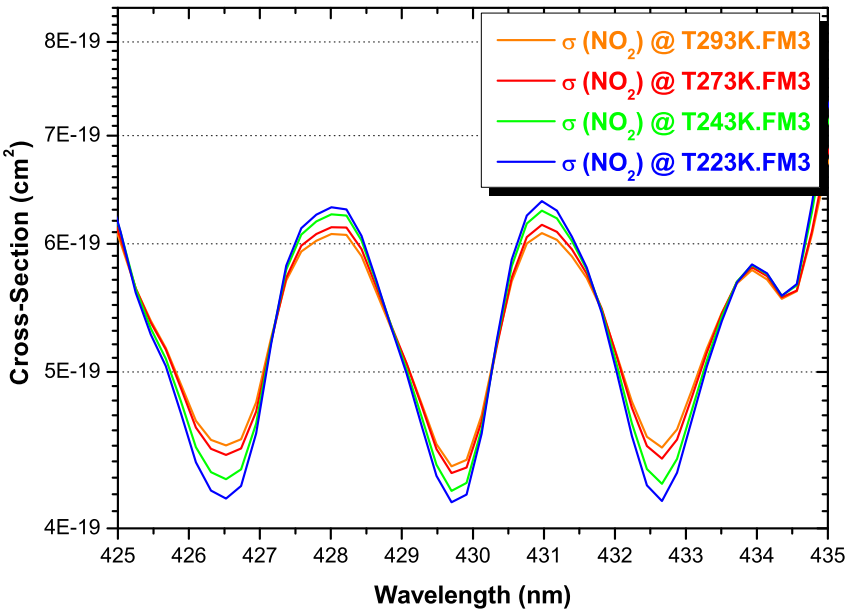

Figure 5.27: NO_2 spectra in the main DOAS window (Zoom II)

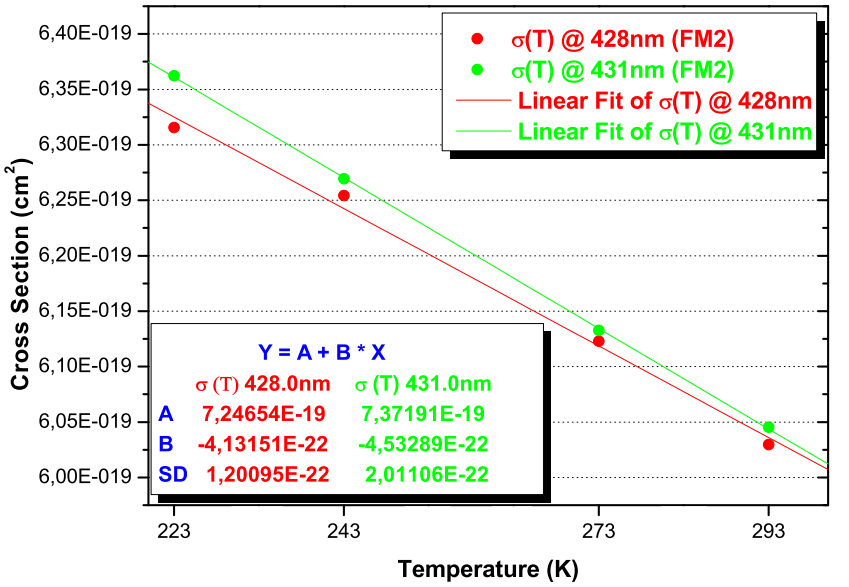

Figure 5.28: Temperature dependence of the NO_2 absorption cross section at two arbitrary wavelengths in the main DOAS window, recorded with GOME-2 FM2

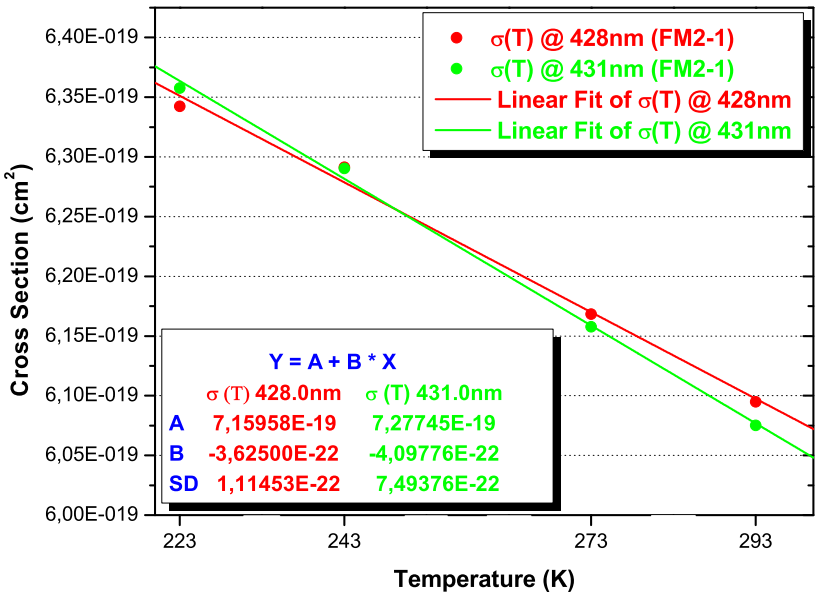

Figure 5.29: Temperature dependence of the NO_2 absorption cross section at two arbitrary wavelengths in the main DOAS window, recorded with GOME-2 FM2-1

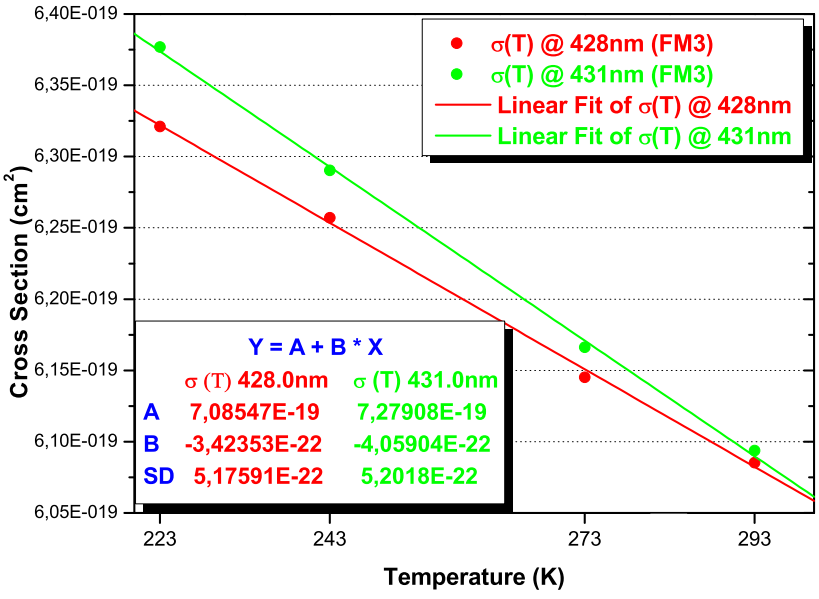

Figure 5.30: Temperature dependence of the NO_2 absorption cross section at two arbitrary wavelengths in the main DOAS window, recorded with GOME-2 FM2-1

5.3 O_2 Absorption Cross Section

In this section we present the obtained absorption spectrum of O_2.

The setup is similar as described in chapter 3.3 for the O_3 system. Only the O_2/O_3 flow is here replaced by an N_2 flow for reference measurements. The pressure in the vessel was 900 mbar, the flows 500 sccm. The optical pathlength was 29 m. Since no temperature dependency was expected only one measurement at ambient temperature was performed.

With these settings a maximum optical density of 0.2 at the A-band around 760 nm was achieved. The A-band was also used for the scaling to absolute absorption cross sections (σ(A-band) $\approx 5 \cdot 10^{-24}$ cm^2). Figures 5.31 and 5.32 show exemplary the O_2 absorption spectra recorded with GOME-2 FM3 in the complete available wavelength range and in a narrower range around the A-band at 760 nm.

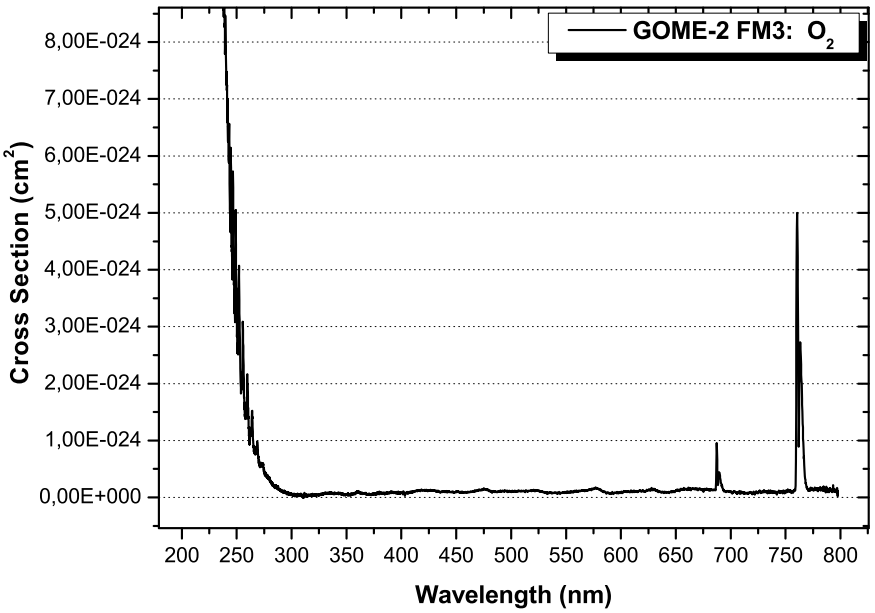

Figure 5.31: O_2 Absorption spectrum

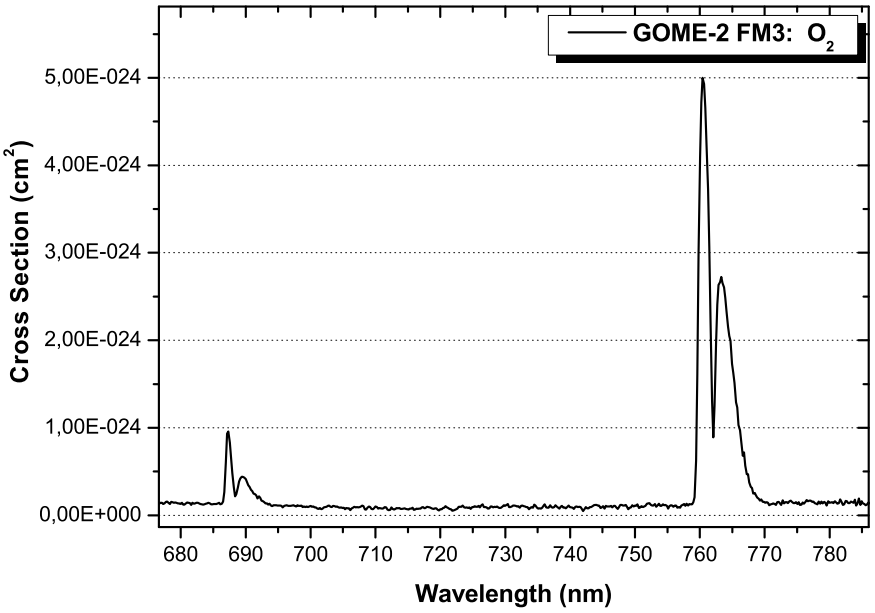

Figure 5.32: A-band of the O_2 absorption around 760 nm

5.4 Wavelength Calibration

5.4.1 General Procedure

For the wavelength calibration[1] a GOME-2 type external spectral line source (SLS), consisting of five individual lamps, is used which illuminates GOME via an integrating sphere to create an uniform field. The light from the external SLS passes through the TVC window, which has a flat transmission over the GOME- 2 spectral range. The dark signal is taken with the lamps of the set-up covered. Further, the internal SLS is used to do a regular monitoring. This means that for each measurement with the internal SLS a wavelength calibration is performed. The dark signal is measured with the scan mirror in dark position.
Before the data is analysed some general pre-processing is performed. In this pre-processing the following steps are performed:

1. The raw data is averaged for each kind of exposure.
2. The dark-signal is subtracted from the light signal.
3. The dark-signal subtracted light-signal is normalised to 1 second by dividing with the integration time.

After the general pre-processing the detailed wavelength calibration is performed. A predefined list of selected lines serves as input for the procedure. This list contains for

[1]Kindly provided by TPD

each line the following information:

1. Literature wavelength in nm
2. Usable pixel window for the line.

Within each pixel window a Gaussian fit is performed to the data. The Gaussian function to be fitted is given by:

$$y = a_0 \exp\left[-\frac{1}{2}\left(\frac{x - a_1}{a_2}\right)^2 + a_3\right] \tag{5.2}$$

where:
y is the predicted signal
x the pixel number
a0,a1,a2,a3 the parameters to be fitted

The FWHM is given by:

$$FWHM = a_2\sqrt{8\ln 2} \tag{5.3}$$

The pixel position of the peak is now equal to a1. After all pixel positions are known for each selected peak the dispersion curve for each FPA channel can be determined. A fourth order polynomial fit through the determined pixel positions is made for each FPA channel, giving the wavelength as a function of pixel.

Please note that the delivered spectra V2.0 contain the wavelength calibration as provided by TPD / TNO.

5.4.2 Deviations in wavelength calibration between individual FMs

A comparison of the results obtained in independent campaigns with different flight models gives a further criterion regarding the consistency of the results and allows a further validation of the wavelength calibration.

Figure 5.33 shows the ratios of the O_3 absorption spectra at ambient temperature between two FM's. In agreement with results discussed before one can see a high consistency between the FM's, especially in the Hartley and Chappuis band. Note that the ratio of two data sets with 1-2 % accuracy each can produce uncertainties of 3-4 %.

A critical region is, as mentioned before, the DOAS window for O_3 between 325 and 345 nm. This range is shown in figure 5.34. The ratios show especially between FM2-1 and FM3 residuals of up to 6 to 8 %. This can be reduced by applying a wavelength shift of - 0.03 nm on the FM2-1 data in channel 2. Note that only a linear shift has been applied. This shift is however highly consistent with the investigations in the Huggins region before, as discussed in section 5.1.6 and shown in table 5.3, i.e. a good agreement of the wavelength axis of FM3 and the high resolution data from Voigt et al. [26].

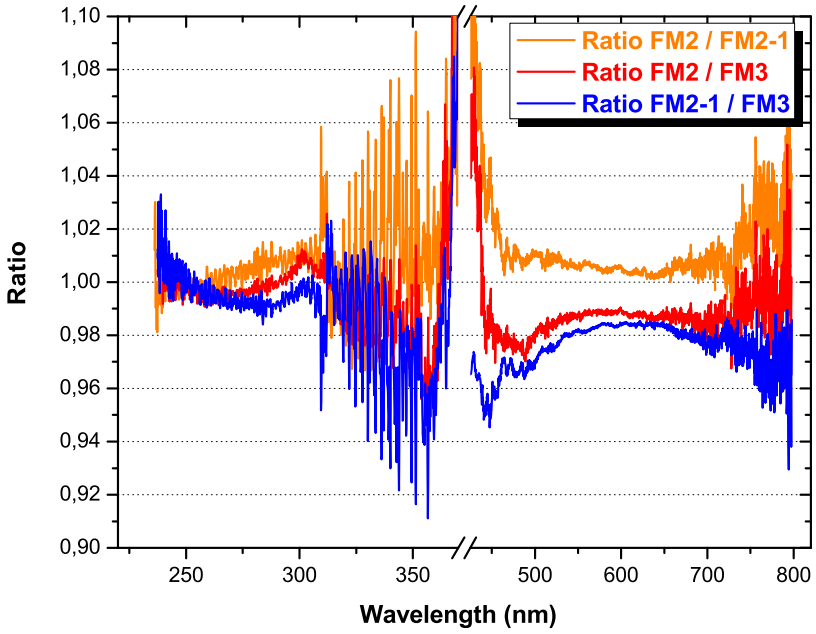

Figure 5.33: Ratios of the O_3 absorption spectra at ambient temperature between different FM's

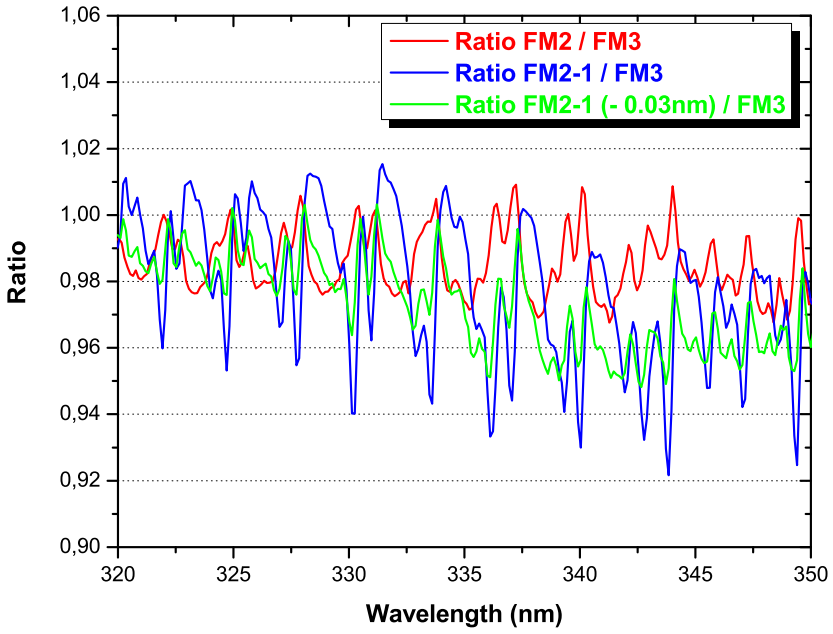

Figure 5.34: Ratios of the O_3 absorption spectra at ambient temperature between different FM's in the Huggins region

For the NO_2 data a different window is important, i.e. the main DOAS region between 400 and 500 nm. Figure 5.35 shows, similar as figures 5.33 and 5.34, the ratios of the NO_2 absorption spectra at ambient temperature between different FM's between 400 and 425 nm. The agreement between the FM's is again very good. The largest residuals appear however again in the ratio between FM2-1 and FM3. A linear wavelength shift of - 0.04 nm leads to a significant improvement (green line).

In order to evaluate the wavelength accuracy of FM3, we can again make a comparison with the high resolution data of Vandaele et al. [7], after convoluting the latter with an approximate GOME-2 ILS (this should not influence the required wavelength shift between both data sets but rather the residuals). This is similar to the procedure described in section 5.1.6. The results are shown in figures 5.36 and 5.37.

The agreement with the data of Vandaele et al [7] is, as shown before, very good, but a wavelength shift of - 0.037 nm appears recommendable for FM3, plus an additional shift of -0.04 nm for FM2-1. This is in consistency with the results illustrated in figure 5.35.

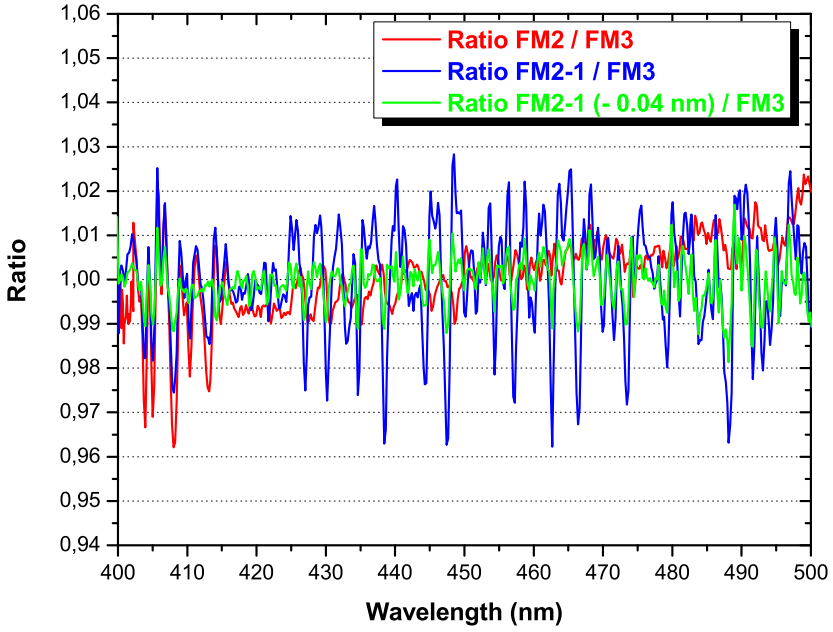

Figure 5.35: Ratios of the NO_2 absorption spectra at ambient temperature between different FM's

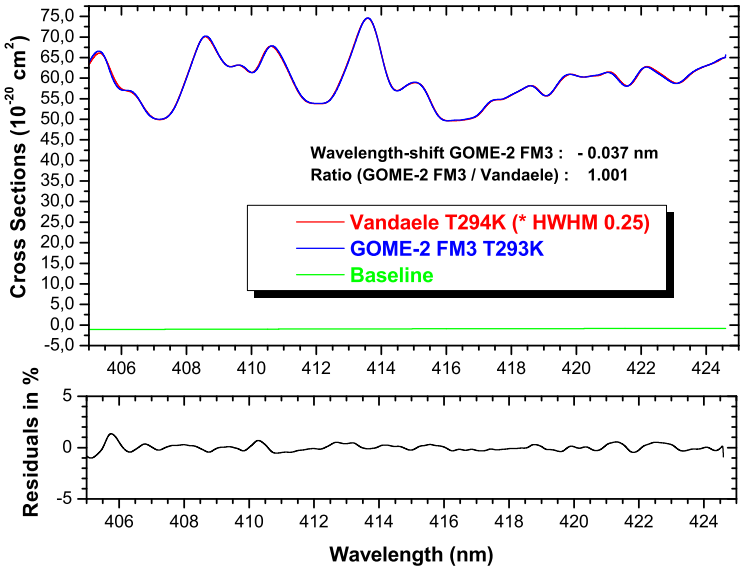

Figure 5.36: Comparison of NO_2 data from GOME-2 FM3 with high resolution data of Vandaele et al. The agreement is very good, the residuals below ± 2 %, however a wavelength shift for FM3 seems appropriate.

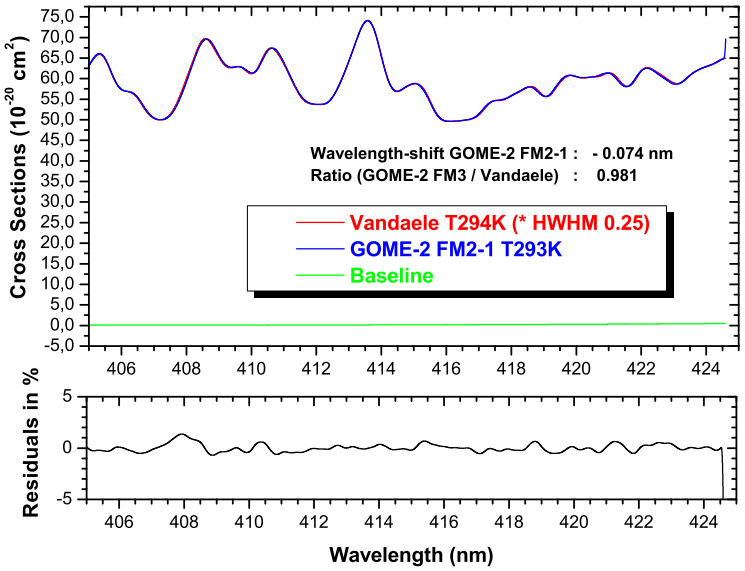

Figure 5.37: Comparison of NO_2 data from GOME-2 FM2-1 with high resolution data of Vandaele et al. The residuals are below ± 2 %, a wavelength shift of -0.074 nm for FM2-1 is recommended.

5.4.3 Origin of Deviations

In the same way as the comparison of GOME-2 O_3 spectra to literature (chapter 5.1.6) also the intercomparison between the FMs indicate contradictions, the origin of which needs to be clarified. The consistency of the deviations found in the comparison to literature data seems to indicate a systematic origin.

A possible reason for the deviations found could be differences in the filling of the GOME-2 instruments' field of view in the SLS measurements on one hand and the CATGAS measurements on the other hand. The wavelength calibration used for the CATGAS spectra in the present version is based on SLS measurements, which used the GOME-2 instruments' internal SLS or the external SLS of the TPD calibration set-up.

Apart from these measurements during the CATGAS campaigns also calibration measurements with a PtCrNe line source from the CATGAS set- up were performed. The key difference between the two types of SLS measurements is in the different optical paths, which the light travels. A comparison of wavelength calibrations obtained by the two types of SLS measurements (either external TPD/internal GOME-2 SLS or external CATGAS SLS) was performed by TPD to clarify this (see e-mail from Gerard Otter: "CATGAS spectral line source measurements", Thursday, 6 Oct 2005 16:42:43 +0200). The availability of SLS measurements with the external CATGAS SLS was also verified based on our measurement protocols (e-mail from Peter Spietz: "CATGAS SLS measurements", Thursday, 06 Oct 2005 18:53:03 +0200). Disagreement between the measurements found by TPD and by us could have occurred if the nomenclature for naming the different types of measurements was disregarded for whatever reason.

The following measurements were found:

- FM2 external CATGAS SLS-measurements:
  - 27.1.2003
  - 28.1.2003
  - 4.2.2003 last measurement(block): stray light from room light, gome2_sls_wk_52
  - 5.2.2003 gome2-sls-wk2-27 (..._26 canceled)
- FM3 external CATGAS SLS measurements:
  - none
- FM2-1 external CATGAS SLS-measurements:
  - 17.8.2004 with SiO2 mirrors in vessel, starting from o3b1m1t293d again with MgF2-mirrors ($\Rightarrow$ mirror mounts in vessel changed in between)
  - 24.8.2004, interrupted by virus attack bling.exe?

The comparison of wavelength calibration obtained from the external TPD SLS to those obtained from the external CATGAS SLS as well as to those obtained from the internal GOME-2 SLS indicates differences, which could be caused by different filling of the field of view. But while for FM2 the agreement between calibrations based on external CATGAS

SLS and internal GOME-2 indicates a reasonable agreement, the situation for FM2- 1 is less satisfying. There discrepancies between the external CATGAS SLS and the instrument's internal SLS on average amount to -0.2 pixel across channels 2, 3, and 4. Channel 1 is difficult to assess, due to low signal levels. The clear disagreement indicates possibly significant difference in the filling of the instrument's field of view. In this context the changes in the CATGAS optical arrangement could be relevant. For FM2 the light bundle was directly focussed on the entrance of the fibre bundle, which caused colored structures and inhomogeneities, as this imaged the light source onto the fibre. For FM3 and FM2-1 a diffusor plate was placed between the off-axis parabolic mirror and the entrance of the fibre bundle to improve the homogeneity of the illumination of the fibre bundle. This reduced the optical throughput slightly.

To obtain correctly calibrated spectra from the CATGAS campaigns, the usage of the external CATGAS SLS measurements for wavelength calibration appears advisable. With respect to usage of CATGAS spectra for O_3 and NO_2 retrieval further considerations are required to transfer the measured CATGAS spectra to a wavelength axis consistent with the internal GOME-2 SLS.

5.5 Least-Square Approach

One goal of the comparative study was the investigation of a potentially new approach regarding compounding a spectrum and data analysis for future studies by using a Least-Square-Method. The motivation for possible alternative illustrates figure 5.38.

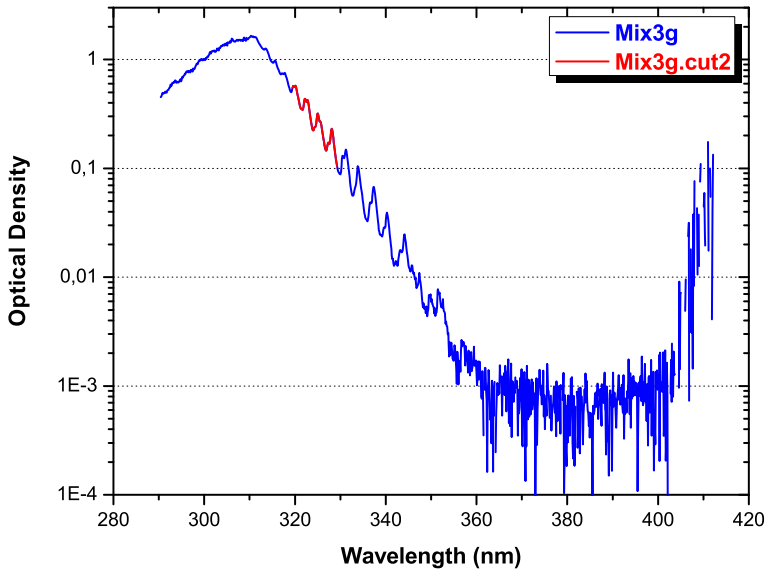

Figure 5.38: Example of a measurement referring to mixture 3 in channel 2. The red part of the spectrum represents the part, which is finally used for the concatenation of the overall absorption spectrum of O_3

Figure 5.38 shows exemplarily a measurement of O_3 in channel 2. The red part of the graphics represents the part of the spectrum, which was finally used for the concatenation of the overall spectrum. It is, as described before, within an optical density window between 0.1 and 1, which is considered to be ideal due to linearity of the detector. Even though the Huggins structures are still visible even at lower optical density, this part is not used for the compounding procedure. The application of a Least-Square-Method though would include this part of a spectra as well, even though with lower weight.

Another advantage would be a further automation of the "gluing" process, which would reduce the time consumed in a manual procedure. For this purpose a software tool was developed, which would read all available measurements and generate an absorption spectrum by applying a Least-Square method. In the following section we compare the spectra, which were generated by this approach, with the manually compounded spectra.

5.5.1 Comparison between manually compounded spectra and LSQ spectra

In a first step we applied the newly developed software by generating several absorption spectra by the method described above and comparing it with the manually compounded spectra. One parameter, which can be varied in the software, is the window of optimal optical density. Depending on this setting the model will use the this range with the highest weight. By building the ratio between a Least-Square (LSQ) spectrum and a manual spectrum we can then compare both methods.

A first illustration is given in figure 5.39. The graphics shows several ratios between manually compounded spectra and LSQ spectra, which were generated by varying the range of optimal optical density: 0.05-1, 0.05-1.5, 0.05-2 and so on, increasing the upper limit in steps of 0.5 till a maximal optical density of 3.5. The same steps were repeated with a minimal value of 0.1 in optical density.

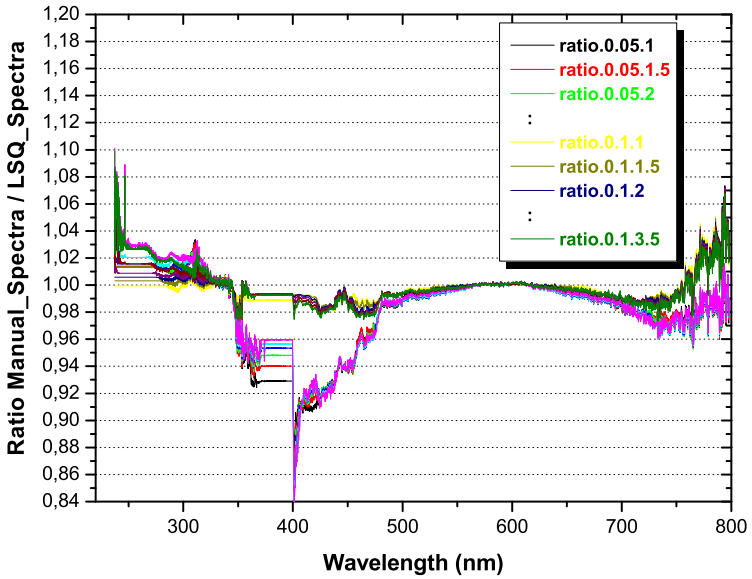

Figure 5.39: Ratio between manual- and LSQ-spectra, which were generated with different settings regarding an optimal optical density range

In figure 5.39 one can see that both methods agree within 2 to 3 % in the Hartley and Chappuis band. In parts of the Huggins bands and especially the minimum range between 370 and 420 nm the deviations are larger and reach up to 8 %. All these measurements though are related to LSQ spectra with a minimal optical density of 0.05, therefore confirming our initial assumption to use optical densities higher than 0.1. This is supported by figure 5.40.

In this figure only the ratios are shown, where the LSQ spectra were generated with a minimal optical density of 0.1. The agreement between both methods is very good in all regions and do not exceed 3 %. The largest deviation results with comparisons of LSQ spectra with a higher upper limit in optical density. The ratios, where an optimal optical density range between 0.1 and 2.5 (and lower) were used for the LSQ spectra, show the best agreement within 2 %.

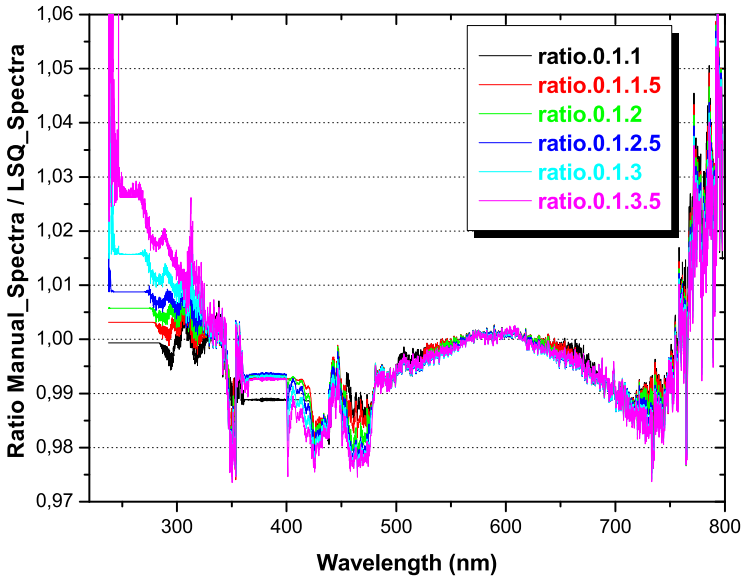

Figure 5.40: Ratio between manual- and LSQ-spectra, which were generated with different settings regarding an optimal optical density range, with a minimal optical density of 0.1

A further comparison is illustrated in figure 5.41. As described in chapter 5.1.6 manually compounded spectra and LSQ spectra have been compared with data from Bass & Paur [22] in the main DOAS window between 325 and 345 nm. Again a very good agreement between both methods can be found.

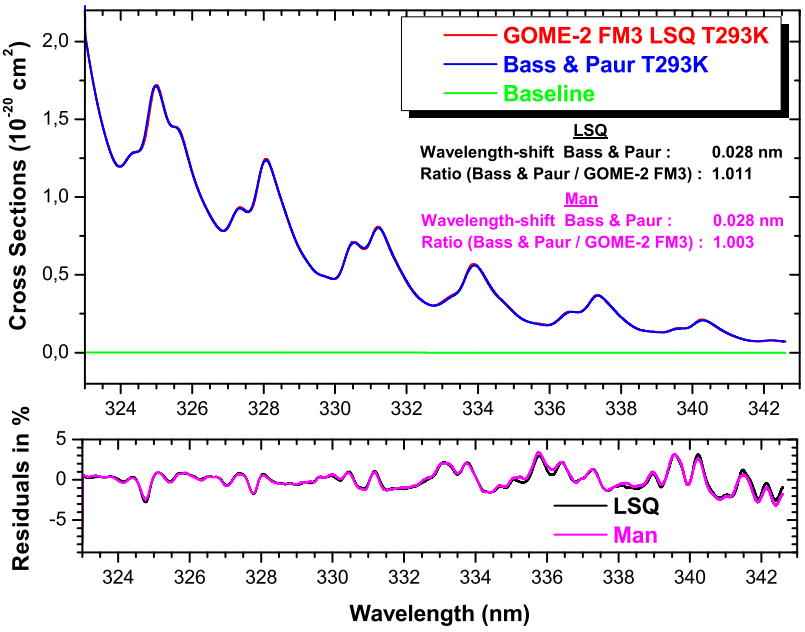

Figure 5.41: Comparison between manual- and LSQ-spectra with data from Bass & Paur

However, some questions remain open. Spectra, which were generated by the LSQ software, show partly high irregularities, which needs further investigation. This is illustrated in figures 5.42 to 5.44.

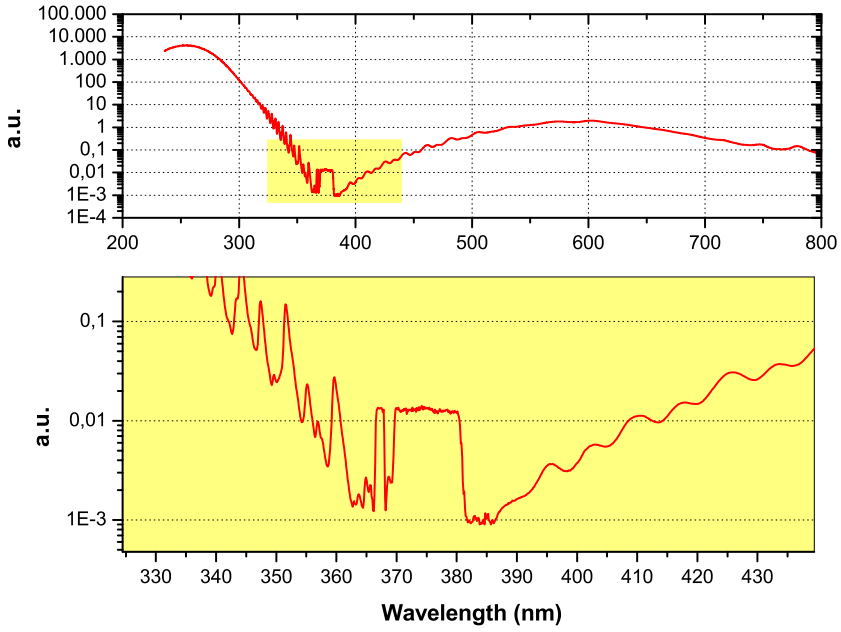

Figure 5.42: Absorption spectra of O_3 at 203 K, which were generated by applying a Least-Square method on the GOME-2 FM2-1 measurements

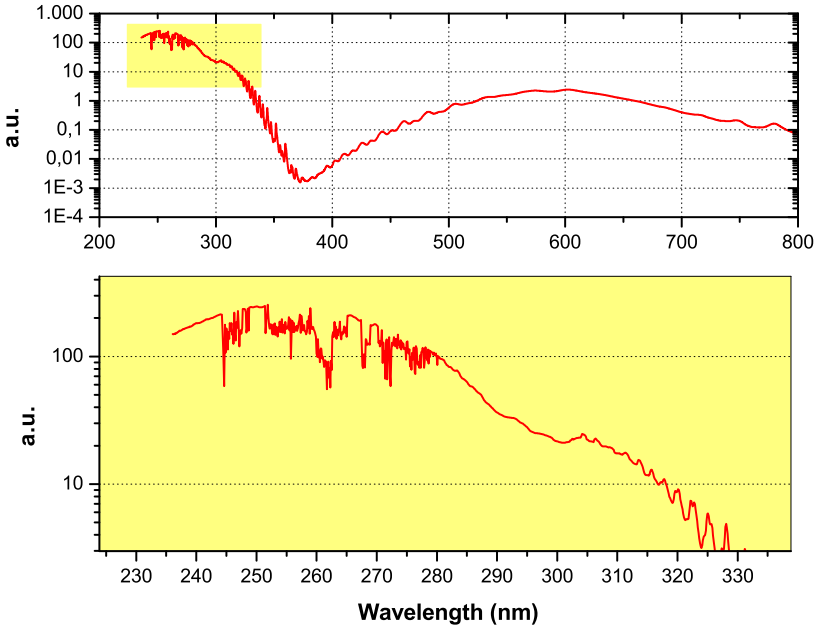

Figure 5.43: Absorption spectra of O_3 at 223 K, which were generated by applying a Least-Square method on the GOME-2 FM2-1 measurements

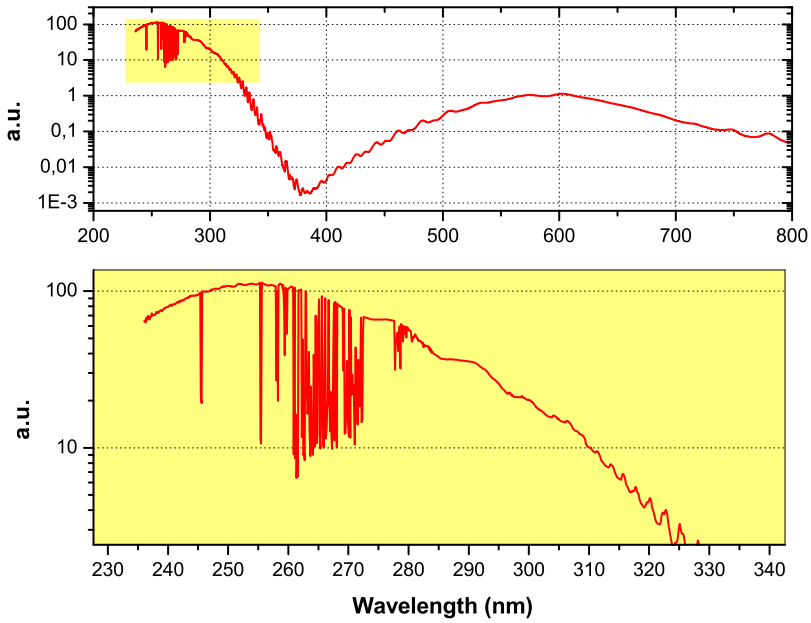

Figure 5.44: Absorption spectra of O_3 at 293 K, which were generated by applying a Least-Square method on the GOME-2 FM2-1 measurements

The following table provides a summary of good and less good LSQ spectra:

Temperature	GOME-2 FM2		GOME-2 FM2-1		GOME-2 FM3	
	good	less good	good	less good	good	less good
293 K	√			X	√	
273 K		X	√		√	
243 K	√		√		√	
223 K		X		X		X
203 K	√			X		X

Seven out of 15 spectra have not been generated correctly by the LSQ software. Furthermore there is no systematic visible in the table. As a conclusion it therefore must be stated that the LSQ software needs further development and that this method should not be used as the only procedure to compound an absorption spectrum out of single measurements.

5.6 Format Description

The data will be available in ascii format containing the following:

1) A header of 20 lines giving information about:

! KEY_DATA_NAME:
! DESCRIPTION:
! INSTRUMENT:
! CHANNEL:
! VERSION:
! HISTORY:
! ORIGIN:
! REF_DOCUMENT:
! DATE:
! MODEL:
! TEMPERATURE:
! NUM_DIM:
! NUM_COLUMNS:
! NUM_ROWS:
! IDL_FORMAT_CODE:
! PARAMETER_COLUMN:
! COLUMN_LABEL_1:
! COLUMN_LABEL_2:
! COLUMN_LABEL_3:
! END_OF_HEADER

2) The actual data set in 3 columns:

! COLUMN_1: WAVELENGTH (VAC) [nm]
! COLUMN_2: ABSORPTION CROSS SECTION [cm^2]
! COLUMN_3: ESTIMATED ERROR

The remaining pages of this chapter contain the headers of the delivered ascii data and the names of the provided origin projects.

GOME-2_FM2-1_O3_T203K.DAT

! KEY_DATA_NAME:	GOME-2_FM2-1_O3_T203K.DAT
! DESCRIPTION:	Absorption Cross-Section
! INSTRUMENT:	GOME-2
! CHANNEL:	1-4
! VERSION:	2.0
! HISTORY:	IUP Bremen
! ORIGIN:	
! REF_DOCUMENT:	
! DATE:	September 2005
! MODEL:	FM 2-1
! TEMPERATURE:	203K
! NUM_DIM:	2
! NUM_COLUMNS:	3
! NUM_ROWS:	3318
! IDL_FORMAT_CODE:	f7.4, E13.4, E13.4
! PARAMETER_COLUMN:	
! COLUMN_LABEL_1:	wavelength (vac) (nm)
! COLUMN_LABEL_2:	sigma (cm^2)
! COLUMN_LABEL_3:	delta sigma (cm^2)
! END_OF_HEADER	

GOME-2_FM2-1_O3_T203K_FPA1.DAT

! KEY_DATA_NAME:	GOME-2_FM2-1_O3_T203K_FPA1.DAT
! DESCRIPTION:	Absorption Cross-Section
! INSTRUMENT:	GOME-2
! CHANNEL:	1
! VERSION:	2.0
! HISTORY:	IUP Bremen
! ORIGIN:	
! REF_DOCUMENT:	
! DATE:	September 2005
! MODEL:	FM 2-1
! TEMPERATURE:	203K
! NUM_DIM:	2
! NUM_COLUMNS:	3
! NUM_ROWS:	1024
! IDL_FORMAT_CODE:	f7.4, E13.4, E13.4
! PARAMETER_COLUMN:	
! COLUMN_LABEL_1:	wavelength (vac) (nm)
! COLUMN_LABEL_2:	sigma (cm^2)
! COLUMN_LABEL_3:	delta sigma (cm^2)
! END_OF_HEADER	

GOME-2_FM2-1_O3_T203K_FPA2.DAT

```
! KEY_DATA_NAME:        GOME-2_FM2-1_O3_T203K_FPA2.DAT
! DESCRIPTION:          Absorption Cross-Section
! INSTRUMENT:           GOME-2
! CHANNEL:              2
! VERSION:              2.0
! HISTORY:              IUP Bremen
! ORIGIN:
! REF_DOCUMENT:
! DATE:                 September 2005
! MODEL:                FM 2-1
! TEMPERATURE:          203K
! NUM_DIM:              2
! NUM_COLUMNS:          3
! NUM_ROWS:             1024
! IDL_FORMAT_CODE:      f7.4, E13.4, E13.4
! PARAMETER_COLUMN:
! COLUMN_LABEL_1:       wavelength (vac) (nm)
! COLUMN_LABEL_2:       sigma (cm^2)
! COLUMN_LABEL_3:       delta sigma (cm^2)
! END_OF_HEADER
```

GOME-2_FM2-1_O3_T203K_FPA3.DAT

```
! KEY_DATA_NAME:        GOME-2_FM2-1_O3_T203K_FPA3.DAT
! DESCRIPTION:          Absorption Cross-Section
! INSTRUMENT:           GOME-2
! CHANNEL:              3
! VERSION:              2.0
! HISTORY:              IUP Bremen
! ORIGIN:
! REF_DOCUMENT:
! DATE:                 September 2005
! MODEL:                FM 2-1
! TEMPERATURE:          203K
! NUM_DIM:              2
! NUM_COLUMNS:          3
! NUM_ROWS:             1024
! IDL_FORMAT_CODE:      f7.4, E13.4, E13.4
! PARAMETER_COLUMN:
! COLUMN_LABEL_1:       wavelength (vac) (nm)
! COLUMN_LABEL_2:       sigma (cm^2)
! COLUMN_LABEL_3:       delta sigma (cm^2)
! END_OF_HEADER
```

GOME-2_FM2-1_O3_T203K_FPA4.DAT

! KEY_DATA_NAME:	GOME-2_FM2-1_O3_T203K_FPA4.DAT
! DESCRIPTION:	Absorption Cross-Section
! INSTRUMENT:	GOME-2
! CHANNEL:	4
! VERSION:	2.0
! HISTORY:	IUP Bremen
! ORIGIN:	
! REF_DOCUMENT:	
! DATE:	September 2005
! MODEL:	FM 2-1
! TEMPERATURE:	203K
! NUM_DIM:	2
! NUM_COLUMNS:	3
! NUM_ROWS:	1024
! IDL_FORMAT_CODE:	f7.4, E13.4, E13.4
! PARAMETER_COLUMN:	
! COLUMN_LABEL_1:	wavelength (vac) (nm)
! COLUMN_LABEL_2:	sigma (cm^2)
! COLUMN_LABEL_3:	delta sigma (cm^2)
! END_OF_HEADER	

GOME-2_FM2-1_O3_T223K.DAT

! KEY_DATA_NAME:	GOME-2_FM2-1_O3_T223K.DAT
! DESCRIPTION:	Absorption Cross-Section
! INSTRUMENT:	GOME-2
! CHANNEL:	1-4
! VERSION:	2.0
! HISTORY:	IUP Bremen
! ORIGIN:	
! REF_DOCUMENT:	
! DATE:	September 2005
! MODEL:	FM 2-1
! TEMPERATURE:	223K
! NUM_DIM:	2
! NUM_COLUMNS:	3
! NUM_ROWS:	3318
! IDL_FORMAT_CODE:	f7.4, E13.4, E13.4
! PARAMETER_COLUMN:	
! COLUMN_LABEL_1:	wavelength (vac) (nm)
! COLUMN_LABEL_2:	sigma (cm^2)
! COLUMN_LABEL_3:	delta sigma (cm^2)
! END_OF_HEADER	

GOME-2_FM2-1_O3_T223K_FPA1.DAT

```
! KEY_DATA_NAME:        GOME-2_FM2-1_O3_T223K_FPA1.DAT
! DESCRIPTION:          Absorption Cross-Section
! INSTRUMENT:           GOME-2
! CHANNEL:              1
! VERSION:              2.0
! HISTORY:              IUP Bremen
! ORIGIN:
! REF_DOCUMENT:
! DATE:                 September 2005
! MODEL:                FM 2-1
! TEMPERATURE:          223K
! NUM_DIM:              2
! NUM_COLUMNS:          3
! NUM_ROWS:             1024
! IDL_FORMAT_CODE:      f7.4, E13.4, E13.4
! PARAMETER_COLUMN:
! COLUMN_LABEL_1:       wavelength (vac) (nm)
! COLUMN_LABEL_2:       sigma (cm^2)
! COLUMN_LABEL_3:       delta sigma (cm^2)
! END_OF_HEADER
```

GOME-2_FM2-1_O3_T223K_FPA2.DAT

```
! KEY_DATA_NAME:        GOME-2_FM2-1_O3_T223K_FPA2.DAT
! DESCRIPTION:          Absorption Cross-Section
! INSTRUMENT:           GOME-2
! CHANNEL:              2
! VERSION:              2.0
! HISTORY:              IUP Bremen
! ORIGIN:
! REF_DOCUMENT:
! DATE:                 September 2005
! MODEL:                FM 2-1
! TEMPERATURE:          223K
! NUM_DIM:              2
! NUM_COLUMNS:          3
! NUM_ROWS:             1024
! IDL_FORMAT_CODE:      f7.4, E13.4, E13.4
! PARAMETER_COLUMN:
! COLUMN_LABEL_1:       wavelength (vac) (nm)
! COLUMN_LABEL_2:       sigma (cm^2)
! COLUMN_LABEL_3:       delta sigma (cm^2)
! END_OF_HEADER
```

GOME-2_FM2-1_O3_T223K_FPA3.DAT

```
! KEY_DATA_NAME:        GOME-2_FM2-1_O3_T223K_FPA3.DAT
! DESCRIPTION:          Absorption Cross-Section
! INSTRUMENT:           GOME-2
! CHANNEL:              3
! VERSION:              2.0
! HISTORY:              IUP Bremen
! ORIGIN:
! REF_DOCUMENT:
! DATE:                 September 2005
! MODEL:                FM 2-1
! TEMPERATURE:          223K
! NUM_DIM:              2
! NUM_COLUMNS:          3
! NUM_ROWS:             1024
! IDL_FORMAT_CODE:      f7.4, E13.4, E13.4
! PARAMETER_COLUMN:
! COLUMN_LABEL_1:       wavelength (vac) (nm)
! COLUMN_LABEL_2:       sigma (cm^2)
! COLUMN_LABEL_3:       delta sigma (cm^2)
! END_OF_HEADER
```

GOME-2_FM2-1_O3_T223K_FPA4.DAT

```
! KEY_DATA_NAME:        GOME-2_FM2-1_O3_T223K_FPA4.DAT
! DESCRIPTION:          Absorption Cross-Section
! INSTRUMENT:           GOME-2
! CHANNEL:              4
! VERSION:              2.0
! HISTORY:              IUP Bremen
! ORIGIN:
! REF_DOCUMENT:
! DATE:                 September 2005
! MODEL:                FM 2-1
! TEMPERATURE:          223K
! NUM_DIM:              2
! NUM_COLUMNS:          3
! NUM_ROWS:             1024
! IDL_FORMAT_CODE:      f7.4, E13.4, E13.4
! PARAMETER_COLUMN:
! COLUMN_LABEL_1:       wavelength (vac) (nm)
! COLUMN_LABEL_2:       sigma (cm^2)
! COLUMN_LABEL_3:       delta sigma (cm^2)
! END_OF_HEADER
```

GOME-2_FM2-1_O3_T243K.DAT

```
! KEY_DATA_NAME:        GOME-2_FM2-1_O3_T243K.DAT
! DESCRIPTION:          Absorption Cross-Section
! INSTRUMENT:           GOME-2
! CHANNEL:              1-4
! VERSION:              2.0
! HISTORY:              IUP Bremen
! ORIGIN:
! REF_DOCUMENT:
! DATE:                 September 2005
! MODEL:                FM 2-1
! TEMPERATURE:          243K
! NUM_DIM:              2
! NUM_COLUMNS:          3
! NUM_ROWS:             3318
! IDL_FORMAT_CODE:      f7.4, E13.4, E13.4
! PARAMETER_COLUMN:
! COLUMN_LABEL_1:       wavelength (vac) (nm)
! COLUMN_LABEL_2:       sigma (cm^2)
! COLUMN_LABEL_3:       delta sigma (cm^2)
! END_OF_HEADER
```

GOME-2_FM2-1_O3_T243K_FPA1.DAT

```
! KEY_DATA_NAME:        GOME-2_FM2-1_O3_T243K_FPA1.DAT
! DESCRIPTION:          Absorption Cross-Section
! INSTRUMENT:           GOME-2
! CHANNEL:              1
! VERSION:              2.0
! HISTORY:              IUP Bremen
! ORIGIN:
! REF_DOCUMENT:
! DATE:                 September 2005
! MODEL:                FM 2-1
! TEMPERATURE:          243K
! NUM_DIM:              2
! NUM_COLUMNS:          3
! NUM_ROWS:             1024
! IDL_FORMAT_CODE:      f7.4, E13.4, E13.4
! PARAMETER_COLUMN:
! COLUMN_LABEL_1:       wavelength (vac) (nm)
! COLUMN_LABEL_2:       sigma (cm^2)
! COLUMN_LABEL_3:       delta sigma (cm^2)
! END_OF_HEADER
```

GOME-2_FM2-1_O3_T243K_FPA2.DAT

```
! KEY_DATA_NAME:        GOME-2_FM2-1_O3_T243K_FPA2.DAT
! DESCRIPTION:          Absorption Cross-Section
! INSTRUMENT:           GOME-2
! CHANNEL:              2
! VERSION:              2.0
! HISTORY:              IUP Bremen
! ORIGIN:
! REF_DOCUMENT:
! DATE:                 September 2005
! MODEL:                FM 2-1
! TEMPERATURE:          243K
! NUM_DIM:              2
! NUM_COLUMNS:          3
! NUM_ROWS:             1024
! IDL_FORMAT_CODE:      f7.4, E13.4, E13.4
! PARAMETER_COLUMN:
! COLUMN_LABEL_1:       wavelength (vac) (nm)
! COLUMN_LABEL_2:       sigma (cm^2)
! COLUMN_LABEL_3:       delta sigma (cm^2)
! END_OF_HEADER
```

GOME-2_FM2-1_O3_T243K_FPA3.DAT

```
! KEY_DATA_NAME:        GOME-2_FM2-1_O3_T243K_FPA3.DAT
! DESCRIPTION:          Absorption Cross-Section
! INSTRUMENT:           GOME-2
! CHANNEL:              3
! VERSION:              2.0
! HISTORY:              IUP Bremen
! ORIGIN:
! REF_DOCUMENT:
! DATE:                 September 2005
! MODEL:                FM 2-1
! TEMPERATURE:          243K
! NUM_DIM:              2
! NUM_COLUMNS:          3
! NUM_ROWS:             1024
! IDL_FORMAT_CODE:      f7.4, E13.4, E13.4
! PARAMETER_COLUMN:
! COLUMN_LABEL_1:       wavelength (vac) (nm)
! COLUMN_LABEL_2:       sigma (cm^2)
! COLUMN_LABEL_3:       delta sigma (cm^2)
! END_OF_HEADER
```

GOME-2_FM2-1_O3_T243K_FPA4.DAT

! KEY_DATA_NAME:	GOME-2_FM2-1_O3_T243K_FPA4.DAT
! DESCRIPTION:	Absorption Cross-Section
! INSTRUMENT:	GOME-2
! CHANNEL:	4
! VERSION:	2.0
! HISTORY:	IUP Bremen
! ORIGIN:	
! REF_DOCUMENT:	
! DATE:	September 2005
! MODEL:	FM 2-1
! TEMPERATURE:	243K
! NUM_DIM:	2
! NUM_COLUMNS:	3
! NUM_ROWS:	1024
! IDL_FORMAT_CODE:	f7.4, E13.4, E13.4
! PARAMETER_COLUMN:	
! COLUMN_LABEL_1:	wavelength (vac) (nm)
! COLUMN_LABEL_2:	sigma (cm^2)
! COLUMN_LABEL_3:	delta sigma (cm^2)
! END_OF_HEADER	

GOME-2_FM2-1_O3_T273K.DAT

! KEY_DATA_NAME:	GOME-2_FM2-1_O3_T273K.DAT
! DESCRIPTION:	Absorption Cross-Section
! INSTRUMENT:	GOME-2
! CHANNEL:	1-4
! VERSION:	2.0
! HISTORY:	IUP Bremen
! ORIGIN:	
! REF_DOCUMENT:	
! DATE:	September 2005
! MODEL:	FM 2-1
! TEMPERATURE:	273K
! NUM_DIM:	2
! NUM_COLUMNS:	3
! NUM_ROWS:	3318
! IDL_FORMAT_CODE:	f7.4, E13.4, E13.4
! PARAMETER_COLUMN:	
! COLUMN_LABEL_1:	wavelength (vac) (nm)
! COLUMN_LABEL_2:	sigma (cm^2)
! COLUMN_LABEL_3:	delta sigma (cm^2)
! END_OF_HEADER	

GOME-2_FM2-1_O3_T273K_FPA1.DAT

! KEY_DATA_NAME:	GOME-2_FM2-1_O3_T273K_FPA1.DAT
! DESCRIPTION:	Absorption Cross-Section
! INSTRUMENT:	GOME-2
! CHANNEL:	1
! VERSION:	2.0
! HISTORY:	IUP Bremen
! ORIGIN:	
! REF_DOCUMENT:	
! DATE:	September 2005
! MODEL:	FM 2-1
! TEMPERATURE:	273K
! NUM_DIM:	2
! NUM_COLUMNS:	3
! NUM_ROWS:	1024
! IDL_FORMAT_CODE:	f7.4, E13.4, E13.4
! PARAMETER_COLUMN:	
! COLUMN_LABEL_1:	wavelength (vac) (nm)
! COLUMN_LABEL_2:	sigma (cm^2)
! COLUMN_LABEL_3:	delta sigma (cm^2)
! END_OF_HEADER	

GOME-2_FM2-1_O3_T273K_FPA2.DAT

! KEY_DATA_NAME:	GOME-2_FM2-1_O3_T273K_FPA2.DAT
! DESCRIPTION:	Absorption Cross-Section
! INSTRUMENT:	GOME-2
! CHANNEL:	2
! VERSION:	2.0
! HISTORY:	IUP Bremen
! ORIGIN:	
! REF_DOCUMENT:	
! DATE:	September 2005
! MODEL:	FM 2-1
! TEMPERATURE:	273K
! NUM_DIM:	2
! NUM_COLUMNS:	3
! NUM_ROWS:	1024
! IDL_FORMAT_CODE:	f7.4, E13.4, E13.4
! PARAMETER_COLUMN:	
! COLUMN_LABEL_1:	wavelength (vac) (nm)
! COLUMN_LABEL_2:	sigma (cm^2)
! COLUMN_LABEL_3:	delta sigma (cm^2)
! END_OF_HEADER	

GOME-2_FM2-1_O3_T273K_FPA3.DAT

```
! KEY_DATA_NAME:        GOME-2_FM2-1_O3_T273K_FPA3.DAT
! DESCRIPTION:          Absorption Cross-Section
! INSTRUMENT:           GOME-2
! CHANNEL:              3
! VERSION:              2.0
! HISTORY:              IUP Bremen
! ORIGIN:
! REF_DOCUMENT:
! DATE:                 September 2005
! MODEL:                FM 2-1
! TEMPERATURE:          273K
! NUM_DIM:              2
! NUM_COLUMNS:          3
! NUM_ROWS:             1024
! IDL_FORMAT_CODE:      f7.4, E13.4, E13.4
! PARAMETER_COLUMN:
! COLUMN_LABEL_1:       wavelength (vac) (nm)
! COLUMN_LABEL_2:       sigma (cm^2)
! COLUMN_LABEL_3:       delta sigma (cm^2)
! END_OF_HEADER
```

GOME-2_FM2-1_O3_T273K_FPA4.DAT

```
! KEY_DATA_NAME:        GOME-2_FM2-1_O3_T273K_FPA4.DAT
! DESCRIPTION:          Absorption Cross-Section
! INSTRUMENT:           GOME-2
! CHANNEL:              4
! VERSION:              2.0
! HISTORY:              IUP Bremen
! ORIGIN:
! REF_DOCUMENT:
! DATE:                 September 2005
! MODEL:                FM 2-1
! TEMPERATURE:          273K
! NUM_DIM:              2
! NUM_COLUMNS:          3
! NUM_ROWS:             1024
! IDL_FORMAT_CODE:      f7.4, E13.4, E13.4
! PARAMETER_COLUMN:
! COLUMN_LABEL_1:       wavelength (vac) (nm)
! COLUMN_LABEL_2:       sigma (cm^2)
! COLUMN_LABEL_3:       delta sigma (cm^2)
! END_OF_HEADER
```

GOME-2_FM2-1_O3_T293K.DAT

! KEY_DATA_NAME:	GOME-2_FM2-1_O3_T293K.DAT
! DESCRIPTION:	Absorption Cross-Section
! INSTRUMENT:	GOME-2
! CHANNEL:	1-4
! VERSION:	2.0
! HISTORY:	IUP Bremen
! ORIGIN:	
! REF_DOCUMENT:	
! DATE:	September 2005
! MODEL:	FM 2-1
! TEMPERATURE:	293K
! NUM_DIM:	2
! NUM_COLUMNS:	3
! NUM_ROWS:	3318
! IDL_FORMAT_CODE:	f7.4, E13.4, E13.4
! PARAMETER_COLUMN:	
! COLUMN_LABEL_1:	wavelength (vac) (nm)
! COLUMN_LABEL_2:	sigma (cm^2)
! COLUMN_LABEL_3:	delta sigma (cm^2)
! END_OF_HEADER	

GOME-2_FM2-1_O3_T293K_FPA1.DAT

! KEY_DATA_NAME:	GOME-2_FM2-1_O3_T293K_FPA1.DAT
! DESCRIPTION:	Absorption Cross-Section
! INSTRUMENT:	GOME-2
! CHANNEL:	1
! VERSION:	2.0
! HISTORY:	IUP Bremen
! ORIGIN:	
! REF_DOCUMENT:	
! DATE:	September 2005
! MODEL:	FM 2-1
! TEMPERATURE:	293K
! NUM_DIM:	2
! NUM_COLUMNS:	3
! NUM_ROWS:	1024
! IDL_FORMAT_CODE:	f7.4, E13.4, E13.4
! PARAMETER_COLUMN:	
! COLUMN_LABEL_1:	wavelength (vac) (nm)
! COLUMN_LABEL_2:	sigma (cm^2)
! COLUMN_LABEL_3:	delta sigma (cm^2)
! END_OF_HEADER	

GOME-2_FM2-1_O3_T293K_FPA2.DAT

```
! KEY_DATA_NAME:        GOME-2_FM2-1_O3_T293K_FPA2.DAT
! DESCRIPTION:          Absorption Cross-Section
! INSTRUMENT:           GOME-2
! CHANNEL:              2
! VERSION:              2.0
! HISTORY:              IUP Bremen
! ORIGIN:
! REF_DOCUMENT:
! DATE:                 September 2005
! MODEL:                FM 2-1
! TEMPERATURE:          293K
! NUM_DIM:              2
! NUM_COLUMNS:          3
! NUM_ROWS:             1024
! IDL_FORMAT_CODE:      f7.4, E13.4, E13.4
! PARAMETER_COLUMN:
! COLUMN_LABEL_1:       wavelength (vac) (nm)
! COLUMN_LABEL_2:       sigma (cm^2)
! COLUMN_LABEL_3:       delta sigma (cm^2)
! END_OF_HEADER
```

GOME-2_FM2-1_O3_T293K_FPA3.DAT

```
! KEY_DATA_NAME:        GOME-2_FM2-1_O3_T293K_FPA3.DAT
! DESCRIPTION:          Absorption Cross-Section
! INSTRUMENT:           GOME-2
! CHANNEL:              3
! VERSION:              2.0
! HISTORY:              IUP Bremen
! ORIGIN:
! REF_DOCUMENT:
! DATE:                 September 2005
! MODEL:                FM 2-1
! TEMPERATURE:          293K
! NUM_DIM:              2
! NUM_COLUMNS:          3
! NUM_ROWS:             1024
! IDL_FORMAT_CODE:      f7.4, E13.4, E13.4
! PARAMETER_COLUMN:
! COLUMN_LABEL_1:       wavelength (vac) (nm)
! COLUMN_LABEL_2:       sigma (cm^2)
! COLUMN_LABEL_3:       delta sigma (cm^2)
! END_OF_HEADER
```

GOME-2_FM2-1_O3_T293K_FPA4.DAT

! KEY_DATA_NAME:	GOME-2_FM2-1_O3_T293K_FPA4.DAT
! DESCRIPTION:	Absorption Cross-Section
! INSTRUMENT:	GOME-2
! CHANNEL:	4
! VERSION:	2.0
! HISTORY:	IUP Bremen
! ORIGIN:	
! REF_DOCUMENT:	
! DATE:	September 2005
! MODEL:	FM 2-1
! TEMPERATURE:	293K
! NUM_DIM:	2
! NUM_COLUMNS:	3
! NUM_ROWS:	1024
! IDL_FORMAT_CODE:	f7.4, E13.4, E13.4
! PARAMETER_COLUMN:	
! COLUMN_LABEL_1:	wavelength (vac) (nm)
! COLUMN_LABEL_2:	sigma (cm^2)
! COLUMN_LABEL_3:	delta sigma (cm^2)
! END_OF_HEADER	

GOME-2_FM3_O3_T203K.DAT

! KEY_DATA_NAME:	GOME-2_FM3_O3_T203K.DAT
! DESCRIPTION:	Absorption Cross-Section
! INSTRUMENT:	GOME-2
! CHANNEL:	1-4
! VERSION:	2.0
! HISTORY:	IUP Bremen
! ORIGIN:	
! REF_DOCUMENT:	
! DATE:	September 2005
! MODEL:	FM 3
! TEMPERATURE:	203K
! NUM_DIM:	2
! NUM_COLUMNS:	3
! NUM_ROWS:	3303
! IDL_FORMAT_CODE:	f7.4, E13.4, E13.4
! PARAMETER_COLUMN:	
! COLUMN_LABEL_1:	wavelength (vac) (nm)
! COLUMN_LABEL_2:	sigma (cm^2)
! COLUMN_LABEL_3:	delta sigma (cm^2)
! END_OF_HEADER	

GOME-2_FM3_O3_T203K_FPA1.DAT

```
! KEY_DATA_NAME:        GOME-2_FM3_O3_T203K_FPA1.DAT
! DESCRIPTION:          Absorption Cross-Section
! INSTRUMENT:           GOME-2
! CHANNEL:              1
! VERSION:              2.0
! HISTORY:              IUP Bremen
! ORIGIN:
! REF_DOCUMENT:
! DATE:                 September 2005
! MODEL:                FM 3
! TEMPERATURE:          203K
! NUM_DIM:              2
! NUM_COLUMNS:          3
! NUM_ROWS:             1024
! IDL_FORMAT_CODE:      f7.4, E13.4, E13.4
! PARAMETER_COLUMN:
! COLUMN_LABEL_1:       wavelength (vac) (nm)
! COLUMN_LABEL_2:       sigma (cm^2)
! COLUMN_LABEL_3:       delta sigma (cm^2)
! END_OF_HEADER
```

GOME-2_FM3_O3_T203K_FPA2.DAT

```
! KEY_DATA_NAME:        GOME-2_FM3_O3_T203K_FPA2.DAT
! DESCRIPTION:          Absorption Cross-Section
! INSTRUMENT:           GOME-2
! CHANNEL:              2
! VERSION:              2.0
! HISTORY:              IUP Bremen
! ORIGIN:
! REF_DOCUMENT:
! DATE:                 September 2005
! MODEL:                FM 3
! TEMPERATURE:          203K
! NUM_DIM:              2
! NUM_COLUMNS:          3
! NUM_ROWS:             1024
! IDL_FORMAT_CODE:      f7.4, E13.4, E13.4
! PARAMETER_COLUMN:
! COLUMN_LABEL_1:       wavelength (vac) (nm)
! COLUMN_LABEL_2:       sigma (cm^2)
! COLUMN_LABEL_3:       delta sigma (cm^2)
! END_OF_HEADER
```

GOME-2_FM3_O3_T203K_FPA3.DAT

! KEY_DATA_NAME:	GOME-2_FM3_O3_T203K_FPA3.DAT
! DESCRIPTION:	Absorption Cross-Section
! INSTRUMENT:	GOME-2
! CHANNEL:	3
! VERSION:	2.0
! HISTORY:	IUP Bremen
! ORIGIN:	
! REF_DOCUMENT:	
! DATE:	September 2005
! MODEL:	FM 3
! TEMPERATURE:	203K
! NUM_DIM:	2
! NUM_COLUMNS:	3
! NUM_ROWS:	1024
! IDL_FORMAT_CODE:	f7.4, E13.4, E13.4
! PARAMETER_COLUMN:	
! COLUMN_LABEL_1:	wavelength (vac) (nm)
! COLUMN_LABEL_2:	sigma (cm^2)
! COLUMN_LABEL_3:	delta sigma (cm^2)
! END_OF_HEADER	

GOME-2_FM3_O3_T203K_FPA4.DAT

! KEY_DATA_NAME:	GOME-2_FM3_O3_T203K_FPA4.DAT
! DESCRIPTION:	Absorption Cross-Section
! INSTRUMENT:	GOME-2
! CHANNEL:	4
! VERSION:	2.0
! HISTORY:	IUP Bremen
! ORIGIN:	
! REF_DOCUMENT:	
! DATE:	September 2005
! MODEL:	FM 3
! TEMPERATURE:	203K
! NUM_DIM:	2
! NUM_COLUMNS:	3
! NUM_ROWS:	1024
! IDL_FORMAT_CODE:	f7.4, E13.4, E13.4
! PARAMETER_COLUMN:	
! COLUMN_LABEL_1:	wavelength (vac) (nm)
! COLUMN_LABEL_2:	sigma (cm^2)
! COLUMN_LABEL_3:	delta sigma (cm^2)
! END_OF_HEADER	

GOME-2_FM3_O3_T223K.DAT

```
! KEY_DATA_NAME:        GOME-2_FM3_O3_T223K.DAT
! DESCRIPTION:          Absorption Cross-Section
! INSTRUMENT:           GOME-2
! CHANNEL:              1-4
! VERSION:              2.0
! HISTORY:              IUP Bremen
! ORIGIN:
! REF_DOCUMENT:
! DATE:                 September 2005
! MODEL:                FM 3
! TEMPERATURE:          223K
! NUM_DIM:              2
! NUM_COLUMNS:          3
! NUM_ROWS:             3303
! IDL_FORMAT_CODE:      f7.4, E13.4, E13.4
! PARAMETER_COLUMN:
! COLUMN_LABEL_1:       wavelength (vac) (nm)
! COLUMN_LABEL_2:       sigma (cm^2)
! COLUMN_LABEL_3:       delta sigma (cm^2)
! END_OF_HEADER
```

GOME-2_FM3_O3_T223K_FPA1.DAT

```
! KEY_DATA_NAME:        GOME-2_FM3_O3_T223K_FPA1.DAT
! DESCRIPTION:          Absorption Cross-Section
! INSTRUMENT:           GOME-2
! CHANNEL:              1
! VERSION:              2.0
! HISTORY:              IUP Bremen
! ORIGIN:
! REF_DOCUMENT:
! DATE:                 September 2005
! MODEL:                FM 3
! TEMPERATURE:          223K
! NUM_DIM:              2
! NUM_COLUMNS:          3
! NUM_ROWS:             1024
! IDL_FORMAT_CODE:      f7.4, E13.4, E13.4
! PARAMETER_COLUMN:
! COLUMN_LABEL_1:       wavelength (vac) (nm)
! COLUMN_LABEL_2:       sigma (cm^2)
! COLUMN_LABEL_3:       delta sigma (cm^2)
! END_OF_HEADER
```

GOME-2_FM3_O3_T223K_FPA2.DAT

! KEY_DATA_NAME:	GOME-2_FM3_O3_T223K_FPA2.DAT
! DESCRIPTION:	Absorption Cross-Section
! INSTRUMENT:	GOME-2
! CHANNEL:	2
! VERSION:	2.0
! HISTORY:	IUP Bremen
! ORIGIN:	
! REF_DOCUMENT:	
! DATE:	September 2005
! MODEL:	FM 3
! TEMPERATURE:	223K
! NUM_DIM:	2
! NUM_COLUMNS:	3
! NUM_ROWS:	1024
! IDL_FORMAT_CODE:	f7.4, E13.4, E13.4
! PARAMETER_COLUMN:	
! COLUMN_LABEL_1:	wavelength (vac) (nm)
! COLUMN_LABEL_2:	sigma (cm^2)
! COLUMN_LABEL_3:	delta sigma (cm^2)
! END_OF_HEADER	

GOME-2_FM3_O3_T223K_FPA3.DAT

! KEY_DATA_NAME:	GOME-2_FM3_O3_T223K_FPA3.DAT
! DESCRIPTION:	Absorption Cross-Section
! INSTRUMENT:	GOME-2
! CHANNEL:	3
! VERSION:	2.0
! HISTORY:	IUP Bremen
! ORIGIN:	
! REF_DOCUMENT:	
! DATE:	September 2005
! MODEL:	FM 3
! TEMPERATURE:	223K
! NUM_DIM:	2
! NUM_COLUMNS:	3
! NUM_ROWS:	1024
! IDL_FORMAT_CODE:	f7.4, E13.4, E13.4
! PARAMETER_COLUMN:	
! COLUMN_LABEL_1:	wavelength (vac) (nm)
! COLUMN_LABEL_2:	sigma (cm^2)
! COLUMN_LABEL_3:	delta sigma (cm^2)
! END_OF_HEADER	

GOME-2_FM3_O3_T223K_FPA4.DAT

```
! KEY_DATA_NAME:        GOME-2_FM3_O3_T223K_FPA4.DAT
! DESCRIPTION:          Absorption Cross-Section
! INSTRUMENT:           GOME-2
! CHANNEL:              4
! VERSION:              2.0
! HISTORY:              IUP Bremen
! ORIGIN:
! REF_DOCUMENT:
! DATE:                 September 2005
! MODEL:                FM 3
! TEMPERATURE:          223K
! NUM_DIM:              2
! NUM_COLUMNS:          3
! NUM_ROWS:             1024
! IDL_FORMAT_CODE:      f7.4, E13.4, E13.4
! PARAMETER_COLUMN:
! COLUMN_LABEL_1:       wavelength (vac) (nm)
! COLUMN_LABEL_2:       sigma (cm^2)
! COLUMN_LABEL_3:       delta sigma (cm^2)
! END_OF_HEADER
```

GOME-2_FM3_O3_T243K.DAT

```
! KEY_DATA_NAME:        GOME-2_FM3_O3_T243K.DAT
! DESCRIPTION:          Absorption Cross-Section
! INSTRUMENT:           GOME-2
! CHANNEL:              1-4
! VERSION:              2.0
! HISTORY:              IUP Bremen
! ORIGIN:
! REF_DOCUMENT:
! DATE:                 September 2005
! MODEL:                FM 3
! TEMPERATURE:          243K
! NUM_DIM:              2
! NUM_COLUMNS:          3
! NUM_ROWS:             3303
! IDL_FORMAT_CODE:      f7.4, E13.4, E13.4
! PARAMETER_COLUMN:
! COLUMN_LABEL_1:       wavelength (vac) (nm)
! COLUMN_LABEL_2:       sigma (cm^2)
! COLUMN_LABEL_3:       delta sigma (cm^2)
! END_OF_HEADER
```

GOME-2_FM3_O3_T243K_FPA1.DAT

! KEY_DATA_NAME:	GOME-2_FM3_O3_T243K_FPA1.DAT
! DESCRIPTION:	Absorption Cross-Section
! INSTRUMENT:	GOME-2
! CHANNEL:	1
! VERSION:	2.0
! HISTORY:	IUP Bremen
! ORIGIN:	
! REF_DOCUMENT:	
! DATE:	September 2005
! MODEL:	FM 3
! TEMPERATURE:	243K
! NUM_DIM:	2
! NUM_COLUMNS:	3
! NUM_ROWS:	1024
! IDL_FORMAT_CODE:	f7.4, E13.4, E13.4
! PARAMETER_COLUMN:	
! COLUMN_LABEL_1:	wavelength (vac) (nm)
! COLUMN_LABEL_2:	sigma (cm^2)
! COLUMN_LABEL_3:	delta sigma (cm^2)
! END_OF_HEADER	

GOME-2_FM3_O3_T243K_FPA2.DAT

! KEY_DATA_NAME:	GOME-2_FM3_O3_T243K_FPA2.DAT
! DESCRIPTION:	Absorption Cross-Section
! INSTRUMENT:	GOME-2
! CHANNEL:	2
! VERSION:	2.0
! HISTORY:	IUP Bremen
! ORIGIN:	
! REF_DOCUMENT:	
! DATE:	September 2005
! MODEL:	FM 3
! TEMPERATURE:	243K
! NUM_DIM:	2
! NUM_COLUMNS:	3
! NUM_ROWS:	1024
! IDL_FORMAT_CODE:	f7.4, E13.4, E13.4
! PARAMETER_COLUMN:	
! COLUMN_LABEL_1:	wavelength (vac) (nm)
! COLUMN_LABEL_2:	sigma (cm^2)
! COLUMN_LABEL_3:	delta sigma (cm^2)
! END_OF_HEADER	

GOME-2_FM3_O3_T243K_FPA3.DAT

```
! KEY_DATA_NAME:        GOME-2_FM3_O3_T243K_FPA3.DAT
! DESCRIPTION:          Absorption Cross-Section
! INSTRUMENT:           GOME-2
! CHANNEL:              3
! VERSION:              2.0
! HISTORY:              IUP Bremen
! ORIGIN:
! REF_DOCUMENT:
! DATE:                 September 2005
! MODEL:                FM 3
! TEMPERATURE:          243K
! NUM_DIM:              2
! NUM_COLUMNS:          3
! NUM_ROWS:             1024
! IDL_FORMAT_CODE:      f7.4, E13.4, E13.4
! PARAMETER_COLUMN:
! COLUMN_LABEL_1:       wavelength (vac) (nm)
! COLUMN_LABEL_2:       sigma (cm^2)
! COLUMN_LABEL_3:       delta sigma (cm^2)
! END_OF_HEADER
```

GOME-2_FM3_O3_T243K_FPA4.DAT

```
! KEY_DATA_NAME:        GOME-2_FM3_O3_T243K_FPA4.DAT
! DESCRIPTION:          Absorption Cross-Section
! INSTRUMENT:           GOME-2
! CHANNEL:              4
! VERSION:              2.0
! HISTORY:              IUP Bremen
! ORIGIN:
! REF_DOCUMENT:
! DATE:                 September 2005
! MODEL:                FM 3
! TEMPERATURE:          243K
! NUM_DIM:              2
! NUM_COLUMNS:          3
! NUM_ROWS:             1024
! IDL_FORMAT_CODE:      f7.4, E13.4, E13.4
! PARAMETER_COLUMN:
! COLUMN_LABEL_1:       wavelength (vac) (nm)
! COLUMN_LABEL_2:       sigma (cm^2)
! COLUMN_LABEL_3:       delta sigma (cm^2)
! END_OF_HEADER
```

GOME-2_FM3_O3_T273K.DAT

```
! KEY_DATA_NAME:        GOME-2_FM3_O3_T273K.DAT
! DESCRIPTION:          Absorption Cross-Section
! INSTRUMENT:           GOME-2
! CHANNEL:              1-4
! VERSION:              2.0
! HISTORY:              IUP Bremen
! ORIGIN:
! REF_DOCUMENT:
! DATE:                 September 2005
! MODEL:                FM 3
! TEMPERATURE:          273K
! NUM_DIM:              2
! NUM_COLUMNS:          3
! NUM_ROWS:             3303
! IDL_FORMAT_CODE:      f7.4, E13.4, E13.4
! PARAMETER_COLUMN:
! COLUMN_LABEL_1:       wavelength (vac) (nm)
! COLUMN_LABEL_2:       sigma (cm^2)
! COLUMN_LABEL_3:       delta sigma (cm^2)
! END_OF_HEADER
```

GOME-2_FM3_O3_T273K_FPA1.DAT

```
! KEY_DATA_NAME:        GOME-2_FM3_O3_T273K_FPA1.DAT
! DESCRIPTION:          Absorption Cross-Section
! INSTRUMENT:           GOME-2
! CHANNEL:              1
! VERSION:              2.0
! HISTORY:              IUP Bremen
! ORIGIN:
! REF_DOCUMENT:
! DATE:                 September 2005
! MODEL:                FM 3
! TEMPERATURE:          273K
! NUM_DIM:              2
! NUM_COLUMNS:          3
! NUM_ROWS:             1024
! IDL_FORMAT_CODE:      f7.4, E13.4, E13.4
! PARAMETER_COLUMN:
! COLUMN_LABEL_1:       wavelength (vac) (nm)
! COLUMN_LABEL_2:       sigma (cm^2)
! COLUMN_LABEL_3:       delta sigma (cm^2)
! END_OF_HEADER
```

GOME-2_FM3_O3_T273K_FPA2.DAT

```
! KEY_DATA_NAME:        GOME-2_FM3_O3_T273K_FPA2.DAT
! DESCRIPTION:          Absorption Cross-Section
! INSTRUMENT:           GOME-2
! CHANNEL:              2
! VERSION:              2.0
! HISTORY:              IUP Bremen
! ORIGIN:
! REF_DOCUMENT:
! DATE:                 September 2005
! MODEL:                FM 3
! TEMPERATURE:          273K
! NUM_DIM:              2
! NUM_COLUMNS:          3
! NUM_ROWS:             1024
! IDL_FORMAT_CODE:      f7.4, E13.4, E13.4
! PARAMETER_COLUMN:
! COLUMN_LABEL_1:       wavelength (vac) (nm)
! COLUMN_LABEL_2:       sigma (cm^2)
! COLUMN_LABEL_3:       delta sigma (cm^2)
! END_OF_HEADER
```

GOME-2_FM3_O3_T273K_FPA3.DAT

```
! KEY_DATA_NAME:        GOME-2_FM3_O3_T273K_FPA3.DAT
! DESCRIPTION:          Absorption Cross-Section
! INSTRUMENT:           GOME-2
! CHANNEL:              3
! VERSION:              2.0
! HISTORY:              IUP Bremen
! ORIGIN:
! REF_DOCUMENT:
! DATE:                 September 2005
! MODEL:                FM 3
! TEMPERATURE:          273K
! NUM_DIM:              2
! NUM_COLUMNS:          3
! NUM_ROWS:             1024
! IDL_FORMAT_CODE:      f7.4, E13.4, E13.4
! PARAMETER_COLUMN:
! COLUMN_LABEL_1:       wavelength (vac) (nm)
! COLUMN_LABEL_2:       sigma (cm^2)
! COLUMN_LABEL_3:       delta sigma (cm^2)
! END_OF_HEADER
```

GOME-2_FM3_O3_T273K_FPA4.DAT

! KEY_DATA_NAME:	GOME-2_FM3_O3_T273K_FPA4.DAT
! DESCRIPTION:	Absorption Cross-Section
! INSTRUMENT:	GOME-2
! CHANNEL:	4
! VERSION:	2.0
! HISTORY:	IUP Bremen
! ORIGIN:	
! REF_DOCUMENT:	
! DATE:	September 2005
! MODEL:	FM 3
! TEMPERATURE:	273K
! NUM_DIM:	2
! NUM_COLUMNS:	3
! NUM_ROWS:	1024
! IDL_FORMAT_CODE:	f7.4, E13.4, E13.4
! PARAMETER_COLUMN:	
! COLUMN_LABEL_1:	wavelength (vac) (nm)
! COLUMN_LABEL_2:	sigma (cm^2)
! COLUMN_LABEL_3:	delta sigma (cm^2)
! END_OF_HEADER	

GOME-2_FM3_O3_T293K.DAT

! KEY_DATA_NAME:	GOME-2_FM3_O3_T293K.DAT
! DESCRIPTION:	Absorption Cross-Section
! INSTRUMENT:	GOME-2
! CHANNEL:	1-4
! VERSION:	2.0
! HISTORY:	IUP Bremen
! ORIGIN:	
! REF_DOCUMENT:	
! DATE:	September 2005
! MODEL:	FM 3
! TEMPERATURE:	293K
! NUM_DIM:	2
! NUM_COLUMNS:	3
! NUM_ROWS:	3303
! IDL_FORMAT_CODE:	f7.4, E13.4, E13.4
! PARAMETER_COLUMN:	
! COLUMN_LABEL_1:	wavelength (vac) (nm)
! COLUMN_LABEL_2:	sigma (cm^2)
! COLUMN_LABEL_3:	delta sigma (cm^2)
! END_OF_HEADER	

GOME-2_FM3_O3_T293K_FPA1.DAT

```
! KEY_DATA_NAME:        GOME-2_FM3_O3_T293K_FPA1.DAT
! DESCRIPTION:          Absorption Cross-Section
! INSTRUMENT:           GOME-2
! CHANNEL:              1
! VERSION:              2.0
! HISTORY:              IUP Bremen
! ORIGIN:
! REF_DOCUMENT:
! DATE:                 September 2005
! MODEL:                FM 3
! TEMPERATURE:          293K
! NUM_DIM:              2
! NUM_COLUMNS:          3
! NUM_ROWS:             1024
! IDL_FORMAT_CODE:      f7.4, E13.4, E13.4
! PARAMETER_COLUMN:
! COLUMN_LABEL_1:       wavelength (vac) (nm)
! COLUMN_LABEL_2:       sigma (cm^2)
! COLUMN_LABEL_3:       delta sigma (cm^2)
! END_OF_HEADER
```

GOME-2_FM3_O3_T293K_FPA2.DAT

```
! KEY_DATA_NAME:        GOME-2_FM3_O3_T293K_FPA2.DAT
! DESCRIPTION:          Absorption Cross-Section
! INSTRUMENT:           GOME-2
! CHANNEL:              2
! VERSION:              2.0
! HISTORY:              IUP Bremen
! ORIGIN:
! REF_DOCUMENT:
! DATE:                 September 2005
! MODEL:                FM 3
! TEMPERATURE:          293K
! NUM_DIM:              2
! NUM_COLUMNS:          3
! NUM_ROWS:             1024
! IDL_FORMAT_CODE:      f7.4, E13.4, E13.4
! PARAMETER_COLUMN:
! COLUMN_LABEL_1:       wavelength (vac) (nm)
! COLUMN_LABEL_2:       sigma (cm^2)
! COLUMN_LABEL_3:       delta sigma (cm^2)
! END_OF_HEADER
```

GOME-2_FM3_O3_T293K_FPA3.DAT

! KEY_DATA_NAME:	GOME-2_FM3_O3_T293K_FPA3.DAT
! DESCRIPTION:	Absorption Cross-Section
! INSTRUMENT:	GOME-2
! CHANNEL:	3
! VERSION:	2.0
! HISTORY:	IUP Bremen
! ORIGIN:	
! REF_DOCUMENT:	
! DATE:	September 2005
! MODEL:	FM 3
! TEMPERATURE:	293K
! NUM_DIM:	2
! NUM_COLUMNS:	3
! NUM_ROWS:	1024
! IDL_FORMAT_CODE:	f7.4, E13.4, E13.4
! PARAMETER_COLUMN:	
! COLUMN_LABEL_1:	wavelength (vac) (nm)
! COLUMN_LABEL_2:	sigma (cm^2)
! COLUMN_LABEL_3:	delta sigma (cm^2)
! END_OF_HEADER	

GOME-2_FM3_O3_T293K_FPA4.DAT

! KEY_DATA_NAME:	GOME-2_FM3_O3_T293K_FPA4.DAT
! DESCRIPTION:	Absorption Cross-Section
! INSTRUMENT:	GOME-2
! CHANNEL:	4
! VERSION:	2.0
! HISTORY:	IUP Bremen
! ORIGIN:	
! REF_DOCUMENT:	
! DATE:	September 2005
! MODEL:	FM 3
! TEMPERATURE:	293K
! NUM_DIM:	2
! NUM_COLUMNS:	3
! NUM_ROWS:	1024
! IDL_FORMAT_CODE:	f7.4, E13.4, E13.4
! PARAMETER_COLUMN:	
! COLUMN_LABEL_1:	wavelength (vac) (nm)
! COLUMN_LABEL_2:	sigma (cm^2)
! COLUMN_LABEL_3:	delta sigma (cm^2)
! END_OF_HEADER	

GOME-2_FM2-1_NO2_T223K.DAT

```
! KEY_DATA_NAME:        GOME-2_FM2-1_NO2_T223K.DAT
! DESCRIPTION:          Absorption Cross-Section
! INSTRUMENT:           GOME-2
! CHANNEL:              1-4
! VERSION:              2.0
! HISTORY:              IUP Bremen
! ORIGIN:
! REF_DOCUMENT:
! DATE:                 September 2005
! MODEL:                FM 2-1
! TEMPERATURE:          223K
! NUM_DIM:              2
! NUM_COLUMNS:          3
! NUM_ROWS:             3256
! IDL_FORMAT_CODE:      f7.4, E13.4, E13.4
! PARAMETER_COLUMN:
! COLUMN_LABEL_1:       wavelength (vac) (nm)
! COLUMN_LABEL_2:       sigma (cm^2)
! COLUMN_LABEL_3:       delta sigma (cm^2)
! END_OF_HEADER
```

GOME-2_FM2-1_NO2_T223K_FPA1.DAT

```
! KEY_DATA_NAME:        GOME-2_FM2-1_NO2_T223K_FPA1.DAT
! DESCRIPTION:          Absorption Cross-Section
! INSTRUMENT:           GOME-2
! CHANNEL:              1
! VERSION:              2.0
! HISTORY:              IUP Bremen
! ORIGIN:
! REF_DOCUMENT:
! DATE:                 September 2005
! MODEL:                FM 2-1
! TEMPERATURE:          223K
! NUM_DIM:              2
! NUM_COLUMNS:          3
! NUM_ROWS:             1024
! IDL_FORMAT_CODE:      f7.4, E13.4, E13.4
! PARAMETER_COLUMN:
! COLUMN_LABEL_1:       wavelength (vac) (nm)
! COLUMN_LABEL_2:       sigma (cm^2)
! COLUMN_LABEL_3:       delta sigma (cm^2)
! END_OF_HEADER
```

GOME-2_FM2-1_NO2_T223K_FPA2.DAT

```
! KEY_DATA_NAME:        GOME-2_FM2-1_NO2_T223K_FPA2.DAT
! DESCRIPTION:          Absorption Cross-Section
! INSTRUMENT:           GOME-2
! CHANNEL:              2
! VERSION:              2.0
! HISTORY:              IUP Bremen
! ORIGIN:
! REF_DOCUMENT:
! DATE:                 September 2005
! MODEL:                FM 2-1
! TEMPERATURE:          223K
! NUM_DIM:              2
! NUM_COLUMNS:          3
! NUM_ROWS:             1024
! IDL_FORMAT_CODE:      f7.4, E13.4, E13.4
! PARAMETER_COLUMN:
! COLUMN_LABEL_1:       wavelength (vac) (nm)
! COLUMN_LABEL_2:       sigma (cm^2)
! COLUMN_LABEL_3:       delta sigma (cm^2)
! END_OF_HEADER
```

GOME-2_FM2-1_NO2_T223K_FPA3.DAT

```
! KEY_DATA_NAME:        GOME-2_FM2-1_NO2_T223K_FPA3.DAT
! DESCRIPTION:          Absorption Cross-Section
! INSTRUMENT:           GOME-2
! CHANNEL:              3
! VERSION:              2.0
! HISTORY:              IUP Bremen
! ORIGIN:
! REF_DOCUMENT:
! DATE:                 September 2005
! MODEL:                FM 2-1
! TEMPERATURE:          223K
! NUM_DIM:              2
! NUM_COLUMNS:          3
! NUM_ROWS:             1024
! IDL_FORMAT_CODE:      f7.4, E13.4, E13.4
! PARAMETER_COLUMN:
! COLUMN_LABEL_1:       wavelength (vac) (nm)
! COLUMN_LABEL_2:       sigma (cm^2)
! COLUMN_LABEL_3:       delta sigma (cm^2)
! END_OF_HEADER
```

GOME-2_FM2-1_NO2_T223K_FPA4.DAT

! KEY_DATA_NAME:	GOME-2_FM2-1_NO2_T223K_FPA4.DAT
! DESCRIPTION:	Absorption Cross-Section
! INSTRUMENT:	GOME-2
! CHANNEL:	4
! VERSION:	2.0
! HISTORY:	IUP Bremen
! ORIGIN:	
! REF_DOCUMENT:	
! DATE:	September 2005
! MODEL:	FM 2-1
! TEMPERATURE:	223K
! NUM_DIM:	2
! NUM_COLUMNS:	3
! NUM_ROWS:	1024
! IDL_FORMAT_CODE:	f7.4, E13.4, E13.4
! PARAMETER_COLUMN:	
! COLUMN_LABEL_1:	wavelength (vac) (nm)
! COLUMN_LABEL_2:	sigma (cm^2)
! COLUMN_LABEL_3:	delta sigma (cm^2)
! END_OF_HEADER	

GOME-2_FM2-1_NO2_T243K.DAT

! KEY_DATA_NAME:	GOME-2_FM2-1_NO2_T243K.DAT
! DESCRIPTION:	Absorption Cross-Section
! INSTRUMENT:	GOME-2
! CHANNEL:	1-4
! VERSION:	2.0
! HISTORY:	IUP Bremen
! ORIGIN:	
! REF_DOCUMENT:	
! DATE:	September 2005
! MODEL:	FM 2-1
! TEMPERATURE:	243K
! NUM_DIM:	2
! NUM_COLUMNS:	3
! NUM_ROWS:	3256
! IDL_FORMAT_CODE:	f7.4, E13.4, E13.4
! PARAMETER_COLUMN:	
! COLUMN_LABEL_1:	wavelength (vac) (nm)
! COLUMN_LABEL_2:	sigma (cm^2)
! COLUMN_LABEL_3:	delta sigma (cm^2)
! END_OF_HEADER	

GOME-2_FM2-1_NO2_T243K_FPA1.DAT

```
! KEY_DATA_NAME:        GOME-2_FM2-1_NO2_T243K_FPA1.DAT
! DESCRIPTION:          Absorption Cross-Section
! INSTRUMENT:           GOME-2
! CHANNEL:              1
! VERSION:              2.0
! HISTORY:              IUP Bremen
! ORIGIN:
! REF_DOCUMENT:
! DATE:                 September 2005
! MODEL:                FM 2-1
! TEMPERATURE:          243K
! NUM_DIM:              2
! NUM_COLUMNS:          3
! NUM_ROWS:             1024
! IDL_FORMAT_CODE:      f7.4, E13.4, E13.4
! PARAMETER_COLUMN:
! COLUMN_LABEL_1:       wavelength (vac) (nm)
! COLUMN_LABEL_2:       sigma (cm^2)
! COLUMN_LABEL_3:       delta sigma (cm^2)
! END_OF_HEADER
```

GOME-2_FM2-1_NO2_T243K_FPA2.DAT

```
! KEY_DATA_NAME:        GOME-2_FM2-1_NO2_T243K_FPA2.DAT
! DESCRIPTION:          Absorption Cross-Section
! INSTRUMENT:           GOME-2
! CHANNEL:              2
! VERSION:              2.0
! HISTORY:              IUP Bremen
! ORIGIN:
! REF_DOCUMENT:
! DATE:                 September 2005
! MODEL:                FM 2-1
! TEMPERATURE:          243K
! NUM_DIM:              2
! NUM_COLUMNS:          3
! NUM_ROWS:             1024
! IDL_FORMAT_CODE:      f7.4, E13.4, E13.4
! PARAMETER_COLUMN:
! COLUMN_LABEL_1:       wavelength (vac) (nm)
! COLUMN_LABEL_2:       sigma (cm^2)
! COLUMN_LABEL_3:       delta sigma (cm^2)
! END_OF_HEADER
```

GOME-2_FM2-1_NO2_T243K_FPA3.DAT

```
! KEY_DATA_NAME:        GOME-2_FM2-1_NO2_T243K_FPA3.DAT
! DESCRIPTION:          Absorption Cross-Section
! INSTRUMENT:           GOME-2
! CHANNEL:              3
! VERSION:              2.0
! HISTORY:              IUP Bremen
! ORIGIN:
! REF_DOCUMENT:
! DATE:                 September 2005
! MODEL:                FM 2-1
! TEMPERATURE:          243K
! NUM_DIM:              2
! NUM_COLUMNS:          3
! NUM_ROWS:             1024
! IDL_FORMAT_CODE:      f7.4, E13.4, E13.4
! PARAMETER_COLUMN:
! COLUMN_LABEL_1:       wavelength (vac) (nm)
! COLUMN_LABEL_2:       sigma (cm^2)
! COLUMN_LABEL_3:       delta sigma (cm^2)
! END_OF_HEADER
```

GOME-2_FM2-1_NO2_T243K_FPA4.DAT

```
! KEY_DATA_NAME:        GOME-2_FM2-1_NO2_T243K_FPA4.DAT
! DESCRIPTION:          Absorption Cross-Section
! INSTRUMENT:           GOME-2
! CHANNEL:              4
! VERSION:              2.0
! HISTORY:              IUP Bremen
! ORIGIN:
! REF_DOCUMENT:
! DATE:                 September 2005
! MODEL:                FM 2-1
! TEMPERATURE:          243K
! NUM_DIM:              2
! NUM_COLUMNS:          3
! NUM_ROWS:             1024
! IDL_FORMAT_CODE:      f7.4, E13.4, E13.4
! PARAMETER_COLUMN:
! COLUMN_LABEL_1:       wavelength (vac) (nm)
! COLUMN_LABEL_2:       sigma (cm^2)
! COLUMN_LABEL_3:       delta sigma (cm^2)
! END_OF_HEADER
```

GOME-2_FM2-1_NO2_T273K.DAT

! KEY_DATA_NAME:	GOME-2_FM2-1_NO2_T273K.DAT
! DESCRIPTION:	Absorption Cross-Section
! INSTRUMENT:	GOME-2
! CHANNEL:	1-4
! VERSION:	2.0
! HISTORY:	IUP Bremen
! ORIGIN:	
! REF_DOCUMENT:	
! DATE:	September 2005
! MODEL:	FM 2-1
! TEMPERATURE:	273K
! NUM_DIM:	2
! NUM_COLUMNS:	3
! NUM_ROWS:	3256
! IDL_FORMAT_CODE:	f7.4, E13.4, E13.4
! PARAMETER_COLUMN:	
! COLUMN_LABEL_1:	wavelength (vac) (nm)
! COLUMN_LABEL_2:	sigma (cm^2)
! COLUMN_LABEL_3:	delta sigma (cm^2)
! END_OF_HEADER	

GOME-2_FM2-1_NO2_T273K_FPA1.DAT

! KEY_DATA_NAME:	GOME-2_FM2-1_NO2_T273K_FPA1.DAT
! DESCRIPTION:	Absorption Cross-Section
! INSTRUMENT:	GOME-2
! CHANNEL:	1
! VERSION:	2.0
! HISTORY:	IUP Bremen
! ORIGIN:	
! REF_DOCUMENT:	
! DATE:	September 2005
! MODEL:	FM 2-1
! TEMPERATURE:	273K
! NUM_DIM:	2
! NUM_COLUMNS:	3
! NUM_ROWS:	1024
! IDL_FORMAT_CODE:	f7.4, E13.4, E13.4
! PARAMETER_COLUMN:	
! COLUMN_LABEL_1:	wavelength (vac) (nm)
! COLUMN_LABEL_2:	sigma (cm^2)
! COLUMN_LABEL_3:	delta sigma (cm^2)
! END_OF_HEADER	

GOME-2_FM2-1_NO2_T273K_FPA2.DAT

```
! KEY_DATA_NAME:        GOME-2_FM2-1_NO2_T273K_FPA2.DAT
! DESCRIPTION:          Absorption Cross-Section
! INSTRUMENT:           GOME-2
! CHANNEL:              2
! VERSION:              2.0
! HISTORY:              IUP Bremen
! ORIGIN:
! REF_DOCUMENT:
! DATE:                 September 2005
! MODEL:                FM 2-1
! TEMPERATURE:          273K
! NUM_DIM:              2
! NUM_COLUMNS:          3
! NUM_ROWS:             1024
! IDL_FORMAT_CODE:      f7.4, E13.4, E13.4
! PARAMETER_COLUMN:
! COLUMN_LABEL_1:       wavelength (vac) (nm)
! COLUMN_LABEL_2:       sigma (cm^2)
! COLUMN_LABEL_3:       delta sigma (cm^2)
! END_OF_HEADER
```

GOME-2_FM2-1_NO2_T273K_FPA3.DAT

```
! KEY_DATA_NAME:        GOME-2_FM2-1_NO2_T273K_FPA3.DAT
! DESCRIPTION:          Absorption Cross-Section
! INSTRUMENT:           GOME-2
! CHANNEL:              3
! VERSION:              2.0
! HISTORY:              IUP Bremen
! ORIGIN:
! REF_DOCUMENT:
! DATE:                 September 2005
! MODEL:                FM 2-1
! TEMPERATURE:          273K
! NUM_DIM:              2
! NUM_COLUMNS:          3
! NUM_ROWS:             1024
! IDL_FORMAT_CODE:      f7.4, E13.4, E13.4
! PARAMETER_COLUMN:
! COLUMN_LABEL_1:       wavelength (vac) (nm)
! COLUMN_LABEL_2:       sigma (cm^2)
! COLUMN_LABEL_3:       delta sigma (cm^2)
! END_OF_HEADER
```

GOME-2_FM2-1_NO2_T273K_FPA4.DAT

! KEY_DATA_NAME:	GOME-2_FM2-1_NO2_T273K_FPA4.DAT
! DESCRIPTION:	Absorption Cross-Section
! INSTRUMENT:	GOME-2
! CHANNEL:	4
! VERSION:	2.0
! HISTORY:	IUP Bremen
! ORIGIN:	
! REF_DOCUMENT:	
! DATE:	September 2005
! MODEL:	FM 2-1
! TEMPERATURE:	273K
! NUM_DIM:	2
! NUM_COLUMNS:	3
! NUM_ROWS:	1024
! IDL_FORMAT_CODE:	f7.4, E13.4, E13.4
! PARAMETER_COLUMN:	
! COLUMN_LABEL_1:	wavelength (vac) (nm)
! COLUMN_LABEL_2:	sigma (cm^2)
! COLUMN_LABEL_3:	delta sigma (cm^2)
! END_OF_HEADER	

GOME-2_FM2-1_NO2_T293K.DAT

! KEY_DATA_NAME:	GOME-2_FM2-1_NO2_T293K.DAT
! DESCRIPTION:	Absorption Cross-Section
! INSTRUMENT:	GOME-2
! CHANNEL:	1-4
! VERSION:	2.0
! HISTORY:	IUP Bremen
! ORIGIN:	
! REF_DOCUMENT:	
! DATE:	September 2005
! MODEL:	FM 2-1
! TEMPERATURE:	293K
! NUM_DIM:	2
! NUM_COLUMNS:	3
! NUM_ROWS:	3256
! IDL_FORMAT_CODE:	f7.4, E13.4, E13.4
! PARAMETER_COLUMN:	
! COLUMN_LABEL_1:	wavelength (vac) (nm)
! COLUMN_LABEL_2:	sigma (cm^2)
! COLUMN_LABEL_3:	delta sigma (cm^2)
! END_OF_HEADER	

GOME-2_FM2-1_NO2_T293K_FPA1.DAT

! KEY_DATA_NAME:	GOME-2_FM2-1_NO2_T293K_FPA1.DAT
! DESCRIPTION:	Absorption Cross-Section
! INSTRUMENT:	GOME-2
! CHANNEL:	1
! VERSION:	2.0
! HISTORY:	IUP Bremen
! ORIGIN:	
! REF_DOCUMENT:	
! DATE:	September 2005
! MODEL:	FM 2-1
! TEMPERATURE:	293K
! NUM_DIM:	2
! NUM_COLUMNS:	3
! NUM_ROWS:	1024
! IDL_FORMAT_CODE:	f7.4, E13.4, E13.4
! PARAMETER_COLUMN:	
! COLUMN_LABEL_1:	wavelength (vac) (nm)
! COLUMN_LABEL_2:	sigma (cm^2)
! COLUMN_LABEL_3:	delta sigma (cm^2)
! END_OF_HEADER	

GOME-2_FM2-1_NO2_T293K_FPA2.DAT

! KEY_DATA_NAME:	GOME-2_FM2-1_NO2_T293K_FPA2.DAT
! DESCRIPTION:	Absorption Cross-Section
! INSTRUMENT:	GOME-2
! CHANNEL:	2
! VERSION:	2.0
! HISTORY:	IUP Bremen
! ORIGIN:	
! REF_DOCUMENT:	
! DATE:	September 2005
! MODEL:	FM 2-1
! TEMPERATURE:	293K
! NUM_DIM:	2
! NUM_COLUMNS:	3
! NUM_ROWS:	1024
! IDL_FORMAT_CODE:	f7.4, E13.4, E13.4
! PARAMETER_COLUMN:	
! COLUMN_LABEL_1:	wavelength (vac) (nm)
! COLUMN_LABEL_2:	sigma (cm^2)
! COLUMN_LABEL_3:	delta sigma (cm^2)
! END_OF_HEADER	

GOME-2_FM2-1_NO2_T293K_FPA3.DAT

! KEY_DATA_NAME:	GOME-2_FM2-1_NO2_T293K_FPA3.DAT
! DESCRIPTION:	Absorption Cross-Section
! INSTRUMENT:	GOME-2
! CHANNEL:	3
! VERSION:	2.0
! HISTORY:	IUP Bremen
! ORIGIN:	
! REF_DOCUMENT:	
! DATE:	September 2005
! MODEL:	FM 2-1
! TEMPERATURE:	293K
! NUM_DIM:	2
! NUM_COLUMNS:	3
! NUM_ROWS:	1024
! IDL_FORMAT_CODE:	f7.4, E13.4, E13.4
! PARAMETER_COLUMN:	
! COLUMN_LABEL_1:	wavelength (vac) (nm)
! COLUMN_LABEL_2:	sigma (cm^2)
! COLUMN_LABEL_3:	delta sigma (cm^2)
! END_OF_HEADER	

GOME-2_FM2-1_NO2_T293K_FPA4.DAT

! KEY_DATA_NAME:	GOME-2_FM2-1_NO2_T293K_FPA4.DAT
! DESCRIPTION:	Absorption Cross-Section
! INSTRUMENT:	GOME-2
! CHANNEL:	4
! VERSION:	2.0
! HISTORY:	IUP Bremen
! ORIGIN:	
! REF_DOCUMENT:	
! DATE:	September 2005
! MODEL:	FM 2-1
! TEMPERATURE:	293K
! NUM_DIM:	2
! NUM_COLUMNS:	3
! NUM_ROWS:	1024
! IDL_FORMAT_CODE:	f7.4, E13.4, E13.4
! PARAMETER_COLUMN:	
! COLUMN_LABEL_1:	wavelength (vac) (nm)
! COLUMN_LABEL_2:	sigma (cm^2)
! COLUMN_LABEL_3:	delta sigma (cm^2)
! END_OF_HEADER	

GOME-2_FM3_NO2_T223K.DAT

```
! KEY_DATA_NAME:        GOME-2_FM3_NO2_T223K.DAT
! DESCRIPTION:          Absorption Cross-Section
! INSTRUMENT:           GOME-2
! CHANNEL:              1-4
! VERSION:              2.0
! HISTORY:              IUP Bremen
! ORIGIN:
! REF_DOCUMENT:
! DATE:                 September 2005
! MODEL:                FM 3
! TEMPERATURE:          223K
! NUM_DIM:              2
! NUM_COLUMNS:          3
! NUM_ROWS:             3294
! IDL_FORMAT_CODE:      f7.4, E13.4, E13.4
! PARAMETER_COLUMN:
! COLUMN_LABEL_1:       wavelength (vac) (nm)
! COLUMN_LABEL_2:       sigma (cm^2)
! COLUMN_LABEL_3:       delta sigma (cm^2)
! END_OF_HEADER
```

GOME-2_FM3_NO2_T223K_FPA1.DAT

```
! KEY_DATA_NAME:        GOME-2_FM3_NO2_T223K_FPA1.DAT
! DESCRIPTION:          Absorption Cross-Section
! INSTRUMENT:           GOME-2
! CHANNEL:              1
! VERSION:              2.0
! HISTORY:              IUP Bremen
! ORIGIN:
! REF_DOCUMENT:
! DATE:                 September 2005
! MODEL:                FM 3
! TEMPERATURE:          223K
! NUM_DIM:              2
! NUM_COLUMNS:          3
! NUM_ROWS:             1024
! IDL_FORMAT_CODE:      f7.4, E13.4, E13.4
! PARAMETER_COLUMN:
! COLUMN_LABEL_1:       wavelength (vac) (nm)
! COLUMN_LABEL_2:       sigma (cm^2)
! COLUMN_LABEL_3:       delta sigma (cm^2)
! END_OF_HEADER
```

GOME-2_FM3_NO2_T223K_FPA2.DAT

```
! KEY_DATA_NAME:        GOME-2_FM3_NO2_T223K_FPA2.DAT
! DESCRIPTION:          Absorption Cross-Section
! INSTRUMENT:           GOME-2
! CHANNEL:              2
! VERSION:              2.0
! HISTORY:              IUP Bremen
! ORIGIN:
! REF_DOCUMENT:
! DATE:                 September 2005
! MODEL:                FM 3
! TEMPERATURE:          223K
! NUM_DIM:              2
! NUM_COLUMNS:          3
! NUM_ROWS:             1024
! IDL_FORMAT_CODE:      f7.4, E13.4, E13.4
! PARAMETER_COLUMN:
! COLUMN_LABEL_1:       wavelength (vac) (nm)
! COLUMN_LABEL_2:       sigma (cm^2)
! COLUMN_LABEL_3:       delta sigma (cm^2)
! END_OF_HEADER
```

GOME-2_FM3_NO2_T223K_FPA3.DAT

```
! KEY_DATA_NAME:        GOME-2_FM3_NO2_T223K_FPA3.DAT
! DESCRIPTION:          Absorption Cross-Section
! INSTRUMENT:           GOME-2
! CHANNEL:              3
! VERSION:              2.0
! HISTORY:              IUP Bremen
! ORIGIN:
! REF_DOCUMENT:
! DATE:                 September 2005
! MODEL:                FM 3
! TEMPERATURE:          223K
! NUM_DIM:              2
! NUM_COLUMNS:          3
! NUM_ROWS:             1024
! IDL_FORMAT_CODE:      f7.4, E13.4, E13.4
! PARAMETER_COLUMN:
! COLUMN_LABEL_1:       wavelength (vac) (nm)
! COLUMN_LABEL_2:       sigma (cm^2)
! COLUMN_LABEL_3:       delta sigma (cm^2)
! END_OF_HEADER
```

GOME-2_FM3_NO2_T223K_FPA4.DAT

```
! KEY_DATA_NAME:        GOME-2_FM3_NO2_T223K_FPA4.DAT
! DESCRIPTION:          Absorption Cross-Section
! INSTRUMENT:           GOME-2
! CHANNEL:              4
! VERSION:              2.0
! HISTORY:              IUP Bremen
! ORIGIN:
! REF_DOCUMENT:
! DATE:                 September 2005
! MODEL:                FM 3
! TEMPERATURE:          223K
! NUM_DIM:              2
! NUM_COLUMNS:          3
! NUM_ROWS:             1024
! IDL_FORMAT_CODE:      f7.4, E13.4, E13.4
! PARAMETER_COLUMN:
! COLUMN_LABEL_1:       wavelength (vac) (nm)
! COLUMN_LABEL_2:       sigma (cm^2)
! COLUMN_LABEL_3:       delta sigma (cm^2)
! END_OF_HEADER
```

GOME-2_FM3_NO2_T243K.DAT

```
! KEY_DATA_NAME:        GOME-2_FM3_NO2_T243K.DAT
! DESCRIPTION:          Absorption Cross-Section
! INSTRUMENT:           GOME-2
! CHANNEL:              1-4
! VERSION:              2.0
! HISTORY:              IUP Bremen
! ORIGIN:
! REF_DOCUMENT:
! DATE:                 September 2005
! MODEL:                FM 3
! TEMPERATURE:          243K
! NUM_DIM:              2
! NUM_COLUMNS:          3
! NUM_ROWS:             3294
! IDL_FORMAT_CODE:      f7.4, E13.4, E13.4
! PARAMETER_COLUMN:
! COLUMN_LABEL_1:       wavelength (vac) (nm)
! COLUMN_LABEL_2:       sigma (cm^2)
! COLUMN_LABEL_3:       delta sigma (cm^2)
! END_OF_HEADER
```

GOME-2_FM3_NO2_T243K_FPA1.DAT

! KEY_DATA_NAME:	GOME-2_FM3_NO2_T243K_FPA1.DAT
! DESCRIPTION:	Absorption Cross-Section
! INSTRUMENT:	GOME-2
! CHANNEL:	1
! VERSION:	2.0
! HISTORY:	IUP Bremen
! ORIGIN:	
! REF_DOCUMENT:	
! DATE:	September 2005
! MODEL:	FM 3
! TEMPERATURE:	243K
! NUM_DIM:	2
! NUM_COLUMNS:	3
! NUM_ROWS:	1024
! IDL_FORMAT_CODE:	f7.4, E13.4, E13.4
! PARAMETER_COLUMN:	
! COLUMN_LABEL_1:	wavelength (vac) (nm)
! COLUMN_LABEL_2:	sigma (cm^2)
! COLUMN_LABEL_3:	delta sigma (cm^2)
! END_OF_HEADER	

GOME-2_FM3_NO2_T243K_FPA2.DAT

! KEY_DATA_NAME:	GOME-2_FM3_NO2_T243K_FPA2.DAT
! DESCRIPTION:	Absorption Cross-Section
! INSTRUMENT:	GOME-2
! CHANNEL:	2
! VERSION:	2.0
! HISTORY:	IUP Bremen
! ORIGIN:	
! REF_DOCUMENT:	
! DATE:	September 2005
! MODEL:	FM 3
! TEMPERATURE:	243K
! NUM_DIM:	2
! NUM_COLUMNS:	3
! NUM_ROWS:	1024
! IDL_FORMAT_CODE:	f7.4, E13.4, E13.4
! PARAMETER_COLUMN:	
! COLUMN_LABEL_1:	wavelength (vac) (nm)
! COLUMN_LABEL_2:	sigma (cm^2)
! COLUMN_LABEL_3:	delta sigma (cm^2)
! END_OF_HEADER	

GOME-2_FM3_NO2_T243K_FPA3.DAT

```
! KEY_DATA_NAME:        GOME-2_FM3_NO2_T243K_FPA3.DAT
! DESCRIPTION:          Absorption Cross-Section
! INSTRUMENT:           GOME-2
! CHANNEL:              3
! VERSION:              2.0
! HISTORY:              IUP Bremen
! ORIGIN:
! REF_DOCUMENT:
! DATE:                 September 2005
! MODEL:                FM 3
! TEMPERATURE:          243K
! NUM_DIM:              2
! NUM_COLUMNS:          3
! NUM_ROWS:             1024
! IDL_FORMAT_CODE:      f7.4, E13.4, E13.4
! PARAMETER_COLUMN:
! COLUMN_LABEL_1:       wavelength (vac) (nm)
! COLUMN_LABEL_2:       sigma (cm^2)
! COLUMN_LABEL_3:       delta sigma (cm^2)
! END_OF_HEADER
```

GOME-2_FM3_NO2_T243K_FPA4.DAT

```
! KEY_DATA_NAME:        GOME-2_FM3_NO2_T243K_FPA4.DAT
! DESCRIPTION:          Absorption Cross-Section
! INSTRUMENT:           GOME-2
! CHANNEL:              4
! VERSION:              2.0
! HISTORY:              IUP Bremen
! ORIGIN:
! REF_DOCUMENT:
! DATE:                 September 2005
! MODEL:                FM 3
! TEMPERATURE:          243K
! NUM_DIM:              2
! NUM_COLUMNS:          3
! NUM_ROWS:             1024
! IDL_FORMAT_CODE:      f7.4, E13.4, E13.4
! PARAMETER_COLUMN:
! COLUMN_LABEL_1:       wavelength (vac) (nm)
! COLUMN_LABEL_2:       sigma (cm^2)
! COLUMN_LABEL_3:       delta sigma (cm^2)
! END_OF_HEADER
```

GOME-2_FM3_NO2_T273K.DAT

! KEY_DATA_NAME:	GOME-2_FM3_NO2_T273K.DAT
! DESCRIPTION:	Absorption Cross-Section
! INSTRUMENT:	GOME-2
! CHANNEL:	1-4
! VERSION:	2.0
! HISTORY:	IUP Bremen
! ORIGIN:	
! REF_DOCUMENT:	
! DATE:	September 2005
! MODEL:	FM 3
! TEMPERATURE:	273K
! NUM_DIM:	2
! NUM_COLUMNS:	3
! NUM_ROWS:	3294
! IDL_FORMAT_CODE:	f7.4, E13.4, E13.4
! PARAMETER_COLUMN:	
! COLUMN_LABEL_1:	wavelength (vac) (nm)
! COLUMN_LABEL_2:	sigma (cm^2)
! COLUMN_LABEL_3:	delta sigma (cm^2)
! END_OF_HEADER	

GOME-2_FM3_NO2_T273K_FPA1.DAT

! KEY_DATA_NAME:	GOME-2_FM3_NO2_T273K_FPA1.DAT
! DESCRIPTION:	Absorption Cross-Section
! INSTRUMENT:	GOME-2
! CHANNEL:	1
! VERSION:	2.0
! HISTORY:	IUP Bremen
! ORIGIN:	
! REF_DOCUMENT:	
! DATE:	September 2005
! MODEL:	FM 3
! TEMPERATURE:	273K
! NUM_DIM:	2
! NUM_COLUMNS:	3
! NUM_ROWS:	1024
! IDL_FORMAT_CODE:	f7.4, E13.4, E13.4
! PARAMETER_COLUMN:	
! COLUMN_LABEL_1:	wavelength (vac) (nm)
! COLUMN_LABEL_2:	sigma (cm^2)
! COLUMN_LABEL_3:	delta sigma (cm^2)
! END_OF_HEADER	

GOME-2_FM3_NO2_T273K_FPA2.DAT

```
! KEY_DATA_NAME:        GOME-2_FM3_NO2_T273K_FPA2.DAT
! DESCRIPTION:          Absorption Cross-Section
! INSTRUMENT:           GOME-2
! CHANNEL:              2
! VERSION:              2.0
! HISTORY:              IUP Bremen
! ORIGIN:
! REF_DOCUMENT:
! DATE:                 September 2005
! MODEL:                FM 3
! TEMPERATURE:          273K
! NUM_DIM:              2
! NUM_COLUMNS:          3
! NUM_ROWS:             1024
! IDL_FORMAT_CODE:      f7.4, E13.4, E13.4
! PARAMETER_COLUMN:
! COLUMN_LABEL_1:       wavelength (vac) (nm)
! COLUMN_LABEL_2:       sigma (cm^2)
! COLUMN_LABEL_3:       delta sigma (cm^2)
! END_OF_HEADER
```

GOME-2_FM3_NO2_T273K_FPA3.DAT

```
! KEY_DATA_NAME:        GOME-2_FM3_NO2_T273K_FPA3.DAT
! DESCRIPTION:          Absorption Cross-Section
! INSTRUMENT:           GOME-2
! CHANNEL:              3
! VERSION:              2.0
! HISTORY:              IUP Bremen
! ORIGIN:
! REF_DOCUMENT:
! DATE:                 September 2005
! MODEL:                FM 3
! TEMPERATURE:          273K
! NUM_DIM:              2
! NUM_COLUMNS:          3
! NUM_ROWS:             1024
! IDL_FORMAT_CODE:      f7.4, E13.4, E13.4
! PARAMETER_COLUMN:
! COLUMN_LABEL_1:       wavelength (vac) (nm)
! COLUMN_LABEL_2:       sigma (cm^2)
! COLUMN_LABEL_3:       delta sigma (cm^2)
! END_OF_HEADER
```

GOME-2_FM3_NO2_T273K_FPA4.DAT

! KEY_DATA_NAME:	GOME-2_FM3_NO2_T273K_FPA4.DAT
! DESCRIPTION:	Absorption Cross-Section
! INSTRUMENT:	GOME-2
! CHANNEL:	4
! VERSION:	2.0
! HISTORY:	IUP Bremen
! ORIGIN:	
! REF_DOCUMENT:	
! DATE:	September 2005
! MODEL:	FM 3
! TEMPERATURE:	273K
! NUM_DIM:	2
! NUM_COLUMNS:	3
! NUM_ROWS:	1024
! IDL_FORMAT_CODE:	f7.4, E13.4, E13.4
! PARAMETER_COLUMN:	
! COLUMN_LABEL_1:	wavelength (vac) (nm)
! COLUMN_LABEL_2:	sigma (cm^2)
! COLUMN_LABEL_3:	delta sigma (cm^2)
! END_OF_HEADER	

GOME-2_FM3_NO2_T293K.DAT

! KEY_DATA_NAME:	GOME-2_FM3_NO2_T293K.DAT
! DESCRIPTION:	Absorption Cross-Section
! INSTRUMENT:	GOME-2
! CHANNEL:	1-4
! VERSION:	2.0
! HISTORY:	IUP Bremen
! ORIGIN:	
! REF_DOCUMENT:	
! DATE:	September 2005
! MODEL:	FM 3
! TEMPERATURE:	293K
! NUM_DIM:	2
! NUM_COLUMNS:	3
! NUM_ROWS:	3294
! IDL_FORMAT_CODE:	f7.4, E13.4, E13.4
! PARAMETER_COLUMN:	
! COLUMN_LABEL_1:	wavelength (vac) (nm)
! COLUMN_LABEL_2:	sigma (cm^2)
! COLUMN_LABEL_3:	delta sigma (cm^2)
! END_OF_HEADER	

GOME-2_FM3_NO2_T293K_FPA1.DAT

```
! KEY_DATA_NAME:        GOME-2_FM3_NO2_T293K_FPA1.DAT
! DESCRIPTION:          Absorption Cross-Section
! INSTRUMENT:           GOME-2
! CHANNEL:              1
! VERSION:              2.0
! HISTORY:              IUP Bremen
! ORIGIN:
! REF_DOCUMENT:
! DATE:                 September 2005
! MODEL:                FM 3
! TEMPERATURE:          293K
! NUM_DIM:              2
! NUM_COLUMNS:          3
! NUM_ROWS:             1024
! IDL_FORMAT_CODE:      f7.4, E13.4, E13.4
! PARAMETER_COLUMN:
! COLUMN_LABEL_1:       wavelength (vac) (nm)
! COLUMN_LABEL_2:       sigma (cm^2)
! COLUMN_LABEL_3:       delta sigma (cm^2)
! END_OF_HEADER
```

GOME-2_FM3_NO2_T293K_FPA2.DAT

```
! KEY_DATA_NAME:        GOME-2_FM3_NO2_T293K_FPA2.DAT
! DESCRIPTION:          Absorption Cross-Section
! INSTRUMENT:           GOME-2
! CHANNEL:              2
! VERSION:              2.0
! HISTORY:              IUP Bremen
! ORIGIN:
! REF_DOCUMENT:
! DATE:                 September 2005
! MODEL:                FM 3
! TEMPERATURE:          293K
! NUM_DIM:              2
! NUM_COLUMNS:          3
! NUM_ROWS:             1024
! IDL_FORMAT_CODE:      f7.4, E13.4, E13.4
! PARAMETER_COLUMN:
! COLUMN_LABEL_1:       wavelength (vac) (nm)
! COLUMN_LABEL_2:       sigma (cm^2)
! COLUMN_LABEL_3:       delta sigma (cm^2)
! END_OF_HEADER
```

GOME-2_FM3_NO2_T293K_FPA3.DAT

```
! KEY_DATA_NAME:       GOME-2_FM3_NO2_T293K_FPA3.DAT
! DESCRIPTION:         Absorption Cross-Section
! INSTRUMENT:          GOME-2
! CHANNEL:             3
! VERSION:             2.0
! HISTORY:             IUP Bremen
! ORIGIN:
! REF_DOCUMENT:
! DATE:                September 2005
! MODEL:               FM 3
! TEMPERATURE:         293K
! NUM_DIM:             2
! NUM_COLUMNS:         3
! NUM_ROWS:            1024
! IDL_FORMAT_CODE:     f7.4, E13.4, E13.4
! PARAMETER_COLUMN:
! COLUMN_LABEL_1:      wavelength (vac) (nm)
! COLUMN_LABEL_2:      sigma (cm^2)
! COLUMN_LABEL_3:      delta sigma (cm^2)
! END_OF_HEADER
```

GOME-2_FM3_NO2_T293K_FPA4.DAT

```
! KEY_DATA_NAME:       GOME-2_FM3_NO2_T293K_FPA4.DAT
! DESCRIPTION:         Absorption Cross-Section
! INSTRUMENT:          GOME-2
! CHANNEL:             4
! VERSION:             2.0
! HISTORY:             IUP Bremen
! ORIGIN:
! REF_DOCUMENT:
! DATE:                September 2005
! MODEL:               FM 3
! TEMPERATURE:         293K
! NUM_DIM:             2
! NUM_COLUMNS:         3
! NUM_ROWS:            1024
! IDL_FORMAT_CODE:     f7.4, E13.4, E13.4
! PARAMETER_COLUMN:
! COLUMN_LABEL_1:      wavelength (vac) (nm)
! COLUMN_LABEL_2:      sigma (cm^2)
! COLUMN_LABEL_3:      delta sigma (cm^2)
! END_OF_HEADER
```

GOME-2_FM2-1_O2_T293K.DAT

! KEY_DATA_NAME:	GOME-2_FM2-1_O2_T293K.DAT
! DESCRIPTION:	Absorption Cross-Section
! INSTRUMENT:	GOME-2
! CHANNEL:	4
! VERSION:	2.0
! HISTORY:	IUP Bremen
! ORIGIN:	
! REF_DOCUMENT:	
! DATE:	September 2005
! MODEL:	FM 2-1
! TEMPERATURE:	293K
! NUM_DIM:	2
! NUM_COLUMNS:	3
! NUM_ROWS:	1024
! IDL_FORMAT_CODE:	f7.4, E13.4, E13.4
! PARAMETER_COLUMN:	
! COLUMN_LABEL_1:	wavelength (vac) (nm)
! COLUMN_LABEL_2:	sigma (cm^2)
! COLUMN_LABEL_3:	delta sigma (cm^2)
! END_OF_HEADER	

GOME-2_FM3_O2_T293K.DAT

! KEY_DATA_NAME:	GOME-2_FM3_O2_T293K.DAT
! DESCRIPTION:	Absorption Cross-Section
! INSTRUMENT:	GOME-2
! CHANNEL:	4
! VERSION:	2.0
! HISTORY:	IUP Bremen
! ORIGIN:	
! REF_DOCUMENT:	
! DATE:	September 2005
! MODEL:	FM 3
! TEMPERATURE:	293K
! NUM_DIM:	2
! NUM_COLUMNS:	3
! NUM_ROWS:	1024
! IDL_FORMAT_CODE:	f7.4, E13.4, E13.4
! PARAMETER_COLUMN:	
! COLUMN_LABEL_1:	wavelength (vac) (nm)
! COLUMN_LABEL_2:	sigma (cm^2)
! COLUMN_LABEL_3:	delta sigma (cm^2)
! END_OF_HEADER	

Delivered Origin projects:

GOME-2_FM2-1_O3_Baselines(T).opj, GOME-2_FM3_O3_Baselines(T).opj

GOME-2_FM2-1_O3_T203K_Data.opj
GOME-2_FM2-1_O3_T223K_Data.opj
GOME-2_FM2-1_O3_T243K_Data.opj
GOME-2_FM2-1_O3_T273K_Data.opj
GOME-2_FM2-1_O3_T293K_Data.opj

GOME-2_FM2-1_O3_T203K_Spectrum.opj
GOME-2_FM2-1_O3_T223K_Spectrum.opj
GOME-2_FM2-1_O3_T243K_Spectrum.opj
GOME-2_FM2-1_O3_T273K_Spectrum.opj
GOME-2_FM2-1_O3_T293K_Spectrum.opj

GOME-2_FM3_O3_T203K_Data.opj
GOME-2_FM3_O3_T223K_Data.opj
GOME-2_FM3_O3_T243K_Data.opj
GOME-2_FM3_O3_T273K_Data.opj
GOME-2_FM3_O3_T293K_Data.opj

GOME-2_FM3_O3_T203K_Spectrum.opj
GOME-2_FM3_O3_T223K_Spectrum.opj
GOME-2_FM3_O3_T243K_Spectrum.opj
GOME-2_FM3_O3_T273K_Spectrum.opj
GOME-2_FM3_O3_T293K_Spectrum.opj

GOME-2_FM2-1_NO2_T223K_Data.opj
GOME-2_FM2-1_NO2_T243K_Data.opj
GOME-2_FM2-1_NO2_T273K_Data.opj
GOME-2_FM2-1_NO2_T293K_Data.opj

GOME-2_FM2-1_NO2_T223K_Spectrum.opj
GOME-2_FM2-1_NO2_T243K_Spectrum.opj
GOME-2_FM2-1_NO2_T273K_Spectrum.opj
GOME-2_FM2-1_NO2_T293K_Spectrum.opj

GOME-2_FM3_NO2_T223K_Data.opj
GOME-2_FM3_NO2_T243K_Data.opj
GOME-2_FM3_NO2_T273K_Data.opj
GOME-2_FM3_NO2_T293K_Data.opj

GOME-2_FM3_NO2_T223K_Spectrum.opj
GOME-2_FM3_NO2_T243K_Spectrum.opj
GOME-2_FM3_NO2_T273K_Spectrum.opj
GOME-2_FM3_NO2_T293K_Spectrum.opj

GOME-2_FM2-1_O2_T293K_Spectrum.opj, GOME-2_FM3_O2_T293K_Spectrum.opj

Chapter 6

Outlook

In this chapter we will give an outlook with respect to possible improvements for future CATGAS measurements.

• **Baseline drift**

Baseline drift was in general clearly smaller than 2 %. But in a number of cases, especially when long purging and measurement periods lay between the first and last reference measurement, it exceeded 2 %. This is likely to be caused by insufficient correction of long term drift by the near-real time light source monitoring. Usually three pairs of vessel and direct measurements were recorded for this correction. By increasing the number of pairs the quality of the correction could be improved as this would be a better approximation to the aimed at near real time measurement. As a draw back this would increase the overall measurement time because the minimum time per pair is determined by the longest PET across the four channels plus overhead time for setting the flip mirror.

• **Unidentified absorption in the O_3 absorption minimum region**

The determination of the O_3 absorption spectrum in the absorption minimum and especially in the neighboring red end of the Huggins band and the blue end of the Chappuis band is still problematic. The observed behavior of absorption was irregular and was clearly not caused by the O_3 absorption. Technical effects like mechanical drift of the mirror mounts or the vessel windows can be excluded after the different efforts made during the study. Two causes appear possible for the observed effect: Firstly an interaction between O_3 (the effect is strongest at high concentrations of O_3) and the surface of the mirrors. And secondly a gas phase absorber, which could be an adduct of O_3 and O_2 or possibly an O_3 dimer. But there is experimental evidence, that the observed effect occurs and disappears with a certain temporal lag relative to the filling and purging of the vessel. This makes an interaction with the mirror surface more likely. Especially an interaction between the at the used pressures and temperatures always present molecular layers of H_2O with O_3 could change the reflectivity of the mirrors slightly and spectrally broad banded. Different approaches can be thought of to improve this.

1. Placing the multipath optics outside of the vessel would inhibit interaction of the surface layer (MgF_2 and H_2O layers) with O_3. But if the same effect takes place

between H_2O layers on the quartz windows and ozone, the effect would thereby not be avoided.

In addition the multiple transition of the analysis beam through the vessel windows would significantly reduce the optical throughput leading to strongly increased exposure times. This is critical with respect to the overall available measurement time per campaign.

2. Purging the mirror surfaces with an inert gas , which in the context of O_3 measurements could be O_2 or N_2, could avoid interaction of O_3 with the mirror surfaces. This necessitates a new design of the mirror mounts and reconsideration of the flow conditions of the different mixtures during the experiment to guarantee stable mixing conditions during measurements. Apart from the later this appears to be the most promising technical approach to overcome the observed problems. Here techniques established in the context of cavity ring down spectroscopy could prove helpful.

3. An analytical approach could use extraction and separation techniques developed in the context of iodine oxides spectroscopy. There concepts of independent component analysis and least squares techniques are being used to separate overlapping absorptions caused by different absorbers [28], [29], [30]. By applying such methods to the already available data obtained in this study the observed unknown absorption could possibly be separated from the ozone spectrum. If the approach could be validated with the present data, this would avoid technical changes to the set-up in future application. Nevertheless a combination of this analytical method and the purging of mirrors appears advisable.

Chapter 7

Conclusion

In this study absorption cross section spectra of O_3 and NO_2 have been measured in three independent campaigns using the three highly stabilized and accurately characterized GOME-2 (Global Ozone Monitoring Experiment 2) satellite spectrometers, flight models FM2, FM2-1, and FM3. The spectra for O_3 were recorded at five temperatures, i.e. 203 K, 223 K, 243 K, 273 K, and 293 K and with a spectral coverage of 240 to 790 nm at a resolution of 0.24 to 0.53 nm full width at half maximum. NO_2 was measured at four temperatures between 223 and 293 K.

The Huggins bands and the Chappuis bands of the O_3 absorption spectrum were covered simultaneously by these measurements. The relative temperature dependence of the O_3 spectrum was determined. For all three campaigns and at the selected wavelengths of 253.65 nm, 289.36 nm, 296.73 nm, 302.15 nm, and 334.15 nm it agrees accurately with the available literature data. For the temperature dependence of the O_3 cross section in the range of 400 to 450 nm an upper limit estimate of no more than 10 % decrease with falling temperature was found at 425 to 430 nm in disagreement with one previous publication. There is some evidence that continuous absorption as measured in the absorption minimum at 429.5 nm drops by a few percent when temperature is reduced from 293 K to 203 K. At the same time the peak of the band at 426.5 nm increases slightly by $\approx$1 %. This is supported by a clear increase of amplitude of differential absorption cross section at 426 nm of 13 % with falling temperature.

At 604.61 nm at the peak of the Chappuis band a slight increase of cross section with falling temperature of $\approx$1 % is found in agreement with three previous publications and in disagreement with one most recent one.

The integrated absorption cross section of the Chappuis region was found to be independent of temperature within less than $\pm$1 %. From simultaneously measured spectra covering the Huggins and Chappuis bands the ratios of integrated absorption cross sections were determined between the different regions providing a robust means for intercomparison of cross section in these regions.

The recorded NO_2 spectra are highly consistent with previous measurements and show an agreement within 2 % in the main DOAS window between 400 and 500 nm for all FM's. Also the linear temperature dependence is in high consistence with previous literature data.

Appendix A

Quality-Analysis Overlap Region

As described in chapter 4.3.1 the following tables give information about the ratio between two mixtures (i.e. two different absorption measurements), the corresponding channel and wavelength range and the mean value with standard deviation.

- **GOME-2 FM2-1 T293K**

Ratio	Channel	Wavelength Range [nm]	Pixel	Mean	SD [%]
ratio m8m7	FPA-1	285 - 292	[680:745]	1.00123	0.12514
ratio m7m6	FPA-1	297 - 304	[790:855]	1.00412	0.29201
ratio m6m3f	FPA-2	309 - 321	[90:190]	1.00762	0.54939
ratio m3fm3e	FPA-2	318 - 323	[170:205]	1.00242	0.22516
ratio m3em3d	FPA-2	321 - 333	[190:285]	1.001	0.26363
ratio m3dm3b	FPA-2	329 - 341	[255:355]	1.00143	0.31525
ratio m3bm2	FPA-2	338 - 345	[335:390]	0.99009	0.97547
ratio m2m1	FPA-2	348 - 354	[420:465]	0.99964	0.4582
ratio m1m2	FPA-3	459 - 479	[320:415]	1.00068	0.12555
ratio m2m3b	FPA-3	476 - 501	[400:520]	0.99643	0.16781
Ø				**1.00047**	**0.34976**

- **GOME-2 FM2-1 T273K**

Ratio	Channel	Wavelength Range [nm]	Pixel	Mean	SD [%]
ratio m8m7	FPA-1	275 - 288	[590:700]	1.00387	0.12509
ratio m7m6	FPA-1	292 - 300	[740:815]	1.00565	0.26512
ratio m6m3f	FPA-2	309 - 316	[95:145]	1.00361	0.86722
ratio m3fm3e	FPA-2	317 - 324	[160:210]	0.99791	0.44255
ratio m3em3d	FPA-2	321 - 328	[190:250]	0.99245	0.62326
ratio m3dm3c	FPA-2	326 - 338	[230:335]	0.99637	0.4611
ratio m3cm3b	FPA-2	329 - 340	[255:355]	1.00003	0.34033
ratio m3bm3a	FPA-2	331 - 345	[275:390]	0.99458	0.75203
ratio m3am2	FPA-2	338 - 346	[335:395]	0.99671	1.06203
ratio m2m1	FPA-2	348 - 353	[415:460]	0.99821	0.79885
ratio m1m2	FPA-3	438 - 471	[220:375]	1.00078	0.09559
ratio m3am2	FPA-3	477 - 514	[405:585]	0.99435	0.37126
Ø				**0.99871**	**0.51704**

- **GOME-2 FM2-1 T243K**

Ratio	Channel	Wavelength Range [nm]	Pixel	Mean	SD [%]
ratio m8m7	FPA-1	281nm - 293nm	[635:745]	1.00552	0.28303
ratio m7m6	FPA-1	294nm - 299nm	[760:800]	1.00221	0.241
ratio m6m3h	FPA-2	309nm - 315nm	[95:140]	1.00424	0.455
ratio m3hm3f	FPA-2	318nm - 324nm	[165:210]	1.00097	0.21032
ratio m3fm3g	FPA-2	319nm - 332nm	[170:280]	0.99983	0.22322
ratio m3gm3e	FPA-2	324nm - 335nm	[210:305]	1.00285	0.19802
ratio m3em3b	FPA-2	328nm - 338nm	[250:330]	0.99999	0.46095
ratio m3bm3c	FPA-2	329nm - 341nm	[255:355]	1.00301	0.55307
ratio m3cm2	FPA-2	338nm - 345nm	[335:390]	0.99762	1.71431
ratio m2m1	FPA-2	348nm - 353nm	[415:460]	1.01527	1.23934
ratio m1m2	FPA-3	459nm - 476nm	[320:400]	1.00125	0.09167
ratio m2m3c	FPA-3	493nm - 519nm	[480:610]	1.00483	0.45083
Ø				**1.00313**	**0.50032**

• **GOME-2 FM2-1 T223K**

Ratio	Channel	Wavelength Range [nm]	Pixel	Mean	SD [%]
ratio m8m7a	FPA-1	278 - 290	[610:725]	1.00698	0.38611
ratio m7am6	FPA-1	294 - 300	[760:815]	1.00226	0.14066
ratio m6m3f	FPA-2	309 - 315	[95:140]	1.00457	0.59446
ratio m3fm3h	FPA-2	310 - 319	[100:170]	1.00272	0.1721
ratio m3hm3g	FPA-2	313 - 324	[125:210]	0.99962	0.29843
ratio m3gm3e	FPA-2	316 - 329	[150:255]	1.00368	0.12971
ratio m3em3d	FPA-2	323 - 332	[205:280]	1.00583	0.32893
ratio m3dm3c	FPA-2	326 - 335	[230:305]	1.00668	0.32032
ratio m3cm3a	FPA-2	329 - 338	[250:335]	1.00394	0.2418
ratio m3am3b	FPA-2	331 - 341	[275:355]	1.00466	0.42356
ratio m3bm2	FPA-2	338 - 345	[335:390]	0.98812	2.47101
ratio m2m1	FPA-2	348 - 353	[415:460]	1.01481	1.5381
ratio m1m2	FPA-3	432 - 471	[235:375]	1.00051	0.11704
ratio m2m3b	FPA-3	482 - 514	[430:585]	1.00059	0.08188
Ø				**1.00321**	**0.51744**

• **GOME-2 FM2-1 T203K**

Ratio	Channel	Wavelength Range [nm]	Pixel	Mean	SD [%]
ratio m8m7	FPA-1	287 - 292	[690:740]	1.00397	0.24017
ratio m7m6	FPA-1	294 - 303	[760:840]	0.99979	0.05617
ratio m6m3h	FPA-2	311 - 317	[110:160]	1.00585	0.81213
ratio m3hm3f	FPA-2	315 - 324	[140:215]	1.00496	0.23021
ratio m3fm3e	FPA-2	319 - 332	[170:280]	1.00514	0.30995
ratio m3em3d	FPA-2	326 - 335	[230:305]	1.00682	0.37984
ratio m3dm3c	FPA-2	328 - 338	[250:335]	1.00341	0.37986
ratio m3cm3a	FPA-2	329 - 341	[255:355]	1.00992	0.6793
ratio m3am1	FPA-2	345 - 348	[390:415]	1.0937	4.94736
ratio m1m3a	FPA-3	459 - 473	[320:385]	1.00016	0.61048
Ø				**1.01337**	**0.86455**

- **GOME-2 FM3 T293K**

Ratio	Channel	Wavelength Range [nm]	Pixel	Mean	SD	SD [%]
ratio m8m7	FPA-1	285 - 294	[680:760]	1.0012	0.00222	0.22145
ratio m7m6	FPA-1	298 - 303	[795:850]	0.99997	0.00336	0.33614
ratio m6m3h	FPA-2	311 - 315	[165:200]	0.99852	0.00302	0.30253
ratio m3gm3h	FPA-2	315 - 326	[200:290]	0.99973	0.00236	0.23603
ratio m3fm3g	FPA-2	318 - 329	[225:315]	1.00078	0.0019	0.19015
ratio m3em3f	FPA-2	323 - 335	[265:360]	0.99993	0.00197	0.19665
ratio m3dm3e	FPA-2	325 - 338	[285:390]	1.00118	0.00252	0.25142
ratio m3cm3d	FPA-2	328 - 340	[310:410]	1.00087	0.00229	0.22907
ratio m3bm3c	FPA-2	328 - 341	[310:415]	1.00095	0.00202	0.2021
ratio m3am3b	FPA-2	331 - 344	[335:445]	0.99982	0.00208	0.20816
ratio m3am2	FPA-2	340 - 345	[410:450]	1.00114	0.00412	0.4118
ratio m2m1	FPA-2	353 - 354	[515:525]	0.97945	0.00307	0.31308
ratio m1m2	FPA-3	439 - 450	[225:280]	0.99938	0.00478	0.47811
ratio m2m3	FPA-3	477 - 502	[405:525]	1.00006	0.00348	0.34791
Ø				**0.99878**	**0.0028**	**0.28033**

- **GOME-2 FM3 T273K**

Ratio	Channel	Wavelength Range [nm]	Pixel	Mean	SD	SD [%]
ratio m8.2m6	FPA-1	290 - 300	[715:815]	1.00155	0.00313	0.31288
ratio m6m3h	FPA-2	312 - 320	[175:240]	0.99856	0.00501	0.50213
ratio m3hm3g	FPA-2	318 - 329	[225:315]	0.99959	0.00201	0.2012
ratio m3gm3e	FPA-2	325 - 334	[285:360]	0.99919	0.00269	0.26964
ratio m3em3b	FPA-2	328 - 338	[310:395]	1.00136	0.00285	0.285
ratio m3bm2	FPA-2	338 - 345	[395:450]	0.9987	0.00633	0.6338
ratio m2m1	FPA-2	352 - 354	[510:525]	0.98692	0.00527	0.53354
ratio m1m2	FPA-3	437 - 453	[215:290]	1.00411	0.00128	0.12794
ratio m2m3b	FPA-3	476 - 493	[400:485]	0.96841	0.00829	0.85632
Ø				**0,99584**	**0,00374**	**0,37759**

- **GOME-2 FM3 T243K**

Ratio	Channel	Wavelength Range [nm]	Pixel	Mean	SD	SD [%]
ratio m8m7	FPA-1	287nm - 293nm	[700:755]	0.99834	0.00241	0.24182
ratio m7m6	FPA-1	300nm - 304nm	[815:860]	0.99909	0.00204	0.20462
ratio m6m3e	FPA-2	312nm - 317nm	[180:215]	1.00147	0.00206	0.20578
ratio m3em3c	FPA-2	319nm - 329nm	[230:315]	1.00095	0.00217	0.21657
ratio m3bm3c	FPA-2	323nm - 334nm	[265:360]	1.00045	0.00342	0.3414
ratio m3am3b	FPA-2	325nm - 335nm	[285:365]	0.99955	0.00222	0.22214
ratio m3am3d	FPA-2	326nm - 338nm	[290:390]	1.001	0.00255	0.25512
ratio m3dm2	FPA-2	337nm - 340nm	[385:410]	0.99411	0.00963	0.96852
ratio m2m1	FPA-2	348nm - 352nm	[475:510]	1.03082	0.01543	1.49683
ratio m1m2*	FPA-3	459nm - 476nm	[320:400]	1.00123	0.00132	0.13166
ratio m2m3d	FPA-3	480nm - 521nm	[420:620]	1.00002	0.00187	0.18656
Ø				**1,00388**	**0,0052**	**0,5146**

- **GOME-2 FM3 T223K**

Ratio	Channel	Wavelength Range [nm]	Pixel	Mean	SD	SD [%]
ratio m8m7a	FPA-1	287 - 293	[700:755]	1.00017	0.00241	0.24079
ratio m7am6	FPA-1	296 - 305	[780:865]	1.0004	0.00165	0.16523
ratio m6m3h	FPA-2	313 - 317	[185:220]	1.00119	0.00354	0.35361
ratio m3hm3g	FPA-2	320 - 331	[240:335]	1.00228	0.00214	0.21354
ratio m3gm3f	FPA-2	323 - 334	[265:360]	1.00243	0.00242	0.24131
ratio m3fm3e	FPA-2	325 - 338	[285:390]	1.0077	0.00566	0.56155
ratio m3em3b	FPA-2	328 - 338	[310:390]	0.98317	0.01891	1.92294
ratio m3bm3a	FPA-2	331 - 345	[335:450]	1.01031	0.00703	0.69573
ratio m3am2	FPA-2	337 - 345	[385:450]	1.16138	0.08974	7.72718
ratio m2m1	FPA-2	347 - 352	[470:510]	1.03299	0.0237	2.29461
ratio m1m2	FPA-3	439 - 457	[225:310]	0.99826	0.00387	0.38806
ratio m2m3a	FPA-3	527 - 558	[650:795]	1.00039	4.49623E-4	0.04494
Ø				**1,01672**	**0,01346**	**1,23746**

- **GOME-2 FM3 T203K**

Ratio	Channel	Wavelength Range [nm]	Pixel	Mean	SD	SD [%]
ratio m8m7	FPA-1	287 - 293	[700:755]	1.00726	0.00365	0.36237
ratio m7m6	FPA-1	297 - 304	[790:860]	1.00135	0.00151	0.15089
ratio m3im6	FPA-2	311 - 315	[170:200]	0.99986	0.00388	0.38851
ratio m3gm3i	FPA-2	320 - 326	[240:290]	0.9949	0.00509	0.51167
ratio m3bm3g	FPA-2	325 - 334	[285:360]	0.98833	0.0103	1.04185
ratio m3am3b	FPA-2	328 - 338	[310:390]	1.00674	0.00683	0.67834
ratio m3cm3a	FPA-2	328 - 341	[310:415]	0.994	0.00535	0.53852
ratio m2m3c	FPA-2	338 - 341	[390:415]	1.01644	0.03105	3.05509
ratio m1m2	FPA-2	347 - 352	[470:510]	0.97037	0.02312	2.383
ratio m1m2	FPA-3	449 - 457	[275:310]	0.99958	0.00124	0.12371
ratio m2m3c	FPA-3	503 - 517	[535:600]	1.00099	0.00134	0.13392
Ø				**0,99816**	**0,00849**	**0,85162**

Appendix B

I_0 - I Documentation

Intensities in b.u. for measurements with GOME-2 FM2-1 at 273K

Mixture	FPA	λ [nm]	I_0 [bu]	I [bu]
1	2	353 - 400	17000 - 20000	5000 - 19000
1	3	400 - 455	3000 - 15000	2500 - 6000
2	2	340 - 360	20000	5000 - 18000
2	3	430 - 490	8000 - 25000	7000 - 15000
3	2	310 - 345	6000 - 20000	2500 - 18000
3	3	475 - 600	15000 - 24000	14000 - 5000
3	4	590 - 790	19000 - 4000	10000 - 2000
6	1	298 - 310	50000 - 15000	25000 - 10000
		Hg(302)	50000	25000
6	2	310 - 315	8000 - 25000	7000 - 22000
7	1	285 - 303	30000 - 50000	12000 - 42000
		Hg(289)	32000	20000
		Hg(296)	45000	35000
8	1	240 - 290	3000 - 35000	2000 - 30000
		Hg(253)	5200	2700

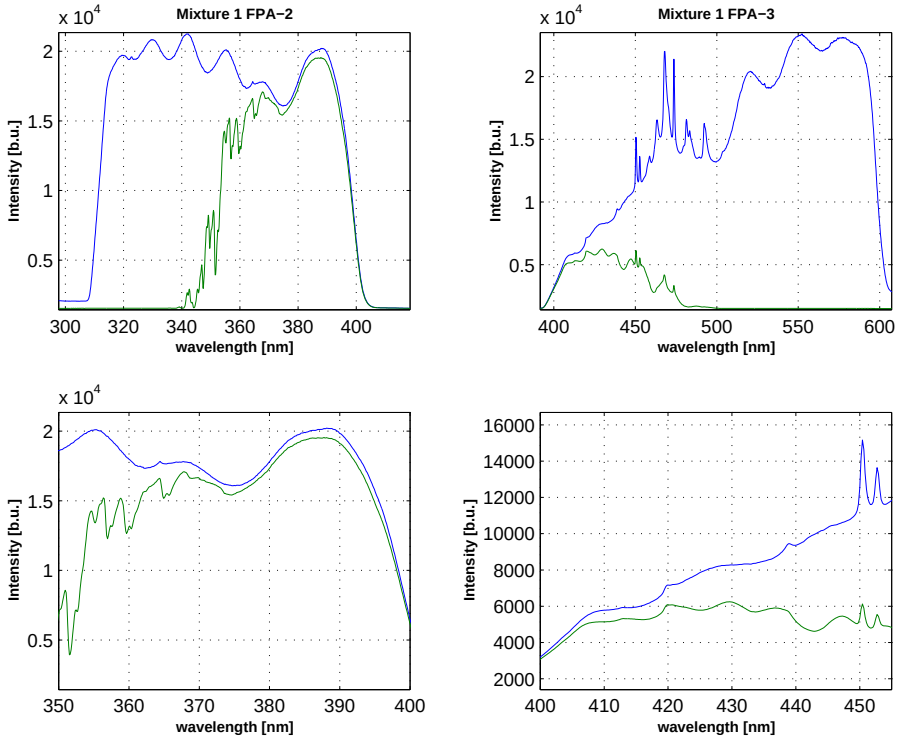

Figure B.1: Intensities regarding mixture 1 measured with GOME-2 FM2-1 @ 273K. The lower graphics show the corresponding relevant wavelength range

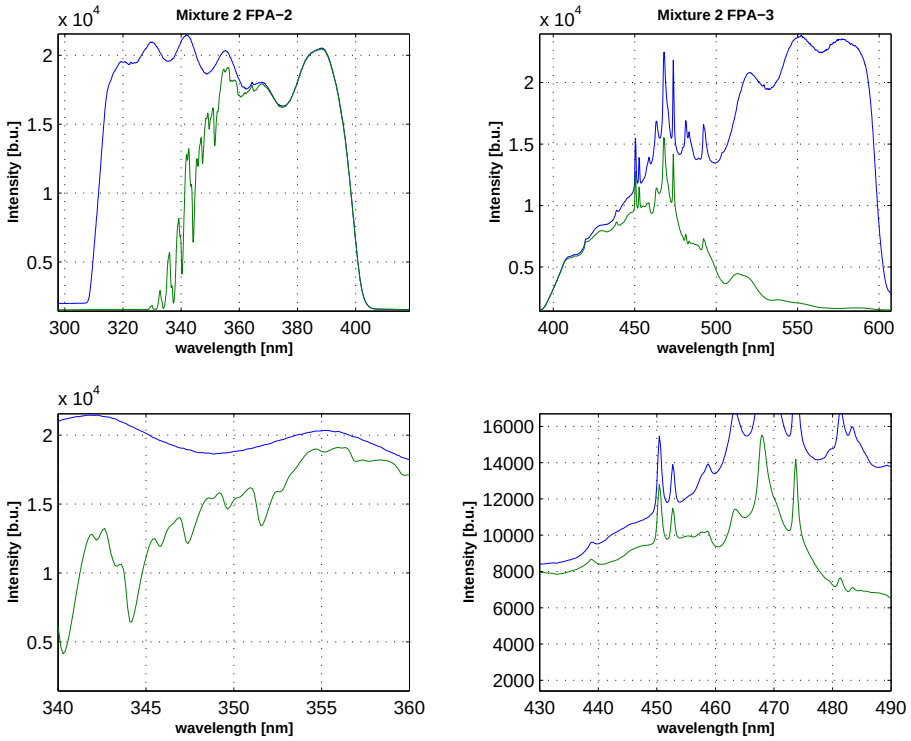

Figure B.2: Intensities regarding mixture 2 measured with GOME-2 FM2-1 @ 273K. The lower graphics show the corresponding relevant wavelength range

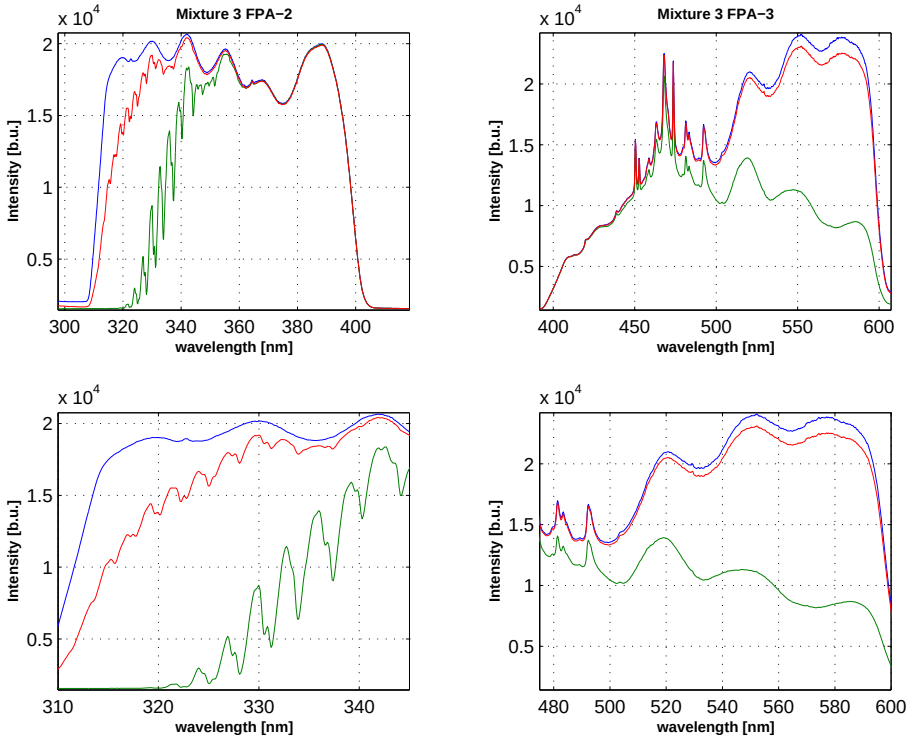

Figure B.3: Intensities regarding mixture 3 measured with GOME-2 FM2-1 @ 273K. As described in the report mixture 3 corresponds to several measurements with slightly different concentrations. The red line shows the intensity with the lowest and the green line the highest concentration regarding mixture 3

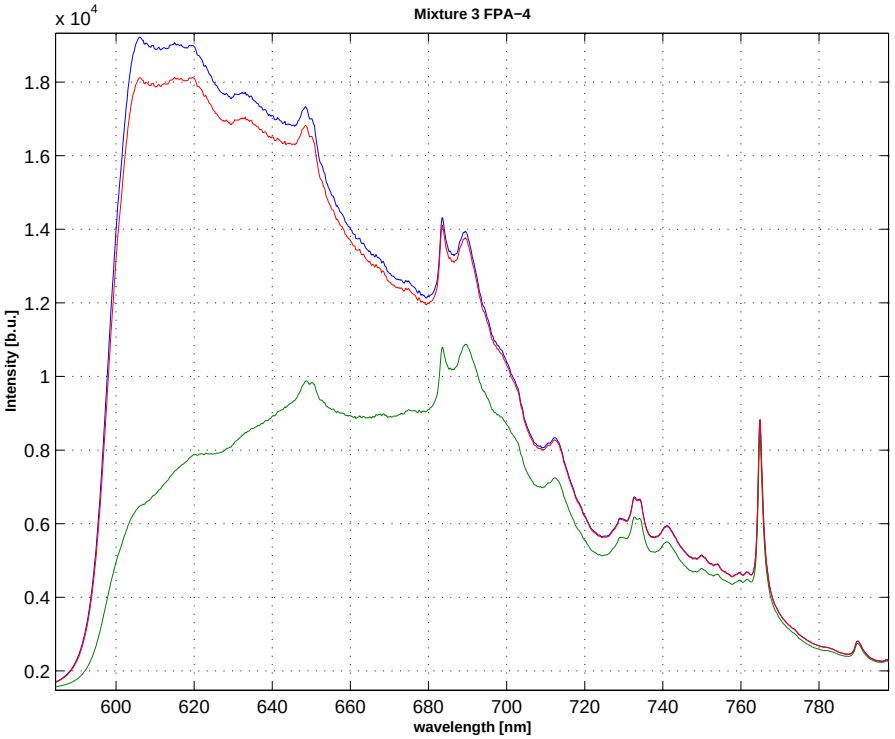

Figure B.4: Intensities regarding mixture 3 in channel 4 measured with GOME-2 FM2-1 @ 273K.

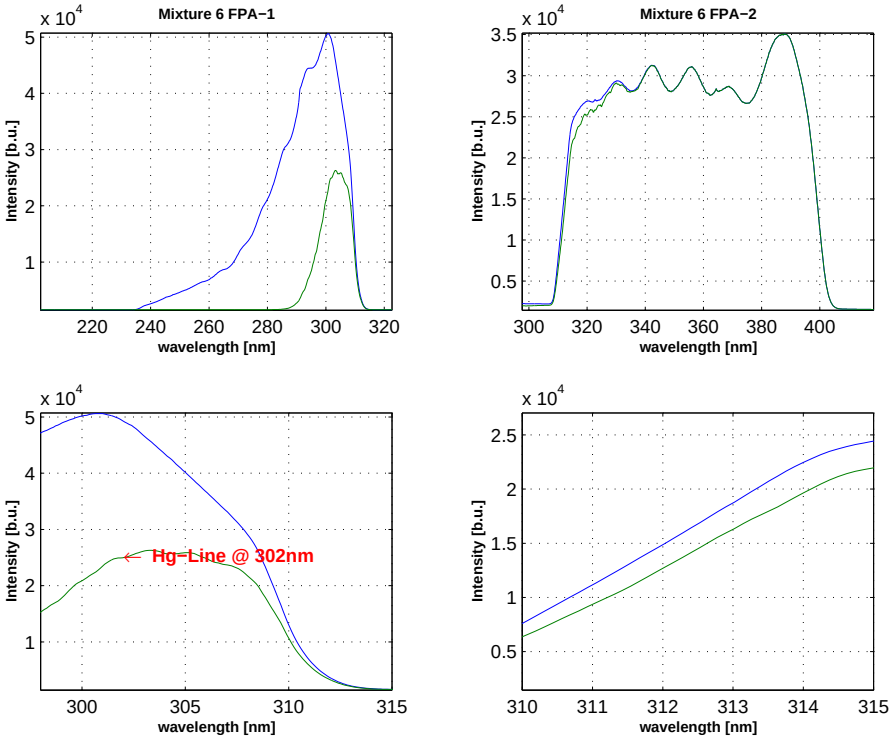

Figure B.5: Intensities regarding mixture 6 measured with GOME-2 FM2-1 @ 273K. The lower graphics show the corresponding relevant wavelength range

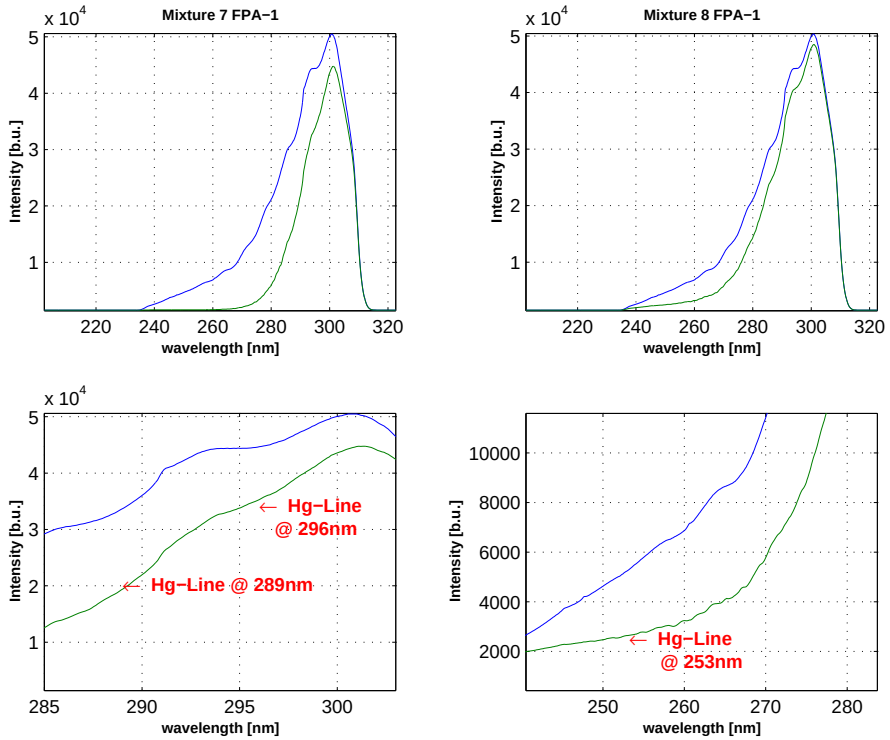

Figure B.6: Intensities regarding mixture 7 and 8 measured with GOME-2 FM2-1 @ 273K. The lower graphics show the corresponding relevant wavelength range together with arrows indicating the location of Hg-Lines, where comparisons with literature data have been done at 293K (At this temperature only at 253nm)

Intensities in b.u. for measurements with GOME-2 FM2-1 at 243K

Mixture	FPA	λ [nm]	I_0 [bu]	I [bu]
1	2	353 - 400	15000 - 18000	5000 - 17000
1	3	400 - 455	3000 - 15000	3000 - 6000
2	2	340 - 360	20000	5000 - 17000
2	3	430 - 490	9000 - 20000	8000 - 15000
3	2	310 - 345	7000 - 20000	6000 - 19000
3	3	475 - 600	16000 - 27000	15000 - 5000
3	4	590 - 790	22000 - 4000	11000 - 2500
6	1	298 - 310	50000 - 15000	10000 - 20000
		Hg(302)	50000	20000
6	2	310 - 315	8000 - 24000	6000 - 21000
7	1	285 - 303	30000 - 49000	11000 - 42000
		Hg(289)	32000	19000
		Hg(296)	42000	32000
8	1	240 - 290	2500 - 33000	2000 - 30000
		Hg(253)	5000	2500

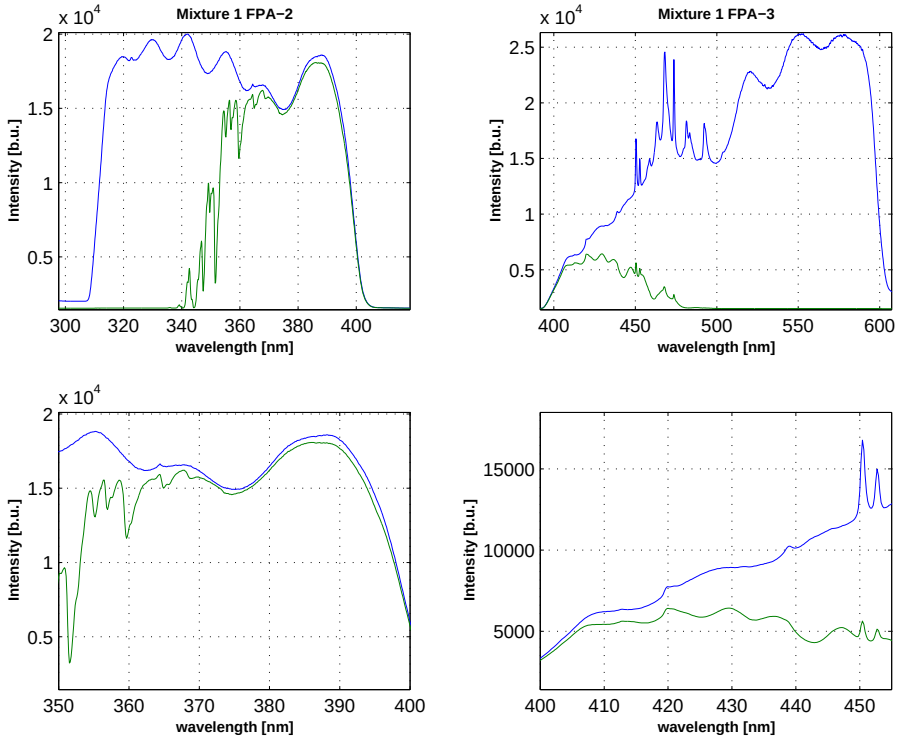

Figure B.7: Intensities regarding mixture 1 measured with GOME-2 FM2-1 @ 243K. The lower graphics show the corresponding relevant wavelength range

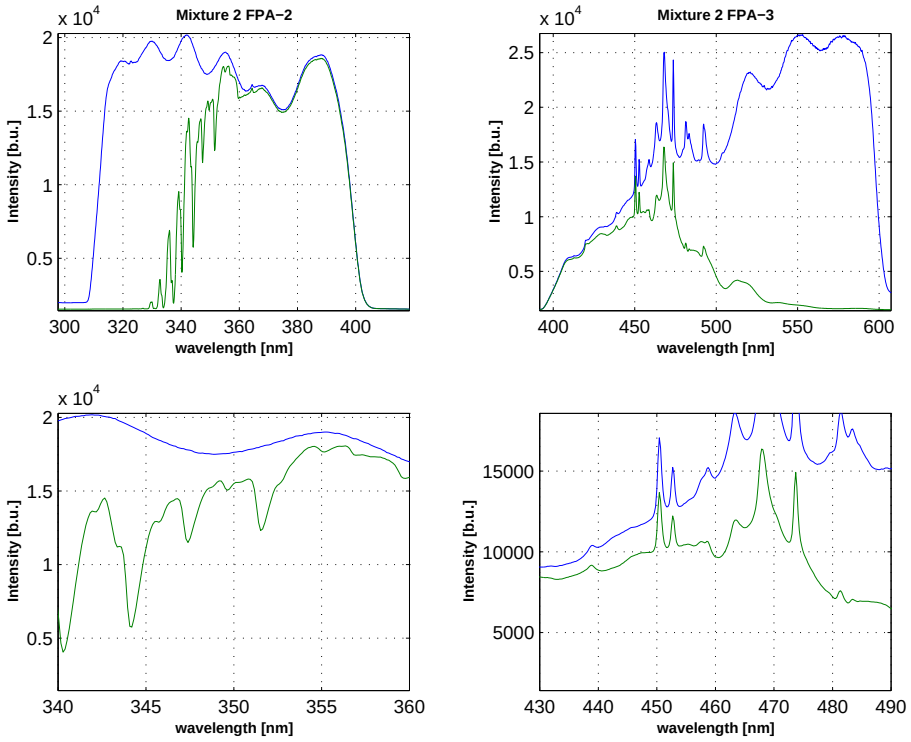

Figure B.8: Intensities regarding mixture 2 measured with GOME-2 FM2-1 @ 243K. The lower graphics show the corresponding relevant wavelength range

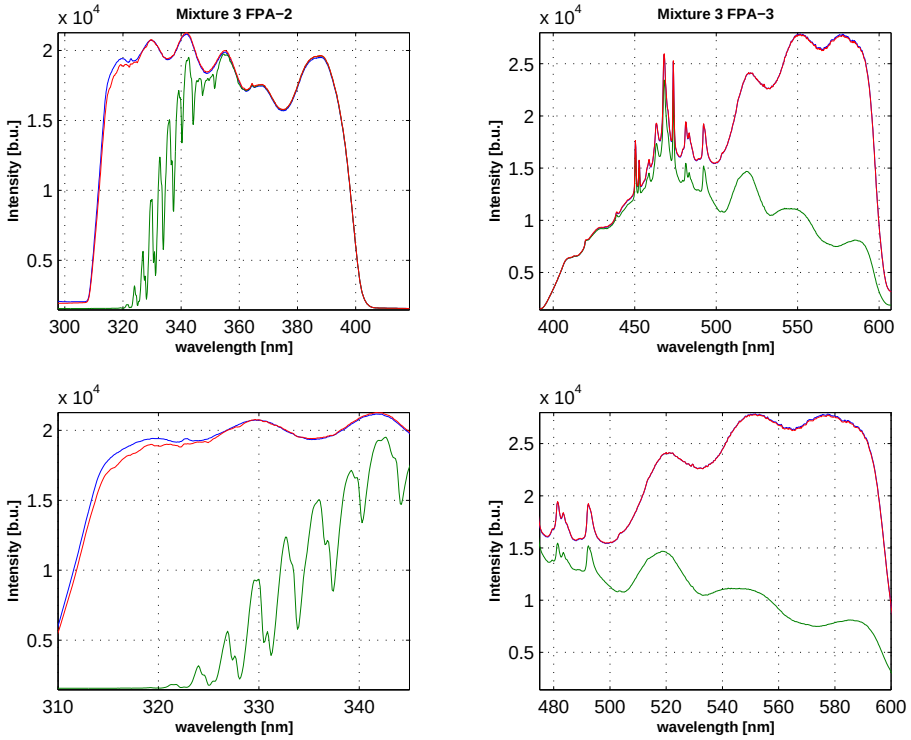

Figure B.9: Intensities regarding mixture 3 measured with GOME-2 FM2-1 @ 243K. As described in the report mixture 3 corresponds to several measurements with slightly different concentrations. The red line shows the intensity with the lowest and the green line the highest concentration regarding mixture 3

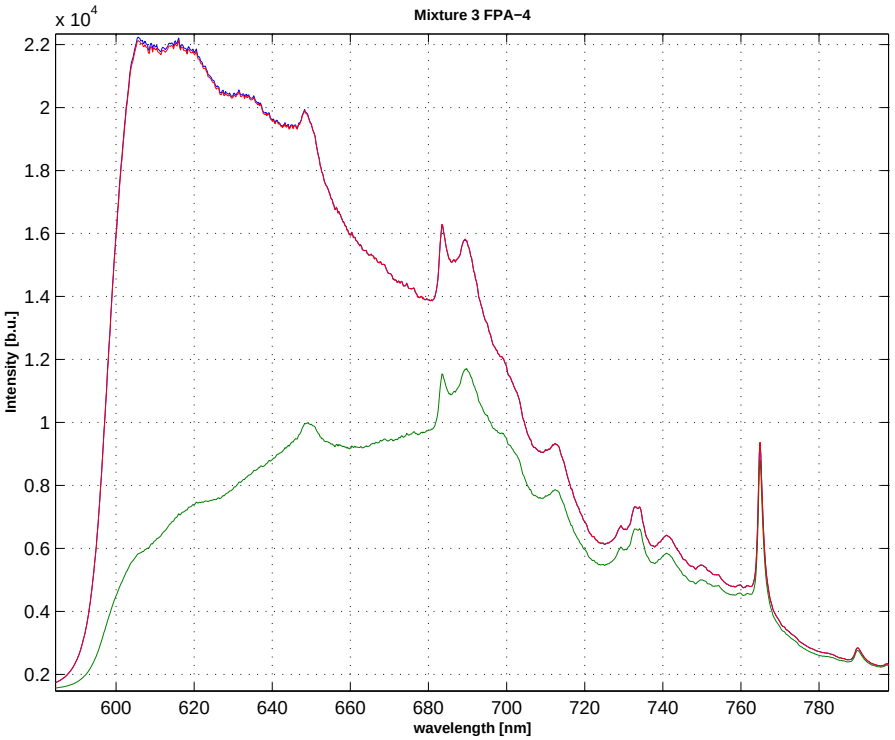

Figure B.10: Intensities regarding mixture 3 in channel 4 measured with GOME-2 FM2-1 @ 243K.

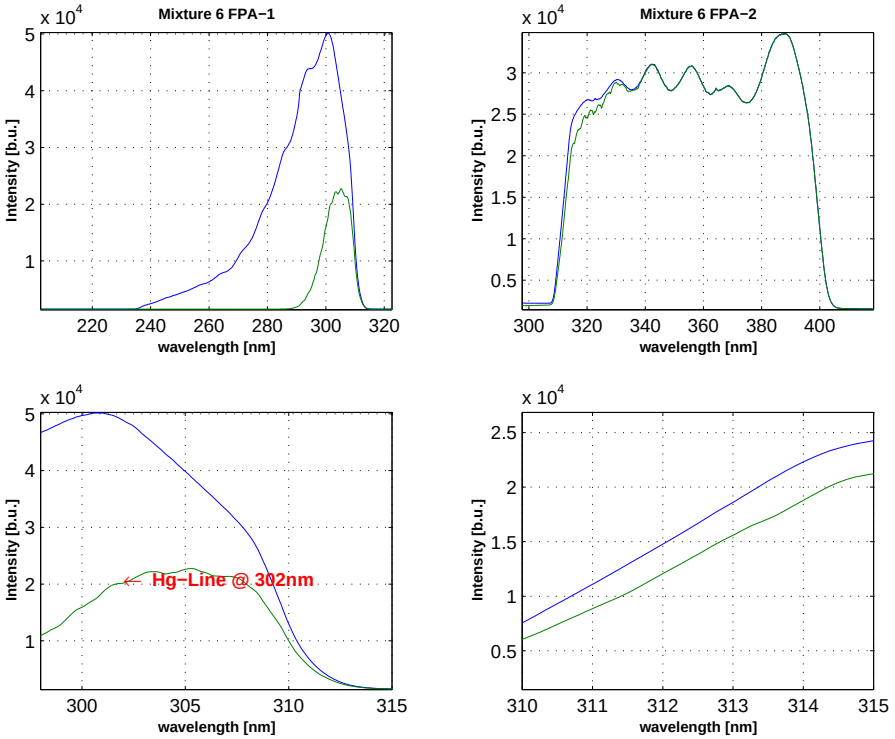

Figure B.11: Intensities regarding mixture 6 measured with GOME-2 FM2-1 @ 243K. The lower graphics show the corresponding relevant wavelength range

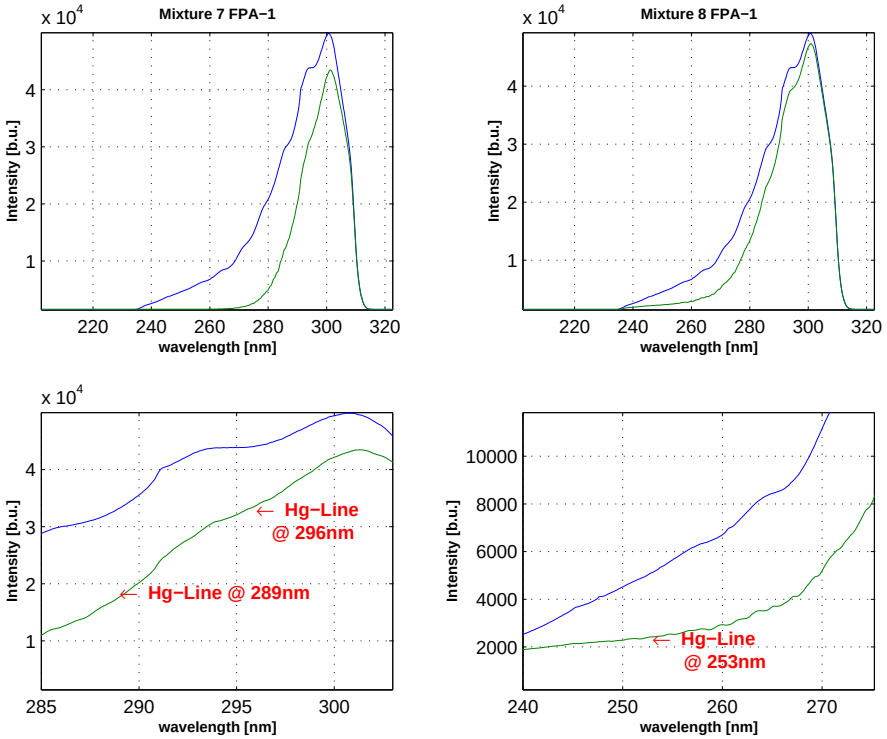

Figure B.12: Intensities regarding mixture 7 and 8 measured with GOME-2 FM2-1 @ 243K. The lower graphics show the corresponding relevant wavelength range together with arrows indicating the location of Hg-Lines, where comparisons with literature data have been done at 293K (At this temperature only at 253nm)

Intensities in b.u. for measurements with GOME-2 FM2-1 at 223K

Mixture	FPA	λ [nm]	I_0 [bu]	I [bu]
1	2	353 - 400	15000 - 18000	3000 - 17000
1	3	400 - 455	3000 - 12000	3000 - 5000
2	2	340 - 360	17000	4000 - 16000
2	3	430 - 490	8000 - 15000	7000 - 10000
3	2	310 - 345	6000 - 20000	5000 - 18000
3	3	475 - 600	14000 - 21000	12000 - 5000
3	4	590 - 790	16000 - 4000	8000 - 2000
6	1	298 - 310	45000 - 12000	25000 - 10000
		Hg(302)	45000	25000
6	2	310 - 315	8000 - 23000	6000 - 21000
7	1	285 - 303	28000 - 45000	10000 - 40000
		Hg(289)	30000	18000
		Hg(296)	41000	31000
8	1	240 - 290	2500 - 31000	2000 - 28000
		Hg(253)	5000	2500

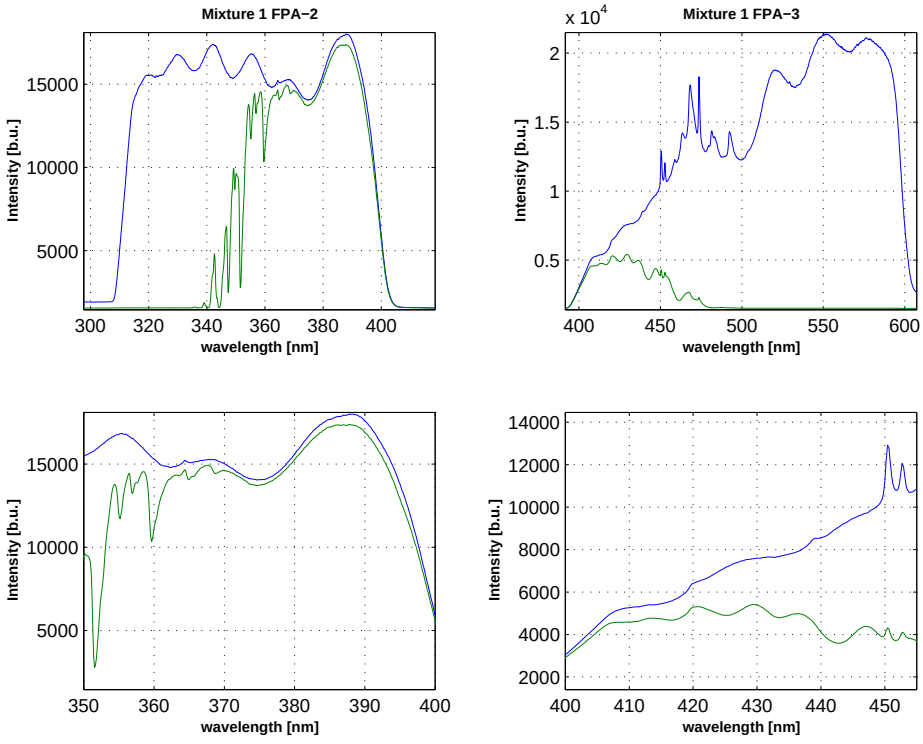

Figure B.13: Intensities regarding mixture 1 measured with GOME-2 FM2-1 @ 223K. The lower graphics show the corresponding relevant wavelength range

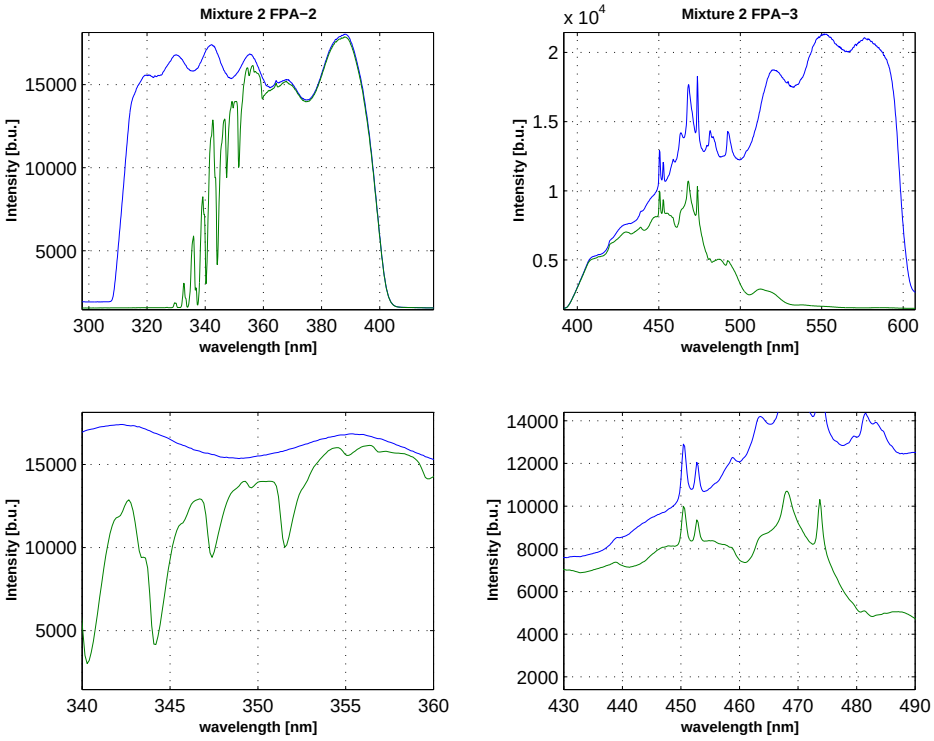

Figure B.14: Intensities regarding mixture 2 measured with GOME-2 FM2-1 @ 223K. The lower graphics show the corresponding relevant wavelength range

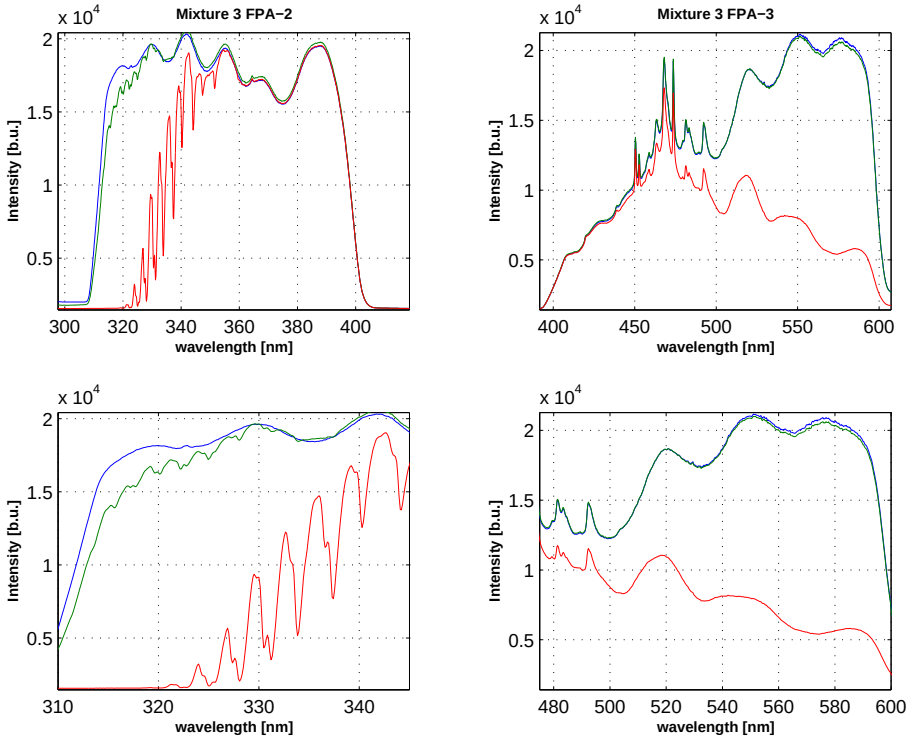

Figure B.15: Intensities regarding mixture 3 measured with GOME-2 FM2-1 @ 223K. As described in the report mixture 3 corresponds to several measurements with slightly different concentrations. The red line shows the intensity with the lowest and the green line the highest concentration regarding mixture 3

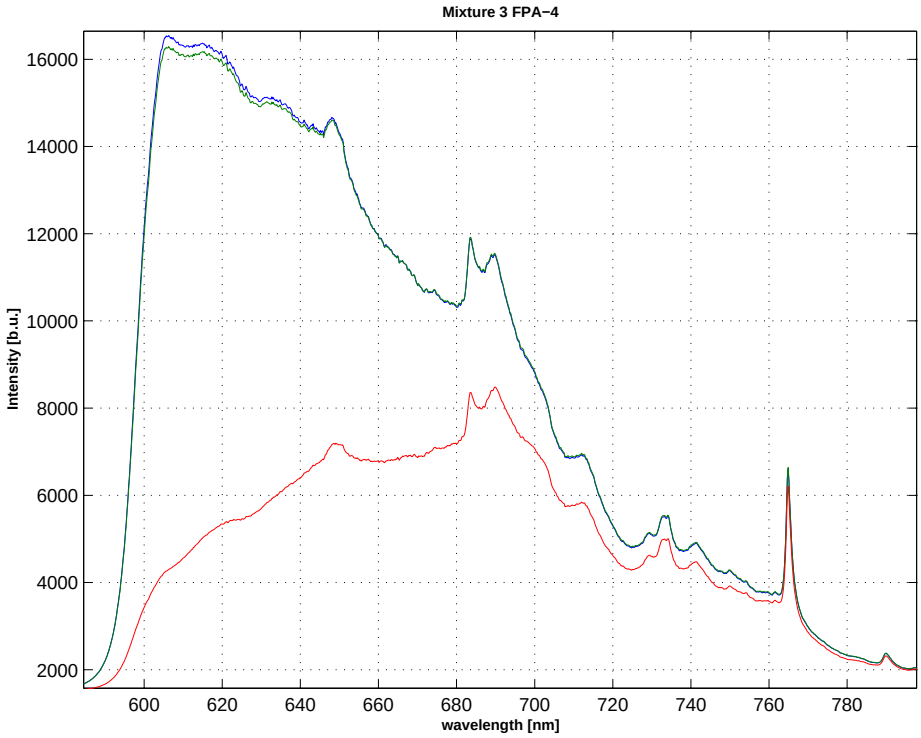

Figure B.16: Intensities regarding mixture 3 in channel 4 measured with GOME-2 FM2-1 @ 223K.

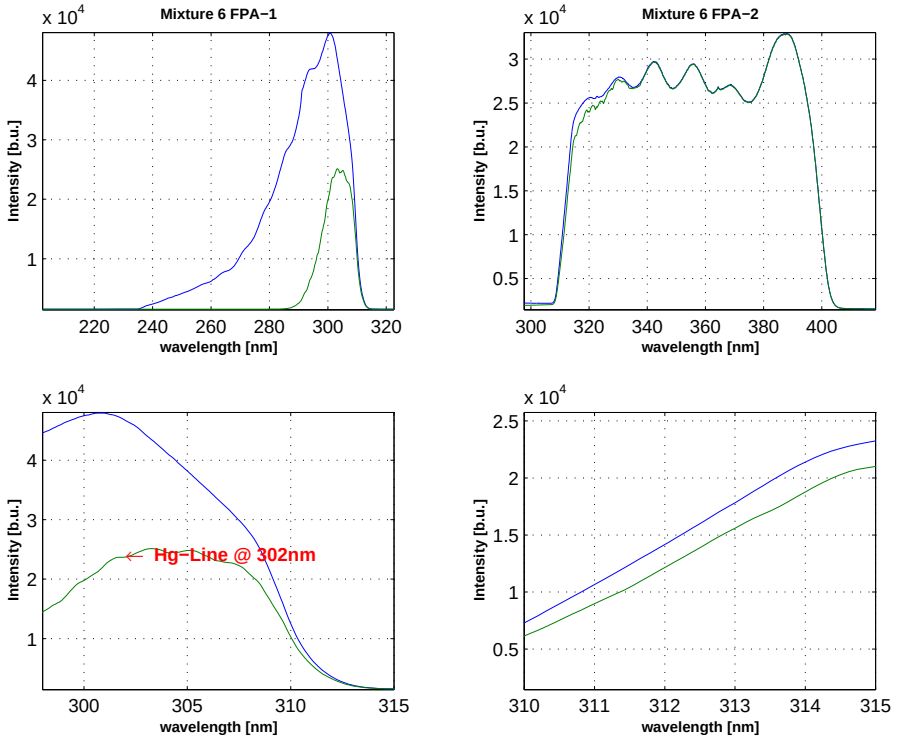

Figure B.17: Intensities regarding mixture 6 measured with GOME-2 FM2-1 @ 223K. The lower graphics show the corresponding relevant wavelength range

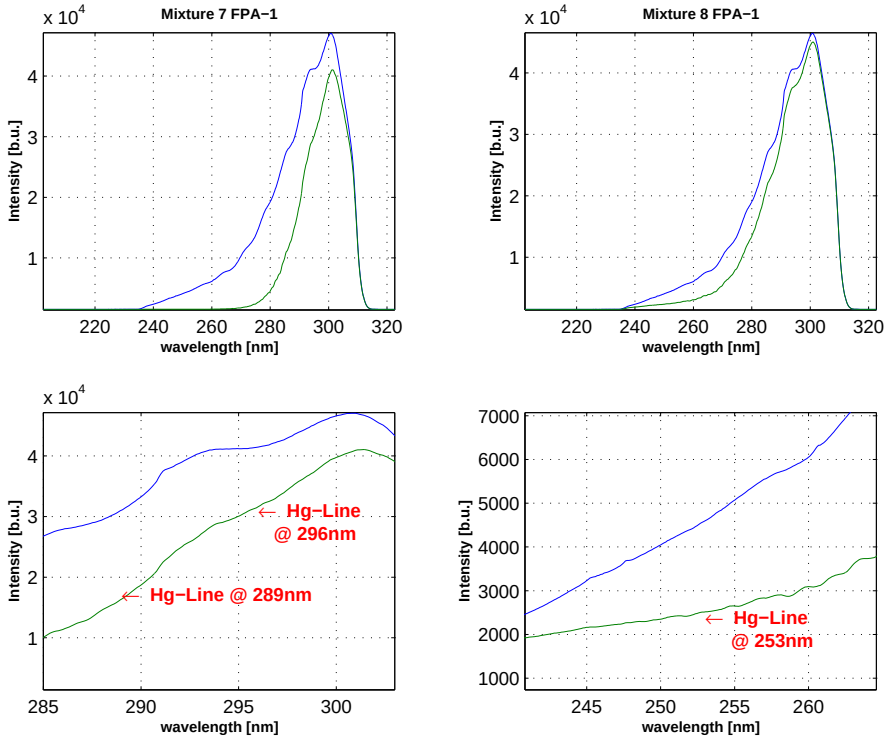

Figure B.18: Intensities regarding mixture 7 and 8 measured with GOME-2 FM2-1 @ 223K. The lower graphics show the corresponding relevant wavelength range together with arrows indicating the location of Hg-Lines, where comparisons with literature data have been done at 293K (At this temperature only at 253nm)

Intensities in b.u. for measurements with GOME-2 FM2-1 at 203K

Mixture	FPA	λ [nm]	I_0 [bu]	I [bu]
1	2	353 - 400	15000 - 18000	3000 - 17000
1	3	400 - 455	3000 - 12000	3000 - 5000
2	2	340 - 360	16000	10000 - 15000
2	3	430 - 490	7000 - 15000	7000 - 12000
3	2	310 - 345	5000 - 17000	2000 - 15000
3	3	475 - 600	12000 - 20000	10000 - 3000
3	4	590 - 790	15000 - 4000	2000 - 7000
6	1	298 - 310	31000 - 8000	15000 - 7000
		Hg(302)	31000	15000
6	2	310 - 315	6000 - 18000	5000 - 16000
7	1	285 - 303	18000 - 31000	5000 - 25000
		Hg(289)	20000	8000
		Hg(296)	27000	19000
8	1	240 - 290	2000 - 22000	1800 - 18000
		Hg(253)	3200	2000

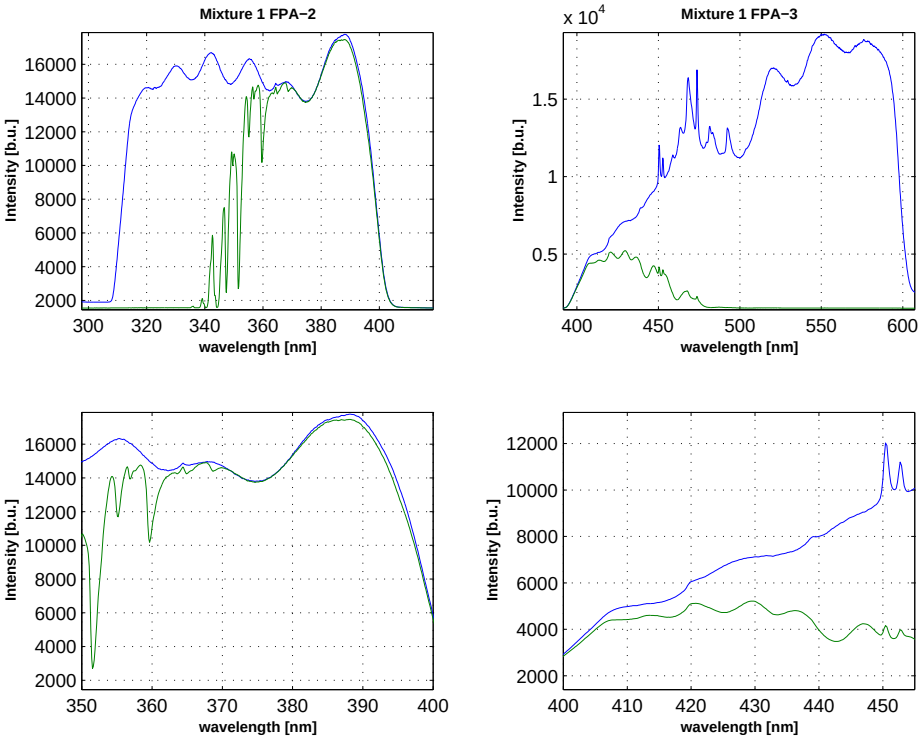

Figure B.19: Intensities regarding mixture 1 measured with GOME-2 FM2-1 @ 203K. The lower graphics show the corresponding relevant wavelength range

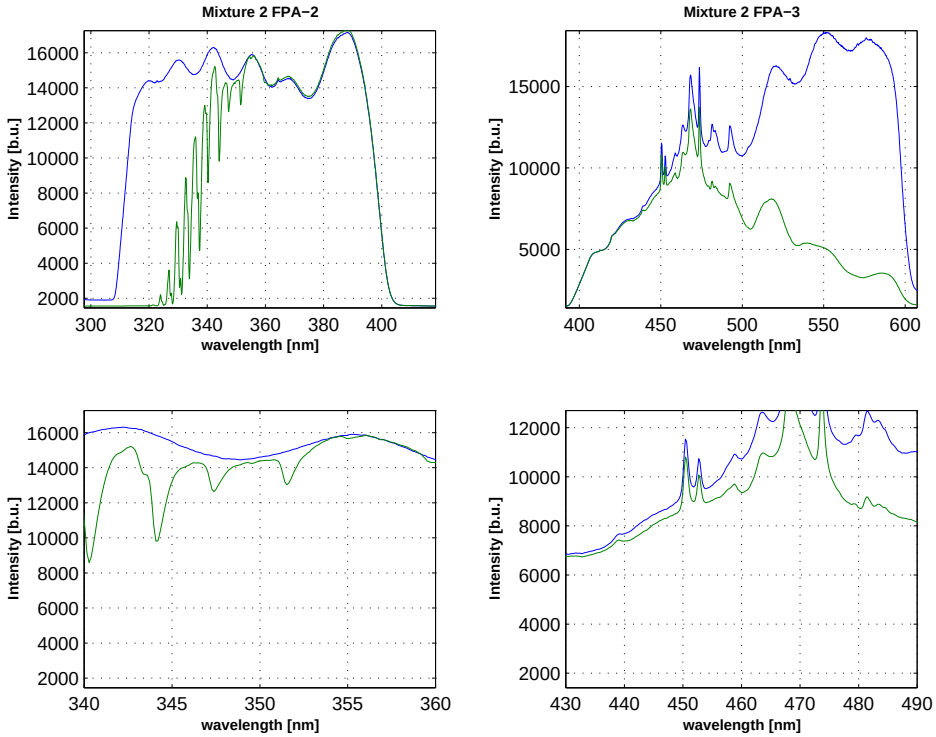

Figure B.20: Intensities regarding mixture 2 measured with GOME-2 FM2-1 @ 203K. The lower graphics show the corresponding relevant wavelength range

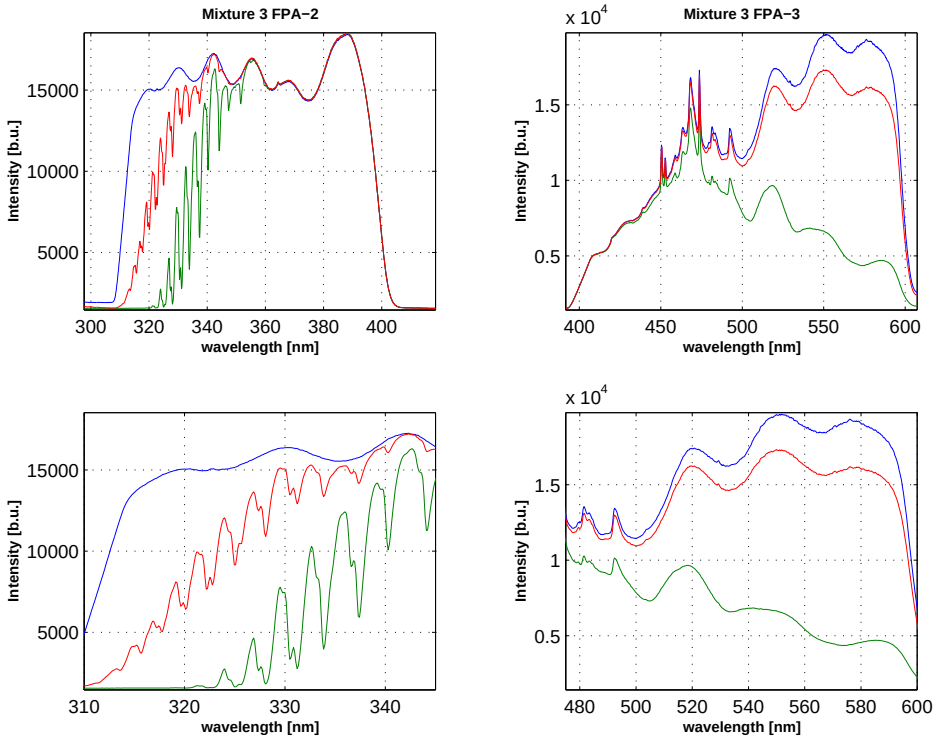

Figure B.21: Intensities regarding mixture 3 measured with GOME-2 FM2-1 @ 203K. As described in the report mixture 3 corresponds to several measurements with slightly different concentrations. The red line shows the intensity with the lowest and the green line the highest concentration regarding mixture 3

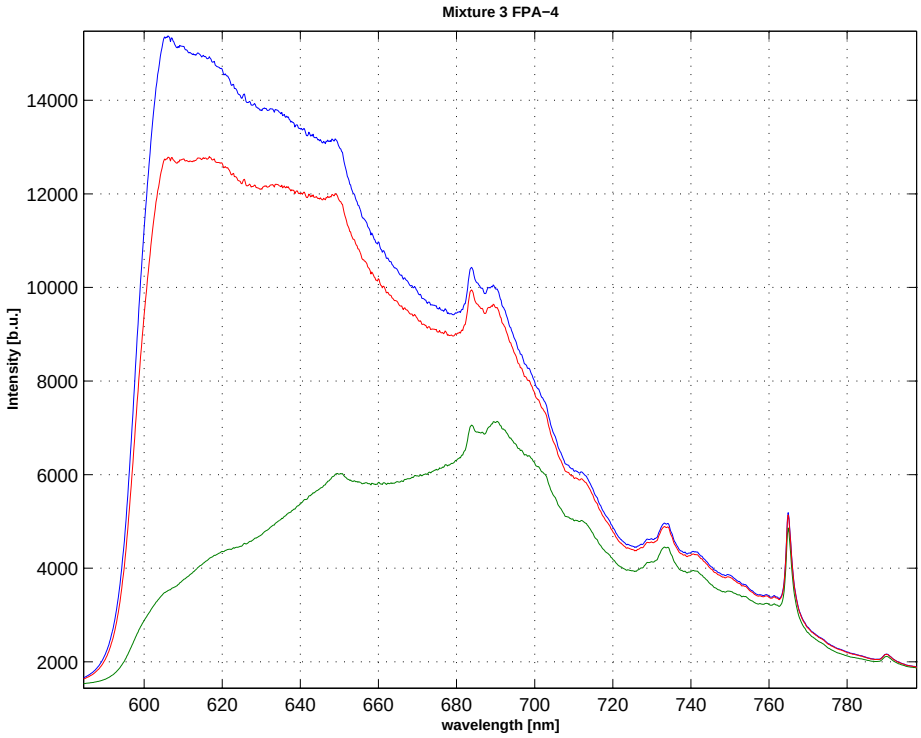

Figure B.22: Intensities regarding mixture 3 in channel 4 measured with GOME-2 FM2-1 @ 203K.

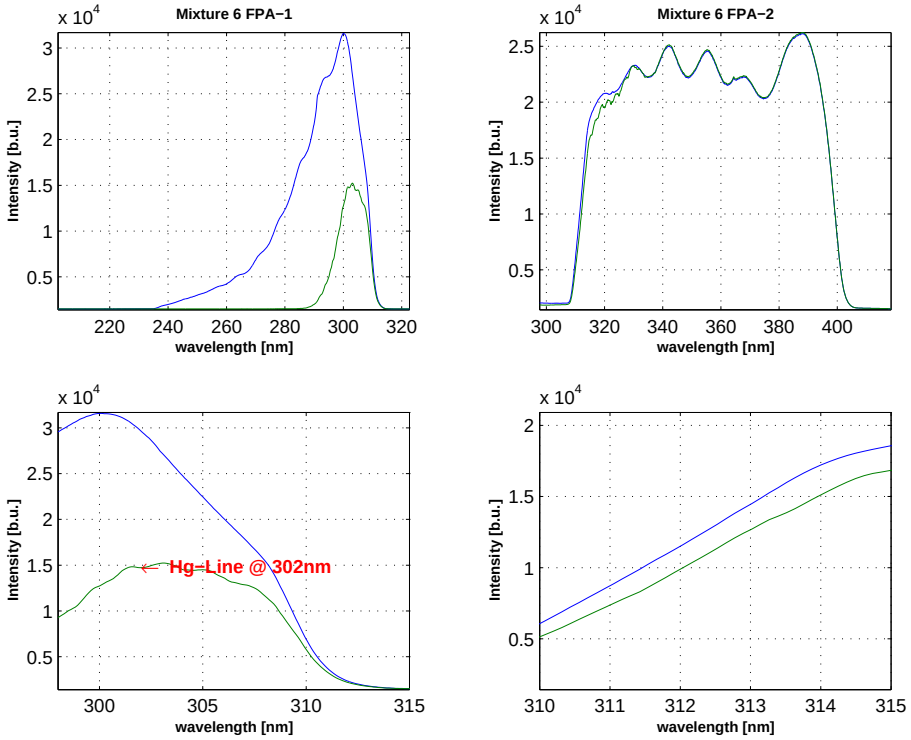

Figure B.23: Intensities regarding mixture 6 measured with GOME-2 FM2-1 @ 203K. The lower graphics show the corresponding relevant wavelength range

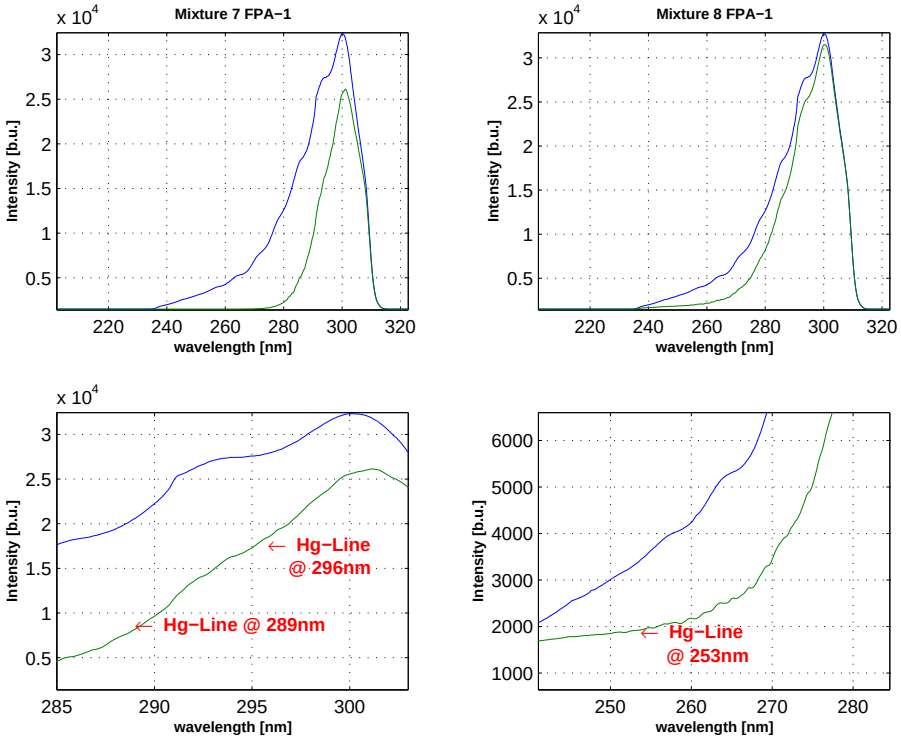

Figure B.24: Intensities regarding mixture 7 and 8 measured with GOME-2 FM2-1 @ 203K. The lower graphics show the corresponding relevant wavelength range together with arrows indicating the location of Hg-Lines, where comparisons with literature data have been done at 293K (At this temperature only at 253nm)

Intensities in b.u. for measurements with GOME-2 FM3 at 293K

Mixture	FPA	λ [nm]	I_0 [bu]	I [bu]
1	2	353 - 400	7000 - 9000	2500 - 9000
1	3	400 - 455	2500 - 20000	2500 - 8000
2	2	340 - 360	7000	3000 - 6000
2	3	430 - 490	10000 - 43000	10000 - 25000
3	2	310 - 345	2000 - 8000	1800(low c) - 7000(high c)
3	3	475 - 600	20000 - 38000	20000
3	4	590 - 790	22000 - 35000	10000 - 20000
6	1	298 - 310	13000 - 8000	11000 - 6000
		Hg(302)	12770	10140
6	2	310 - 315	2400 - 15000	2200 - 10000
7	1	285 - 303	8000 - 14000	3500 - 12000
		Hg(289)	10060	5550
		Hg(296)	13070	10045
8	1	240 - 290	1800 - 12000	1600 - 9000
		Hg(253)	2560	1780

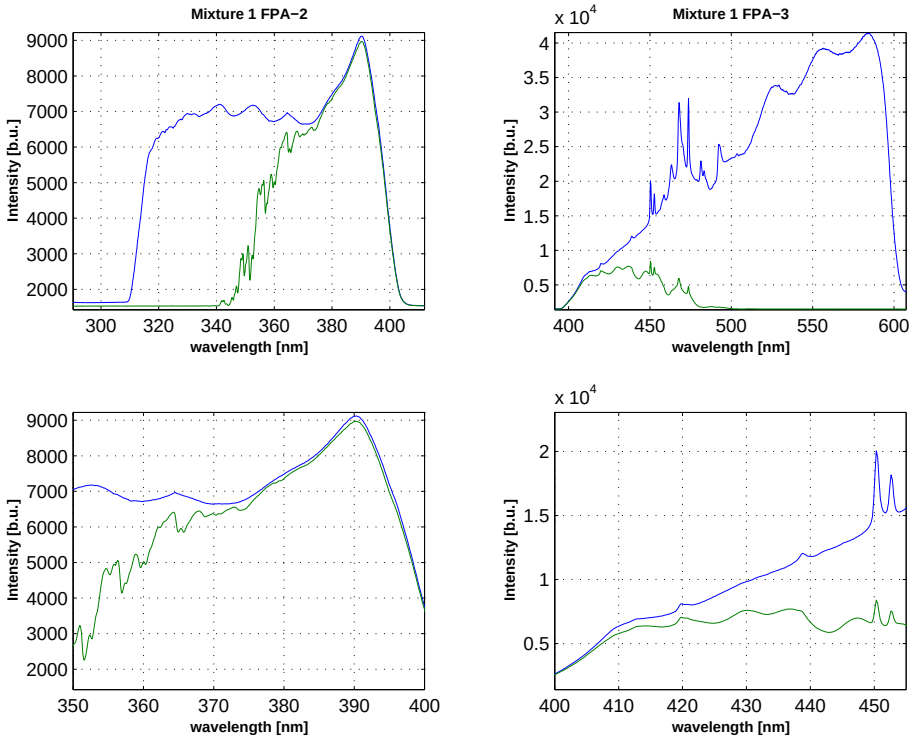

Figure B.25: Intensities regarding mixture 1 measured with GOME-2 FM3 @ 293K. The lower graphics show the corresponding relevant wavelength range

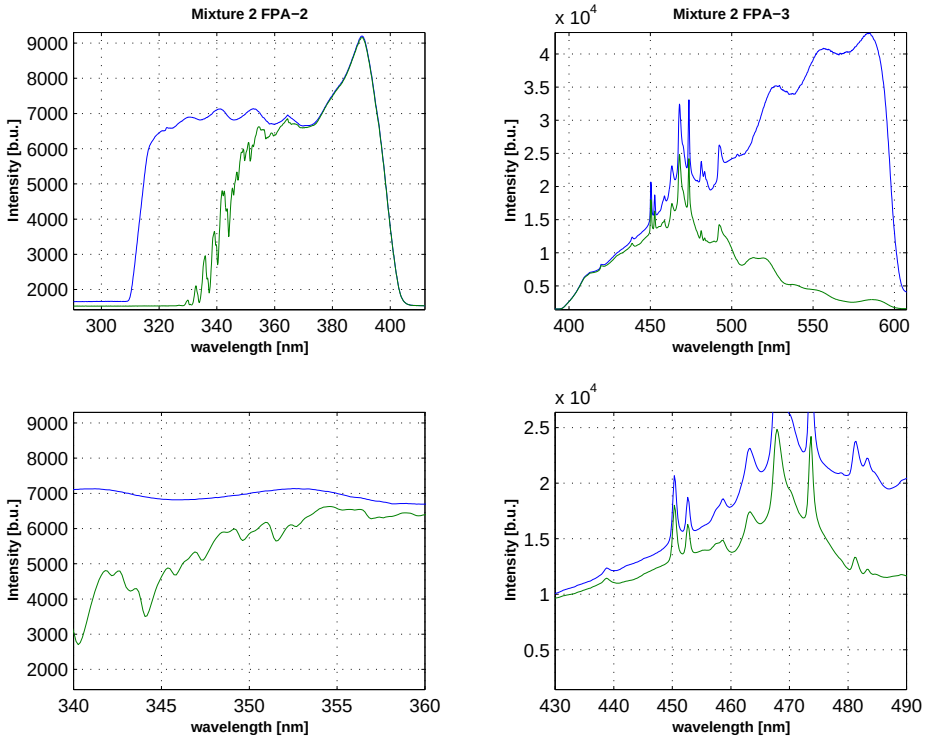

Figure B.26: Intensities regarding mixture 2 measured with GOME-2 FM3 @ 293K. The lower graphics show the corresponding relevant wavelength range

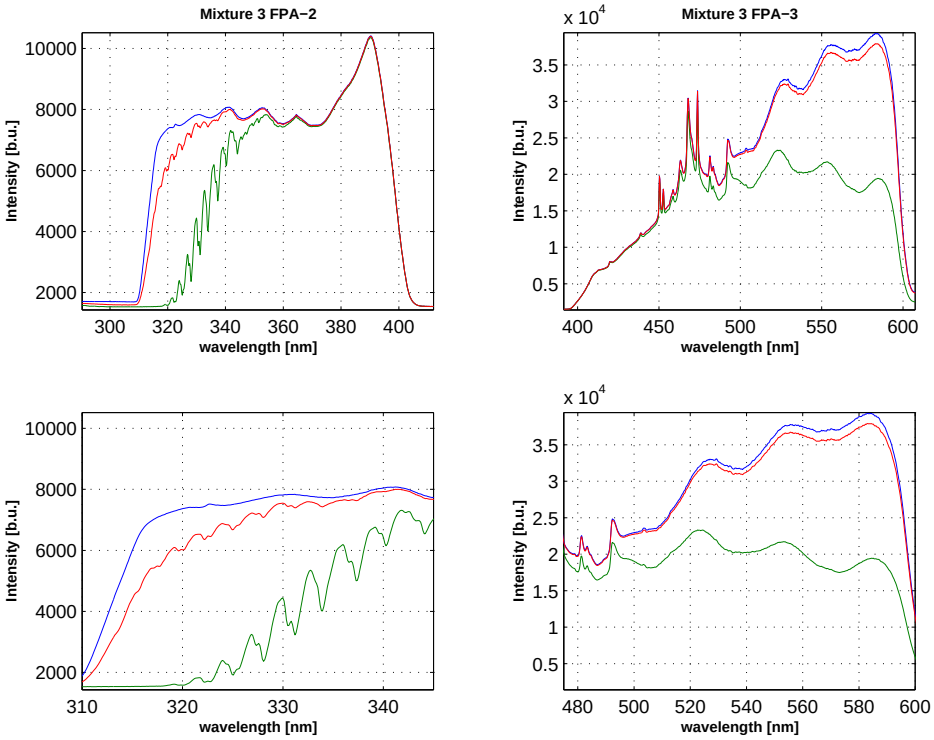

Figure B.27: Intensities regarding mixture 3 measured with GOME-2 FM3 @ 293K. As described in the report mixture 3 corresponds to several measurements with slightly different concentrations. The red line shows the intensity with the lowest and the green line the highest concentration regarding mixture 3

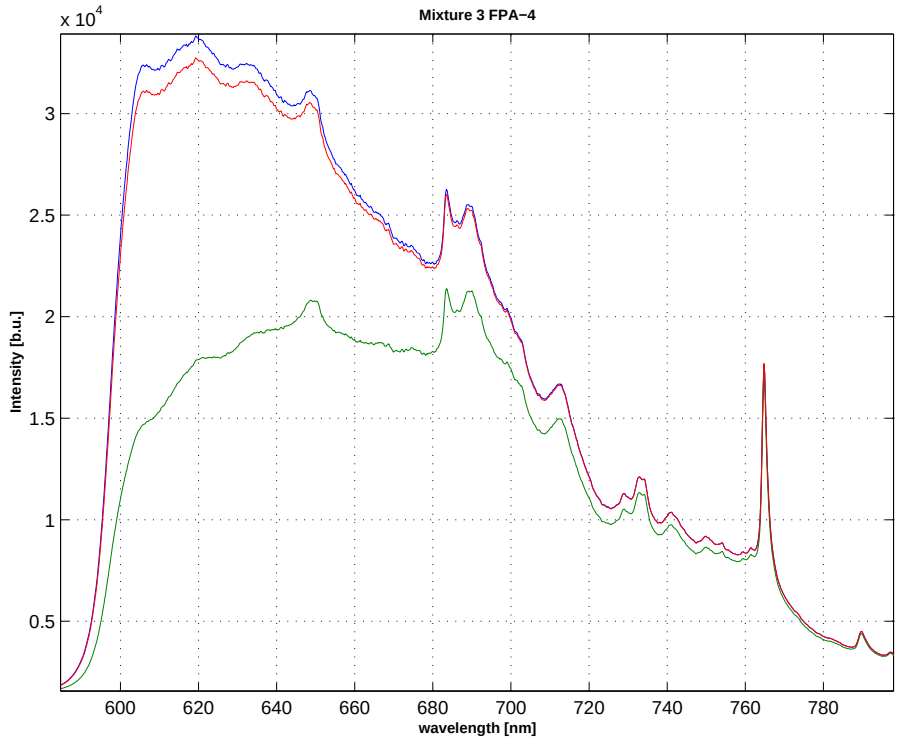

Figure B.28: Intensities regarding mixture 3 in channel 4 measured with GOME-2 FM3 @ 293K.

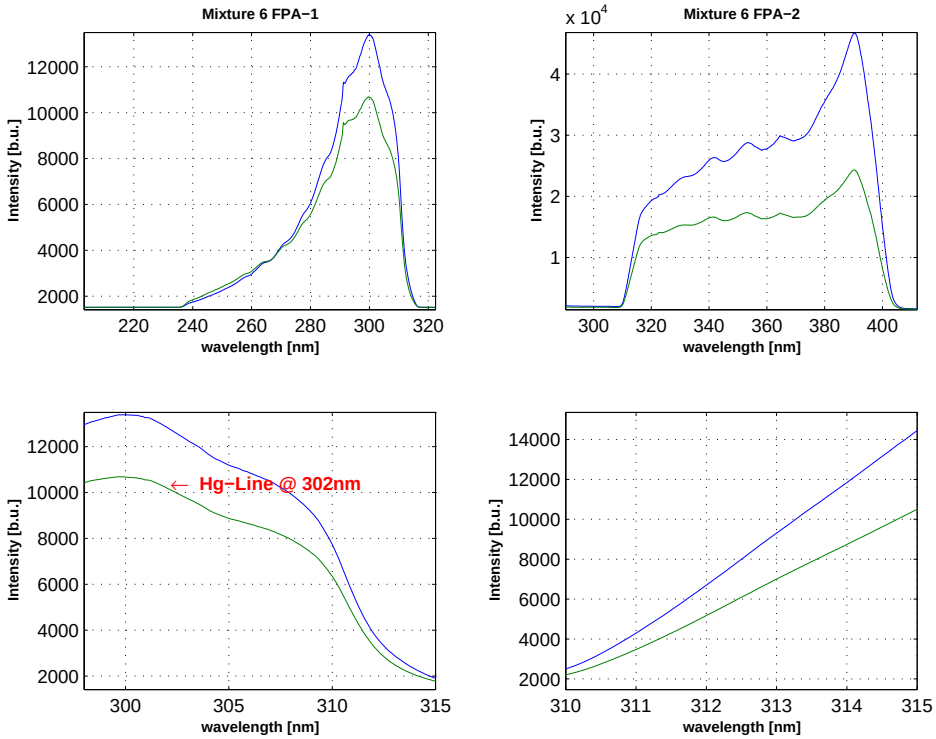

Figure B.29: Intensities regarding mixture 6 measured with GOME-2 FM3 @ 293K. The lower graphics show the corresponding relevant wavelength range

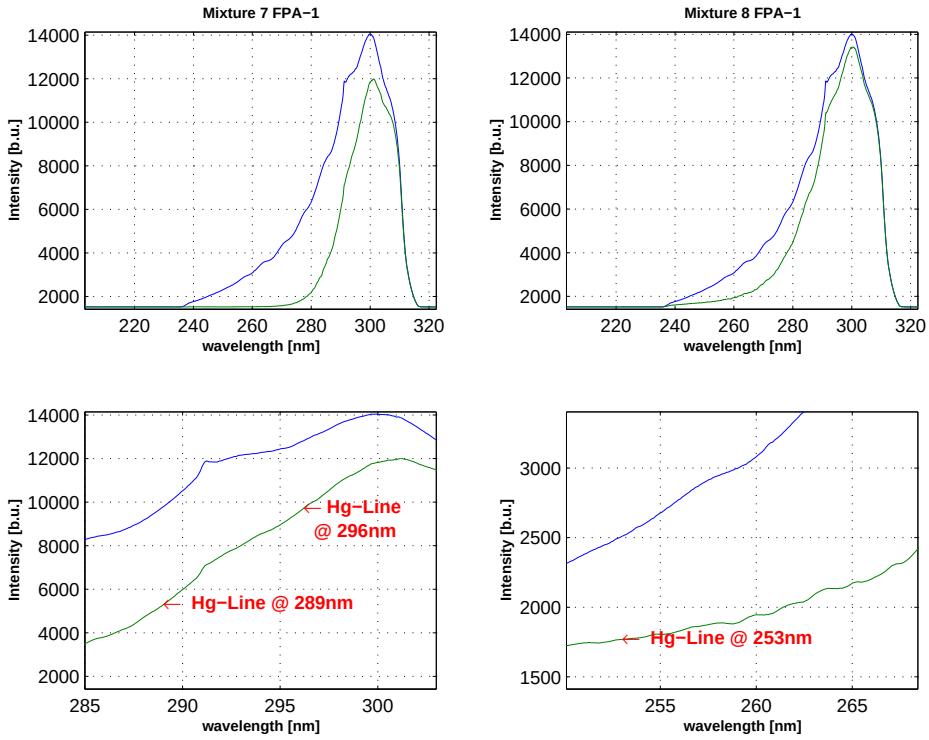

Figure B.30: Intensities regarding mixture 7 and 8 measured with GOME-2 FM3 @ 293K. The lower graphics show the corresponding relevant wavelength range together with arrows indicating the location of Hg-Lines, where comparisons with literature data have been done.

Intensities in b.u. for measurements with GOME-2 FM3 at 273K

Mixture	FPA	λ [nm]	I_0 [bu]	I [bu]
1	2	353 - 400	7000 - 9000	2500 - 9000
1	3	400 - 455	2000 - 17000	2000 - 7000
2	2	340 - 360	7000	2300 - 6500
2	3	430 - 490	8000 - 25000	7500 - 17000
3	2	310 - 345	1700 - 7000	1600 - 6000
3	3	475 - 600	17000 - 35000	15000 - 5000
3	4	590 - 790	30000 - 2500	16000 - 2500
6	1	298 - 310	11000 - 7000	4000 - 6000
		Hg(302)	10500	5800
6	2	310 - 315	2500 - 12000	2200 - 10500
7	1	285 - 303	6300 - 11000	3000 - 9000
		Hg(289)	7500	4400
		Hg(296)	9700	7500
8	1	240 - 290	1700 - 8000	1550 - 7000
		Hg(253)	2200	1670

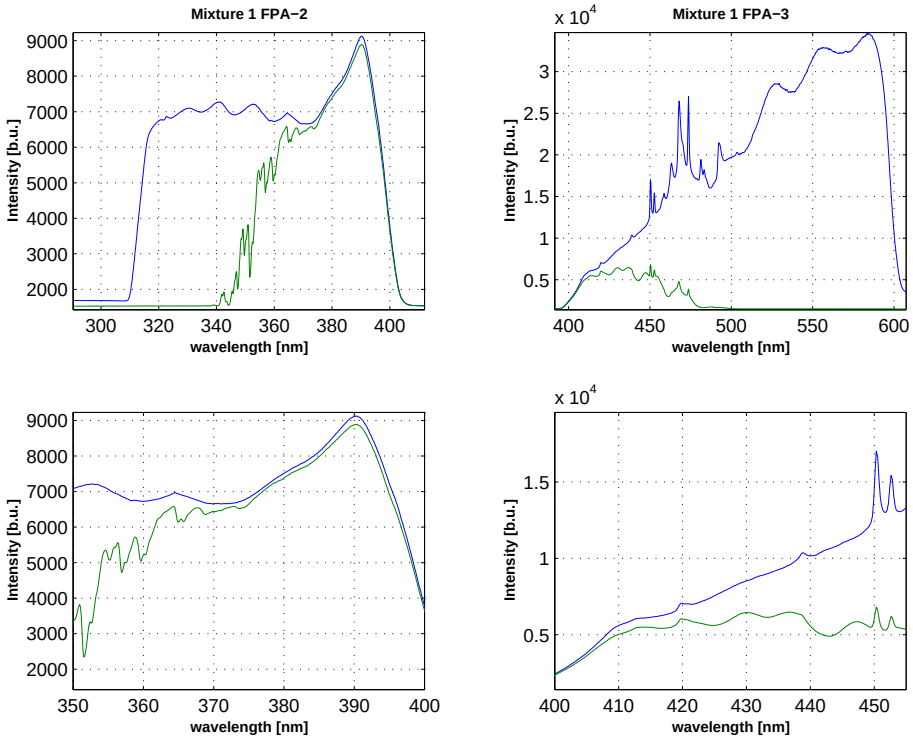

Figure B.31: Intensities regarding mixture 1 measured with GOME-2 FM3 @ 273K. The lower graphics show the corresponding relevant wavelength range

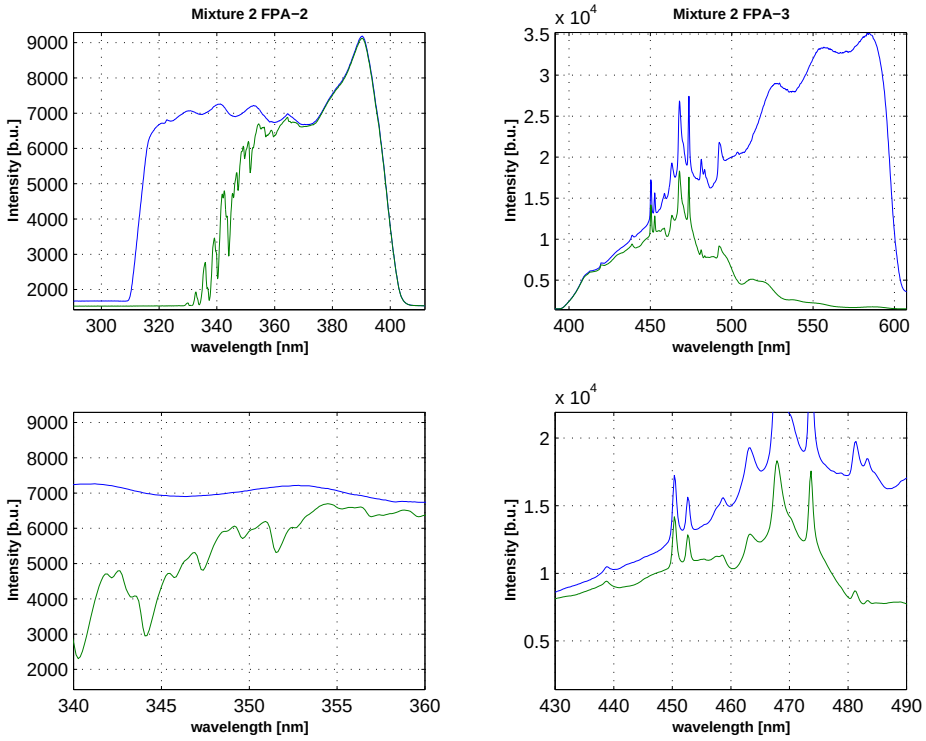

Figure B.32: Intensities regarding mixture 2 measured with GOME-2 FM3 @ 273K. The lower graphics show the corresponding relevant wavelength range

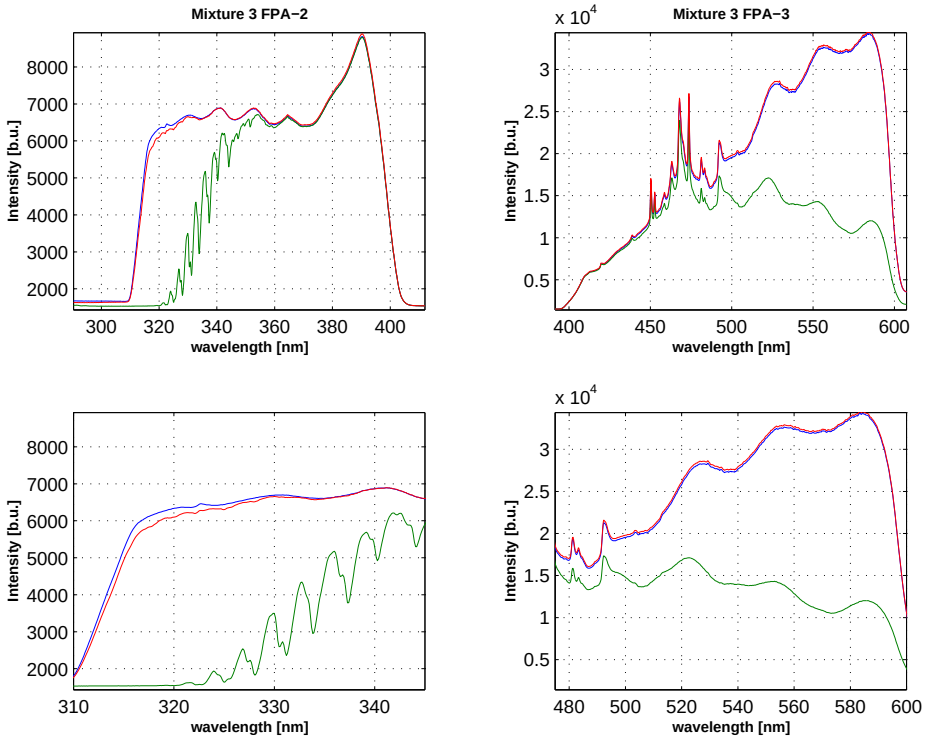

Figure B.33: Intensities regarding mixture 3 measured with GOME-2 FM3 @ 273K. As described in the report mixture 3 corresponds to several measurements with slightly different concentrations. The red line shows the intensity with the lowest and the green line the highest concentration regarding mixture 3

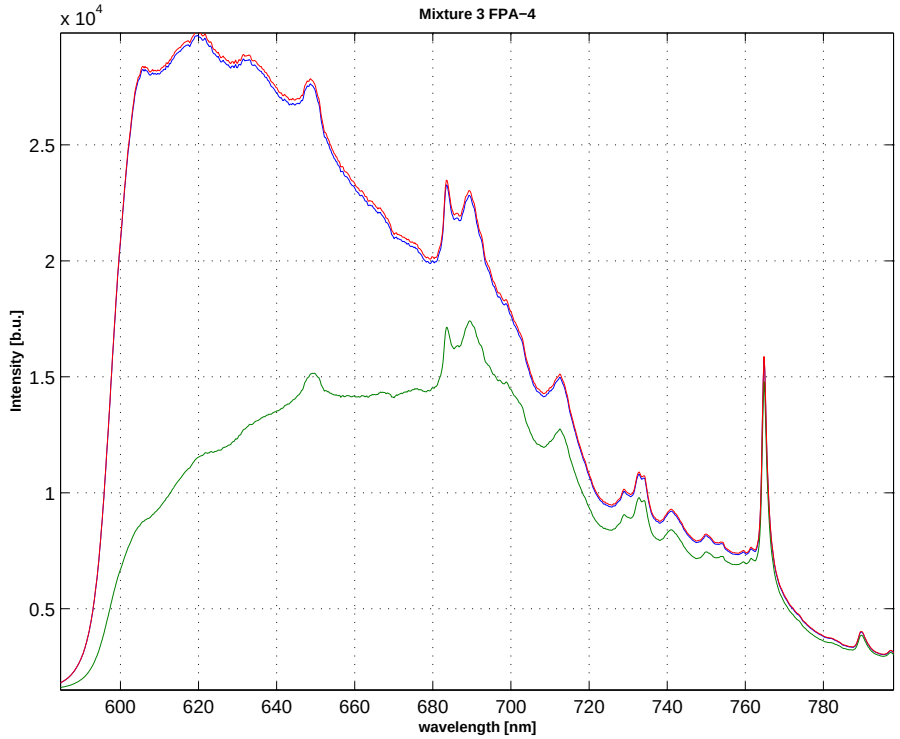

Figure B.34: Intensities regarding mixture 3 in channel 4 measured with GOME-2 FM3 @ 273K.

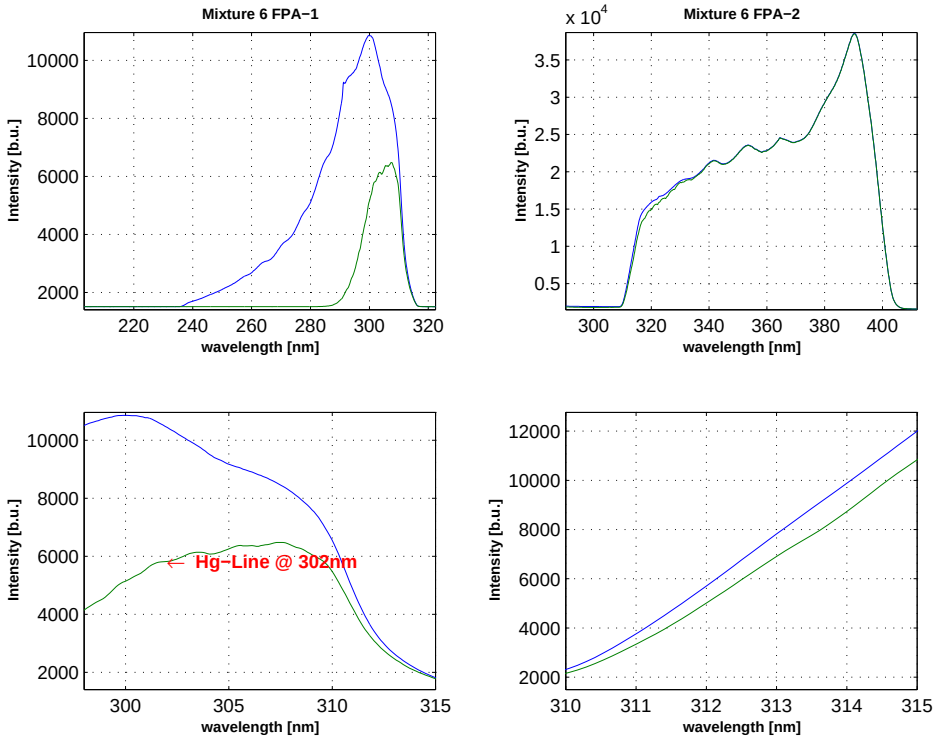

Figure B.35: Intensities regarding mixture 6 measured with GOME-2 FM3 @ 273K. The lower graphics show the corresponding relevant wavelength range

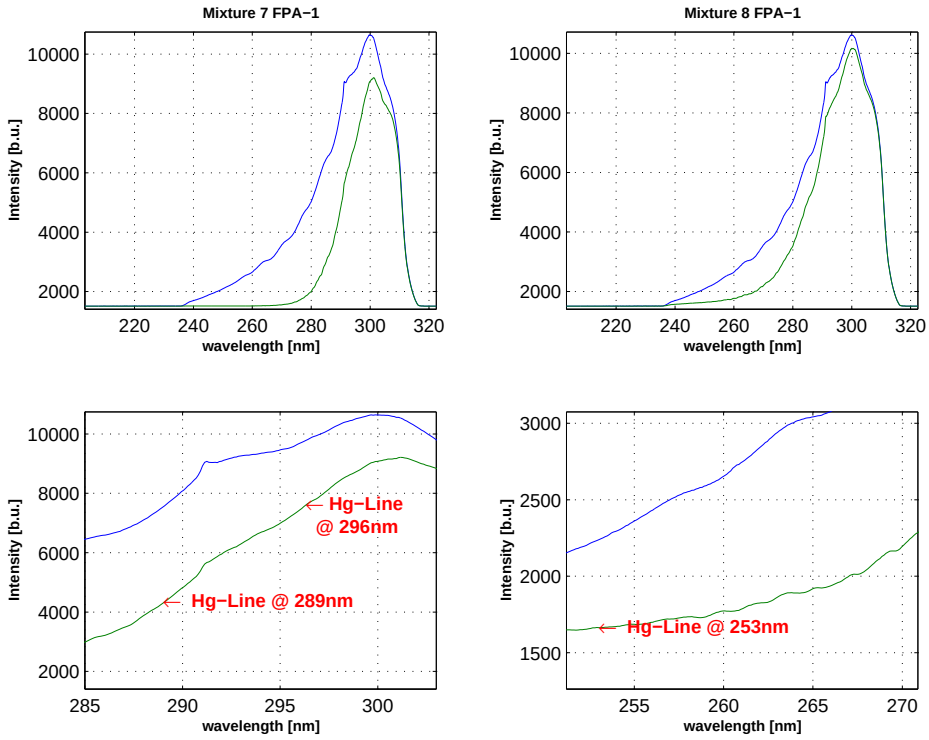

Figure B.36: Intensities regarding mixture 7 and 8 measured with GOME-2 FM3 @ 273K. The lower graphics show the corresponding relevant wavelength range together with arrows indicating the location of Hg-Lines, where comparisons with literature data have been done at 293K (At this temperature only at 253nm)

Intensities in b.u. for measurements with GOME-2 FM3 at 243K

Mixture	FPA	λ [nm]	I_0 [bu]	I [bu]
1	2	353 - 400	9000 - 1000	2500 - 10500
1	3	400 - 455	2000 - 18000	2000 - 7000
2	2	340 - 360	9000	4500 - 8500
2	3	430 - 490	10000 - 25000	9000 - 20000
3	2	310 - 345	1800 - 6300	1530 - 6000
3	3	475 - 600	17000 - 35000	15000 - 5000
3	4	590 - 790	22000 - 3000	10000 - 2500
6	1	298 - 310	10000 - 5500	3500 - 5500
		Hg(302)	9000	4800
6	2	310 - 315	2300 - 10500	2100 - 9500
7	1	285 - 303	5700 - 9000	2500 - 7500
		Hg(289)	6500	3500
		Hg(296)	8200	6200
8	1	240 - 290	1700 - 7000	1590 - 6000
		Hg(253)	2150	1690

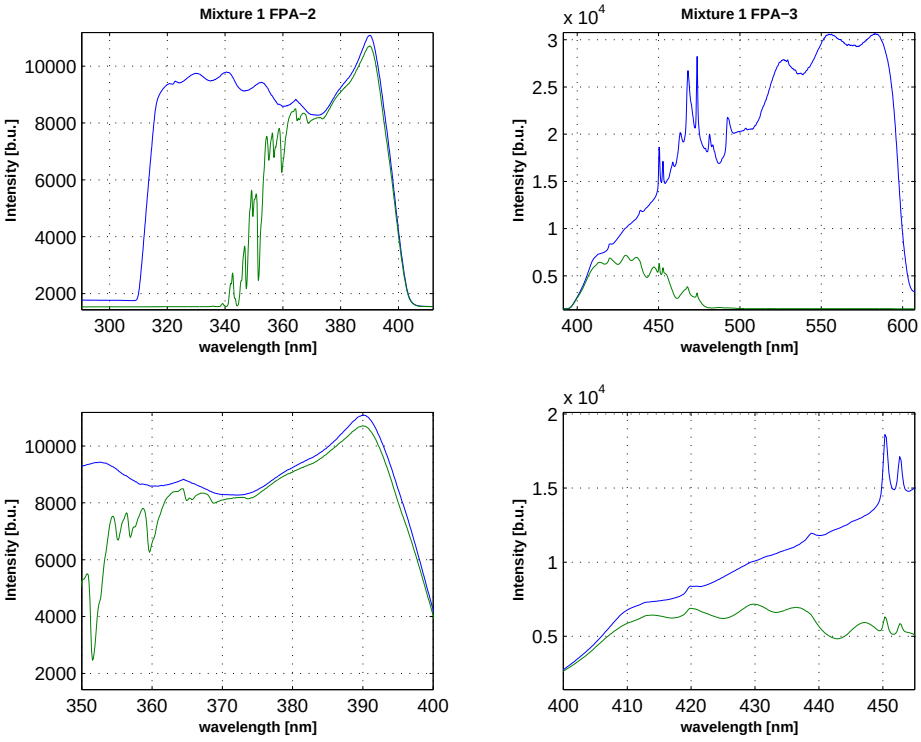

Figure B.37: Intensities regarding mixture 1 measured with GOME-2 FM3 @ 243K. The lower graphics show the corresponding relevant wavelength range

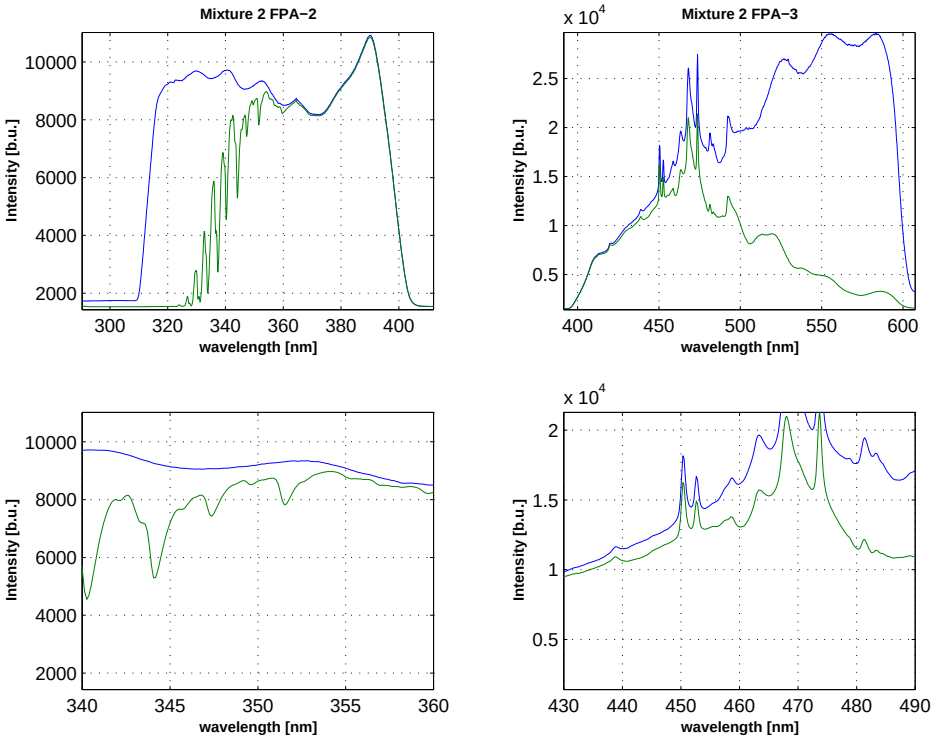

Figure B.38: Intensities regarding mixture 2 measured with GOME-2 FM3 @ 243K. The lower graphics show the corresponding relevant wavelength range

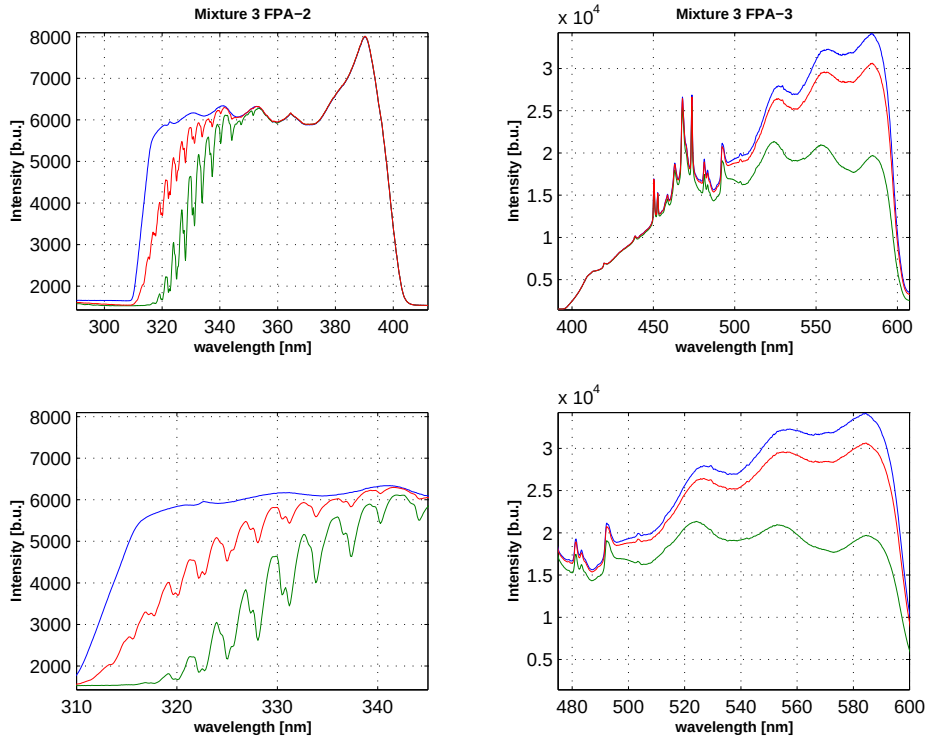

Figure B.39: Intensities regarding mixture 3 measured with GOME-2 FM3 @ 243K. As described in the report mixture 3 corresponds to several measurements with slightly different concentrations. The red line shows the intensity with the lowest and the green line the highest concentration regarding mixture 3

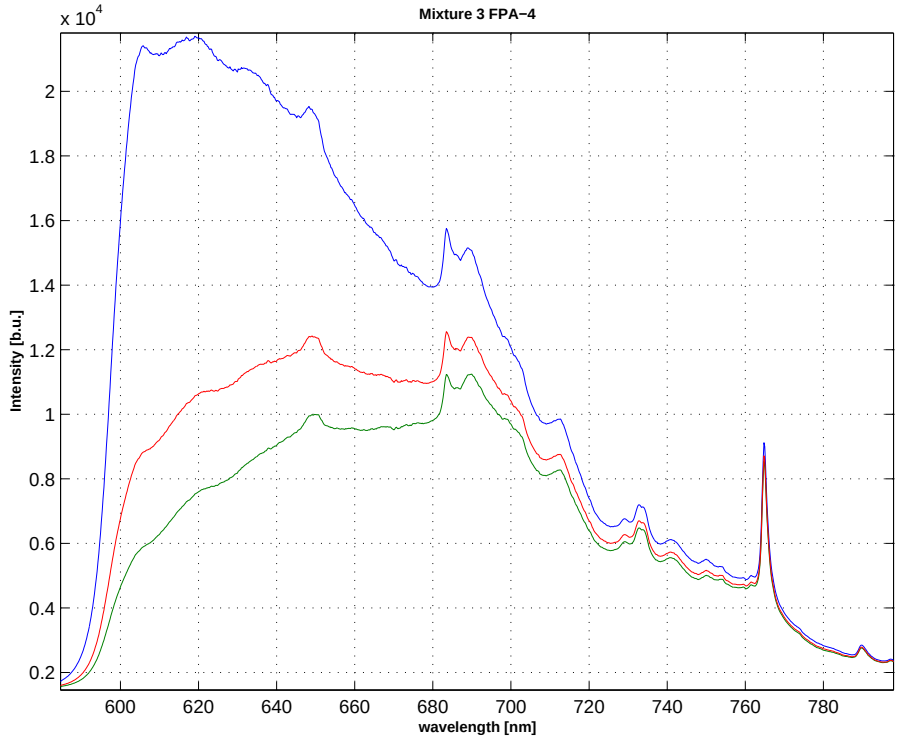

Figure B.40: Intensities regarding mixture 3 in channel 4 measured with GOME-2 FM3 @ 243K.

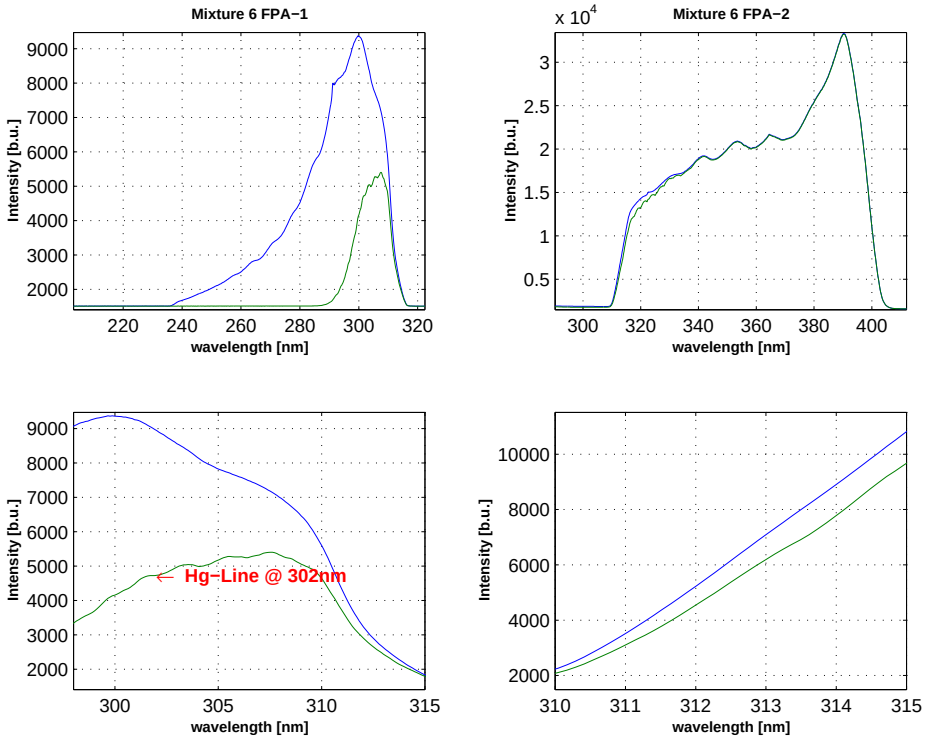

Figure B.41: Intensities regarding mixture 6 measured with GOME-2 FM3 @ 243K. The lower graphics show the corresponding relevant wavelength range

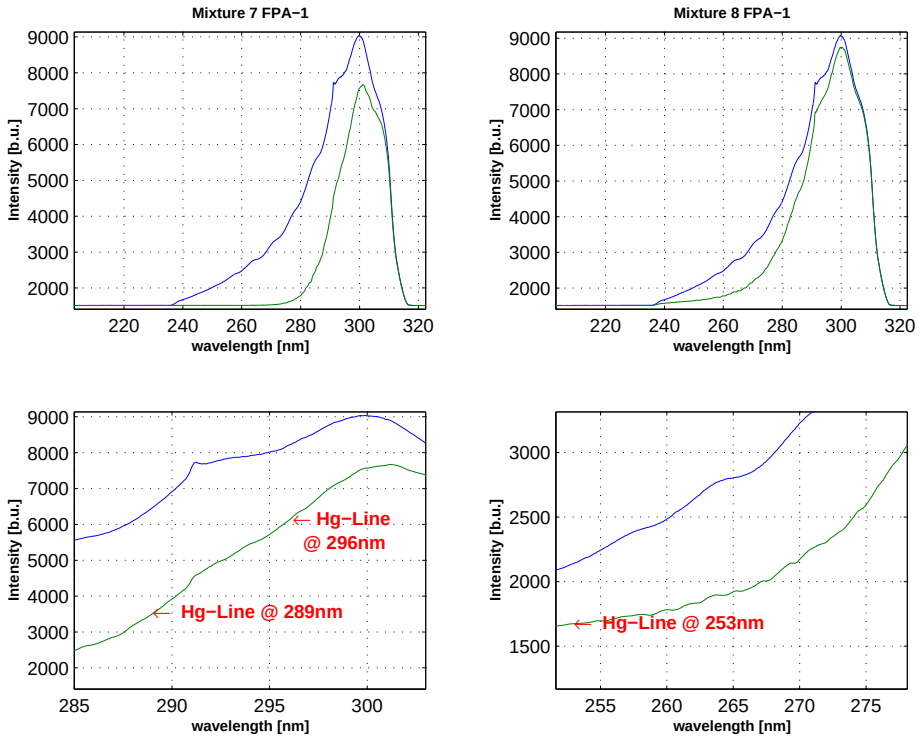

Figure B.42: Intensities regarding mixture 7 and 8 measured with GOME-2 FM3 @ 243K. The lower graphics show the corresponding relevant wavelength range together with arrows indicating the location of Hg-Lines, where comparisons with literature data have been done at 293K (At this temperature only at 253nm)

Intensities in b.u. for measurements with GOME-2 FM3 at 223K

Mixture	FPA	λ [nm]	I_0 [bu]	I [bu]
1	2	353 - 400	5000 - 6500	2000 - 6000
1	3	400 - 455	2000 - 12000	2000 - 5000
2	2	340 - 360	8000	4000 - 7800
2	3	430 - 490	10000 - 25000	9000 - 19000
3	2	310 - 345	3200 - 28000	1900 - 26000
3	3	475 - 600	22000 - 35000	20000 - 5000
3	4	590 - 790	30000 - 3500	15000 - 3300
6	1	298 - 310	9000 - 2000	5000 - 1900
		Hg(302)	8500	5500
6	2	310 - 315	2300 - 10000	2100 - 9500
7	1	285 - 303	5500 - 8500	2300 - 7000
		Hg(289)	6300	3300
		Hg(296)	8000	5800
8	1	240 - 290	1700 - 6500	1590 - 5800
		Hg(253)	2100	1700

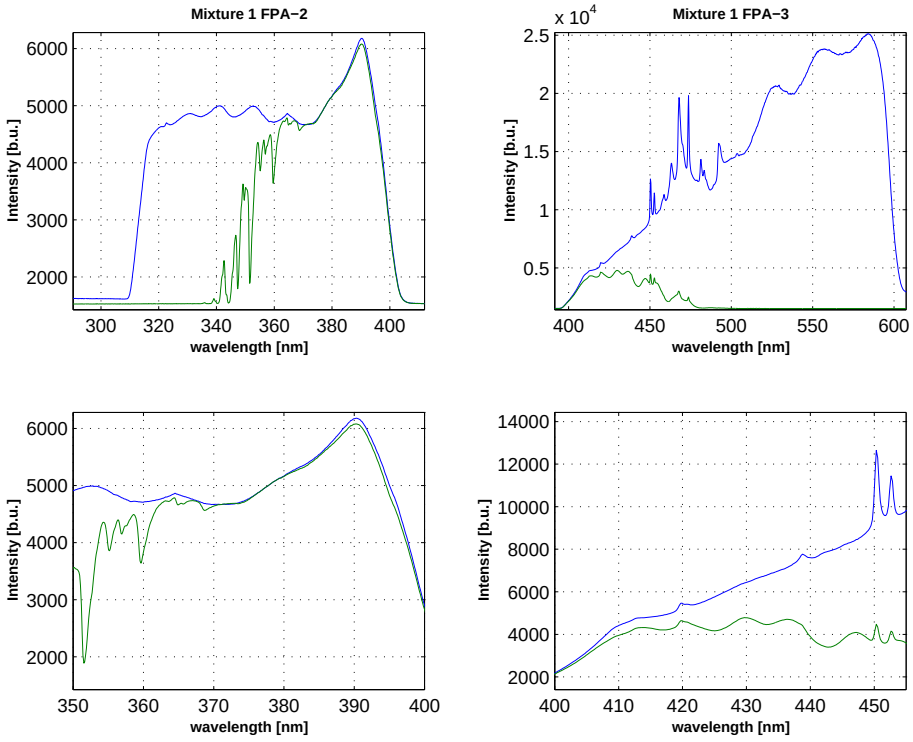

Figure B.43: Intensities regarding mixture 1 measured with GOME-2 FM3 @ 223K. The lower graphics show the corresponding relevant wavelength range

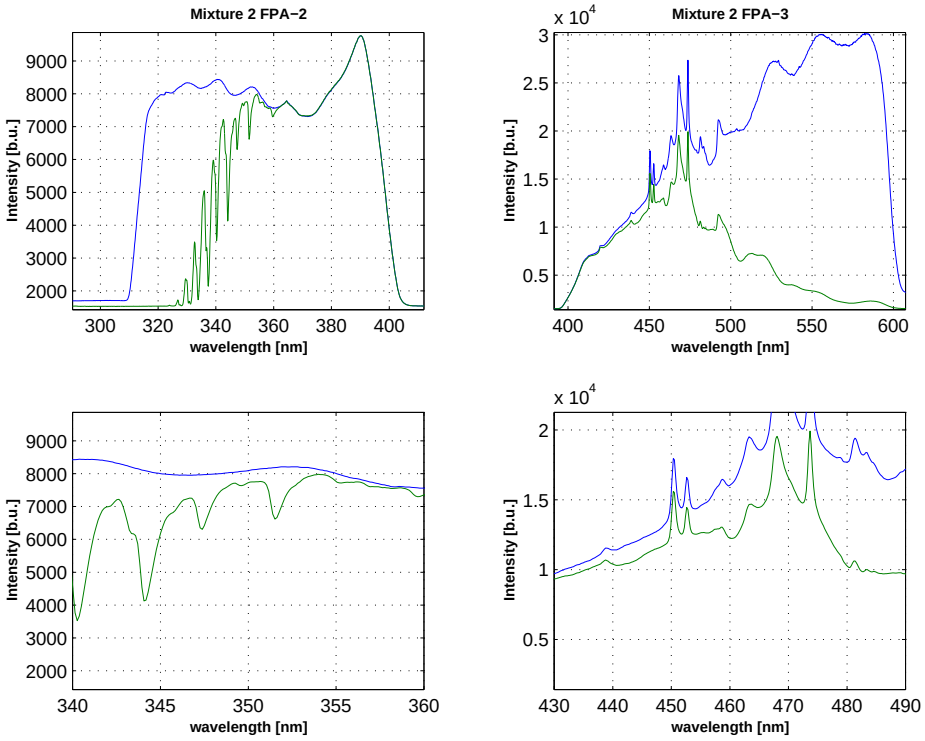

Figure B.44: Intensities regarding mixture 2 measured with GOME-2 FM3 @ 223K. The lower graphics show the corresponding relevant wavelength range

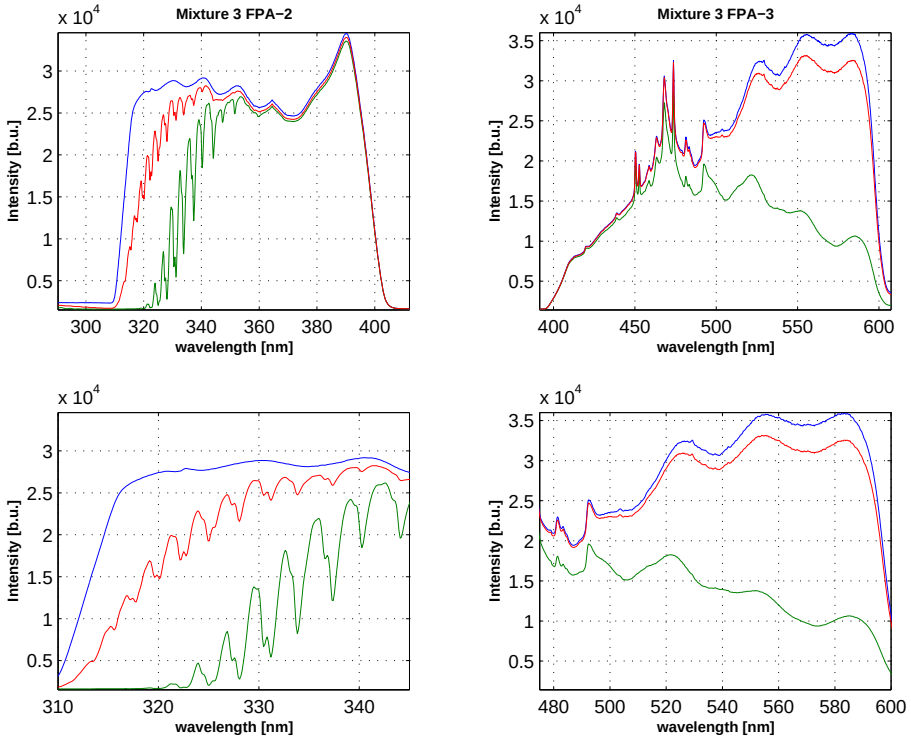

Figure B.45: Intensities regarding mixture 3 measured with GOME-2 FM3 @ 223K. As described in the report mixture 3 corresponds to several measurements with slightly different concentrations. The red line shows the intensity with the lowest and the green line the highest concentration regarding mixture 3

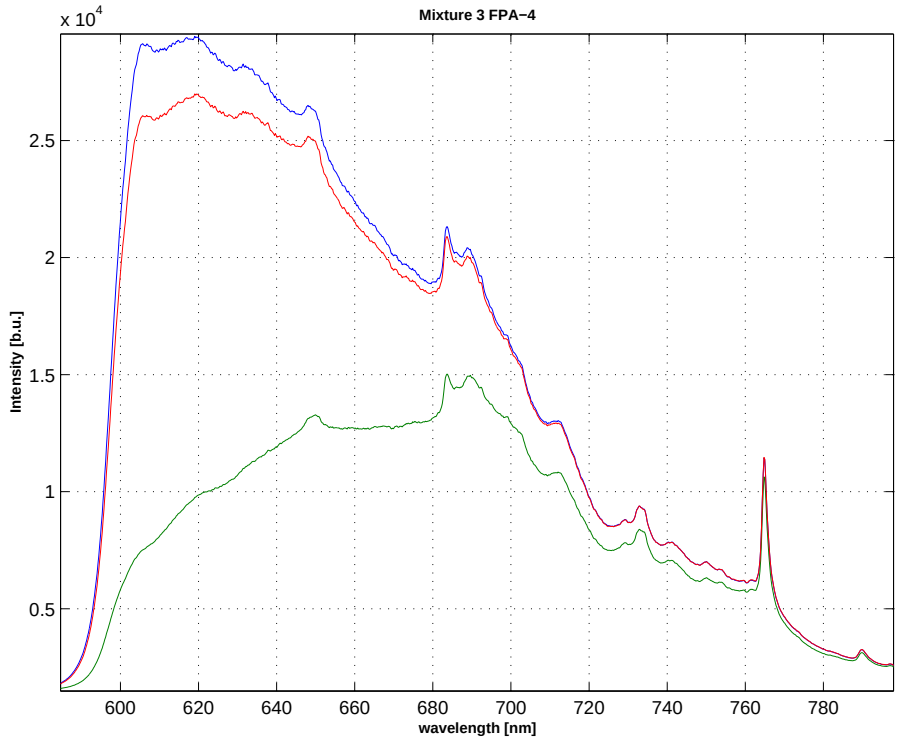

Figure B.46: Intensities regarding mixture 3 in channel 4 measured with GOME-2 FM3 @ 223K.

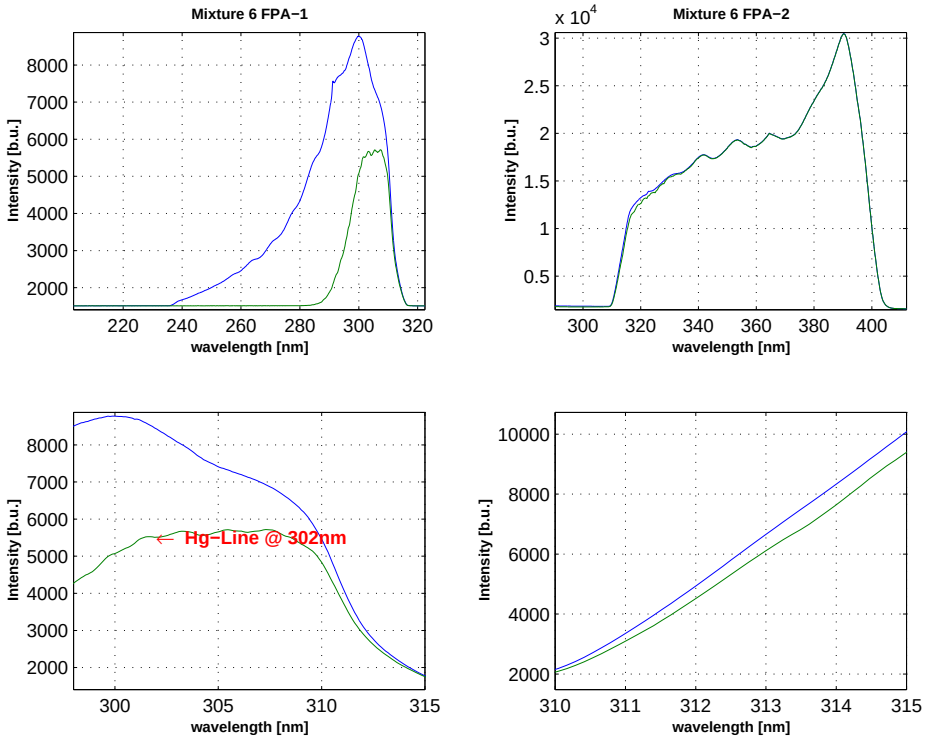

Figure B.47: Intensities regarding mixture 6 measured with GOME-2 FM3 @ 223K. The lower graphics show the corresponding relevant wavelength range

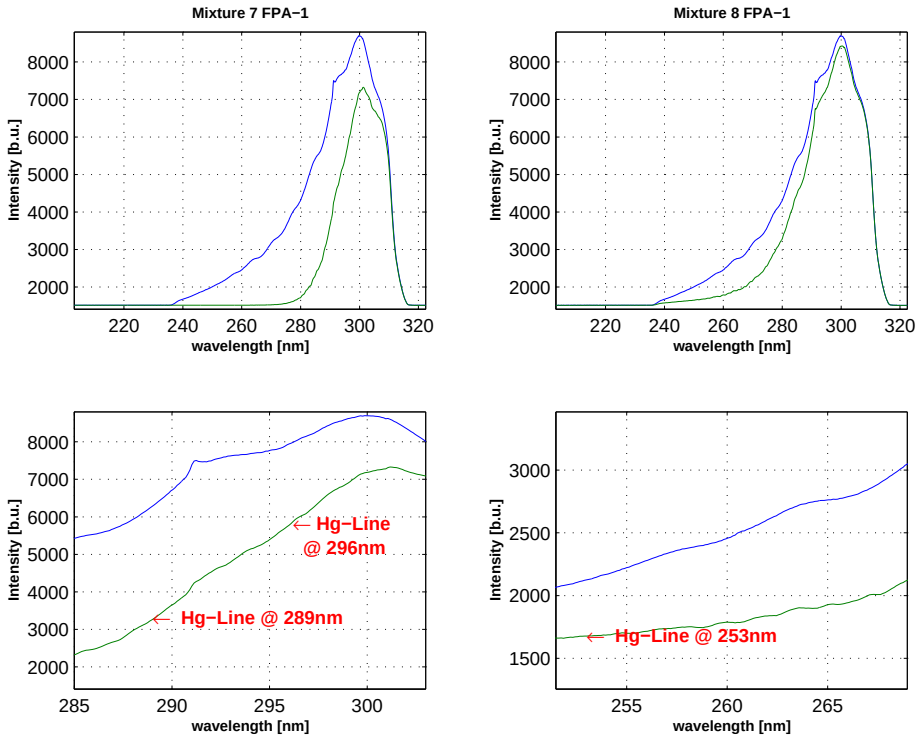

Figure B.48: Intensities regarding mixture 7 and 8 measured with GOME-2 FM3 @ 223K. The lower graphics show the corresponding relevant wavelength range together with arrows indicating the location of Hg-Lines, where comparisons with literature data have been done at 293K (At this temperature only at 253nm)

Intensities in b.u. for measurements with GOME-2 FM3 at 203K

Mixture	FPA	λ [nm]	I_0 [bu]	I [bu]
1	2	353 - 400	5000 - 6500	1800 - 5000
1	3	400 - 455	2000 - 12000	2000 - 4000
2	2	340 - 360	4800	2000 - 4500
2	3	430 - 490	6000 - 15000	5000 - 12000
3	2	310 - 345	2000 - 6800	1600 - 6000
3	3	475 - 600	15000 - 25000	12000 - 2400
3	4	590 - 790	16000 - 2200	3000 - 9000
6	1	298 - 310	11000 - 7000	14200 - 6400
		Hg(302)	12770	10140
6	2	310 - 315	2300 - 12000	2100 - 10000
7	1	285 - 303	6000 - 10000	2600 - 8700
		Hg(289)	7200	3800
		Hg(296)	9400	7000
8	1	240 - 290	1700 - 8000	1590 - 7000
		Hg(253)	2200	1700

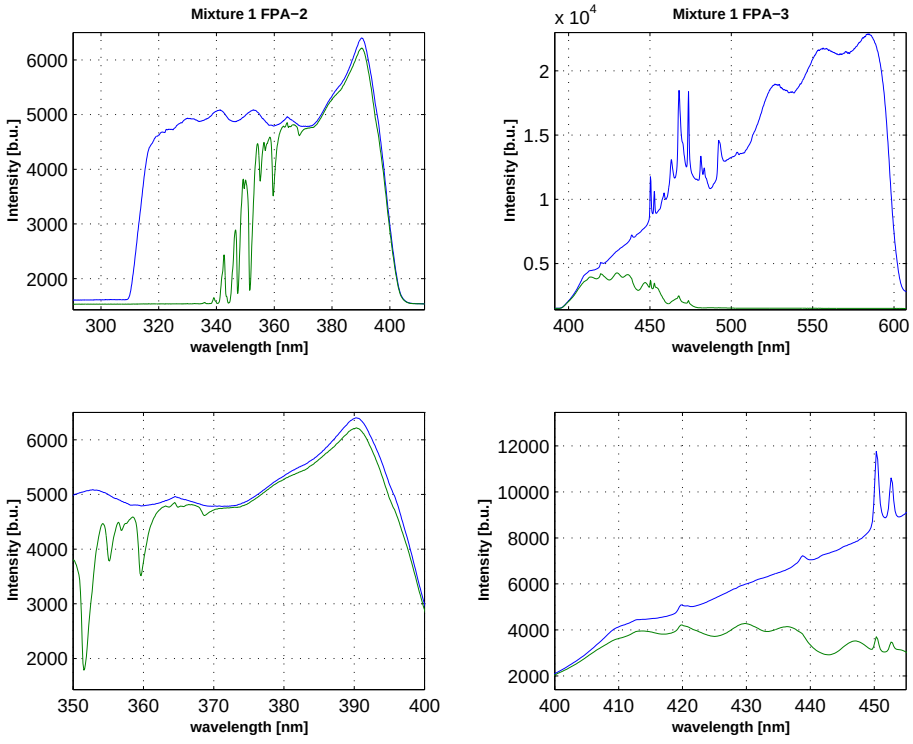

Figure B.49: Intensities regarding mixture 1 measured with GOME-2 FM3 @ 203K. The lower graphics show the corresponding relevant wavelength range

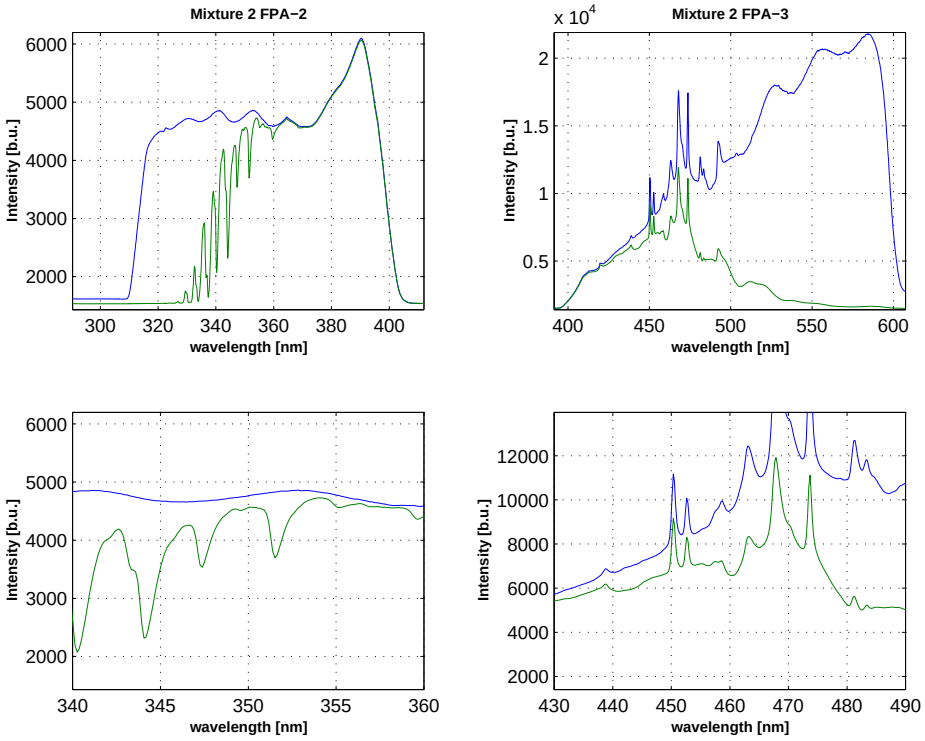

Figure B.50: Intensities regarding mixture 2 measured with GOME-2 FM3 @ 203K. The lower graphics show the corresponding relevant wavelength range

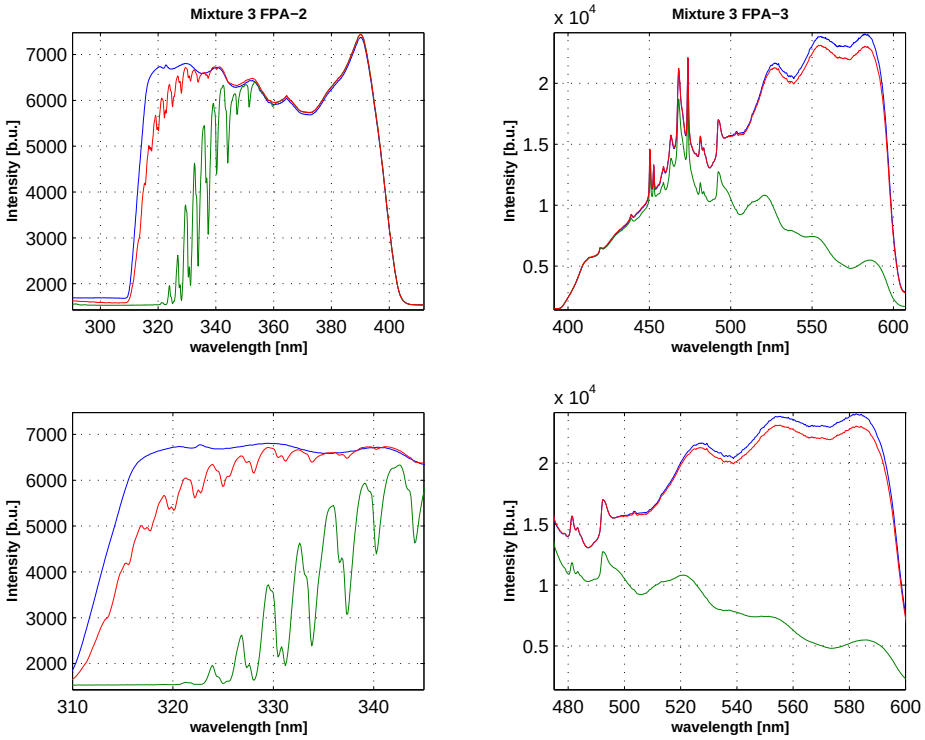

Figure B.51: Intensities regarding mixture 3 measured with GOME-2 FM3 @ 203K. As described in the report mixture 3 corresponds to several measurements with slightly different concentrations. The red line shows the intensity with the lowest and the green line the highest concentration regarding mixture 3

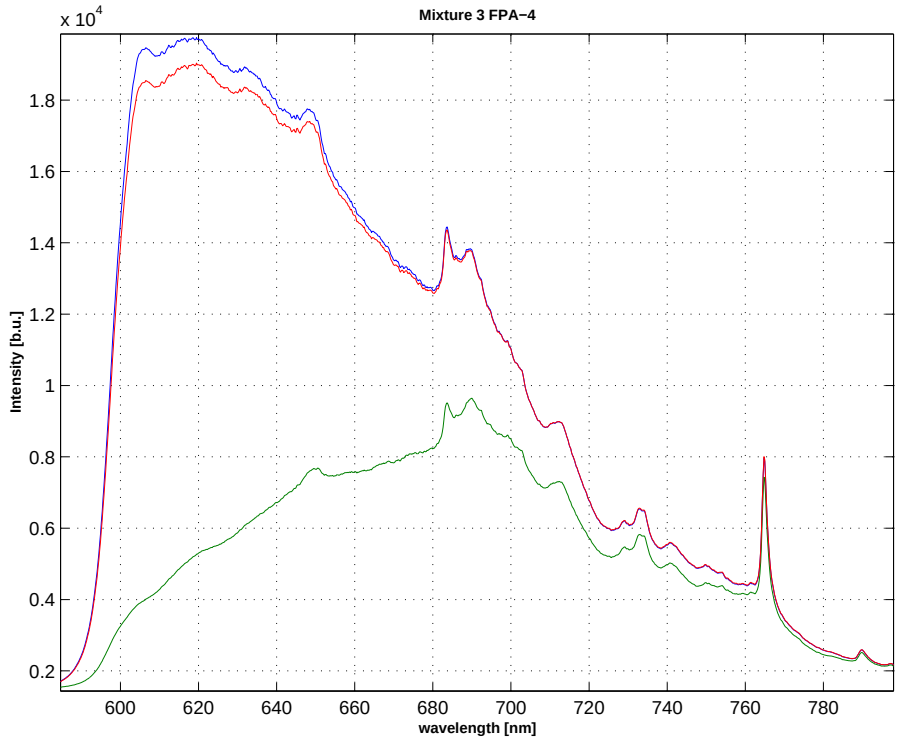

Figure B.52: Intensities regarding mixture 3 in channel 4 measured with GOME-2 FM3 @ 203K.

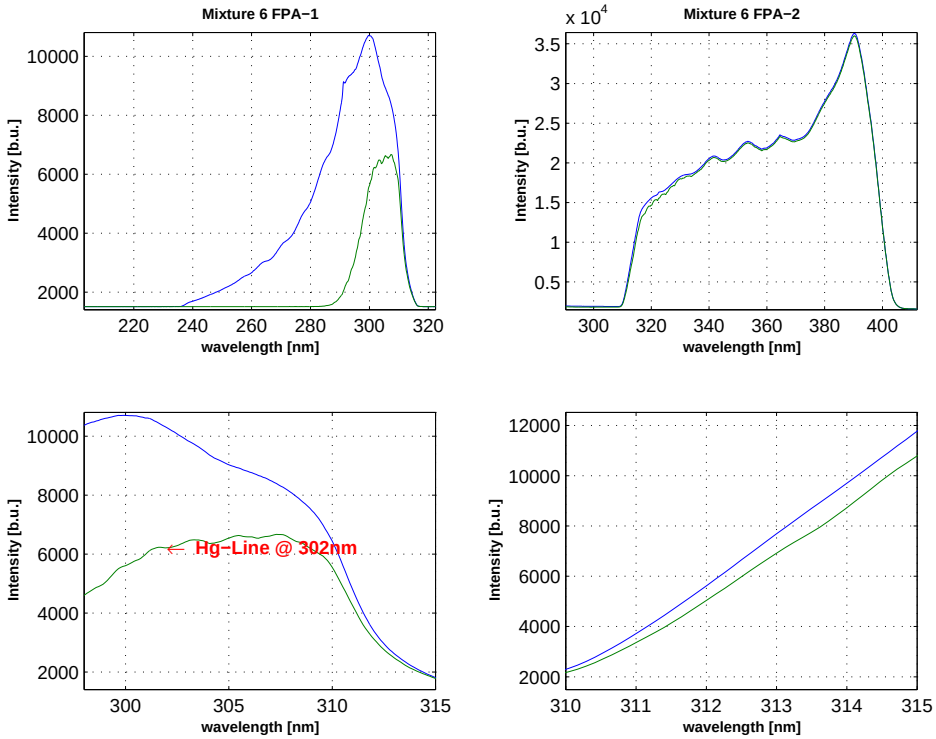

Figure B.53: Intensities regarding mixture 6 measured with GOME-2 FM3 @ 203K. The lower graphics show the corresponding relevant wavelength range

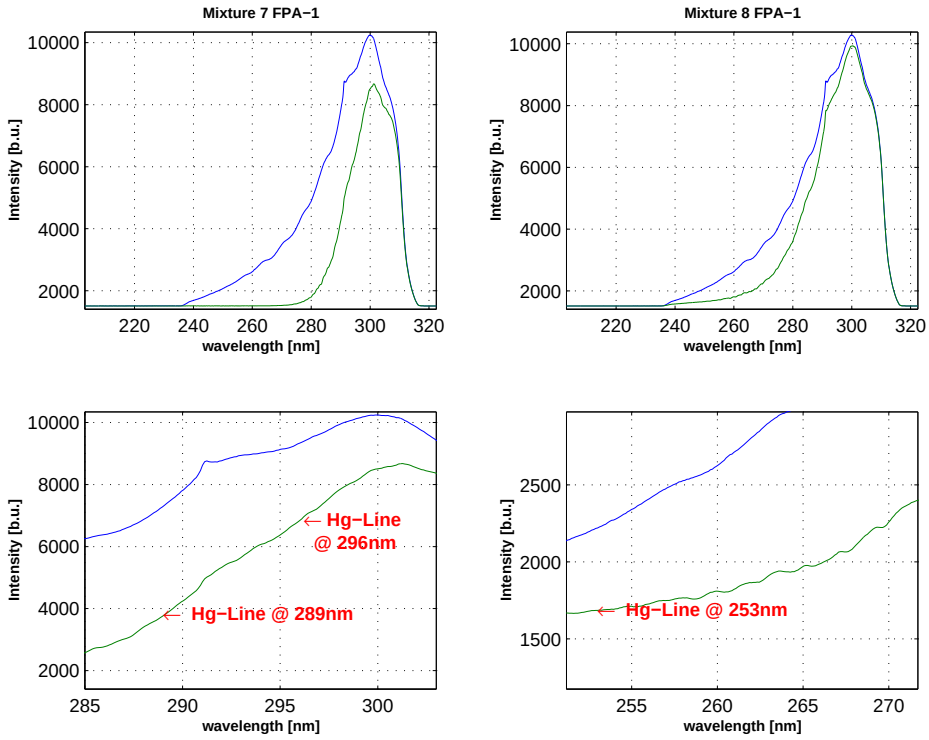

Figure B.54: Intensities regarding mixture 7 and 8 measured with GOME-2 FM3 @ 203K. The lower graphics show the corresponding relevant wavelength range together with arrows indicating the location of Hg-Lines, where comparisons with literature data have been done at 293K (At this temperature only at 253nm)

Appendix C

Publications

Poster Sessions

- B. Gür, P. Spietz, J. Orphal and J.P. Burrows *"Improved On-Ground Absorption Measurements with the GOME-2 Satellite Spectrometers by using the IFE / IUP CATGAS set-up"*, European Geophysical Union Assembly, Nice, France, April 2004
- B. Gür , P. Spietz , J. Orphal and J.P. Burrows *"Atmospheric Remote-Sensing Reference Data from GOME-2: Absorption Cross-Sections of Ozone at ambient Temperature in the 240 - 795 nm Range"* German Physical Society Conference, Berlin, Germany, March 2005
- B. Gür , P. Spietz , J. Orphal and J.P. Burrows *"Atmospheric Remote-Sensing Reference Data from GOME-2: Temperature-Dependent Absorption Cross-Sections of Ozone in the 240 - 795 nm Range""* European Geophysical Union Assembly, Vienna, Austria, April 2005
- B. Gür , P. Spietz , J. Orphal, C. Albers and J.P. Burrows *"Atmospheric Remote-Sensing Reference Data from GOME-2: Temperature-Dependent Absorption Cross-Sections of NO_2 in the 240 - 795 nm Range"* European Geophysical Union Assembly, Vienna, Austria, April 2005

Paper

- B. Gür , P. Spietz , J. Orphal and J.P. Burrows *"Spectra and temperature dependence of the ozone absorption cross section between 203 and 293 K in the 240 to 790 nm range determined by using the GOME-2 satellite spectrometers"*, manuscript in preparation
- B. Gür , P. Spietz , J. Orphal, C. Albers and J.P. Burrows *"Atmospheric Remote-Sensing Reference Data from GOME-2: Temperature-Dependent Absorption Cross-Sections of NO_2 in the 240 - 795 nm Range"*, manuscript in preparation

Bibliography

[1] J. Orphal, *"Critical Review of the Absorption Cross Sections of Ozone and NO_2 in the 240 - 790 nm Region" Part 1: Ozone*", ESA Technical Note MO-TN-ESA-GO-0302, see also Journal of Photochemistry and Photobiology A: Chemistry, 157, 185-209 (2003)

[2] J. Orphal, *"Critical Review of the Absorption Cross Sections of Ozone and NO_2 in the 240 - 790 nm Region" Part 2: Nitrogen Dioxide*", see also Journal of Photochemistry and Photobiology A: Chemistry, 157, 185-209 (2003)

[3] J.U. White, *"Long Optical Paths of Large Aperture"* Journal of the Optical Society America, 32, 285-288 (1942)

[4] M. Eisinger, *"Nachweis von BrO über mittleren nördlichen Breiten mit differentieller Absorbtionsspektroskopie*", Diploma-Thesis, University Bremen (1994)

[5] H.K. Roscoe, A.K. Hind, *"The Equilibrium Constant of NO_2 with N_2O_4 and the Temperature Dependence of the Visible Spectrum of NO_2: A Critical Review and the Implications for Measurements of NO_2 in the Polar Stratosphere*", Journal of Atmospheric Chemistry, 16, 257 - 276 (1993)

[6] S. A. Nizkorodov, S. P. Sander and L. R. Brown *"Temperature and Pressure Dependence of High-Resolution Air-Broadened Absorption Cross Sections of NO2 (415-525 nm)"*, Journal of Physical Chemistry A, 108(22), 4864 - 4872 (2004)

[7] A.C. Vandaele, C. Hermans, P.C. Simon, M. Carleer, R. Colin, S. Fally, M.F. Merienne, A. Jenouvrier and B. Coquart *"Measurements of the NO_2 Absorption Cross Section from 42000 cm^{-1} to 10000 cm^{-1} (238-1000 nm) at 220 K and 294 K"* Journal of Quantitative Spectroscopy and Radiative Transfer, 59, No. 3-5, 171-184 (1998)

[8] R.S. Mulliken, Journal of Chemical Physics, 7, 14-20 (1939)

[9] Z. El Helou, S. Churassy, G. Wannous, R. Bacis and E. Boursey, *"Absolute cross sections of ozone at atmospheric temperatures for the Wulf and the Chappuis bands*", Journal of Chemical Physics, 122, 244311 (2005)

[10] S. Solomon, A.L. Schmeltekopf, and W.R. Sanders, Journal of Geophysical Research, 92, 8311-8319 (1987)

[11] U. Platt, *"Differential optical absorption spectroscopy (DOAS), in Air Monitoring by Spectroscopic Techniques*, Chemical Analysis Series 127, Wiley, New York, (1994)

[12] L.T. Molina, M.J. Molina, *"Absolute Absorption Cross Section of Ozone in the 185-350 nm Wavelength Range"*, Journal of Geophysical Research 91, 14501-14508 (1986)

[13] J. Barnes and K. Mauersberger, *"Temperature Dependence of the Ozone Absorption Cross Section at the 253.7 nm Mercury Line"*, Journal of Geophysical Research, 92 D12, 14861-14864 (1987)

[14] K. Yoshino, D.E. Freeman, J.R. Esmond, W.H. Parkinson, *"Absolute Absorption Cross Section Measurements of Ozone in the Wavelength Region 238-335 nm and the Temperature Dependence"*, Planetary Space Science 36 No.4, 395-398 (1988)

[15] J. Malicet, J. Brion, and D. Daumont, *"Temperature Dependence of the Absorption Cross Section of Ozone at 254 nm"*, Chemical Physics Letters 158, 293-296 (1989)

[16] J. Brion, A. Chakir, D. Daumont, J. Malicet, C. Parisse, *"High Resolution Laboratory Absorption Cross Section of O_3. Temperature Effect"*, Chemical Physics Letters 213, 610-612 (1993)

[17] A. Amoruso, M. Cacciani, A. Di Sarra, G. Fiocco, *"Apsorption Cross Sections of Ozone in the 590-610 nm Region at T=230 K and T=299 K"*, Journal of Geophysical Research 95 D12, 20565-20568 (1990)

[18] J. B. Burkholder and R. K. Talukdar, *"Temperature Dependence of the Ozone Absorption Spectrum over the Wavelength Range 410 to 760 nm"*, Geophysical Research Letters 21, No. 7, 581-584 (1994)

[19] J.P. Burrows, A. Richter, A. Dehn, B. Deters, S. Himmelmann, S. Voigt, J. Orphal, *"Atmospheric Remote-Sensing Reference Data from GOME-2. Temperature-Dependent Absorption Cross Sections of O_3 in the 231-794 nm Range"*, Journal of Quantitative Spectroscopy and Radiative Transfer 61, 509-517 (1999)

[20] J. Brion, A. Chakir, D. Daumont, C. Parisse, J. Malicet, *"Absorption Spectra Measurements for the Ozone Molecule in the 350-830 nm Region"*, Journal of Atmospheric Chemistry 30, 291-299 (1998)

[21] A.M. Bass, R.J. Paur, *"The Ultraviolet Cross-Sections of Ozone, Part I, The Measurements"*, C.S. Zerefos, A. Ghazi, D. Reidel (Eds.), Proceedings of the Quadrennial Ozone Symposium on Atmospheric Ozone, Norwell, Mass., 606-610 (1985)

[22] R.J. Paur, A.M. Bass, *"The Ultraviolet Cross-sections of Ozone, Part II, Result and Temperature Dependence"*, C.S. Zerefos, A. Ghazi, D. Reidel (Eds.), Proceedings of the Quadrennial Ozone Symposium on Atmospheric Ozone, Norwell, Mass., 611-616 (1985)

[23] J. Brion, D. Daumont, J. Malicet, *"New Measurements of the Absolute Absorption Cross Sections of Ozone at 294 and 223 K in the 310-350 nm Spectral Range"*, Journal of Physics Letters (Paris) 45, L57-L60 (1984)

[24] D. Daumont, J. Brion, J. Charbonnier, J. Malicet, *"Ozone UV-Spectroscopy. I: Absorption Cross Sections at Room Temperature"*, Journal of Atmospheric Chemistry 15, 145-155 (1992)

[25] J. Malicet, D. Daumont, J. Charbonnier, C. Chakir, A. Parisse, J. Brion, *"Ozone UV-Spectroscopy. II: Absorption Cross Sections and Temperature Dependence"*, Journal of Atmospheric Chemistry 21, 263-273 (1995)

[26] S. Voigt, J. Orphal, K. Bogumil, J.P. Burrows, *"The Temperature Dependence (203-293 K) of the Absorption Cross Sections of O_3 in the 230-850 nm Region Measured by Fourier-Transform Spectroscopy"*, Journal of Photochemistry and Photobiology A: Chemistry 143, 1-9 (2001)

[27] EUMETSAT Document EUM/OPS-EPS/MAN/05/2005, Issue: 1.0 Date: 28/02/05 GOME-2 Products Guide

[28] J.C. Gómez Martín, P. Spietz, J. Orphal and J. P. Burrows, *"Principal and Independent Component Analysis of Overlapping Spectra in the Context of Mulichannel Time-resolved Absorption Spectroscopy"* Spectro. Chim. Acta A, Vol. 60, pp. 2673-2693 (2004)

[29] P. Spietz, *"Absorption cross sections for iodine species of relevance to the photolysis of mixtures of I_2 and O_3 and for the atmosphere"*, Thesis, Doctoral Program "Dr. rer. nat.", Department of Physics, University of Bremen, March 2005

[30] P. Spietz, J.C. Gómez Martín and J.P. Burrows, *"Spectroscopic Studies of the I_2/O_3 Photochemistry, Part 2: Improved Spectra of Iodine Oxides and analysis of the IO Absorption Spectrum"*, Manuscript submitted for publication at the Journal of Photochemistry and Photobiology A, July 2005